Cytokinin-promoted secondary growth and storage of high molecular weight carbon compounds in the perennial stem zone of *Arabis alpina*

Inaugural-Dissertation

zur Erlangung des Doktorgrades
der Mathematisch-Naturwissenschaftlichen Fakultät
der Heinrich-Heine-Universität Düsseldorf

vorgelegt von

Anna Sergeeva
aus Neustrelitz

Düsseldorf, September 2020

aus dem Institut für Botanik
der Heinrich-Heine-Universität Düsseldorf

Gedruckt mit der Genehmigung der
Mathematisch-Naturwissenschaftlichen Fakultät der
Heinrich-Heine-Universität Düsseldorf

Berichterstatter:

1. Prof. Dr. Petra Bauer

2. apl. Prof. Dr. Nicole Linka

Tag der mündlichen Prüfung: 20.10.2020

Eidesstattliche Erklärung

Ich versichere an Eides Statt, dass die Dissertation von mir selbständig und ohne unzulässige fremde Hilfe unter Beachtung der „Grundsätze zur Sicherung guter wissenschaftlicher Praxis an der Heinrich-Heine-Universität Düsseldorf“ erstellt worden ist.

Ich habe die Dissertation in dieser oder ähnlicher Form bisher keiner anderen Fakultät vorgelegt.

Ich habe bisher keine erfolglosen Promotionsversuche unternommen.

Anna Sergeeva
Düsseldorf, 01.09.2020

Acknowledgements

First of all, I would like to thank Prof. Dr. Petra Bauer for giving me the opportunity to work on a project which was part of a bigger network of interesting researchers. Thank you, Petra, for supporting me during this time. Thank you for all the detailed discussions and all the help. I learned a lot during this time. Also, my personality changed a lot. My personal growing and development during this time could only happen because you gave me this opportunity to be part of your group.

I would like to thank apl. Prof. Dr. Nicole Linka for reviewing my thesis and being the second examiner. Thank you, a lot, for accepting this task that shortly before submission of my thesis.

Thank you, Prof. Dr. Stanislav Kopriva, for being my mentor during the CEPLAS time of my project. I would like to thank you for your valuable input during my yearly meetings.

I am really thankful to Dr. Tabea Mettler-Altmann. Thank you, Tabea, for your great ideas, support, help, your time, and long discussions. Thank you for providing me the opportunity to perform some of the experiments and to analyze my data in your laboratory. I learned a lot from you and I am really happy that I could get to know you. I was always impressed how great you manage this huge amount of work and how you can keep and combine all these details of that many projects in your head. I would also like to thank Maria, Katrin, and Elisabeth for their immensely friendly way of support. I always felt really comfortable in your laboratory.

I would like to thank Dr. Hans-Jörg Mai for analyzing the data that fast when there was not that much time left. Also, thank you, Hansi, for your valuable great input and of course technical support. I really appreciate the fact that you invest a lot of time in helping when help is needed. Thank you for that.

Thank you, Dani, for accompanying me, starting from the first year of this whole period. Thank you for morally supporting me and for sharing the good and the bad moments with me. I am really thankful to you for being there for me, especially during these harsh times with my “knee issue”. Thank you for being my best friend.

I would like to thank all the members of our laboratory. It was a pleasure to work together with all of you. Thank you, Birte, for all the conversations we had. Especially with you and Dani, we could share this sometimes-heavy weight of the “package”. I am thankful to Ksenia, Moni, Aron, Jannik, Inga, Tzvetina, Rumen, Ginte, Elke, and all the previous members for creating a pleasant working atmosphere. Thank you, Hongjiu, for helping me with some of the experiments during your stay in our laboratory.

Thank you Sieglinde, Meng-Ying, and Kumari. I am happy that I could get to know you and thankful to you for the wonderful time we spent together.

Thank you, Sohail. I am really happy that you accompany me now in my life. Thank you for your support, long conversations, and wonderful time together full of harmony. Dher sara pyar.

Und natürlich möchte ich den wohl wichtigsten Menschen in meinem Leben danken, meinen Eltern. Danke euch für eure Liebe und Unterstützung in den ganzen Jahren. Ohne euch würde ich wahrscheinlich nicht so viel Kraft haben, alles zu bewältigen. Weiterhin würde ich mich gerne bei meinem Bruder bedanken. Trotz allem weiß ich, dass ich mich immer auf dich verlassen kann. Schließlich möchte ich mich bei dem kleinsten Mitglied unserer Familie bedanken, meiner Nichte. Du bist noch ziemlich jung und verstehst vieles noch nicht, aber du gibst jetzt schon sehr viel Kraft und positive Energie. Спасибо вам!

Table of Contents

1 Preface

This thesis is divided into three parts. The overview is provided by a short summary in English and German. The first part comprises the introduction, subdivided into three sections. The first section describes perennial and annual life cycle strategies, including the description of the used perennial model species *Arabis alpina*. The second section provides an overview about primary and secondary growth and reflects on the influence of phytohormones on secondary growth. The third section informs about storage in perennial plants, whereat starch and lipid metabolism are depicted in more detail. The first part is completed by presenting the thesis objectives. The second part includes two manuscripts:

1. **Cytokinin-promoted secondary growth and nutrient storage in the perennial stem zone of *Arabis alpina***

   Anna Sergeeva, Hongjiu Liu, Hans-Jörg Mai, Tabea Mettler-Altmann, Christiane Kiefer, George Coupland, Petra Bauer

   - *in press* - The Plant Journal (*online ahead of print*: DOI: https://doi.org/10.1111/tpj.15123)

In this study, we identify that the vegetative lateral stem zone of *A. alpina* exhibits secondary growth and accumulation of starch and triacylglycerol (TAG) in cambium and cambium derivatives (termed perennial growth zone (PZ)). By contrast, the inflorescence of lateral stems is marked by primary growth (termed annual growth zone (AZ)). Storage characteristics of starch and TAG differ here from the PZ. We provide evidence that cytokinin promotes secondary growth in stems of *A. alpina*. Cytokinin application enhanced cambium activity and formation of secondary phloem parenchyma in the PZ and even in the AZ. Cytokinin-related gene ontology terms were enriched in the PZ. Concomitantly, cytokinin biosynthesis and signaling genes were expressed at a higher level in the PZ than in the AZ. With these findings we provide novel factors important for studies regarding the perennial growth of *A. alpina*.

2. **Lipid metabolism distinguishes perennial and annual stem zones in the perennial model plant *Arabis alpina***

   Anna Sergeeva, Tabea Mettler-Altmann, Hongjiu Liu, Hans-Jörg Mai, Petra Bauer

   - *in press* - Plant Direct

This study provides a detailed analysis of lipid metabolism in lateral stems of *A. alpina*. We demonstrate that glycerolipids, including neutral lipids, phospholipids, and glycolipids, are present at higher levels in the PZ as compared to the AZ. In addition, evidence is provided that glycerolipid-related genes may be involved in the development of the PZ. We suggest lipid metabolism genes to be targets of regulatory mechanisms specifying the PZ differentiation in *A. alpina*.

The third part, containing concluding remarks, completes the thesis by stating the answers to the major research questions, summarizing the most important findings, reflecting on the outcome, and providing several starting points for future analyses.

2 Summary

Based on the reproductive strategy, plants can be classified into two groups, annuals and perennials. Monocarpic annual plants reproduce once during their life cycle and finally senesce. Polycarpic perennial plants grow for several seasons and cycle between vegetative and reproductive mode. Growth is maintained through vegetative behavior of meristems, while senescence is restricted only to reproductive branches. One characteristic trait of perennial species is the efficient use of nutrients that are partitioned between sustained plant organs and developing seeds. Resources, stored in vegetative plant structures, are used to re-initiate growth after unfavorable growth periods. Thus, persistence of perennial plants is marked by a high above-ground and below-ground tissue density. Vegetative above-ground shoots of perennial plants may increase in diameter with development. This increase in girth is termed secondary growth and is initiated by two secondary lateral meristems, the vascular and cork cambium. Cambial activity in stems is influenced by a diverse set of phytohormones. Here, cytokinin is claimed to be a key regulator in cambium establishment and activity. Secondary growth is linked to nutrient storage. Various storage compounds are known to be present in stem tissues of perennial herbaceous plant species and trees.

Nutrient allocation to storage tissues is fundamental for perennial life cycle and must be precisely regulated. We used perennial Brassicaceae model species *Arabis alpina* to study perennial trait of nutrient storage. *A. alpina* Pajares (Paj), the accession requiring vernalization for flowering, has a complex stem architecture. Lateral stems of Paj and its vernalization-independent mutant derivative *A. alpina perpetual flowering 1-1* (*pep1-1*) have a proximal vegetative zone, that is retained after flowering, and a distal senescing inflorescence zone. We investigated this zonation pattern on anatomical and biochemical level and identified the vegetative zone to be marked by secondary growth (termed perennial growth zone (PZ)). Starch and triacylglycerol (TAG)-containing lipid bodies accumulated in cambium and cambium derivatives in the PZ. In addition to TAG, glycolipids and phospholipids were present at higher levels in the PZ. Secondary growth and storage were independent from vernalization or flowering. By contrast, primary growth was characteristic for the inflorescence zone (termed annual growth zone (AZ)). The AZ and roots exhibited different storage characteristics. Application of cytokinin enhanced cambial activity and secondary phloem parenchyma formation in the PZ and in the AZ. Transcriptome analysis revealed cytokinin and lipid metabolism-related gene ontology terms to be enriched in the PZ. Cytokinin biosynthesis and signaling genes were expressed at a higher level in the PZ in comparison to the AZ. In addition, a set of glycerolipid metabolism-related genes had higher expression levels during development of the PZ. These genes strongly correlated with single fatty acids of each investigated glycerolipid fraction of the PZ.

With this study we show that nutrient storage is coupled to cytokinin-promoted secondary growth in the vegetative PZ of *A. alpina*. Moreover, we identify lipid metabolism genes that might be potential targets of regulatory mechanisms specifying the PZ development.

3 Zusammenfassung

Pflanzen können anhand der Fortpflanzungsstrategie in zwei Gruppen, die einjährigen und die mehrjährigen, unterteilt werden. Monokarpe einjährige Pflanzen pflanzen sich einmal während ihres Lebenszykluses fort und seneszieren schließlich. Polykarpe mehrjährige Pflanzen überdauern mehrere Jahre und wechseln dabei zwischen dem vegetativen und reproduktiven Lebensmodus. Das Wachstum wird durch das vegetative Verhalten der Meristeme aufrechterhalten, während die Seneszenz sich nur auf die reproduktiven Äste beschränkt. Ein charakteristisches Merkmal der mehrjährigen Spezies ist die effiziente Nährstoffnutzung. Die Nährstoffe werden dabei zwischen den überdauernden Pflanzenorganen und den sich entwickelnden Samen aufgeteilt. Ressourcen, die in den vegetativen Pflanzenstrukturen gespeichert werden, werden nach den ungünstigen Wachstumsperioden für die erneute Wachstumsaufnahme genutzt. Die Langlebigkeit der mehrjährigen Pflanzen ist daher durch eine hohe oberirdische und unterirdische Gewebedichte gekennzeichnet. Vegetative oberirdische Sprosse der mehrjährigen Pflanzen können mit fortschreitender Entwicklung im Durchmesser zunehmen. Diese Zunahme im Umfang wird als sekundäres Dickenwachstum bezeichnet, und wird durch die Aktivität der zwei sekundärer Lateralmeristeme, des Kambiums und des Korkkambiums, ausgelöst. Kambiumaktivität in Stämmen wird durch eine Reihe unterschiedlicher Phytohormone beeinflusst. Hierbei wird Cytokinin als ein Hauptregulator der Kambiumetablierung und -aktivität angesehen. Sekundäres Dickenwachstum ist an die Nährstoffspeicherung gekoppelt. Das Vorkommen zahlreicher Speicherstoffe in Geweben der Stämme der mehrjährigen krautigen Pflanzen und Bäume ist bekannt.

Nährstoffallokation zu den Speichergeweben ist grundlegend für den Lebenszyklus der mehrjährigen Pflanzen und muss präzise reguliert werden. Um das mehrjährige Merkmal der Nährstoffspeicherung zu untersuchen, wurde die mehrjährige Modellspezies *Arabis alpina*, die zur Familie der Brassicaceae gehört, genutzt. *A. alpina* Pajares (Paj), die Akzession, die Vernalisation zur Förderung der Blütenbildung benötigt, weist eine komplexe Stammarchitektur auf. Die lateralen Stämme von Paj können in eine proximale vegetative Zone, welche nach der Blütenbildung aufrechterhalten wird, und in eine distale seneszierende Infloreszenz-Zone unterteilt werden. Die gleiche Struktur ist auch beim mutierten Abkömmling von Paj, *A. alpina perpetual flowering 1-1* (*pep1-1*), die keine Vernalisation zur Blütenbildung braucht, zu finden. Dieses Zonierungsmuster wurde auf anatomischer und biochemischer Ebene untersucht. Dabei wurde festgestellt, dass die vegetative Zone durch das sekundäre Dickenwachstum gekennzeichnet ist (benannt als mehrjährige Wachstumszone (engl., PZ)), und Stärke sowie Triacylglycerol (TAG) in den Lipidkörperchen im Kambium und in den Kambiumderivaten dieser Zone akkumulieren. Zudem wurden höhere Mengen an Glyko- und Phospholipiden in der PZ ermittelt. Sekundäres Dickenwachstum und Speicherung waren dabei nicht von der Vernalisation oder der Blütenbildung abhängig. Im Gegensatz dazu war das primäre Dickenwachstum charakteristisch für die Infloreszenz-Zone (benannt als einjährige Zone (engl., AZ)). Die AZ und die Wurzeln wiesen andere Speichermerkmale auf. Die Anwendung von Cytokinin förderte

die Kambiumaktivität und die Bildung des sekundären Phloemparenchyms in der PZ und auch in der AZ. Mit Hilfe der Transkriptomanalyse wurden die Genontologie-Begriffe, die sich auf Cytokinin und den Lipidmetabolismus bezogen, als angereichert in der PZ nachgewiesen. Im Vergleich zu der AZ waren Cytokinin Biosynthese- und Signalgene höher exprimiert in der PZ. Zudem wies eine Reihe an Genen des Glycerolipid-Metabolismus eine stärkere Expression während der Entwicklung der PZ auf. Diese Gene korrelierten mit den einzelnen Fettsäuren jeder untersuchten Glycerolipid-Fraktion der PZ.

In der vorliegenden Arbeit wird gezeigt, dass die Nährstoffspeicherung in der vegetativen PZ von *A. alpina* in Verbindung mit dem sekundären Dickenwachstum, welches durch Cytokinin beeinflusst wird, steht. Darüber hinaus werden in dieser Arbeit Gene des Lipidmetabolismus identifiziert. Diese Gene stellen potentielle Ziele der regulatorischen Mechanismen, welche die Entwicklung der PZ bestimmen könnten, dar.

4 Abbreviation list

ACC	aminocyclopropane-1-carboxylate
ACX	acyl-CoA oxidase
ADP	adenosine diphosphate
AGPase	adenosine diphosphate glucose pyrophosphorylase
AHK2	ARABIDOPSIS HISTIDINE KINASE 2
AIM1	ABNORMAL INFLORESCENCE MERISTEM 1
ANT	AINTEGUMENTA
ARF5	AUXIN RESPONSE FACTOR 5
AZ	annual growth zone
BIL1	BRASSINOSTEROID-INSENSITIVE 2-LIKE 1
C	carbon
CKX	CYTOKININ OXIDASE
CLE41	EMBRYO SURROUNDING REGION RELATED 41
CLV3	CLAVATA3
CRE1	CYTOKININ RESPONSE 1
DBE	debranching enzyme
DGAT	diacylglycerol acyltransferase
ECH2	ENOYL-COA HYDRATASE 2
ER	endoplasmic reticulum
ERF	ETHYLENE RESPONSE FACTOR
ETO1	ETHYLENE OVERPRODUCER 1
FA	fatty acid
FLC	FLOWERING LOCUS C
FUL	FRUITFULL
GA	gibberellic acid
GA20ox	Gibberellin 20-oxidase
GL	glycolipid
GO	gene ontology
GPAT	glycerol-3-phosphate acyltransferase
GWD	glucan, water dikinase
HPt	histidine phosphotransfer protein
IPT	Isopentenyltransferase

ISA1	isoamylase 1
JA	jasmonic acid
JAZ	JASMONATE ZIM-DOMAIN
KAT	3-ketoacyl-CoA thiolase
LFY	LEAFY
LB	lipid body
LD	lipid droplet
LDA	limit dextrinase
LDAP	LD-associated protein
LOG	LONELY GUY
LPAAT	lysophosphatidic acid acyltransferase
LRR-RLK	leucine-rich repeat receptor-like kinase
MAX	MORE AXILLARY BRANCHES
MFP	multifunctional protein
miR156	microRNA156
MP	MONOPTEROS
N	nitrogen
NL	neutral lipid
NSC	non-structural carbohydrate
OB	oil body
P	phosphorus
Paj	Pajares
PDAT	phospholipid:diacylglycerol acyltransferase
PEP1	PERPETUAL FLOWERING 1
PGPP	phosphatidylglycerol phosphate phosphatase
PGPS	phosphatidylglycerol phosphate synthase
P_i	phosphate
PIN	PIN-FORMED
PIS	phosphatidylinositol synthases
PL	phospholipid
PP	phosphatidate phosphatase
PWD	phosphoglucan, water dikinase
PXY	PHLOEM INTERCALATED WITH XYLEM
PZ	perennial growth zone

RAM	Root apical meristem
RNA	ribonucleic acid
RR	response regulator
S	sulfur
SAM	Shoot apical meristem
SBE	starch-branching enzyme
SDP1	SUGAR-DEPENDENT 1
SEX1	STARCH EXCESS 1
SOC1	SUPPRESSOR OF OVEREXPRESSION OF CONSTANS 1
SPL15	SQUAMOSA PROMOTER BINDING PROTEIN-LIKE 15
SS	starch synthase
TAG	triacylglycerol
TDIF	TRACHEARY ELEMENT DIFFERENTIATION INHIBITORY FACTOR
TDR	TDIF RECEPTOR
TFL1	TERMINAL FLOWER 1
VLCFA	very long-chain fatty acid
WOX4	WUSCHEL-RELATED HOMEOBOX 4

5 Introduction

5.1 Perennial and annual life cycle strategies

Plants can be categorized into two general groups according to their reproductive strategy, annuals and perennials. Annuals are usually monocarpic (semelparous) and reproduce only once during their one-year life cycle prior to senescence and death of the plant (Thomas, 2013). Transition from vegetative to reproductive growth occurs fast, generally following inductive seasonal cues. Energy is predominantly invested into rapid seed production to maximize the reproductive effort (Pitelka, 1977; Bazzaz *et al.*, 1987). Many plants adopted this life cycle strategy in harsh environments to avoid stress factors like drought, frost, and grazing, which is accomplished by rapid reproduction (Whyte, 1977; Pettit *et al.*, 1995; Evans *et al.*, 2005; Cruz-Mazo *et al.*, 2009).

By contrast, growth and development of perennial plants encompasses several growth seasons. The majority of perennial plants is polycarpic (iteroparous) and characterized by repeated cycles between vegetative and reproductive mode throughout their lifespan (Bergonzi and Albani, 2011). An important factor that differentiates perennials from annuals is the distinctive behavior of meristems. Some remain vegetative, while others are committed to reproductive development (Battey and Tooke, 2002; Amasino, 2009; Albani and Coupland, 2010). Senescence is confined only to reproductive branches, while growth is sustained through vegetative axillary branches and dormant buds (Amasino, 2009; Albani and Coupland, 2010). The available resources are used efficiently by partitioning them between the maintained plant organs and offspring production. Perennial plant species rely on stored resources in vegetative structures in order to re-initiate growth after unfavorable growth periods, thus maximizing persistence, defense, and stress tolerance (De Souza and Da Silva, 1987). Maximized persistence is reflected in perennials by high above-ground and below-ground tissue density and allocation of biomass predominantly into roots (De Souza and Da Silva, 1987; Garnier, 1992; Roumet *et al.*, 2006). Therefore, nutrient allocation either to persisting storage tissues/organs or to developing seeds must be precisely regulated.

Perennial life strategy is usually regarded to be ancestral (Hu *et al.*, 2003; Grillo *et al.*, 2009). Transitions from perennial to annual life histories are common among angiosperms and are generally considered as an adaptive strategy to avoid seasonal stress factors, especially arid periods (Sherrard and Maherali, 2006; Cruz-Mazo *et al.*, 2009; Friedman and Rubin, 2015). These switches between different life strategies resulted in closely related annual and perennial species (Lowry *et al.*, 2008; Grillo *et al.*, 2009; Lindberg *et al.*, 2020). Mechanisms that regulate whether a plant is annual or perennial remain unexplored to a great extent. However, the availability of closely related annual and perennial species offers an opportunity to elucidate the molecular regulators conferring perennial or annual traits by a direct comparison within the phylogenetic framework.

Perennial plant species are marked by longer lifespan, greater biomass production, higher nutrient storage capacity, and better performance in harsh environments (Glover, 2005). Nevertheless, annual crops rather form the basis of human diet. Examples include wheat, barley, rye, maize, and rice. To date, there are no perennial species that may produce grain harvests covering the needs of world population. Remarkable differences between annuals and perennials involve mechanisms of maintenance of dormant buds and vegetative structures (Amasino, 2009; Albani and Coupland, 2010; Vayssières *et al.*, 2020), spatiotemporal separation of flowering response (Zhou *et al.*, 2013; Friedman and Rubin, 2015; Lazaro *et al.*, 2018), pronounced juvenile, adult vegetative, and reproductive phase (Usami *et al.*, 2009; Bergonzi and Albani, 2011; Willmann and Poethig, 2011), and resource allocation to developed perennating storage tissues/organs (Hu et al., 2003; Wang *et al.*, 2007; Hartmann *et al.*, 2011; Hartmann and Trumbore, 2016). Therefore, elucidation of these mechanisms may be beneficial for the development of perennial grain cropping systems.

5.2 Perennial model plant *Arabis alpina*

Annuality has evolved multiple times independently from a perennial background in different lineages of the tribe Arabideae within the Brassicaceae (Karl and Koch, 2013). Phylogenetic analysis of the main branches of Arabideae showed that the annual *Arabis montbretiana* is a sister species of the perennial *Arabis alpina* (Kiefer *et al.*, 2017). In recent years, these two taxa have been established as a model system to investigate perennial to annual transition. The sequenced genome (Willing *et al.*, 2015), and the techniques and tools developed for *Arabidopsis thaliana* and other Brassicaceae can be directly employed to study *A. alpina*.

According to the Raunkiaer's system of plant life forms, *A. alpina* is a herbaceous hemicryptophyte with above-ground perennial vegetative branches. *A. alpina* originates from migrations out of Asia Minor and has a wide arctic-alpine distribution range (Koch *et al.*, 2006; Ansell *et al.*, 2011; Karl *et al.*, 2012). The perennial life-cycle of *A. alpina* was characterized using *A. alpina* Pajares (Paj), an accession from Spain. In accordance with the polycarpic perennial life strategy, Paj plants cycle between vegetative and reproductive development for several growth seasons (Wang *et al.*, 2009). While reproductive main and axillary stem segments senesce and finally die, vegetative stem parts of the plant are retained. The developmental cycle of Paj comprises pronounced juvenile, vegetative, and reproductive phase (Bergonzi and Albani, 2011; Hyun *et al.*, 2017).

Stem architecture of *A. alpina* Paj is marked by varying positions of individual flowers, dormant buds, non-flowering and flowering lateral branches (Lazaro *et al.*, 2018). During and after vernalization, three types of vegetative (V1, V2, V3) and two inflorescence (I1, I2) subzones are established from bottom to top (Figure 1). Zonation pattern of V1 branches resembles this of the main shoot axis. V2 bears dormant axillary buds, while axillary vegetative branches are characteristic for the small V3 subzone. Lateral branches with inflorescences are formed in the I1 subzone. The terminal I2 subzone is defined by individual flowers. Vayssières *et al.* (2020) demonstrated that auxin polar transport is

involved in the establishment of this complex stem architecture, especially regarding the maintenance of the V2 dormant bud zone.

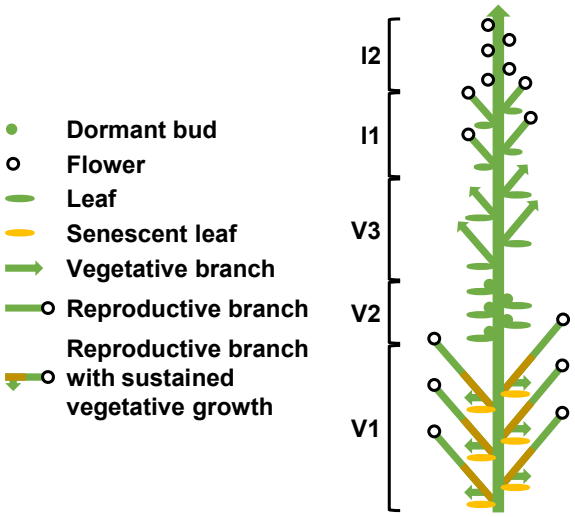

Figure 1. Schematic representation of the stem architecture of *A. alpina* Pajares (Paj), established after vernalization. Stems are divided into two zones, vegetative (with subzones V1, V2, and V3) and inflorescence (with subzones I1 and I2). V1 zone is characterized by reproductive axillary branches that retain vegetative character after flowering. V2 bears dormant axillary buds, while V3 zone is marked by branches with vegetative character. Lateral branches with inflorescences are representative for I1 subzone. Individual flowers are formed in the I2 subzone. The schematic plant representation was partially adopted from Wang *et al.* (2009), Lazaro *et al.* (2018), and Vayssières *et al.* (2020).

An ecologically relevant adaptive trait of the requirement for vernalization prevents plants from flowering before winter and permits flowering in the favorable conditions afterwards (Kim *et al.*, 2009). Vernalization suppresses flowering in *A. alpina* Paj until the action of repressors is released (Wang *et al.*, 2009). The *A. alpina* orthologue of *Arabidopsis FLOWERING LOCUS C* (*FLC*), *PERPETUAL FLOWERING 1* (*PEP1*), acts as a floral repressor and regulates flowering of *A. alpina* in response to vernalization (Wang *et al.*, 2009). FLC is a MADS box transcription factor with a well-known function in flowering delay before vernalization (Michaels and Amasino, 1999). In *Arabidopsis*, FLC represses transcription of genes involved in transition to reproductive development (Helliwell *et al.*, 2006; Searle *et al.*, 2006; Deng *et al.*, 2011). The stable repression of *FLC* transcription occurs due to the trimethylation on lysine 27 of histone 3 (H3K27me3) at the *FLC* gene (Finnegan and Dennis, 2007; Angel *et al.*, 2011). In *A. alpina*, PEP1 not only prevents flowering before vernalization, but also effects reversion to vegetative growth after reproduction (Wang *et al.*, 2009; Castaings *et al.*, 2014). Contrary to *Arabidopsis* and *A. montbretiana*, where *FLC* or *FLC* orthologue respectively is stably repressed by vernalization (Kiefer *et al.*, 2017), *PEP1* is temporarily repressed by the cold period in *A. alpina* (Wang *et al.*, 2009). Expression levels of *PEP1* increase again when plants are returned to warm temperatures. Contrary to *FLC* in *A. thaliana*, the H3K27me3 mark at the *PEP1* locus is not sustained after vernalization, correlating with enhanced levels of *PEP1* (Finnegan and Dennis, 2007; Wang *et al.*, 2009; Angel *et al.*, 2011). Moreover, flowering does not occur in axillary branches that are initiated during vernalization due to high *PEP1* expression levels (Wang *et al.*, 2009; Park *et al.*, 2017). Flowering is not dependent on vernalization and is induced simultaneously in all branches of the *pep1-1* mutant, a derivative of Paj, that carries lesions in *PEP1* (Wang *et al.*, 2009; Albani *et al.*, 2012). In comparison to Paj, *pep1-1* has lower longevity and an absent sub-zonation of the vegetative stem zone (Wang *et al.*, 2009; Hughes *et al.*, 2019). Despite this, *pep1-1* mutants still display perennial growth characteristics

and repeatedly form new axillary branches with proximal vegetative and distal reproductive character until the end of the growth season.

Further analyses of the obligate vernalization response in *A. alpina* demonstrated the involvement of the microRNA156 (miR156) in regulating age-dependent competence to flower in response to vernalization (Bergonzi *et al.*, 2013). *A. alpina* responds to cold treatment only if a certain age is reached (Wang *et al.*, 2011; Bergonzi *et al.*, 2013). This time span of gaining competence to flower encompasses five weeks, stressing the presence of a pronounced juvenile phase in *A. alpina*. Vernalized younger plants remain vegetative. Older plants that were competent to induce flowering after vernalization were characterized by lowest levels of miR156 (Bergonzi *et al.*, 2013). Analyses of transgenic plants supported the relationship between miR156 activity and the age-dependent competence to flower in response to vernalization. Flowering in response to the prolonged cold treatment was prevented in transgenic *A. alpina* plants overexpressing miR156. Reduced miR156 activity resulted in plants responding to vernalization sooner after germination.

Hyun *et al.* (2019) demonstrated a link between PEP1 and miR156-dependent regulation of flowering, involving the flowering promoting factor SQUAMOSA PROMOTER BINDING PROTEIN-LIKE 15 (SPL15). In *A. alpina*, down-regulation of *PEP1* is not affected by age or miR156 (Wang *et al.*, 2011; Bergonzi *et al.*, 2013), indicating that the age-dependent competence to flower is established downstream of *PEP1* (Hyun *et al.*, 2019). PEP1 was shown to bind to certain regions of the *Arabis SPL15* promoter (Mateos *et al.*, 2017). The importance of PEP1 binding for *AaSPL15* transcription was supported by high *AaSPL15* mRNA levels in *pep1-1* mutants and in older vernalized Paj plants (Hyun *et al.*, 2019). In addition, the majority of mutant plants with inactivated *AaSPL15* in the background of Paj did not flower after cold treatment, supporting the involvement of *AaSPL15* in vernalization. In *A. thaliana*, miR156 targets *SPL15* mRNA and flowering under short days is enhanced by SPL15 (Hyun *et al.*, 2016; Xu *et al.*, 2016). Shoot apical meristems (SAMs) of young *A. alpina* plants contained high levels of miR156 and prolonged cold treatment failed to promote *AaSPL15* expression here (Bergonzi *et al.*, 2013; Hyun *et al.*, 2019). To test whether miR156 influences vernalization through *AaSPL15*, transgenic Paj plants with a miR156-resistant form of *AaSPL15* mRNA were generated (Hyun *et al.*, 2019). Indeed, these plants accumulated AaSPL15 at the SAM of young and old plants during vernalization. Furthermore, young plants with the resistant form of *AaSPL15* mRNA even flowered after vernalization. Therefore, Hyun *et al.* (2019) suggested *AaSPL15* to coordinate vernalization and age-derived signals at the SAM of *A. alpina*.

In addition, a role in the extension of the vegetative phase during which plants are not responsive to inductive signals was demonstrated for the floral repressor TERMINAL FLOWER 1 (TFL1) (Wang *et al.*, 2011). In Paj, transition to flowering is characterized by enhanced expression of the floral meristem identity gene *LEAFY* (*LFY*) (Wang *et al.*, 2009). *LFY* is blocked by TFL1 during vernalization in young *A. alpina* plants. This effect was abolished in RNA interference lines with

reduced *TFL1* expression and flowering occurred during vernalization in young plants (Wang *et al.*, 2011).

To date, perennial growth habit of *A. alpina* was extensively investigated regarding the non-simultaneous development of meristems within the same plant. However, an important trait conferring perennial growth habit was overlooked until now. In order to sustain growth after the cold season and flowering, the resources are supposedly allocated not only to developing seeds in *A. alpina*, but also to putative storage tissues. *A. alpina* plants do not form obvious perennating storage organs. Thus, putative long-term storage tissues may occur in maintained vegetative stems and roots.

5.3 Primary and secondary growth

A unique feature of plants is the ability to grow indefinitely, resulting in the formation of new tissues and organs. This process is driven by the mitotic activity of meristematic stem cell populations, enabled of self-maintenance and production of daughter cells, which may differentiate into at least one specialized cell type (Laux, 2003; Sablowski, 2004; Scheres, 2007). Primary growth or shoot, and root elongation occur due to the activity of stem cell populations present in the SAM and the root apical meristem (RAM). SAM and RAM can be found at the tips of the main and lateral shoots and roots. SAM and RAM formation takes place during embryogenesis (Scheres *et al.*, 1994; Long and Barton, 1998). The vascular system of the *Arabidopsis* embryo is marked by a continuous network consisting of procambial cells spread along the hypocotyl-root axis and the cotyledons (Busse and Evert, 1999). After seed germination, the activity of meristematic cells in the SAM and the RAM leads to the establishment of the primary vasculature (Evert, 2006). The primary vasculature of dicot and gymnosperm stems is composed of separate bundles arranged around the pith (Figure 2) (Fischer *et al.*, 2019). The vascular stem cells are contained in the procambium of each bundle. Primary xylem and primary phloem, tissues involved in long-distance transport, are formed by the activity of procambium cells toward the inner pith and outside of the stem respectively (Esau, 1960). Composition of xylem includes tracheary elements, fibers, and parenchyma cells. Phloem tissue is composed of sieve elements, companion cells, fibers, and parenchyma cells. The interfascicular cells between the vascular bundles differentiate into parenchyma.

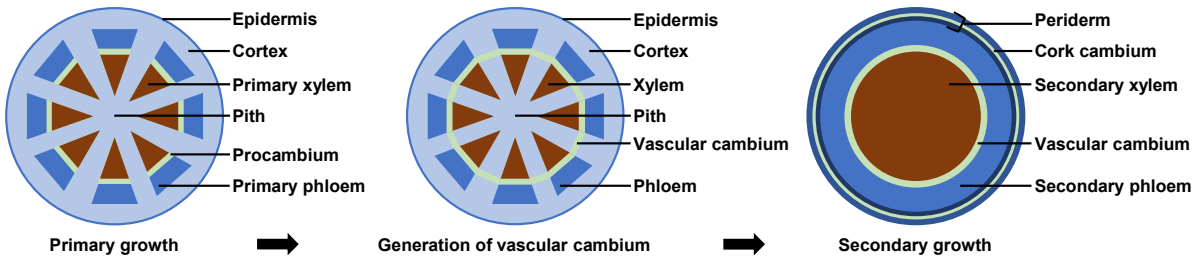

Figure 2. Schematic representation of secondary growth progression in a stem from primary growth to generation of vascular cambium and secondary growth tissues. Left: primary xylem (brown) and primary phloem (dark blue) are formed by the activity of procambium cells (green) during primary growth. Middle: a closed ring of vascular cambium (green) is formed during secondary growth. *(legend continued on next page)*

Right: activity of vascular cambium results in the production of secondary xylem (brown) and secondary phloem (dark blue). Periderm is generated by the activity of cork cambium (green), the second lateral meristem. The schematic illustration was partially adopted from Fischer *et al.* (2019).

With increasing apical growth new tissues are produced in the lateral dimension in stems and roots in order to provide more structural support, water, and nutrients. (Larson, 1994; Evert, 2006). This increase in girth is termed secondary growth and is initiated in stems by two secondary lateral meristems, the vascular and cork cambium (Figure 2). Secondary growth is restricted to gymnosperms and most dicotyledonous species and does not occur in monocotyledons and ferns (Baucher *et al.*, 2007). Secondary growth is initiated by reactivation of procambial cells of the vascular bundles. Concurrently, meristematic activity is acquired by the parenchyma cells in the interfascicular region between the vascular bundles, resulting in differentiation of these cells into interfascicular cambial cells. Thus, a closed ring of vascular cambium is formed (Figure 2). Cell divisions in the vascular cambium lead to the production of secondary xylem and secondary phloem with the corresponding parenchyma, resulting in wood and bast formation. Periderm, the new protective outer tissue against water loss, wounding, and pathogen attack, is generated by the cork cambium or phellogen. The cork cambium produces inward phelloderm and outward cork.

Secondary growth may occur in annual plant species, including the model *A. thaliana*. Thus, the current knowledge about the major molecular regulators of secondary growth mainly comes from studies using *Arabidopsis* or *Populus*. In *Arabidopsis*, secondary growth takes place in the root, hypocotyl, and stem region in close proximity to the rosette. Tips of *Arabidopsis* stems display only primary growth characteristics (Dolan and Roberts, 1995; Altamura *et al.*, 2001). Interestingly, mechanical stress may influence cambial activity and thus the establishment of secondary rays in the *Arabidopsis* stem (Ragni and Greb, 2018). Many regulators of secondary growth identified in *Arabidopsis* are conserved in perennial woody species (Etchells *et al.*, 2015; Barra-Jiménez and Ragni, 2017; Kucukoglu *et al.*, 2017). Here, *Populus* represents the preferred perennial model organism to study molecular mechanisms inducing secondary growth. The important signals and molecular mechanisms influencing vascular cambium initiation, maintenance and activity, and development of secondary growth tissues will be described in the following sections.

5.4 Influence of phytohormones on secondary growth

Phytohormones represent key regulators of plant growth and development and are generally active at very low concentrations (Wani *et al.*, 2016). They comprise a diverse set of chemical compounds, including cytokinins, auxin, gibberellin (GA), ethylene, jasmonic acid (JA), strigolactones, abscisic acid, brassinosteroids, and salicylic acid. Examples of their functions encompass regulation of stem elongation, vegetative growth, flowering, cell division and elongation, apical dominance, axillary bud growth, seed and bud dormancy, senescence, fruit ripening, and stomatal closure (Asami and

Nakagawa, 2018). In addition, an array of studies demonstrated phytohormones to impact secondary growth development. The major findings are represented in more detail in the following.

5.4.1 Cytokinin

In the past decades, cytokinin was demonstrated to be one of the most important regulators positively influencing the establishment and the activity of the vascular cambium during secondary growth (Matsumoto-Kitano *et al.*, 2008; Nieminen *et al.*, 2008; Ohashi-Ito *et al.*, 2014; Immanen *et al.*, 2016). Cytokinin homeostasis includes cytokinin biosynthetic enzymes ISOPENTENYLTRANSFERASEs (IPTs), LONELY GUYs (LOGs), involved in the conversion of inactive cytokinins to bioactive forms, and the cytokinin-degrading enzymes CYTOKININ OXIDASEs (CKXs) (Sakakibara, 2006). The cytokinin signaling pathway consists of a multistep two-component signal transduction pathway (Hwang *et al.*, 2002). The phosphorelay transduction pathway is initiated by the binding of the hormone to the cytoplasmic CYTOKININ RESPONSE 1 (CRE1)-like receptors which is followed by the phosphorylation of histidine phosphotransfer (HPt) proteins. HPts move from the cytosol to the nucleus where they transfer a phosphoryl group to transcription factors type B response regulators (RRs). Type B RRs trigger the activation of cytokinin primary response genes. Cytokinin primary response genes include type A RRs that inhibit the activity of type B RRs, thus participating in a negative feedback mechanism of the cytokinin phosphorelay transduction pathway.

Importance of cytokinin in the establishment of cambium was shown in *Arabidopsis* roots by generation of mutants affected in IPTs (Matsumoto-Kitano *et al.*, 2008). Cambium formation and secondary growth were completely abolished in quadruple *atipt1;3;5;7* mutants. Transgenic hybrid poplar trees, overexpressing *CKX2* and thus having reduced cytokinin levels, exhibited decreased cambial cell divisions and thinner stems in comparison to wild type trees (Nieminen *et al.*, 2008). *Arabidopsis* mutants with impaired function in cytokinin receptors ARABIDOPSIS HISTIDINE KINASE 2 (AHK2) and AHK3 were marked by the absence of interfascicular cambium and consequently secondary growth (Hejátko *et al.*, 2009). Influence of increased cytokinin levels on the vascular development in *Populus* trees was shown by overexpression of *Arabidopsis AtIPT7* under the *PttLMX5* promoter, enhancing the expression in the cambial and developing xylem region (Immanen *et al.*, 2016). In comparison to wild type plants, cambial cell files of transgenic lines were comprised of increased number of meristematic cells, resulting in enhanced biomass production. Moreover, increased cytokinin levels and cytokinin signaling response in the cambial and xylem region of the *pLMX5:AtIPT7* lines enhanced cambial auxin levels and gene expression of auxin-responsive genes (Immanen *et al.*, 2016). This supported the already known observation of the connection of the homeostasis of these two hormones (Jones *et al.*, 2010; Šimášková *et al.*, 2015). Hormonal profiling across the *Populus trichocarpa* stem demonstrated a specific but interconnected distribution of cytokinin, auxin, and GA (Immanen *et al.*, 2016). Cytokinins had the highest concentrations in the developing phloem. Auxin levels peaked in the actively dividing cambial zone and the developing

xylem tissue was marked by bioactive GA. Furthermore, the concentration gradient of cytokinins was supported by gene expression of cytokinin biosynthesis and signaling genes (Nieminen *et al.*, 2008; Immanen *et al.*, 2016).

Downstream of the cytokinin signaling pathway, transcription factors AINTEGUMENTA (ANT) and D-type cyclin CYCD3;1 might be the important regulators of secondary growth (Randall *et al.*, 2015). In *Arabidopsis*, these transcription factors are expressed in the vascular cambium and respond to cytokinin during root secondary growth. Single mutants displayed reduction in the number of cambial cells and decreased secondary growth (Randall *et al.*, 2015; Collins *et al.*, 2015). Another example of the regulation of cambial development in *Arabidopsis* involves auxin-cytokinin signaling and a glycogen synthase kinase 3, BRASSINOSTEROID-INSENSITIVE 2-LIKE 1 (BIL1) (Han *et al.*, 2018). BIL1 influences inhibition of cambial activity, by mediating phosphorylation of the auxin-dependent transcription factor MONOPTEROS/AUXIN RESPONSE FACTOR 5 (MP/ARF5). The inflorescence stems and hypocotyls of *Arabidopsis bil1* mutants are marked by enhanced cambial activity and formation of vascular tissues. The *bil1* mutant phenotype was abolished, when a phosphorylated version of MP/ARF5 was overexpressed, indicating the involvement of BIL1 in the negative regulation of cambial activity. Moreover, BIL1 influences cambial activity acting via negative regulators of cytokinin signaling, the A-type *Arabidopsis* RRs, ARR7 and ARR15. BIL1-induced phosphorylation of MP/ARF5 leads to up-regulation of ARR7 and ARR15 and thus suppression of the cytokinin response.

5.4.2 Auxin

In addition to cytokinin, evidence exists for auxin being an important positive regulator of cambial activity and differentiation of secondary growth tissues. In fact, interfascicular cambium formation is initiated in decapitated stems by exogenously applied auxin, while radial development is inhibited in decapitated stems alone (Little *et al.*, 2002). Interestingly, auxin may be required for cambial identity maintenance, as cambial cells differentiate into parenchyma in explants of pine stems without a source of auxin (Savidge, 1983). Basipetal auxin transport along the stem axis relies on the activity of auxin efflux carriers of the PIN-FORMED (PIN) family (Okada *et al.*, 1991). In inflorescence stems of *Arabidopsis*, PIN1 is expressed in the procambial and cambial regions and in xylem parenchyma with a localization toward the root apex (Gälweiler *et al.*, 1998; Benková *et al.*, 2003; Bennett *et al.*, 2006; Sauer *et al.*, 2006; Bennett *et al.*, 2016). PIN2 and PIN3 accumulate mainly in xylem parenchyma (Bennett *et al.*, 2016). Consistently, Agusti *et al.* (2011) demonstrated in *Arabidopsis pin* mutants that PIN1 and PIN3 and hence basipetal auxin transport are required for the lateral growth initiated by the vascular cambium activity. The mutant plants displayed reduced interfascicular cambium formation. In addition, an auxin gradient across the lateral dimension of stems may be involved in the regulation of cambial activity and differentiation of cambium-derived tissues by providing spatial information to cells of these tissues (Sundberg *et al.*, 2000; Bhalerao and Fischer,

2014). The highest auxin concentrations are present in the cambial region of poplar and spruce stems. Auxin levels decrease gradually toward secondary phloem or xylem (Tuominen *et al.*, 1997; Uggla *et al.*, 1996; Uggla *et al.*, 1998; Björklund *et al.*, 2007; Immanen *et al.*, 2016). Thus, cells with a high division rate are influenced by high auxin concentrations, expanding cells are exposed to intermediate auxin levels, and cells experiencing low concentrations undergo differentiation processes including secondary cell wall deposition (Fischer *et al.*, 2019). Reduced cambial cell divisions took place in transgenic hybrid aspen trees with ubiquitously reduced auxin responsiveness, supporting the role of auxin to promote cambial activity (Nilsson *et al.*, 2008).

The transcription factor WUSCHEL-RELATED HOMEOBOX 4 (WOX4) is required for auxin-dependent cambium stimulation downstream of auxin signaling. *WOX4* expression increases with enhanced accumulation of auxin (Suer *et al.*, 2011). Moreover, cambial cell divisions in fascicular and interfascicular regions are reduced in *Arabidopsis wox4* mutants, even with enhanced auxin accumulation (Suer *et al.*, 2011). WOX4 is a downstream target of the peptide-receptor signaling module, TRACHEARY ELEMENT DIFFERENTIATION INHIBITORY FACTOR/EMBRYO SURROUNDING REGION RELATED 41-PHLOEM INTERCALATED WITH XYLEM/TDIF RECEPTOR (TDIF/CLE41-PXY/TDR) (Hirakawa *et al.*, 2010; Etchells *et al.*, 2013). In the *Arabidopsis* genome, *CLAVATA3* (*CLV3*)/*CLE41* and *CLE44* genes encode for TDIF which is a 12-amino-acid-long mobile peptide ligand (Ito *et al.*, 2006; Hirakawa *et al.*, 2008; Ohyama *et al.*, 2008; Etchells and Turner, 2010). TDIF is bound by the plasma membrane-associated leucine-rich repeat receptor-like kinase (LRR-RLK) PXY/TDR in the cambial region (Fischer and Turner, 2007; Hirakawa *et al.*, 2008; Etchells and Turner, 2010). Vascular development-associated processes are influenced in several ways via interactions between TDIF/CLE41 and PXY/TDR. These include the regulation of procambial/cambial cell division rate, inhibition of differentiation of xylem cells, and control of the vascular patterning (Hirakawa *et al.*, 2008; Whitford *et al.*, 2008; Etchells and Turner, 2010; Hirakawa *et al.*, 2010). Positive regulation of WOX4 by the TDIF/CLE41-PXY/TDR signaling pathway was supported by the enhanced expression of WOX4, when CLE41 was overexpressed and synthetic TDIF/CLE41 peptide was applied. A similar regulation pattern was demonstrated for WOX14 that was suggested to act redundantly with WOX4 (Etchells *et al.*, 2013). Therefore, WOX transcription factors, downstream of CLE peptide signaling, may have important regulatory effects on cambial activity (Fischer *et al.*, 2019). The described observations in *Arabidopsis* were supported with studies in which hybrid aspen was used as model plant (Etchells *et al.*, 2015; Kucukoglu *et al.*, 2017). Cambial activity and wood formation were severely reduced in RNA interference lines with down-reguation of *WOX4* homologs (Kucukoglu *et al.*, 2017).

5.4.3 Gibberellin

In addition to cytokinin and auxin, an important role in secondary growth is attributed to GA. However, while cytokinin and auxin rather influence cambial activity, GA acts in the xylem region

where it promotes xylem cell differentiation and lignification (Denis *et al.*, 2017). The highest levels of bioactive GA are present in the developing xylem tissue of *Populus*, coinciding with its role in the regulation of xylem development (Israelsson *et al.*, 2005; Immanen *et al.*, 2016). Longer xylem fibers and an increased number of xylem fibers were produced in *Populus* trees, either overexpressing the biosynthetic gene *Gibberellin 20-oxidase* (*GA20ox*) or after exogenous treatment with GA (Eriksson *et al.*, 2000; Mauriat and Moritz, 2009; Johnsson *et al.*, 2019). Moreover, shoot-derived GA was demonstrated to promote xylem expansion in hypocotyls of *Arabidopsis* in grafting experiments (Ragni *et al.*, 2011). Upstream of GA, the transcription factor WOX14 may play an important role in vascular cell differentiation and lignification (Denis *et al.*, 2017). Thus, defects in *Arabidopsis* mutants with impaired WOX14 function were eliminated by exogeneous GA application, and overexpression of *WOX14* resulted in enhanced GA biosynthesis.

5.4.4 Other hormones

The effects on cambium regulation and formation of secondary growth tissues were further reported for ethylene, strigolactone and JA. Ethylene is involved in both, formation of tension wood and promotion of cambial cell divisions (Andersson-Gunnerås *et al.*, 2003; Love *et al.*, 2009; Etchells *et al.*, 2012). Ethylene, applied either as gaseous ethylene or in the form of the precursor aminocyclopropane-1-carboxylate (ACC), stimulated cambial cell proliferation and wood formation in *Populus* (Love *et al.*, 2009). Furthermore, overexpression of *ACC oxidase*, encoding the enzyme involved in the conversion of ACC to ethylene, resulted in transgenic *Populus* trees with enhanced cambial cell divisions and secondary xylem formation. Etchells *et al.* (2012) demonstrated ethylene to be involved in the regulation of cell divisions during vascular development using *Arabidopsis* as model organism. *Arabidopsis* plants with a loss-of-function mutations in *ETHYLENE RESPONSE FACTOR* (*ERF*) genes displayed reduced number of vascular cells during primary and secondary growth. In addition, the *ethylene overproducer 1* (*eto1*) mutant exhibited an enhanced cambial proliferation in hypocotyls and inflorescence stems.

In a study using *Arabidopsis*, strigolactone was reported to promote cambial activity and secondary growth in inflorescence stems by local application of GR24, a synthetic strigolactone analog (Agusti *et al.*, 2011). Moreover, *Arabidopsis* mutants with impaired strigolactone signaling or biosynthesis had reduced cambium-initiated secondary growth. Interestingly, auxin signaling may influence the regulatory effect of strigolactone on meristematic activity of the vascular cambium. Strigolactone activity is tightly linked to the auxin signaling pathway and the expression of strigolactone biosynthesis genes, *MORE AXILLARY BRANCHES 3* (*MAX3*) and (*MAX4*), is up-regulated by auxin (Hayward *et al.*, 2009; Waldie *et al.*, 2014).

Sehr *et al.* (2010) demonstrated a stimulatory role for JA signaling in secondary growth, using histological, molecular and genetic approaches. In *Arabidopsis*, JA application resulted in an increase of interfascicular cambium, cell wall thickening of xylem tissues and production of phloem fibers.

Furthermore, mutants with impaired function of the *JASMONATE ZIM-DOMAIN10* (*JAZ10*) and *JAZ7* genes, the repressors of JA signaling, exhibited a significant increase in longitudinal interfascicular cambium extension. Interestingly, JA biosynthesis and signaling genes were up-regulated in a transcriptome analysis during secondary growth in the woody genotype of *Arabidopsis*, *suppressor of overexpression of constans 1* (*soc1*) *fruitfull* (*ful*) loss-of-function double mutant (Melzer *et al.*, 2008; Davin *et al.*, 2016). Both genes, *SOC1* and *FUL*, encode MADS-box flowering time transcription factors. Knock-out of these genes in *Arabidopsis* results in a shrubby phenotype, accompanied by increased production of woody tissue.

5.5 Storage organs, storage tissues, and storage compounds

Secondary growth is coupled with nutrient allocation. Tissues produced during secondary growth represent a potential storage site for directing a variety of diverse energy-rich compounds therein. Due to the presence of remarkably advanced secondary growth in stems and clearly traceable seasonal cycling of stored resources, extensive investigations regarding storage were performed using different tree species in the past decades. A special feature of deciduous trees is the nutrient allocation from senescing leaves and subsequent storage in stems for rapid production of new tissues in spring, independent from available resources and nutrient uptake (Millard and Grelet, 2010; Rennenberg and Schmidt, 2010). Here, small branches are used for seasonal storage, while large branches and tree stems serve as decadal storage sites (Hartmann and Trumbore, 2016). Nutrients transported from senescing leaves are stored in bark parenchyma, wood ray, and pith cells as carbon (C)-containing metabolites, such as carbohydrates and lipids (Sauter and Kloth, 1987; Sauter and van Cleve, 1989, Sauter and van Cleve, 1994; Sauter and Wellenkamp, 1998), nitrogen (N)-containing compounds, including mainly proteins and amino acids (Coleman *et al.*, 1991; Gessler *et al.*, 1998; Cooke and Weih, 2005; Millard and Grelet, 2010; Wildhagen *et al.*, 2010), glutathione and sulfate for sulfur (S) (Herschbach and Rennenberg, 1996; Dürr *et al.*, 2010; Herschbach *et al.*, 2012; Malcheska *et al.*, 2013), and phosphorus (P), represented by phosphate (P_i) and organic-bound P_i (Netzer *et al.*, 2017; Netzer *et al.*, 2018).

Among the above-described storage compounds, C-containing metabolites, such as sugars, starch, and lipids, comprise probably the greatest pool of stored resources in plants. Principal metabolites involved in carbohydrate storage in vegetative tissues are either starch, sucrose or sucrose derivatives (Scofield *et al.*, 2009). Sugars and starch are summarized under the term non-structural carbohydrates (NSCs) and are present in the cytosol of cells, plastids, vacuoles, and apoplast (Secchi and Zwieniecki, 2016). In woody plants, long-term storage of extensive amounts of NSCs occurs in amyloplasts of ray and axial parenchyma cells (Furze *et al.*, 2018). Seasonal variation was present for NSC levels in stems of several tree species excluding poplar, with higher concentrations in the growing season and lower in the dormant period (Richardson *et al.*, 2013). Contrary to that, NSC amounts increased during dormancy in wood and bark tissues of poplar (Sauter and van Cleve, 1994; Sauter and Wellenkamp, 1998; Watanabe *et al.*, 2018). In addition, the C storage pool of deciduous trees was

reported to contain triacylglycerol (TAG) in lipid bodies (LBs) accumulated in bark and wood (Sauter and van Cleve, 1994; Watanabe *et al.*, 2018). Here, amounts of lipids were enhanced in autumn and during dormancy and declined in spring.

N and S storage in the form of proteins, amino acids arginine, histidine, tyrosine and ornithine, sulfate, and glutathione occurred in poplar plants in bark and wood of stems during dormancy, while remobilization of both nutrients for leaf development took place in spring after bud break (Dürr *et al.*, 2010; Wildhagen *et al.*, 2010; Malcheska *et al.*, 2013; Watanabe *et al.*, 2018). Interestingly, N availability strongly influences C metabolism. N deficiency is known to induce accumulation of C-containing metabolites in plants, generally in the form of starch, fructan, and other soluble carbohydrates (Wang and Tillberg, 1996; Scheible *et al.*, 1997; Wang *et al.*, 2000; Ruuska *et al.*, 2008).

Beside N and S, P represents another essential nutrient involved in plant growth and development (Lambers and Plaxton, 2018; Lang *et al.*, 2016). Plants rely on the stored P-containing resources under growth-limiting conditions, such as P-impoverished soils. Beech trees of Tuttlingen forest, which are exposed to growing conditions on P-depleted soil, provide an example of an efficient P storage in stems (Netzer *et al.*, 2018). Here, P storage pools in bark were marked by enhanced accumulation of phospholipids and glucosamine-6-phosphate, while N-acetyl-D-glucosamine-6-phosphate was stored in wood tissues. P stored in this way in tree stems contributed to P cycling during annual growth. P accumulation in bark and wood tissues occurred during dormancy, while its mobilization took place in spring (Netzer *et al.*, 2017).

The above-described examples regarding storage tissues and storage compounds relate to tree species. But how do storage pools look like in the case of perennial herbaceous plant species and which storage tissues/organs are involved? Many reports exist also here.

In order to sustain perennial life cycle, herbaceous plants evolved a diversity of perennating storage structures. These include specialized carbohydrate and N-storing underground organs, such as xylopodia, rhizophores, rhizomes, tubers, bulbs, and tuberous roots (de Moraes *et al.*, 2016). Potato tubers accumulating starch and storage proteins are probably one of the most prominent examples regarding such underground organs (Visser *et al.*, 1994; Hartmann *et al.*, 2011). Furthermore, parenchyma tissues of rhizophores and tuberous roots store starch and fructans in some herbaceous species of *Asteraceae*, *Dioscoreaceae*, *Smilacaceae*, *Amaranthaceae*, and *Bixaceae* (Isejima *et al.*, 1991; Vieira and Figueiredo-Ribeiro, 1993; Carvalho and Dietrich, 1996; Hayashi and Appezzato-da-Glória, 2005; Carvalho *et al.*, 2007; Appezzato-da-Glória *et al.*, 2008; Silva *et al.*, 2013). Interestingly, high levels of lipids accumulate in the underground tubers of yellow nutsedge, the only plant species known so far to accumulate high amounts of oils in tubers (Linssen *et al.*, 1989). In addition, N storage in the form of proteins occurs in the underground reserve organs of several *Fabaceae* species (Figueiredo-Ribeiro *et al.*, 1986).

However, long-term storage tissues in herbaceous species occur not only in the underground organs, but also in the above-ground vegetative plant segments. Here, *Tetraena mongolica*, an endemic

species from western Mongolia, represents an example of starch and TAG-containing LB storage in phloem and xylem parenchyma of stems, which is considered to be a C supply for the development of new shoots in the next growth period (Wang *et al.*, 2007). Another example includes *Oxytropis sericea*. Branches of this alpine perennial leguminous herb accumulate NSCs in the fall (Wyka, 1999). Levels of accumulated NSCs decrease during winter and reach minimal amounts after growth initiation in spring.

In general, plants store resources to support growth after the dormant period/for the next growth cycle (Cyr *et al.*, 1990; Millard and Grelet, 2010; Wildhagen *et al.*, 2010), to recover from damage (Wyka, 1999; Scheidel and Bruelheide, 2004), and to integrate compounds that are in excess (Servaites *et al.*, 1989; Li *et al.*, 1992). Various tissues serve as long-term storage sites for a diverse set of metabolites. However, the prominent role of long-term storage in plants is attributed to high-energy C compounds, starch and lipids, which will be described in more detail in the following sections.

5.5.1 Starch

Generally, starch in plant cells functions as a dense, osmotically inert sugar reserve for growth and development when photosynthesis is absent or limited (Smith and Zeeman, 2020). Plants are prevented from photosynthesis at night, after damage, during seed germination, and during bud outgrowth following the dormant period. Based on its biological function, this non-structural carbohydrate is defined as transitory starch or storage starch.

Semi-crystalline starch granules with diameters between 1-100 µm are composed of two glucose polymers, amylopectin and amylose (Pérez and Bertoft, 2010). The branched molecule amylopectin consists of groups of linear chains of α-1,4-linked glucose residues connected to branch regions by α-1,6 linkages. Amylose is composed of long α-1,4-linked glucose units with few branch points. In general, amylose fraction in starches of leaves amounts to 10 %, while starch in storage organs may contain 20-30 % (Smith and Zeeman, 2020). While amylopectin forms the structural framework of the granule, amylose is considered to fill spaces within the amylopectin-shaped matrix.

5.5.1.1 Starch biosynthesis

The pathway of starch biosynthesis is initiated by the plastid-localized enzyme adenosine diphosphate (ADP) glucose pyrophosphorylase (AGPase), catalyzing production of the glucose donor ADP-glucose (Figure 3) (Smith and Zeeman, 2020). Glucose 1-phosphate, the substrate for AGPase, derives from the Calvin-Benson cycle in chloroplasts (Fettke *et al.*, 2011; Stitt and Zeeman, 2012). In amyloplasts of non-photosynthetic tissues, hexose phosphates have to be first imported from the cytosol (Flügge *et al.*, 2011). Synthesis of starch polymers from ADP-glucose includes the cooperative and simultaneous action of three enzymes, starch synthases (SSs), starch-branching enzymes (SBEs), and debranching enzymes (DBEs) (Figure 3). SSs transfer the glucosyl moiety from ADP-glucose to non-reducing ends of glucose chains at the surface of the starch granule, creating an α-1,4 glucosidic bond. Branching and thus generation of an α-1,6 linkage within the structure of glucose chains is introduced

by SBEs. SBEs transfer terminal parts consisting of several glucoses to the same or a neighboring chain. The importance of SBEs for the branching structure of amylopectin was confirmed in studies using potato, maize, and rice (Schwall *et al.*, 2000; Blauth *et al.*, 2002; Satoh *et al.*, 2003). Impaired function of SBE isoforms severely altered amylopectin structure affecting the chain length of branches in mutant plants. DBEs are involved in the selective removal of extraneous branches of the synthesized molecules via hydrolysis of α-1,6 linkages (Smith and Zeeman, 2020). Significance of debranching in amylopectin synthesis was supported in studies with *Arabidopsis*, potato, cereals, and *Chlamydomonas* mutants deficient in isoforms of isoamylase 1 (ISA1) type (James *et al.*, 1995; Delrue and Ball, 1996; Bustos *et al.*, 2004; Delatte *et al.*, 2005). Impaired function of DBE ISA1 resulted in formation of highly branched glucans. This fraction remained soluble and lost competency to crystallize into a granular form.

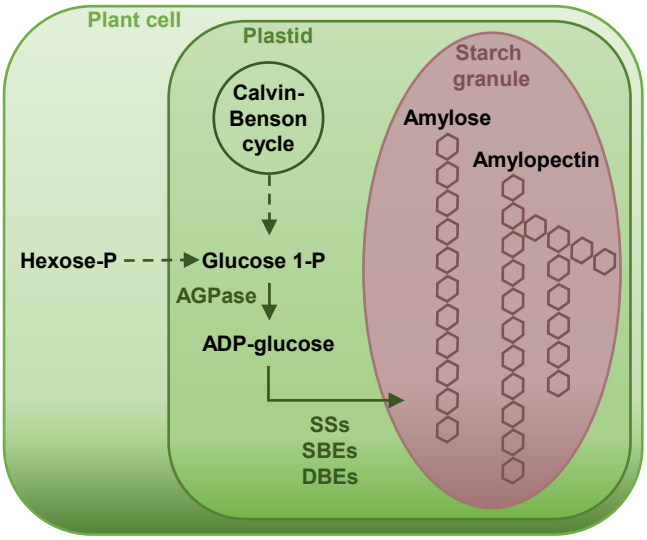

Figure 3. Pathway of starch biosynthesis. In a photosynthetic cell, fructose 6-P, deriving from the Calvin-Benson cycle, is converted to glucose 1-P in the plastid. In non-photosynthetic cells, hexose-Ps are imported into the plastid from the cytosol. The AGPase catalyzes conversion of glucose 1-P to ADP-glucose. Starch is synthesized from ADP-glucose via simultaneous activity of three enzymes, SSs, SBEs, and DBEs. Steps that are not shown are indicated by dashed lines. Abbreviations: ADP, adenosine diphosphate; AGPase, ADP glucose pyrophosphorylase; DBE, debranching enzyme; P, phosphate; SBE, starch-branching enzyme; SS, starch synthase. The schematic illustration was partially adopted from Smith and Zeeman (2020).

The described pathway of starch biosynthesis is well conserved among plant species, indicating a common origin (Deschamps *et al.*, 2008). Differences among species and organs may rather be related to starch mobilization. Starch mobilization and the mechanism behind starch turnover is well studied in *Arabidopsis* leaves, but poorly investigated until now in other species and in diverse organs.

5.5.1.2 Starch mobilization

In *Arabidopsis* leaves, biosynthesis of transitory starch and mobilization follow a diurnal cycle and involve the circadian clock. Sucrose and starch are synthesized during the day. During the night, almost all starch is converted to sucrose to maintain metabolism in the absence of photosynthesis. Hydrolytic enzymes, exoamylase β-amylase and DBE isoamylase, are involved in starch degradation predominantly yielding the disaccharide maltose (Figure 4) (Smith and Zeeman, 2020). β-amylase cleaves α-1,4 linkages, while isoamylase is responsible for cleavage of α-1,6 linkages. Knockout mutants in isoforms of β-amylase had elevated starch levels in comparison to wild type (Fulton *et al.*, 2008). DBEs involved in starch mobilization, ISOAMYLASE 3 (ISA3) and limit dextrinase (LDA), differ from debranching enzymes participating in starch biosynthesis (Delatte *et al.*, 2006). Similar to

reports regarding β-amylase, starch contents and soluble branched glucans were increased in *isa3 lda* double mutants. In addition, the organization of amylopectin molecules at the surface of the granule is essential for starch degradation. Two sets of enzymes, glucan, water dikinase (GWD/STARCH EXCESS 1 (SEX1)) and phosphoglucan, water dikinase (PWD), alter organization of amylopectin by phosphorylation and dephosphorylation of glucose units, thus enabling hydrolytic enzymes to access the granule (Figure 4) (Yu *et al.*, 2001; Baunsgaard *et al.*, 2005; Kötting *et al.*, 2005; Edner *et al.*, 2007; Blennow and Engelsen, 2010).

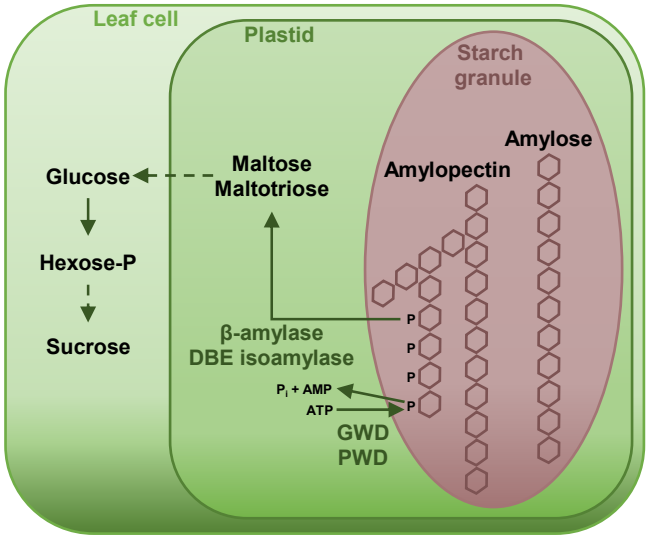

Figure 4. Pathway of starch mobilization. GWD and PWD alter organization of amylopectin by phosphorylation and dephosphorylation events. Thus, hydrolytic enzymes, β-amylase and DBE isoamylase, are enabled to access the granule. Hydrolysis, catalyzed by β-amylase and DBE isoamylase, results in production of maltose and maltotriose. Maltotriose is further metabolized to yield glucose. Maltose and glucose are transported to the cytosol, where they are converted in several steps to sucrose. Steps that are not shown are indicated by dashed lines. Abbreviations: AMP, adenosine monophosphate; ATP, adenosine triphosphate; DBE, debranching enzyme; GWD, glucan, water dikinase; P, phosphate; P_i, inorganic phosphate; PWD, phosphoglucan, water dikinase. The schematic illustration was partially adopted from Smith and Zeeman (2020).

Despite photosynthetically active leaves, accumulation and mobilization of starch occurs in many non-photosynthetic plant tissues, as already described above for trees and several perennial herbaceous species. This accumulation of starch is regarded as long-term storage starch. In annual *Arabidopsis*, the corresponding storage tissues comprise embryos, testas, stems, root columella, petals, anthers, and pollen (Caspar *et al.*, 1991). Studies with mutants in components of the starch metabolism mechanism, described above, revealed alterations in starch levels in non-photosynthetic tissues of *Arabidopsis* (Caspar *et al.*, 1985; Andriotis *et al.*, 2010; Feike *et al.*, 2016). This indicates that enzymes of starch metabolism playing a role in leaves may also be involved in other compartments of the plant (Smith and Zeeman, 2020). However, the mechanism of starch degradation described for *Arabidopsis* leaves may indeed also function in reserves laid down in other plant species. This is supported by the presence of transcripts corresponding to elements of the leaf starch mobilization pathway of *Arabidopsis* in cambium and wood of tree stems (Hoffman *et al.*, 2010; Resman *et al.*, 2010; Berrocal-Lobo *et al.*, 2011). However, the difference between the annual *Arabidopsis* and perennial plant species may concern here the regulation occurring not only in a diurnal but also in a seasonal manner.

5.5.2 Lipids

Starch is an efficient and compact form of stored energy in plants. However, lipids represent another alternative. In comparison to starch, lipid reserves provide more than twice the energy per weight (Pfister *et al.*, 2020). Plants store lipids predominantly as TAG in specialized compartments, the so-called LBs/lipid droplets (LDs). LBs were reported to be present in oilseeds of diverse plant species (Cao and Huang, 1986; Loer and Herman, 1993; Lee *et al.*, 1995; Lacey *et al.*, 1999; Shockey *et al.*, 2006; Cai *et al.*, 2017), but also in vegetative tissues, such as roots (Næsted *et al.*, 2000; Chinnasamy *et al.*, 2003), stems (Sauter and Cleve, 1994; Madey *et al.*, 2002; Wang *et al.*, 2007), and leaves (Pyc *et al.*, 2017; Brocard *et al.*, 2017). In addition to the storage function, lipids play key roles in the general plant metabolism, including membrane remodeling and lipid signaling. Lipid composition is a key for membrane identity of cells and cellular organelles. Here, predominant constituents of the plasma membrane are phosphoglycerolipids (Simon, 1974; Wewer *et al.*, 2011), while chloroplast thylakoid membranes contain primarily galactoglycerolipids (Hurlock *et al.*, 2014; LaBrant *et al.*, 2018; Karki *et al.*, 2019). In order to produce energy, fatty acids (FAs) from both, storage and membrane lipids, are subjected to catabolic processes occurring in peroxisomal β-oxidation pathway.

5.5.2.1 Lipid bodies

LBs are composed of a core of neutral lipids (NLs) (mainly TAG, but also steryl/wax esters) surrounded by a phospholipid (PL) monolayer with various surface-associated proteins (Thiam *et al.*, 2013; Ohsaki *et al.*, 2014; Huang, 2018). Thus, key functions of these cell compartments are energy and C supply for plant metabolism, as well as lipid provision for membrane biosynthesis. Formation and budding of LBs occurs on the endoplasmic reticulum (ER), which is promoted here by enzymes involved in TAG biosynthesis (Walther *et al.*, 2017). Synthesized TAG is sequestered in the hydrophobic area of the PL bilayer, finally resulting in budding. Depending on the cell type, developmental stage, and growth conditions, LBs released into the cytoplasm may differ in size, shape, and mobility (Pyc *et al.*, 2017).

Current knowledge on LBs mainly derives from studies on oilseeds. However, investigations using vegetative tissues from various plant species and green algae hint to their additional involvement in diverse physiological processes, which mainly occurs due to the presence of a group of proteins within the LB structure. LB proteins can be categorized depending on their single, dual or multiple functions (Huang, 2018). These comprise structural, enzymatic, membrane protein trafficking, and signaling roles, as well as use of LB surface as a platform for other cellular processes. In plant seeds, oleosin represents the most abundant structural protein involved in stabilization, formation, and turnover of LBs (Huang, 1996; Schmidt and Herman, 2008; Shimada *et al.*, 2008; Miquel *et al.*, 2014). LBs are predominantly involved in metabolic processes due to enzymatic activities and binding characteristics of two sets of proteins, caleosin/dioxygenase/steroleosin and LD-associated proteins (LDAPs)/oil body (OB)-associated proteins. Enzymatic activity of caleosin, dioxygenase, and

steroleosin results in products which are related to stress responses. Caleosin has a peroxygenase activity and catalyzes conversion of hydroperoxides of α-linolenic acid to different oxylipins functioning as phytoalexins (Hanano *et al.*, 2006; Blée *et al.*, 2014). Dioxygenase was extensively studied in relation to pathogen and senescence-induced response (Sanz *et al.*, 1998; Marcos *et al.*, 2015). Dioxygenase may catalyze production of oxylipins for defense of abiotic and biotic stresses together with caleosin (Shimada and Hara-Nishimura, 2015). Steroleosin belongs to the family of hydroxysteroid dehydrogenases and is involved in the production of brassinosteroids from sterol substrates (Lin *et al.*, 2002; Zhang *et al.*, 2016).

An abundant occurrence in non-seed cell types was recently reported for LDAPs (Gidda *et al.*, 2016). LDAPs appear to be involved in drought stress in *Arabidopsis* (Kim *et al.*, 2016). Moreover, LDAP3 influences LB morphology and contents of NLs in seeds through an interaction with a plant-specific protein of unknown function, exhibiting an LB targeting signal (Pyc *et al.*, 2017). LB amounts are enhanced under N-deprived conditions in green algae and in leaves of higher plants (Tsai *et al.*, 2015; Brocard *et al.*, 2017). Furthermore, plastoglobuli, a specific type of LBs deriving from plastids, were proposed to be involved in abiotic stress response and developmental transitions (van Wijk and Kessler, 2017). In addition, LBs were reported to function in cytoplasmic signaling (van der Schoot *et al.*, 2011).

Catabolism of LBs is driven by two major mechanisms (Poxleitner *et al.*, 2006; Barbosa and Siniossoglou, 2017; Walther *et al.*, 2017). The first includes lipolysis catalyzed by a lipase on the surface of LBs. In the second pathway, LBs are recycled via autophagy or by vacuoles. SUGAR-DEPENDENT 1 (SDP1) and its related SDP1-LIKE are lipases involved in hydrolysis of LB-derived TAG (Eastmond, 2006). In *Arabidopsis*, SDP1 exhibits a broad substrate specificity regarding different FAs and its transcript is ubiquitously present in various organs (Eastmond, 2006; Kelly *et al.*, 2013).

Taken together, LBs represent not solely inert energy stores, but additionally have a broad range of functions in diverse physiological processes.

5.5.2.2 Biosynthesis of glycerolipids

Glycerolipids play key roles in plant metabolism. As mentioned above, TAG, consisting of a glycerol backbone and three FAs, functions as a source of energy stored in LBs in plants. Further examples for glycerolipids include phosphoglycerolipids and galactoglycerolipids, which are major constituents of plant membranes. The plasma membrane contains primarily phosphoglycerolipids, such as phosphatidylcholine and phosphatidylethanolamine (Simon, 1974; Wewer *et al.*, 2011). Predominant constituents of the chloroplast thylakoid membranes are galactoglycerolipids (hereafter termed glycolipids (GLs)), monogalactosyldiacylglycerol and digalactosyldiacylglycerol (Hurlock *et al.*, 2014; LaBrant *et al.*, 2018; Karki *et al.*, 2019). Similar to PLs, digalactosyldiacylglycerol is a bilayer-forming lipid. Therefore, digalactosyldiacylglycerol can replace PLs in membranes during P-limited conditions,

thus ensuring membrane homeostasis (Härtel *et al.*, 2000; Andersson *et al.*, 2003; Jouhet *et al.*, 2004; Andersson *et al.*, 2005).

Biosynthesis pathways of different lipid classes are interconnected. In plant tissues, lipids are synthesized in the prokaryotic pathway in the chloroplast and in the eukaryotic pathway in the ER (Figure 5) (Li-Beisson *et al.*, 2013; Jayawardhane *et al.*, 2018). Chloroplast lipid synthesis relies on diacylglycerol backbones that derive from both, prokaryotic and eukaryotic pathway (Ohlrogge and Browse, 1995; Li-Beisson *et al.*, 2013). Phosphatidic acid, the precursor of GLs and also PLs, is transformed to phosphatidylglycerol on the inner chloroplast envelope (Li-Beisson *et al.*, 2013) or dephosphorylated to diacylglycerol by phosphatidate phosphatase (PP) (Figure 5) (Carman, 1997; Ohlrogge and Browse, 1995). The transfer of a galactose moiety from UDP-galactose to diacylglycerol or monogalactosyldiacylglycerol, catalyzed by two distinct galactosyltransferases in the inner or outer envelope, results in the synthesis of GLs (Kelly and Dörmann, 2004; Andersson and Dörmann, 2008).

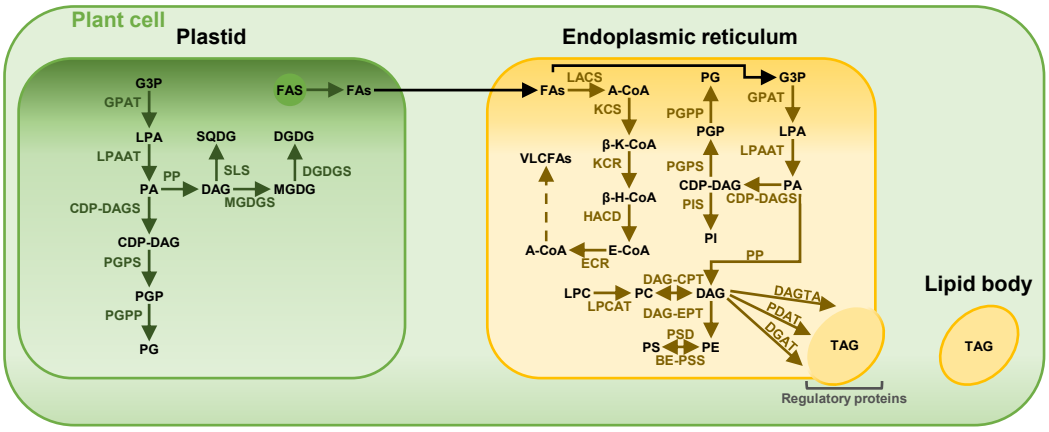

Figure 5. Overview of prokaryotic and eukaryotic glycerolipid biosynthesis pathways in the plastid and in the endoplasmic reticulum. Abbreviations: A-CoA: acyl-CoA; β-K-CoA: β-ketoacyl-CoA; BE-PSS: base-exchange-type phosphatidylserine synthase; CDP-DAGS: CDP-DAG synthase; CoA: coenzyme A; DAG: diacylglycerol; DAGTA: diacylglycerol transacylase; DAG-CPT: CDP-choline:diacylglycerol cholinephosphotransferase; DAG-EPT: CDP-ethanolamine:diacylglycerol cholinephosphotransferase; DGAT: diacylglycerol acyltransferase; DGDG: digalactosyldiacylglycerol; DGDGS: digalactosyldiacylglycerol transferase; E-CoA: enoyl-CoA; ECR: enoyl-CoA reductase; FAS: fatty acid synthase; FAs: fatty acids; G3P: glycerol 3-phosphate; GPAT: glycerol-3-phosphate acyltransferase; HACD: hydroxyacyl-CoA dehydratase; KCR: ketoacyl-CoA reductase; KCS: 3-ketoacyl-CoA synthase; LACS: long-chain acyl-CoA synthetase; LPA: lysophosphatidic acid; LPAAT: lysophosphatidic acid acyltransferase; LPC: lysophosphatidylcholine; LPCAT: lysophosphatidylcholine acyltransferase; MGDG: monogalactosyldiacylglycerol; MGDGS: monogalactosyldiacylglycerol transferase; PA: phosphatidic acid; PC: phosphatidylcholine; PDAT: phospholipid:diacylglycerol acyltransferase; PE: phosphatidylethanolamine; PG: phosphatidylglycerol; PGP: phosphatidylglycerol phosphate; PGPP: phosphatidylglycerol phosphate phosphatase; PGPS: phosphatidylglycerol phosphate synthase; PI: phosphatidylinositol; PIS: PI synthase; PP: phosphatidate phosphatase; PS: phosphatidylserine; PSD: phosphatidylserine decarboxylae; SLS: sulfolipid synthase; SQDG: sulfoquinovosyldiacylglycerol; TAG: triacylglycerol; VLCFAs: very long-chain fatty acids. Steps that are not shown are indicated by dashed lines. Adopted from Li-Beisson *et al.* (2013).

PL synthesis takes place in the ER (Li-Beisson *et al.*, 2013). Phosphatidic acid is produced in the reactions involving acyl-CoA:glycerol-3-phosphate acyltransferase (GPAT) and acyl-

CoA:lysophosphatidic acid acyltransferase (LPAAT) (Figure 5). Phosphatidylinositol is further synthesized from *myo*-inositol and CDP-diacylglycerol, the conversion product of phosphatidic acid, via phosphatidylinositol synthases (PIS) (Xue *et al.*, 2000; Löfke *et al.*, 2008). Phosphatidylglycerol synthesis occurs via phosphatidylglycerol phosphate synthase (PGPS) and phosphatidylglycerol phosphate phosphatase (PGPP). PGPS catalyzes the conversion of CDP-diacylglycerol and glycerol-3-phosphate to phosphatidylglycerol phosphate. Subsequently, PGPP participates in dephosphorylation of phosphatidylglycerol phosphate to produce phosphatidylglycerol (Müller and Frentzen, 2001; Hagio *et al.*, 2002; Xu *et al.*, 2002).Diacylglycerol, deriving from phosphatidic acid, can be used for TAG biosynthesis (Han *et al.*, 2006) or converted to phosphatidylcholine and phosphatidylethanolamine in the reactions with CDP-choline and CDP-ethanolamine respectively. In addition, phosphatidylethanolamine can be synthesized via phosphatidylserine decarboxylation pathway (Li-Beisson *et al.*, 2013).

Biosynthesis of TAG takes place in the ER in the *Kennedy* or *glycerol phosphate pathway*. Some of its steps are common to the already described synthesis of membrane lipids (Figure 5) (Li-Beisson *et al.*, 2013). A GPAT is involved in the acylation of glycerol-3-phosphate in the first step (Zheng *et al.*, 2003; Beisson *et al.*, 2007), followed by a second acylation catalyzed by an LPAAT (Kim and Huang, 2004; Kim *et al.*, 2005). The second acylation results in the formation of phosphatidic acid. To produce diacylglycerol, phosphatidic acid is dephosphorylated by PP (Nakamura *et al.*, 2009; Eastmond *et al.*, 2010). Therefore, diacylglycerol is an important intermediate for the synthesis of storage and membrane lipids. A third acylation reaction is specific for TAG biosynthesis and three processes, varying in the acyl donor origin identified so far, are involved in this step (Li-Beisson *et al.*, 2013). In one of these reactions, an acyl-CoA molecule is acylated to diacylglycerol via the activity of a diacylglycerol acyltransferase (DGAT) (Katavic *et al.*, 1995; Routaboul *et al.*, 1999; Zou *et al.*, 1999; Saha *et al.*, 2006; Yen *et al.*, 2008). Acyl moieties also derive from phosphatidylcholine in order to acylate diacylglycerol via the activity of a phospholipid:diacylglycerol acyltransferase (PDAT) (Dahlqvist *et al.*, 2000; Ståhl *et al.*, 2004; Zhang *et al.*, 2009). Moreover, the importance of phosphatidylcholine in TAG biosynthesis is stressed by the additional desaturation of FAs on phosphatidylcholine itself (Ohlrogge and Jaworski, 1997). Dependency between the phosphatidylcholine pool and the TAG synthesis was supported in studies using *Arabidopsis* mutants impaired in PDAT function (Zhang *et al.*, 2009). The TAG content decreased dramatically in seeds of mutant plants. According to investigations with safflower seeds, the third possible mechanism of the last acylation reaction of diacylglycerol was hypothesized to involve a diacylglycerol:diacylglycerol transacylase (Stobart *et al*., 1997).

The nature of FAs of glycerolipids is indicative for their function and for the lipid species. For example, GLs of chloroplasts consist to a large extent of trienoic FAs (Moreau *et al.*, 1998; Andersson and Dörmann, 2008). The abundant FAs of TAG have chain lengths of 18 and 20 carbons with one to three double bonds (Chapman and Ohlrogge, 2012; Bates *et al.*, 2013). Interestingly, senescing

Arabidopsis leaves accumulate TAG enriched in 16:3 and 18:3 FAs. These FAs usually occur in GLs of thylakoids (Kaup *et al.*, 2002). The observed TAG accumulation was suggested to be related to sequestration of free FAs deriving from the breakdown of thylakoid membranes.

The *De novo* FA synthesis takes place in the plastid in reactions catalyzed by enzymes of the FA synthase complex (Figure 5) (Li-Beisson *et al.*, 2013). FAs produced in the plastid are transported to the ER. In the ER, they can be either subjected to the FA elongase complex or to the esterification of glycerol-3-phosphate to form glycerolipids. The FA elongase complex involves four enzymatic activities in order to produce very long-chain fatty acids (VLCFAs) (Figure 5) (Joubès *et al.*, 2008).

5.5.2.3 Fatty acid β-oxidation

Mobilization of glycerolipid-derived FAs is required to provide building blocks and energy for plant metabolic processes. FAs are subjected to peroxisomal β-oxidation in order to be degraded (Figure 6) (Li-Beisson *et al.*, 2013). FA β-oxidation consists of a repetitive oxidation spiral. In each cycle, one acetyl-CoA unit (C_2) is cleaved from an acyl-CoA chain (C_n) and the oxidation spiral is repeated resulting in acyl-CoA (C_{n-2}). This four-step process comprises reactions catalyzed by three enzymes, acyl-CoA oxidase (ACX), multifunctional protein (MFP), and 3-ketoacyl-CoA thiolase (KAT). Two different strategies had evolved in order to enable the enzymes to convert substrates with decreasing chain length in each round of the core β-oxidation pathway. These include multiple isoforms specific to differing chain length and enzymes accepting a broad range of substrates.

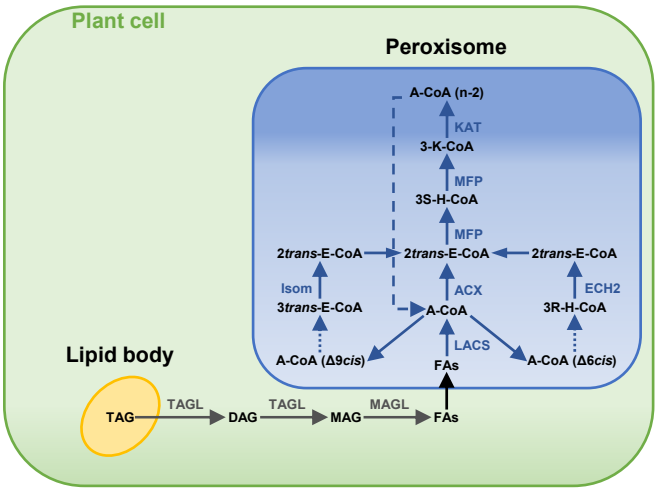

Figure 6. Overview of fatty acid β-oxidation in the peroxisome. Degradation of FAs deriving from the hydrolysis of TAG contained in the lipid body is represented. Abbreviations: A-CoA: acyl-CoA; ACX: acyl-CoA thioesterase; 3R/3S-H-CoA: 3R/3S-hydroxyacyl-CoA; 3-K-CoA: 3-ketoacyl-CoA; CoA: coenzyme A; DAG: diacylglycerol; E-CoA: enoyl-CoA; FAs: fatty acids; Isom: isomerase; KAT: 3-ketothiolase; LACS: long-chain acyl-CoA synthetase; MAG: monoacylglycerol; MAGL: monoacylglycerol lipase; MFP: multifunctional protein; TAG: triacylglycerol; TAGL: triacylglycerol lipase; Acyl-CoA chains with a *cis* double bond on an even-numbered carbon are exemplified by Δ6*cis*, while fatty acids with *cis* double bonds at odd-numbered positions are exemplified by Δ9*cis*. Steps that are not shown are indicated by small dashed arrows. The repetitive oxidation spiral is indicated by the big dashed arrow. Adopted from Li-Beisson *et al.* (2013).

In the first step of β-oxidation, ACXs catalyze the conversion of activated acyl-CoA to 2-trans-enoyl-CoA (Figure 6). In *Arabidopsis*, six ACX genes have been identified (Adham *et al.*, 2005; Graham, 2008). Thus, rapid catabolism of TAG-derived FAs during seed germination and early postgerminative development in *Arabidopsis* was reported to correlate with upregulated gene expression of *ACX1*, *ACX2*, *ACX3* and *ACX4* (Rylott *et al.*, 2001).

Second and third reaction of the core β-oxidation pathway, 2-trans-enoyl-CoA hydratase and L-3-hydroxyacyl-CoA dehydrogenase, involve MFP (Figure 6) (Graham, 2008). Two isoforms of MFP are present in *Arabidopsis*, ABNORMAL INFLORESCENCE MERISTEM 1 (AIM1) and MFP2 (Richmond and Bleecker, 1999; Eastmond and Graham, 2000). MFP2 involvement in storage oil breakdown was supported in studies with *A. thaliana* T-DNA insertion mutants (Rylott *et al.*, 2006). Catabolism of storage lipids occurred more slowly in *mfp2* mutant seedlings than in wild type.

The final reaction of the oxidation cycle is catalyzed by KAT (Figure 6). KAT is involved in the thiolytic cleavage of 3-ketoacyl-CoA to acyl-CoA and acetyl-CoA (Li-Beisson *et al.*, 2013). Three loci encode KAT enzymes, KAT1, KAT2, and KAT5, in the genome of *Arabidopsis* (Carrie *et al.*, 2007). LB-derived TAG breakdown was hindered in *kat2* mutant *Arabidopsis* seedlings (Germain *et al.*, 2001).

Unsaturated FAs with *cis* double bonds at even-numbered or odd-numbered positions on the carbon chain have to undergo conversion reactions in the auxiliary β-oxidation pathway before they can enter the core oxidation spiral (Figure 6) (Li-Beisson *et al.*, 2013). FAs with a *cis* double bond on an even-numbered carbon can be processed either by an epimerase or ENOYL-COA HYDRATASE 2 (ECH2/hydratase) to 2-*trans*-enoyl-CoA, which then enters the core β-oxidation pathway (Schulz and Kunau, 1987; Goepfert *et al.*, 2006). FAs with *cis* double bonds at odd-numbered carbons are subjected to the auxiliary pathway involving isomerases (Goepfert *et al.*, 2005; Goepfert *et al.*, 2008).

Taken together, nutrient allocation to perennating storage tissues was not investigated so far in the perennial model species *A. alpina*. Thus, elucidation of the development of such tissues, examination of the accumulation and turnover of high-energy C compounds, starch and lipids, in these tissues, and uncovering of the regulation behind these processes will contribute greatly to the already obtained knowledge about the perennial growth habit of *A. alpina*. The development of perennial grain cropping systems may profit from these findings in the future.

6 Thesis Objectives

In recent years, *Arabis alpina* has been established as a model Brassicaceae species to study perennial traits. In previous studies, the perennial life-cycle of *A. alpina* was characterized using the vernalization-dependent accession Pajares (Paj) (Wang *et al.*, 2009; Wang *et al.*, 2011; Bergonzi *et al.*, 2013; Park *et al.*, 2017; Lazaro *et al.*, 2018; Hyun *et al.*, 2019; Vayssières *et al.*, 2020). The preceding research generally concentrated on non-simultaneous development of meristems regarding vegetative and reproductive growth. However, the resource allocation to putative perennating organs/tissues was not investigated in *A. alpina* so far. Lateral stems of Paj, which are formed prior to vernalization, can be subdivided into two different zones, when flowering occurs. The proximal vegetative zone with a dormant bud region and newly formed axillary branches is maintained after reproduction, while the distal seed-producing inflorescence zone senesces. The observed zonation pattern of lateral stems raised the following questions: (i) is this zonation related to the long-term nutrient storage, (ii) which signals affect this zonation, and (iii) do these signals confer perennial traits to *A. alpina*? In order to answer these questions, the following objectives of the thesis were formulated:

1. Identify long-term nutrient storage tissues and determine the abundant accumulated carbon (C) storage biopolymers in lateral stems of perennial *A. alpina*.

The anatomy of internode stem cross sections is inspected in vegetative and inflorescence zones at different growth stages with and without the prolonged cold treatment to identify long-term nutrient storage. In order to perform a detailed analysis of the development of stem tissues, the selected growth stages are distributed along a developmental gradient. To investigate the dependency on vernalization, the vernalization-independent mutant *A. alpina perpetual flowering 1-1* (*pep1-1*), a derivative of Paj, is included. Perennial lines, Paj and *pep1-1*, are compared to the annual sister species *A. montbretiana*. Deposition of C storage biopolymers, starch and lipids, is investigated in stem internodes by staining of tissue sections. Microscopic observations are supported by biochemical quantification. Fatty acid profiles, deriving from storage and membrane glycerolipids, are analyzed in more detail. Qualitative and quantitative analyses are performed to identify striking development and storage-related dissimilarities between the different stem zones as well as between perennial and annual species. The vegetative stem zone of perennial *A. alpina* is expected to accumulate high amounts of C-containing compounds in specified storage tissues.

2. Identify signals that differentiate between the vegetative and the inflorescence lateral stem zone and potentially confer perennial traits to *A. alpina*

Secondary growth-related formation of pronounced storage tissues in vegetative lateral stem internodes is identified in perennial Paj and *pep1-1*. The *pep1-1* mutant is used for further analyses, as the trait of secondary growth and nutrient storage occurs irrespective of differential flowering behavior. The

influence of hormones (cytokinin, auxin, gibberellin, and ethylene) on vascular cambium activity is tested by direct application either to juvenile vegetative or developing inflorescence stem internodes. To identify gene expression differences related to secondary growth and nutrient deposition between the vegetative and the inflorescence stem internodes, a gene expression profiling experiment using RNA sequencing is performed with *pep1-1*. To cover a broad range of possible developmental processes, the investigated stages comprise a juvenile, an adult vegetative, and an adult reproductive phase. Gene ontology enrichment analysis is performed to narrow down the search for putative candidate genes, demarcating the vegetative stem zone from the inflorescence. Candidates, which may represent targets of regulatory mechanisms specifying differentiation of the vegetative stem zone in *A. alpina*, are extracted for downstream analyses. The potential candidate genes are expected to be expressed at higher levels during development of the vegetative stem zone in comparison to the inflorescence.

References

Adham, A. R., Zolman, B. K., Millius, A., & Bartel, B. (2005). Mutations in Arabidopsis acyl-CoA oxidase genes reveal distinct and overlapping roles in beta-oxidation. *Plant J, 41*(6), 859-874.

Agusti, J., Herold, S., Schwarz, M., Sanchez, P., Ljung, K., Dun, E. A., Brewer, P. B., Beveridge, C. A., Sieberer, T., Sehr, E. M., Greb, T. (2011). Strigolactone signaling is required for auxin-dependent stimulation of secondary growth in plants. *Proc Natl Acad Sci U S A, 108*(50), 20242-20247.

Albani, M. C., Castaings, L., Wotzel, S., Mateos, J. L., Wunder, J., Wang, R.,Reymond, M., Coupland, G. (2012). PEP1 of Arabis alpina is encoded by two overlapping genes that contribute to natural genetic variation in perennial flowering. *PLoS Genet, 8*(12), e1003130.

Albani, M. C., & Coupland, G. (2010). Comparative Analysis of Flowering in Annual and Perennial Plants. In *Plant Development* (pp. 323-348).

Altamura, M. M., Possenti, M., Matteucci, A., Baima, S., Ruberti, I., & Morelli, G. (2001). Development of the vascular system in the inflorescence stem of Arabidopsis. *New Phytologist, 151*(2), 381-389.

Amasino, R. (2009). Floral induction and monocarpic versus polycarpic life histories. *Genome biology, 10*(7), 1-3.

Andersson, M., & Dörmann, P. (2008). Chloroplast membrane lipid biosynthesis and transport. In: Plant Cell Monographs. Springer, Berlin, Heidelberg.

Andersson, M. X., Larsson, K. E., Tjellstrom, H., Liljenberg, C., & Sandelius, A. S. (2005). Phosphate-limited oat. The plasma membrane and the tonoplast as major targets for phospholipid-to-glycolipid replacement and stimulation of phospholipases in the plasma membrane. *J Biol Chem, 280*(30), 27578-27586.

Andersson, M. X., Stridh, M. H., Larsson, K. E., Liljenberg, C., & Sandelius, A. S. (2003). Phosphate-deficient oat replaces a major portion of the plasma membrane phospholipids with the galactolipid digalactosyldiacylglycerol. *FEBS Letters, 537*(1-3), 128-132.

Andersson□Gunnerås, S., Hellgren, J. M., Björklund, S., Regan, S., Moritz, T., & Sundberg, B. (2003). Asymmetric expression of a poplar ACC oxidase controls ethylene production during gravitational induction of tension wood. *The Plant Journal, 34*(3), 339-349.

Andriotis, V. M., Pike, M. J., Kular, B., Rawsthorne, S., & Smith, A. M. (2010). Starch turnover in developing oilseed embryos. *New Phytol, 187*(3), 791-804.

Angel, A., Song, J., Dean, C., & Howard, M. (2011). A Polycomb-based switch underlying quantitative epigenetic memory. *Nature, 476*(7358), 105-108.

Ansell, S. W., Stenoien, H. K., Grundmann, M., Russell, S. J., Koch, M. A., Schneider, H., & Vogel, J. C. (2011). The importance of Anatolian mountains as the cradle of global diversity in Arabis alpina, a key arctic-alpine species. *Ann Bot, 108*(2), 241-252.

Appezzato-da-Glória, B., Cury, G., Kasue Misaki Soares, M., Rocha, R., & Hissae Hayashi, A. (2008). Underground systems of Asteraceae species from the Brazilian Cerrado1. *The Journal of the Torrey Botanical Society, 135*(1), 103-113.

Asami, T., & Nakagawa, Y. (2018). Preface to the Special Issue: Brief review of plant hormones and their utilization in agriculture. *J Pestic Sci, 43*(3), 154-158.

Barbosa, A. D., & Siniossoglou, S. (2017). Function of lipid droplet-organelle interactions in lipid homeostasis. *Biochim Biophys Acta Mol Cell Res, 1864*(9), 1459-1468.

Barra-Jiménez, A., & Ragni, L. (2017). Secondary development in the stem: when Arabidopsis and trees are closer than it seems. *Curr Opin Plant Biol, 35*, 145-151. doi:10.1016/j.pbi.2016.12.002

Bates, P. D., Stymne, S., & Ohlrogge, J. (2013). Biochemical pathways in seed oil synthesis. *Curr Opin Plant Biol, 16*(3), 358-364.

Battey, N. H., & Tooke, F. (2002). Molecular control and variation in the floral transition. *Current opinion in plant biology, 5*(1), 62-68.

Baucher, M., El Jaziri, M., & Vandeputte, O. (2007). From primary to secondary growth: origin and development of the vascular system. *Journal of experimental botany, 58*(13), 3485-3501.

Baunsgaard, L., Lutken, H., Mikkelsen, R., Glaring, M. A., Pham, T. T., & Blennow, A. (2005). A novel isoform of glucan, water dikinase phosphorylates pre-phosphorylated alpha-glucans and is involved in starch degradation in Arabidopsis. *Plant J, 41*(4), 595-605.

Bazzaz, F. A., Chiariello, N. R., Coley, P. D., & Pitelka, L. F. (1987). Allocating resources to reproduction and defense. *BioScience, 37*(1), 58-67.

Beisson, F., Li, Y., Bonaventure, G., Pollard, M., & Ohlrogge, J. B. (2007). The acyltransferase GPAT5 is required for the synthesis of suberin in seed coat and root of Arabidopsis. *Plant Cell, 19*(1), 351-368.

Benková, E., Michniewicz, M., Sauer, M., Teichmann, T., Seifertová, D., Jürgens, G., & Friml, J. (2003). Local, efflux-dependent auxin gradients as a common module for plant organ formation. *Cell, 115*(5), 591-602.

Bennett, T., Liang, Y., Seale, M., Ward, S., Müller, D., & Leyser, O. (2016). Strigolactone regulates shoot development through a core signalling pathway. *Biology open, 5*(12), 1806-1820.

Bennett, T., Sieberer, T., Willett, B., Booker, J., Luschnig, C., & Leyser, O. (2006). The Arabidopsis MAX pathway controls shoot branching by regulating auxin transport. *Curr Biol, 16*(6), 553-563.

Bergonzi, S., & Albani, M. C. (2011). Reproductive competence from an annual and a perennial perspective. *J Exp Bot, 62*(13), 4415-4422.

Bergonzi, S., Albani, M. C., van Themaat, E. V. L., Nordström K. J., Wang, R., Schneeberger, K., Moerland, P. D., & Coupland, G. (2013) Mechanisms of age-dependent response to winter temperature in perennial flowering of Arabis alpina. *Science*, 340, 1094-1097.

Berrocal-Lobo, M., Ibanez, C., Acebo, P., Ramos, A., Perez-Solis, E., Collada, C., Casado, R., Aragoncillo, C., & Allona, I. (2011). Identification of a homolog of Arabidopsis DSP4 (SEX4) in chestnut: its induction and accumulation in stem amyloplasts during winter or in response to the cold. *Plant Cell Environ, 34*(10), 1693-1704.

Bhalerao, R. P., & Fischer, U. (2014). Auxin gradients across wood-instructive or incidental? *Physiol Plant, 151*(1), 43-51.

Björklund, S., Antti, H., Uddestrand, I., Moritz, T., & Sundberg, B. (2007). Cross-talk between gibberellin and auxin in development of Populus wood: gibberellin stimulates polar auxin transport and has a common transcriptome with auxin. *Plant J, 52*(3), 499-511.

Blauth, S. L., Kim, K., Klucinec, J., Shannon, J. C., Thompson, D., & Guiltinan, M. (2002). Identification of Mutator insertional mutants of starch-branching enzyme 1 (sbe1) in Zea mays L.. *Plant Mol Biol,* 48, 287–297.

Blée, E., Boachon, B., Burcklen, M., Le Guedard, M., Hanano, A., Heintz, D., Ehlting, J., Herrfurth, C., Feussner, I., & Bessoule, J. J. (2014). The reductase activity of the Arabidopsis caleosin RESPONSIVE TO DESSICATION20 mediates gibberellin-dependent flowering time, abscisic acid sensitivity, and tolerance to oxidative stress. *Plant Physiol, 166*(1), 109-124.

Blennow, A., & Engelsen, S. B. (2010). Helix-breaking news: fighting crystalline starch energy deposits in the cell. *Trends Plant Sci, 15*(4), 236-240.

Brocard, L., Immel, F., Coulon, D., Esnay, N., Tuphile, K., Pascal, S., Claverol, S., Fouillen, L., Bessoule, J-J., & Brehelin, C. (2017). Proteomic Analysis of Lipid Droplets from Arabidopsis Aging Leaves Brings New Insight into Their Biogenesis and Functions. *Front Plant Sci, 8*, 894.

Busse, J. S., & Evert, R. F. (1999). Pattern of differentiation of the first vascular elements in the embryo and seedling of Arabidopsis thaliana. *International Journal of Plant Sciences, 160*(1), 1-13.

Bustos, R., Fahy, B., Hylton, C. M., Seale, R., Nebane, N. M., Edwards, A., Martin, C., & Smith, A. M. (2004). Starch granule initiation is controlled by a heteromultimeric isoamylase in potato tubers. *Proceedings of the National Academy of Sciences, 101*(7), 2215-2220.

Cai, Y., McClinchie, E., Price, A., Nguyen, T. N., Gidda, S. K., Watt, S. C., Yurchenko, O., Park, S., Sturtevant, D., Mullen, R. T., Dyer, J. M., & Chapman, K. D. (2017). Mouse fat storage-inducing transmembrane protein 2 (FIT2) promotes lipid droplet accumulation in plants. *Plant Biotechnol J, 15*(7), 824-836.

Cao, Y.-z., & Huang, A. H. (1986). Diacylglycerol acyltransferase in maturing oil seeds of maize and other species. *Plant Physiology, 82*(3), 813-820.

Carman, G. M. (1997). Phosphatidate phosphatases and diacylglycerol pyrophosphate phosphatases in Saccharomyces cerevisiae and Escherichia coli. *Biochimica et Biophysica Acta (BBA)-Lipids and Lipid Metabolism, 1348*(1-2), 45-55.

Carrie, C., Murcha, M. W., Millar, A. H., Smith, S. M., & Whelan, J. (2007). Nine 3-ketoacyl-CoA thiolases (KATs) and acetoacetyl-CoA thiolases (ACATs) encoded by five genes in Arabidopsis thaliana are targeted either to peroxisomes or cytosol but not to mitochondria. *Plant Mol Biol, 63*(1), 97-108.

Carvalho, C., & Dietrich, S. (1996). Carbohydrates in tuberous roots of Cochlospermum regium (Mart. & Schr) Pilger at different stages of development. *Revista brasileira de Botânica, 19*(2), 127-131.

Carvalho, M. (2007). Fructans in Asteraceae from the Brazilian cerrado. *Recent advances in fructooligosaccharides research*, 69-91.

Caspar, T., Huber, S. C., & Somerville, C. (1985). Alterations in growth, photosynthesis, and respiration in a starchless mutant of Arabidopsis thaliana (L.) deficient in chloroplast phosphoglucomutase activity. *Plant Physiology, 79*(1), 11-17.

Caspar, T., Lin, T.-P., Kakefuda, G., Benbow, L., Preiss, J., & Somerville, C. (1991). Mutants of Arabidopsis with altered regulation of starch degradation. *Plant Physiology, 95*(4), 1181-1188.

Castaings, L., Bergonzi, S., Albani, M. C., Kemi, U., Savolainen, O., & Coupland, G. (2014). Evolutionary conservation of cold-induced antisense RNAs of FLOWERING LOCUS C in Arabidopsis thaliana perennial relatives. *Nat Commun, 5*, 4457.

Chapman, K. D., & Ohlrogge, J. B. (2012). Compartmentation of triacylglycerol accumulation in plants. *J Biol Chem, 287*(4), 2288-2294.

Chinnasamy, G., Davis, P. J., & Bal, A. K. (2003). Seasonal changes in oleosomic lipids and fatty acids of perennial root nodules of beach pea. *J Plant Physiol, 160*(4), 355-365.

Coleman, G. D., Chen, T. H., Ernst, S. G., & Fuchigami, L. (1991). Photoperiod control of poplar bark storage protein accumulation. *Plant Physiology, 96*(3), 686-692.

Collins, C., Maruthi, N. M., & Jahn, C. E. (2015). CYCD3 D-type cyclins regulate cambial cell proliferation and secondary growth in Arabidopsis. *J Exp Bot, 66*(15), 4595-4606.

Cooke, J. E., & Weih, M. (2005). Nitrogen storage and seasonal nitrogen cycling in Populus: bridging molecular physiology and ecophysiology. *New Phytol, 167*(1), 19-30.

Cruz-Mazo, G., Buide, M. L., Samuel, R., & Narbona, E. (2009). Molecular phylogeny of Scorzoneroides (Asteraceae): evolution of heterocarpy and annual habit in unpredictable environments. *Mol Phylogenet Evol, 53*(3), 835-847.

Cyr, D., Bewley, J., & Dumbroff, E. (1990). Seasonal dynamics of carbohydrate and nitrogenous components in the roots of perennial weeds. *Plant, Cell & Environment, 13*(4), 359-365.

Dahlqvist, A., Ståhl, U., Lenman, M., Banas, A., Lee, M., Sandager, L., Ronne, H., & Stymne, S. (2000). Phospholipid: diacylglycerol acyltransferase: an enzyme that catalyzes the acyl-CoA-independent formation of triacylglycerol in yeast and plants. *Proceedings of the National Academy of Sciences, 97*(12), 6487-6492.

Davin, N., Edger, P. P., Hefer, C. A., Mizrachi, E., Schuetz, M., Smets, E., Myburg, A. A., Douglas, C., J., Schranz, M. E., & Lens, F. (2016). Functional network analysis of genes differentially expressed during xylogenesis in soc1ful woody Arabidopsis plants. *Plant J, 86*(5), 376-390.

de Moraes, M. G., de Carvalho, M. A. M., Franco, A. C., Pollock, C. J., & Figueiredo-Ribeiro, Rita de Cássia L. (2016). Fire and Drought: Soluble Carbohydrate Storage and Survival Mechanisms in Herbaceous Plants from the Cerrado. *BioScience, 66*(2), 107-117.

De Souza, J. G., & Da Silv, J. V. (1987). Partitioning of carbohydrates in annual and perennial cotton (Gossypium hirsutum L.). *Journal of experimental botany, 38*(7), 1211-1218.

Delatte, T., Trevisan, M., Parker, M. L., & Zeeman, S. C. (2005). Arabidopsis mutants Atisa1 and Atisa2 have identical phenotypes and lack the same multimeric isoamylase, which influences the branch point distribution of amylopectin during starch synthesis. *Plant J, 41*(6), 815-830.

Delatte, T., Umhang, M., Trevisan, M., Eicke, S., Thorneycroft, D., Smith, S. M., & Zeeman, S. C. (2006). Evidence for distinct mechanisms of starch granule breakdown in plants. *J Biol Chem, 281*(17), 12050-12059.

Delrue, B., & Ball, S. (1996). Preamylopectin Pmcessing: A Mandatory Step for Starch Biosynthesis in Plants.

Deng, W., Ying, H., Helliwell, C. A., Taylor, J. M., Peacock, W. J., & Dennis, E. S. (2011). FLOWERING LOCUS C (FLC) regulates development pathways throughout the life cycle of Arabidopsis. *Proc Natl Acad Sci U S A, 108*(16), 6680-6685.

Denis, E., Kbiri, N., Mary, V., Claisse, G., Conde, E. S. N., Kreis, M., & Deveaux, Y. (2017). WOX14 promotes bioactive gibberellin synthesis and vascular cell differentiation in Arabidopsis. *Plant J, 90*(3), 560-572.

Deschamps, P., Haferkamp, I., d'Hulst, C., Neuhaus, H. E., & Ball, S. G. (2008). The relocation of starch metabolism to chloroplasts: when, why and how. *Trends Plant Sci, 13*(11), 574-582.

Dolan, L., & Roberts, K. (1995). Secondary thickening in roots of Arabidopsis thaliana: anatomy and cell surface changes. *New Phytologist, 131*(1), 121-128.

Dürr, J., Bucking, H., Mult, S., Wildhagen, H., Palme, K., Rennenberg, H., Ditengou, F., & Herschbach, C. (2010). Seasonal and cell type specific expression of sulfate transporters in the phloem of Populus reveals tree specific characteristics for SO(4)(2-) storage and mobilization. *Plant Mol Biol, 72*(4-5), 499-517.

Eastmond, P. J. (2006). SUGAR-DEPENDENT1 encodes a patatin domain triacylglycerol lipase that initiates storage oil breakdown in germinating Arabidopsis seeds. *Plant Cell, 18*(3), 665-675.

Eastmond, P., & Graham, I. (2000). The multifunctional protein At MFP2 is co-ordinately expressed with other genes of fatty acid β-oxidation during seed germination in Arabidopsis thaliana (L.) Heynh. In: Portland Press Ltd.

Eastmond, P. J., Quettier, A. L., Kroon, J. T., Craddock, C., Adams, N., & Slabas, A. R. (2010). Phosphatidic acid phosphohydrolase 1 and 2 regulate phospholipid synthesis at the endoplasmic reticulum in Arabidopsis. *Plant Cell, 22*(8), 2796-2811.

Edner, C., Li, J., Albrecht, T., Mahlow, S., Hejazi, M., Hussain, H., Kaplan, F., Guy, C., Smith, S. M., Steup, M., & Ritte, G. (2007). Glucan, water dikinase activity stimulates breakdown of starch granules by plastidial beta-amylases. *Plant Physiol, 145*(1), 17-28.

Eriksson, M. E., Israelsson, M., Olsson, O., & Moritz, T. (2000). Increased gibberellin biosynthesis in transgenic trees promotes growth, biomass production and xylem fiber length. *Nature biotechnology, 18*(7), 784-788.

Esau, K. (1960). Anatomy of seed plants. *Soil Science, 90*(2), 149.

Etchells, J. P., Mishra, L. S., Kumar, M., Campbell, L., & Turner, S. R. (2015). Wood Formation in Trees Is Increased by Manipulating PXY-Regulated Cell Division. *Curr Biol, 25*(8), 1050-1055.

Etchells, J. P., Provost, C. M., Mishra, L., & Turner, S. R. (2013). WOX4 and WOX14 act downstream of the PXY receptor kinase to regulate plant vascular proliferation independently of any role in vascular organisation. *Development, 140*(10), 2224-2234.

Etchells, J. P., Provost, C. M., & Turner, S. R. (2012). Plant vascular cell division is maintained by an interaction between PXY and ethylene signalling. *PLoS Genet, 8*(11), e1002997.

Etchells, J. P., & Turner, S. R. (2010). The PXY-CLE41 receptor ligand pair defines a multifunctional pathway that controls the rate and orientation of vascular cell division. *Development, 137*(5), 767-774.

Evans, M. E. K., Hearn, D. J., Hahn, W. J., Spangle, J. M., & Venable, D. L. (2005). Climate and Life-History Evolution in Evening Primroses (Oenothera, Onagraceae): A Phylogenetic Comparative Analysis. *Evolution, 59*(9).

Evert, R. F. (2006). *Esau's plant anatomy: meristems, cells, and tissues of the plant body: their structure, function, and development*: John Wiley & Sons.

Feike, D., Seung, D., Graf, A., Bischof, S., Ellick, T., Coiro, M., Soyk, S., Eicke, S., Mettler-Altmann, T., Lu, K. J., Trick, M., Zeeman, S. C., & Smith, A. M. (2016). The Starch Granule-Associated Protein EARLY STARVATION1 Is Required for the Control of Starch Degradation in Arabidopsis thaliana Leaves. *Plant Cell, 28*(6), 1472-1489.

Fettke, J., Malinova, I., Albrecht, T., Hejazi, M., & Steup, M. (2011). Glucose-1-phosphate transport into protoplasts and chloroplasts from leaves of Arabidopsis. *Plant Physiol, 155*(4), 1723-1734.

Figueiredo-Ribeiro, R. (1986). Reserve carbohydrates in underground organs of native Brazilian plants. *Revta. brasil. Bot., 9*, 159-166.

Finnegan, E. J., & Dennis, E. S. (2007). Vernalization-induced trimethylation of histone H3 lysine 27 at FLC is not maintained in mitotically quiescent cells. *Current biology, 17*(22), 1978-1983.

Fischer, U., Kucukoglu, M., Helariutta, Y., & Bhalerao, R. P. (2019). The Dynamics of Cambial Stem Cell Activity. *Annu Rev Plant Biol, 70*, 293-319.

Fisher, K., & Turner, S. (2007). PXY, a receptor-like kinase essential for maintaining polarity during plant vascular-tissue development. *Curr Biol, 17*(12), 1061-1066.

Flügge, U. I., Hausler, R. E., Ludewig, F., & Gierth, M. (2011). The role of transporters in supplying energy to plant plastids. *J Exp Bot, 62*(7), 2381-2392. doi:10.1093/jxb/erq361

Friedman, J., & Rubin, M. J. (2015). All in good time: understanding annual and perennial strategies in plants. *Am J Bot, 102*(4), 497-499.

Fulton, D. C., Stettler, M., Mettler, T., Vaughan, C. K., Li, J., Francisco, P., Gil, M., Reinhold, H., Eicke, S., Messerli, G., Dorken, G., Halliday, K., Smith, A. M., Smith, S. M., & Zeeman, S. C. (2008). Beta-AMYLASE4, a noncatalytic protein required for starch breakdown, acts upstream of three active beta-amylases in Arabidopsis chloroplasts. *Plant Cell, 20*(4), 1040-1058.

Furze, M. E., Trumbore, S., & Hartmann, H. (2018). Detours on the phloem sugar highway: stem carbon storage and remobilization. *Curr Opin Plant Biol, 43*, 89-95.

Gälweiler, L., Guan, C., Müller, A., Wisman, E., Mendgen, K., Yephremov, A., & Palme, K. (1998). Regulation of polar auxin transport by AtPIN1 in Arabidopsis vascular tissue. *Science, 282*(5397), 2226-2230.

Garnier, E. (1992). Growth analysis of congeneric annual and perennial grass species. *Journal of ecology*, 665-675.

Germain, V., Rylott, E. L., Larson, T. R., Sherson, S. M., Bechtold, N., Carde, J. P., Bryce, J. H., Graham, I. A., & Smith, S. M. (2001). Requirement for 3□ketoacyl□CoA thiolase□2 in peroxisome development, fatty acid β□oxidation and breakdown of triacylglycerol in lipid bodies of Arabidopsis seedlings. *The Plant Journal, 28*(1), 1-12.

Gessler, A., Schneider, S., Weber, P., Hanemann, U., & Rennenberg, H. (1998). Soluble N compounds in trees exposed to high loads of N: a comparison between the roots of Norway spruce (Picea abies) and beech (Fagus sylvatica) trees grown under field conditions. *New Phytologist, 138*(3), 385-399.

Gidda, S. K., Park, S., Pyc, M., Yurchenko, O., Cai, Y., Wu, P., Andrews, D. W., Chapman, K. D., Dyer, J. M., & Mullen, R. T. (2016). Lipid Droplet-Associated Proteins (LDAPs) Are Required for the Dynamic Regulation of Neutral Lipid Compartmentation in Plant Cells. *Plant Physiol, 170*(4), 2052-2071.

Glover, J. D. (2005). The necessity and possibility of perennial grain production systems. *Renewable Agriculture and Food Systems, 20*(1), 1-4.

Goepfert, S., Hiltunen, J. K., & Poirier, Y. (2006). Identification and functional characterization of a monofunctional peroxisomal enoyl-CoA hydratase 2 that participates in the degradation of even cis-unsaturated fatty acids in Arabidopsis thaliana. *J Biol Chem, 281*(47), 35894-35903.

Goepfert, S., Vidoudez, C., Rezzonico, E., Hiltunen, J. K., & Poirier, Y. (2005). Molecular identification and characterization of the Arabidopsis delta(3,5),delta(2,4)-dienoyl-coenzyme A isomerase, a peroxisomal enzyme participating in the beta-oxidation cycle of unsaturated fatty acids. *Plant Physiol, 138*(4), 1947-1956.

Goepfert, S., Vidoudez, C., Tellgren-Roth, C., Delessert, S., Hiltunen, J. K., & Poirier, Y. (2008). Peroxisomal Delta(3),Delta(2)-enoyl CoA isomerases and evolution of cytosolic paralogues in embryophytes. *Plant J, 56*(5), 728-742.

Graham, I. A. (2008). Seed storage oil mobilization. *Annu Rev Plant Biol, 59*, 115-142.

Grillo, M. A., Li, C., Fowlkes, A. M., Briggeman, T. M., Zhou, A., Schemske, D. W., & Sang, T. (2009). Genetic architecture for the adaptive origin of annual wild rice, oryza nivara. *Evolution, 63*(4), 870-883.

Hagio, M., Sakurai, I., Sato, S., Kato, T., Tabata, S., & Wada, H. (2002). Phosphatidylglycerol is essential for the development of thylakoid membranes in Arabidopsis thaliana. *Plant and cell physiology, 43*(12), 1456-1464.

Han, G. S., Wu, W. I., & Carman, G. M. (2006). The Saccharomyces cerevisiae Lipin homolog is a Mg2+-dependent phosphatidate phosphatase enzyme. *J Biol Chem, 281*(14), 9210-9218.

Han, S., Cho, H., Noh, J., Qi, J., Jung, H. J., Nam, H., Lee, S., Hwang, D., Greb, T., & Hwang, I. (2018). BIL1-mediated MP phosphorylation integrates PXY and cytokinin signalling in secondary growth. *Nat Plants, 4*(8), 605-614.

Hanano, A., Burcklen, M., Flenet, M., Ivancich, A., Louwagie, M., Garin, J., & Blee, E. (2006). Plant seed peroxygenase is an original heme-oxygenase with an EF-hand calcium binding motif. *J Biol Chem, 281*(44), 33140-33151.

Härtel, H., Dörmann, P., & Benning, C. (2000). DGD1-independent biosynthesis of extraplastidic galactolipids after phosphate deprivation in Arabidopsis. *Proceedings of the National Academy of Sciences, 97*(19), 10649-10654.

Hartmann, A., Senning, M., Hedden, P., Sonnewald, U., & Sonnewald, S. (2011). Reactivation of meristem activity and sprout growth in potato tubers require both cytokinin and gibberellin. *Plant Physiol, 155*(2), 776-796.

Hartmann, H., & Trumbore, S. (2016). Understanding the roles of nonstructural carbohydrates in forest trees - from what we can measure to what we want to know. *New Phytol, 211*(2), 386-403.

Hayashi, A. H., & Appezzato-da-Glória, B. (2005). The origin and anatomy of rhizophores in Vernonia herbacea and V. platensis (Asteraceae) from the Brazilian Cerrado. *Australian Journal of Botany, 53*(3), 273-279.

Hayward, A., Stirnberg, P., Beveridge, C., & Leyser, O. (2009). Interactions between auxin and strigolactone in shoot branching control. *Plant Physiol, 151*(1), 400-412.

Hejátko, J., Ryu, H., Kim, G. T., Dobesova, R., Choi, S., Choi, S. M., Souček, P., Horák, J., Pekárová, B., Palme, K., Brzobohatý, B., & Hwang, I. (2009). The histidine kinases CYTOKININ-INDEPENDENT1 and ARABIDOPSIS HISTIDINE KINASE2 and 3 regulate vascular tissue development in Arabidopsis shoots. *Plant Cell, 21*(7), 2008-2021.

Helliwell, C. A., Wood, C. C., Robertson, M., James Peacock, W., & Dennis, E. S. (2006). The Arabidopsis FLC protein interacts directly in vivo with SOC1 and FT chromatin and is part of a high-molecular-weight protein complex. *Plant J, 46*(2), 183-192.

Herschbach, C., Gessler, A., & Rennenberg, H. (2012). Long-Distance Transport and Plant Internal Cycling of N- and S-Compounds. In *Progress in Botany Vol. 73* (pp. 161-188).

Herschbach, C., & Rennenberg, H. (1996). Storage and remobilisation of sulphur in beech trees (Fagus sylvatica). *Physiologia Plantarum, 98*(1), 125-132.

Hirakawa, Y., Kondo, Y., & Fukuda, H. (2010). TDIF peptide signaling regulates vascular stem cell proliferation via the WOX4 homeobox gene in Arabidopsis. *Plant Cell, 22*(8), 2618-2629.

Hirakawa, Y., Shinohara, H., Kondo, Y., Inoue, A., Nakanomyo, I., Ogawa, M., Sawa, S., Ohashi-Ito, K., Matsubayashi, Y., & Fukuda, H. (2008). Non-cell-autonomous control of vascular stem cell fate by a CLE peptide/receptor system. *Proceedings of the National Academy of Sciences, 105*(39), 15208-15213.

Hoffman, D. E., Jonsson, P., Bylesjo, M., Trygg, J., Antti, H., Eriksson, M. E., & Moritz, T. (2010). Changes in diurnal patterns within the Populus transcriptome and metabolome in response to photoperiod variation. *Plant Cell Environ, 33*(8), 1298-1313.

Hu, F. Y., Tao, D. Y., Sacks, E., Fu, B. Y., Xu, P., Li, J., Yang, Y., McNally, K., Khush, G. S., Paterson, A. H., & Li, Z. K. (2003). Convergent evolution of perenniality in rice and sorghum. *Proceedings of the National Academy of Sciences, 100*(7), 4050-4054.

Huang, A. (1996). Oleosins and oil bodies in seeds and other organs. *Plant Physiology, 110*(4), 1055.

Huang, A. H. C. (2018). Plant Lipid Droplets and Their Associated Proteins: Potential for Rapid Advances. *Plant Physiol, 176*(3), 1894-1918.

Hughes, P. W., Soppe, W. J. J., & Albani, M. C. (2019). Seed traits are pleiotropically regulated by the flowering time gene PERPETUAL FLOWERING 1 (PEP1) in the perennial Arabis alpina. *Mol Ecol, 28*(5), 1183-1201.

Hurlock, A. K., Roston, R. L., Wang, K., & Benning, C. (2014). Lipid trafficking in plant cells. *Traffic, 15*(9), 915-932.

Hwang, I., Chen, H. C., & Sheen, J. (2002). Two-component signal transduction pathways in Arabidopsis. *Plant Physiol, 129*(2), 500-515.

Hyun, Y., Richter, R., & Coupland, G. (2017). Competence to Flower: Age-Controlled Sensitivity to Environmental Cues. *Plant Physiol, 173*(1), 36-46.

Hyun, Y., Richter, R., Vincent, C., Martinez-Gallegos, R., Porri, A., & Coupland, G. (2016). Multi-layered Regulation of SPL15 and Cooperation with SOC1 Integrate Endogenous Flowering Pathways at the Arabidopsis Shoot Meristem. *Dev Cell, 37*(3), 254-266.

Hyun, Y., Vincent, C., Tilmes, V., Bergonzi, S., Kiefer, C., Richter, R., Martinez-Gallegos, R., Severing, E., & Coupland, G. (2019). A regulatory circuit conferring varied flowering response to cold in annual and perennial plants. *Science, 363*, 409-412.

Immanen, J., Nieminen, K., Smolander, O. P., Kojima, M., Alonso Serra, J., Koskinen, P., Zhang, J., Elo, A., Mähönen, P., Street, N., Bhalerao, R. P., Paulin, L., Auvinen, P., Sakakibara, H., & Helariutta, Y. (2016). Cytokinin and Auxin Display Distinct but Interconnected Distribution and Signaling Profiles to Stimulate Cambial Activity. *Curr Biol, 26*(15), 1990-1997.

Isejima, E., FIGUEIREDO RRIEIRO, R., & Zaidan, L. (1991). Fructan composition in adventitious tuberous roots of Viguiera discolor Baker (Asteraceae) as influenced by daylength. *New Phytologist, 119*(1), 149-154.

Israelsson, M., Sundberg, B., & Moritz, T. (2005). Tissue-specific localization of gibberellins and expression of gibberellin-biosynthetic and signaling genes in wood-forming tissues in aspen. *Plant J, 44*(3), 494-504.

Ito, Y., Nakanomyo, I., Motose, H., Iwamoto, K., Sawa, S., Dohmae, N., & Fukuda, H. (2006). Dodeca-CLE peptides as suppressors of plant stem cell differentiation. *Science, 313*(5788), 842-845.

James, M. G., Robertson, D. S., & Myers, A. M. (1995). Characterization of the maize gene sugary1, a determinant of starch composition in kernels. *The Plant Cell, 7*(4), 417-429.

Jayawardhane, K. N., Singer, S. D., Weselake, R. J., & Chen, G. (2018). Plant sn-Glycerol-3-Phosphate Acyltransferases: Biocatalysts Involved in the Biosynthesis of Intracellular and Extracellular Lipids. *Lipids, 53*(5), 469-480.

Johnsson, C., Jin, X., Xue, W., Dubreuil, C., Lezhneva, L., & Fischer, U. (2019). The plant hormone auxin directs timing of xylem development by inhibition of secondary cell wall deposition through repression of secondary wall NAC-domain transcription factors. *Physiol Plant, 165*(4), 673-689.

Jones, B., Gunneras, S. A., Petersson, S. V., Tarkowski, P., Graham, N., May, S., Dolezal, K., Sandberg, G., & Ljung, K. (2010). Cytokinin regulation of auxin synthesis in Arabidopsis involves a homeostatic feedback loop regulated via auxin and cytokinin signal transduction. *Plant Cell, 22*(9), 2956-2969.

Joubès, J., Raffaele, S., Bourdenx, B., Garcia, C., Laroche-Traineau, J., Moreau, P., Domergue, F., & Lessire, R. (2008). The VLCFA elongase gene family in Arabidopsis thaliana: phylogenetic analysis, 3D modelling and expression profiling. *Plant Mol Biol, 67*(5), 547-566.

Jouhet, J., Marechal, E., Baldan, B., Bligny, R., Joyard, J., & Block, M. A. (2004). Phosphate deprivation induces transfer of DGDG galactolipid from chloroplast to mitochondria. *J Cell Biol, 167*(5), 863-874.

Karki, N., Johnson, B. S., & Bates, P. D. (2019). Metabolically Distinct Pools of Phosphatidylcholine Are Involved in Trafficking of Fatty Acids out of and into the Chloroplast for Membrane Production. *Plant Cell, 31*(11), 2768-2788.

Karl, R., Kiefer, C., Ansell, S. W., & Koch, M. A. (2012). Systematics and evolution of Arctic-Alpine Arabis alpina (Brassicaceae) and its closest relatives in the eastern Mediterranean. *Am J Bot, 99*(4), 778-794.

Karl, R., & Koch, M. A. (2013). A world-wide perspective on crucifer speciation and evolution: phylogenetics, biogeography and trait evolution in tribe Arabideae. *Ann Bot, 112*(6), 983-1001.

Katavic, V., Reed, D. W., Taylor, D. C., Giblin, E. M., Barton, D. L., Zou, J., Mackenzie, S. L., Covello, P. S., & Kunst, L. (1995). Alteration of seed fatty acid composition by an ethyl methanesulfonate-induced mutation in Arabidopsis thaliana affecting diacylglycerol acyltransferase activity. *Plant Physiology, 108*(1), 399-409.

Kaup, M. T., Froese, C. D., & Thompson, J. E. (2002). A role for diacylglycerol acyltransferase during leaf senescence. *Plant Physiol, 129*(4), 1616-1626.

Kelly, A. A., & Dörmann, P. (2004). Green light for galactolipid trafficking. *Curr Opin Plant Biol, 7*(3), 262-269.

Kelly, A. A., van Erp, H., Quettier, A. L., Shaw, E., Menard, G., Kurup, S., & Eastmond, P. J. (2013). The sugar-dependent1 lipase limits triacylglycerol accumulation in vegetative tissues of Arabidopsis. *Plant Physiol, 162*(3), 1282-1289.

Kiefer, C., Severing, E., Karl, R., Bergonzi, S., Koch, M., Tresch, A., & Coupland, G. (2017). Divergence of annual and perennial species in the Brassicaceae and the contribution of cis-acting variation at FLC orthologues. *Mol Ecol, 26*(13), 3437-3457.

Kim, D. H., Doyle, M. R., Sung, S., & Amasino, R. M. (2009). Vernalization: winter and the timing of flowering in plants. *Annu Rev Cell Dev Biol, 25*, 277-299.

Kim, E. Y., Park, K. Y., Seo, Y. S., & Kim, W. T. (2016). Arabidopsis Small Rubber Particle Protein Homolog SRPs Play Dual Roles as Positive Factors for Tissue Growth and Development and in Drought Stress Responses. *Plant Physiol, 170*(4), 2494-2510.

Kim, H. U., & Huang, A. H. (2004). Plastid lysophosphatidyl acyltransferase is essential for embryo development in Arabidopsis. *Plant Physiol, 134*(3), 1206-1216.

Kim, H. U., Li, Y., & Huang, A. H. (2005). Ubiquitous and endoplasmic reticulum-located lysophosphatidyl acyltransferase, LPAT2, is essential for female but not male gametophyte development in Arabidopsis. *Plant Cell, 17*(4), 1073-1089.

Koch, M. A., Kiefer, C., Ehrich, D., Vogel, J., Brochmann, C., & Mummenhoff, K. (2006). Three times out of Asia Minor: the phylogeography of Arabis alpina L. (Brassicaceae). *Mol Ecol, 15*(3), 825-839.

Kötting, O., Pusch, K., Tiessen, A., Geigenberger, P., Steup, M., & Ritte, G. (2005). Identification of a novel enzyme required for starch metabolism in Arabidopsis leaves. The phosphoglucan, water dikinase. *Plant Physiol, 137*(1), 242-252.

Kucukoglu, M., Nilsson, J., Zheng, B., Chaabouni, S., & Nilsson, O. (2017). WUSCHEL-RELATED HOMEOBOX4 (WOX4)-like genes regulate cambial cell division activity and secondary growth in Populus trees. *New Phytol, 215*(2), 642-657.

LaBrant, E., Barnes, A. C., & Roston, R. L. (2018). Lipid transport required to make lipids of photosynthetic membranes. *Photosynth Res, 138*(3), 345-360.

Lacey, D. J., Beaudoin, F., Dempsey, C. E., Shewry, P. R., & Napier, J. A. (1999). The accumulation of triacylglycerols within the endoplasmic reticulum of developing seeds of Helianthus annuus. *The Plant Journal, 17*(4), 397-405.

Lambers, H., & Plaxton, W. C. (2018). Phosphorus: back to the roots. *Annual Plant Reviews online*, 3-22.

Lang, F., Bauhus, J., Frossard, E., George, E., Kaiser, K., Kaupenjohann, M., Krüger, J., Matzner, E., Polle, A., Prietzel, J., Rennenberg, H., & Wellbrock, N. (2016). Phosphorus in forest ecosystems: New insights from an ecosystem nutrition perspective. *Journal of Plant Nutrition and Soil Science, 179*(2), 129-135.

Larson, P. (1994). Springer series in wood science: the vascular cambium. *Development and Structure. Springer-Verlag, Berlin*.

Laux, T. (2003). The stem cell concept in plants: a matter of debate. *Cell, 113*(3), 281-283.

Lazaro, A., Obeng-Hinneh, E., & Albani, M. C. (2018). Extended Vernalization Regulates Inflorescence Fate in Arabis alpina by Stably Silencing PERPETUAL FLOWERING1. *Plant Physiol, 176*(4), 2819-2833.

Lee, K., Ratnayake, C., & Huang, A. H. (1995). Genetic dissection of the co□expression of genes encoding the two isoforms of oleosins in the oil bodies of maize kernel. *The Plant Journal, 7*(4), 603-611.

Li, B., Geiger, D. R., & Shieh, W.-J. (1992). Evidence for circadian regulation of starch and sucrose synthesis in sugar beet leaves. *Plant Physiology, 99*(4), 1393-1399.

Li-Beisson, Y., Shorrosh, B., Beisson, F., Andersson, M. X., Arondel, V., Bates, P. D., Baud, S., Bird, D., Debono, A., Durrett, T. P., Franke, R. B., Graham, I. A., Katayama, K., Kelly, A.A., Larson, T., Markham, J. E., Miquel, M., Molina, I., Nishida, I., Rowland, O., Samuels, L., Schmid, K. M., Wada, H., Welti, R., Xu, C., Zallot, R., & Ohlrogge, J. (2013). Acyl-lipid metabolism. *Arabidopsis Book, 11*, e0161.

Lin, L.-J., Tai, S. S., Peng, C.-C., & Tzen, J. T. (2002). Steroleosin, a sterol-binding dehydrogenase in seed oil bodies. *Plant Physiology, 128*(4), 1200-1211.

Lindberg, C. L., Hanslin, H. M., Schubert, M., Marcussen, T., Trevaskis, B., Preston, J. C., & Fjellheim, S. (2020). Increased above-ground resource allocation is a likely precursor for independent evolutionary origins of annuality in the Pooideae grass subfamily. *New Phytol*.

Linssen, J. P., Cozijnsen, J. L., & Pilnik, W. (1989). Chufa (Cyperus esculentus): a new source of dietary fibre. *Journal of the Science of Food and Agriculture, 49*(3), 291-296.

Little, C. A., MacDonald, J. E., & Olsson, O. (2002). Involvement of indole-3-acetic acid in fascicular and interfascicular cambial growth and interfascicular extraxylary fiber differentiation in Arabidopsis thaliana inflorescence stems. *International Journal of Plant Sciences, 163*(4), 519-529.

Loer, D. S., & Herman, E. M. (1993). Cotranslational integration of soybean (Glycine max) oil body membrane protein oleosin into microsomal membranes. *Plant Physiology, 101*(3), 993-998.

Löfke, C., Ischebeck, T., Konig, S., Freitag, S., & Heilmann, I. (2008). Alternative metabolic fates of phosphatidylinositol produced by phosphatidylinositol synthase isoforms in Arabidopsis thaliana. *Biochem J, 413*(1), 115-124.

Long, J. A., & Barton, M. K. (1998). The development of apical embryonic pattern in Arabidopsis. *Development, 125*(16), 3027-3035.

Love, J., Björklund, S., Vahala, J., Hertzberg, M., Kangasjärvi, J., & Sundberg, B. (2009). Ethylene is an endogenous stimulator of cell division in the cambial meristem of Populus. *Proceedings of the National Academy of Sciences, 106*(14), 5984-5989.

Lowry, D. B., Rockwood, R. C., & Willis, J. H. (2008). Ecological reproductive isolation of coast and inland races of Mimulus guttatus. *Evolution, 62*(9), 2196-2214.

Madey, E., Nowack, L. M., & Thompson, J. E. (2002). Isolation and characterization of lipid in phloem sap of canola. *Planta, 214*(4), 625-634.

Malcheska, F., Honsel, A., Wildhagen, H., Durr, J., Larisch, C., Rennenberg, H., & Herschbach, C. (2013). Differential expression of specific sulphate transporters underlies seasonal and spatial patterns of sulphate allocation in trees. *Plant Cell Environ, 36*(7), 1285-1295.

Marcos, R., Izquierdo, Y., Vellosillo, T., Kulasekaran, S., Cascon, T., Hamberg, M., & Castresana, C. (2015). 9-Lipoxygenase-Derived Oxylipins Activate Brassinosteroid Signaling to Promote Cell Wall-Based Defense and Limit Pathogen Infection. *Plant Physiol, 169*(3), 2324-2334.

Mateos, J. L., Tilmes, V., Madrigal, P., Severing, E., Richter, R., Rijkenberg, C. W. M., Krajewski, P., & Coupland, G. (2017). Divergence of regulatory networks governed by the orthologous transcription factors FLC and PEP1 in Brassicaceae species. *Proc Natl Acad Sci U S A, 114*(51), E11037-E11046.

Matsumoto-Kitano, M., Kusumoto, T., Tarkowski, P., Kinoshita-Tsujimura, K., Vaclavikova, K., Miyawaki, K., & Kakimoto, T. (2008). Cytokinins are central regulators of cambial activity. *Proc Natl Acad Sci U S A 105,* 20027-20031.

Mauriat, M., & Moritz, T. (2009). Analyses of GA20ox- and GID1-over-expressing aspen suggest that gibberellins play two distinct roles in wood formation. *Plant J, 58*(6), 989-1003.

Melzer, S., Lens, F., Gennen, J., Vanneste, S., Rohde, A., & Beeckman, T. (2008). Flowering-time genes modulate meristem determinacy and growth form in Arabidopsis thaliana. *Nat Genet, 40*(12), 1489-1492.

Michaels, S. D., & Amasino, R. M. (1999). FLOWERING LOCUS C encodes a novel MADS domain protein that acts as a repressor of flowering. *The Plant Cell, 11*(5), 949-956.

Millard, P., & Grelet, G. A. (2010). Nitrogen storage and remobilization by trees: ecophysiological relevance in a changing world. *Tree Physiol, 30*(9), 1083-1095.

Miquel, M., Trigui, G., d'Andrea, S., Kelemen, Z., Baud, S., Berger, A., Deruyffelaere, C., Trubuil, A., Lepiniec, L., & Dubreucq, B. (2014). Specialization of oleosins in oil body dynamics during seed development in Arabidopsis seeds. *Plant Physiol, 164*(4), 1866-1878.

Moreau, P., Bessoule, J., Mongrand, S., Testet, E., Vincent, P., & Cassagne, C. (1998). Lipid trafficking in plant cells. *Progress in lipid research, 37*(6), 371.

Müller, F., & Frentzen, M. (2001). Phosphatidylglycerophosphate synthases from Arabidopsis thaliana. *FEBS Letters, 509*(2), 298-302.

Næsted, H., Frandsen, G. I., Jauh, G.-Y., Hernandez-Pinzon, I., Nielsen, H. B., Murphy, D. J., Rogers, J. C., & Mundy, J. (2000). Caleosins: Ca 2+-binding proteins associated with lipid bodies. *Plant Molecular Biology, 44*(4), 463-476.

Nakamura, Y., Koizumi, R., Shui, G., Shimojima, M., Wenk, M. R., Ito, T., & Ohta, H. (2009). Arabidopsis lipins mediate eukaryotic pathway of lipid metabolism and cope critically with

phosphate starvation. *Proceedings of the National Academy of Sciences, 106*(49), 20978-20983.

Netzer, F., Herschbach, C., Oikawa, A., Okazaki, Y., Dubbert, D., Saito, K., & Rennenberg, H. (2018). Seasonal Alterations in Organic Phosphorus Metabolism Drive the Phosphorus Economy of Annual Growth in F. sylvatica Trees on P-Impoverished Soil. *Front Plant Sci, 9*, 723.

Netzer, F., Schmid, C., Herschbach, C., & Rennenberg, H. (2017). Phosphorus-nutrition of European beech (Fagus sylvatica L.) during annual growth depends on tree age and P-availability in the soil. *Environmental and Experimental Botany, 137*, 194-207.

Nieminen, K., Immanen, J., Laxell, M., Kauppinen, L., Tarkowski, P., Dolezal, K., Tähtiharju, S., Elo, A., Decourteix, M., Ljung, K., Bhalerao, R., Keinonen, K., Albert, V. A., & Helariutta, Y. (2008). Cytokinin signaling regulates cambial development in poplar. *Proceedings of the National Academy of Sciences, 105*(50), 20032-20037.

Nilsson, J., Karlberg, A., Antti, H., Lopez-Vernaza, M., Mellerowicz, E., Perrot-Rechenmann, C., Sandberg., G., & Bhalerao, R. P. (2008). Dissecting the molecular basis of the regulation of wood formation by auxin in hybrid aspen. *Plant Cell, 20*(4), 843-855.

Ohashi-Ito, K., Saegusa, M., Iwamoto, K., Oda, Y., Katayama, H., Kojima, M., Sakakibara, H., & Fukuda, H. (2014). A bHLH complex activates vascular cell division via cytokinin action in root apical meristem. *Curr Biol, 24*(17), 2053-2058.

Ohlrogge, J., & Browse, J. (1995). Lipid biosynthesis. *The Plant Cell, 7*(7), 957.

Ohlrogge, J. B., & Jaworski, J. G. (1997). Regulation of fatty acid synthesis. *Annual review of plant biology, 48*(1), 109-136.

Ohsaki, Y., Suzuki, M., & Fujimoto, T. (2014). Open questions in lipid droplet biology. *Chem Biol, 21*(1), 86-96.

Ohyama, K., Ogawa, M., & Matsubayashi, Y. (2008). Identification of a biologically active, small, secreted peptide in Arabidopsis by in silico gene screening, followed by LC-MS-based structure analysis. *Plant J, 55*(1), 152-160.

Okada, K., Ueda, J., Komaki, M. K., Bell, C. J., & Shimura, Y. (1991). Requirement of the auxin polar transport system in early stages of Arabidopsis floral bud formation. *The Plant Cell, 3*(7), 677-684.

Palmer, N. A., Saathoff, A. J., Scully, E. D., Tobias, C. M., Twigg, P., Madhavan, S., Schmer, M., Cahoon, R., Sattler, S. E., Edmé, S. J., Mitchell, R. B., & Sarath, G. (2017). Seasonal below-ground metabolism in switchgrass. *Plant J, 92*(6), 1059-1075.

Park, J. Y., Kim, H., & Lee, I. (2017). Comparative analysis of molecular and physiological traits between perennial Arabis alpina Pajares and annual Arabidopsis thaliana Sy-0. *Sci Rep, 7*(1), 13348.

Pérez, S., & Bertoft, E. (2010). The molecular structures of starch components and their contribution to the architecture of starch granules: A comprehensive review. *Starch - Stärke, 62*(8), 389-420.

Pettit, N. E., Froend, R. H., & Ladd, P. G. (1995). Grazing in remnant woodland vegetation: changes in species composition and life form groups. *Journal of vegetation science, 6*(1), 121-130.

Pfister, B., Zeeman, S. C., Rugen, M. D., Field, R. A., Ebenhoh, O., & Raguin, A. (2020). Theoretical and experimental approaches to understand the biosynthesis of starch granules in a physiological context. *Photosynth Res, 145*(1), 55-70.

Pitelka, L. F. (1977). Energy allocations in annual and perennial lupines (Lupinus: Leguminosae). *Ecology, 58*(5), 1055-1065.

Poxleitner, M., Rogers, S. W., Lacey Samuels, A., Browse, J., & Rogers, J. C. (2006). A role for caleosin in degradation of oil-body storage lipid during seed germination. *Plant J, 47*(6), 917-933.

Pyc, M., Cai, Y., Gidda, S. K., Yurchenko, O., Park, S., Kretzschmar, F. K., Ischebeck, T., Valerius, O., Braus, G. H., Chapman, K. D., Dyer, J. M., & Mullen, R. T. (2017). Arabidopsis lipid droplet-associated protein (LDAP) - interacting protein (LDIP) influences lipid droplet size and neutral lipid homeostasis in both leaves and seeds. *Plant J, 92*(6), 1182-1201.

Pyc, M., Cai, Y., Greer, M. S., Yurchenko, O., Chapman, K. D., Dyer, J. M., & Mullen, R. T. (2017). Turning Over a New Leaf in Lipid Droplet Biology. *Trends Plant Sci, 22*(7), 596-609.

Qin, C., & Wang, X. (2002). The Arabidopsis Phospholipase D Family. Characterization of a Calcium-Independent and Phosphatidylcholine-Selective PLDζ1 with Distinct Regulatory Domains. *Plant Physiology, 128*(3), 1057-1068.

Ragni, L., & Greb, T. (2018). Secondary growth as a determinant of plant shape and form. *Semin Cell Dev Biol, 79*, 58-67.

Ragni, L., Nieminen, K., Pacheco-Villalobos, D., Sibout, R., Schwechheimer, C., & Hardtke, C. S. (2011). Mobile gibberellin directly stimulates Arabidopsis hypocotyl xylem expansion. *Plant Cell, 23*(4), 1322-1336.

Randall, R. S., Miyashima, S., Blomster, T., Zhang, J., Elo, A., Karlberg, A., Immanen, J., Nieminen, K., Lee, J-Y., Kakimoto, T., Blajecka, K., Melnyk, C. W., Alcasabas, A., Forzani, C., Matsumoto-Kitano, M., Mähönen, A. P., Bhalerao, R., Dewitte, W., Helariutta, Y., & Murray, J. A. (2015). AINTEGUMENTA and the D-type cyclin CYCD3;1 regulate root secondary growth and respond to cytokinins. *Biol Open, 4*(10), 1229-1236.

Rennenberg, H., & Schmidt, S. (2010). Perennial lifestyle--an adaptation to nutrient limitation? *Tree Physiol, 30*(9), 1047-1049.

Resman, L., Howe, G., Jonsen, D., Englund, M., Druart, N., Schrader, J., Antti, H., Skinner, J., Sjödin, A., Chen, T., & Bhalerao, R. P. (2010). Components acting downstream of short day perception regulate differential cessation of cambial activity and associated responses in early and late clones of hybrid poplar. *Plant Physiol, 154*(3), 1294-1303.

Richardson, A. D., Carbone, M. S., Keenan, T. F., Czimczik, C. I., Hollinger, D. Y., Murakami, P., Schaberg, P. G., & Xu, X. (2013). Seasonal dynamics and age of stemwood nonstructural carbohydrates in temperate forest trees. *New Phytol, 197*(3), 850-861.

Richmond, T. A., & Bleecker, A. B. (1999). A defect in β-oxidation causes abnormal inflorescence development in Arabidopsis. *The Plant Cell, 11*(10), 1911-1923.

Roumet, C., Urcelay, C., & Diaz, S. (2006). Suites of root traits differ between annual and perennial species growing in the field. *New Phytol, 170*(2), 357-368.

Routaboul, J.-M., Benning, C., Bechtold, N., Caboche, M., & Lepiniec, L. (1999). The TAG1 locus of Arabidopsis encodes for a diacylglycerol acyltransferase. *Plant Physiology and Biochemistry, 37*(11), 831-840.

Ruuska, S. A., Lewis, D. C., Kennedy, G., Furbank, R. T., Jenkins, C. L., & Tabe, L. M. (2008). Large scale transcriptome analysis of the effects of nitrogen nutrition on accumulation of stem carbohydrate reserves in reproductive stage wheat. *Plant Mol Biol, 66*(1-2), 15-32.

Rylott, E. L., Eastmond, P. J., Gilday, A. D., Slocombe, S. P., Larson, T. R., Baker, A., & Graham, I. A. (2006). The Arabidopsis thaliana multifunctional protein gene (MFP2) of peroxisomal beta-oxidation is essential for seedling establishment. *Plant J, 45*(6), 930-941.

Rylott, E. L., Hooks, M., & Graham, I. A. (2001). Co-ordinate regulation of genes involved in storage lipid mobilization in Arabidopsis thaliana. In: Portland Press Ltd.

Sablowski, R. (2004). Plant and animal stem cells: conceptually similar, molecularly distinct? *Trends Cell Biol, 14*(11), 605-611.

Saha, S., Enugutti, B., Rajakumari, S., & Rajasekharan, R. (2006). Cytosolic triacylglycerol biosynthetic pathway in oilseeds. Molecular cloning and expression of peanut cytosolic diacylglycerol acyltransferase. *Plant Physiol, 141*(4), 1533-1543. doi:10.1104/pp.106.082198

Sakakibara, H. (2006). Cytokinins: activity, biosynthesis, and translocation. *Annu Rev Plant Biol, 57*, 431-449.

Sanz, A., Moreno, J. I., & Castresana, C. (1998). PIOX, a new pathogen-induced oxygenase with homology to animal cyclooxygenase. *The Plant Cell, 10*(9), 1523-1537.

Satoh, H., Nishi, A., Yamashita, K., Takemoto, Y., Tanaka, Y., Hosaka, Y., Sakurai, A., Fujita, N., & Nakamura, Y. (2003). Starch-branching enzyme I-deficient mutation specifically affects the structure and properties of starch in rice endosperm. *Plant Physiol, 133*(3), 1111-1121.

Sauer, M., Balla, J., Luschnig, C., Wisniewska, J., Reinohl, V., Friml, J., & Benkova, E. (2006). Canalization of auxin flow by Aux/IAA-ARF-dependent feedback regulation of PIN polarity. *Genes Dev, 20*(20), 2902-2911.

Sauter, J., & Kloth, S. (1987). Changes in carbohydrates and ultrastructure in xylem ray cells ofPopulus in response to chilling. *Protoplasma, 137*(1), 45-55.

Sauter, J. J., & Van Cleve, B. (1989). Micromorphometric determination of organelles and of storage material in wood ray cells-a useful method for detecting differentiation within a tissue. *IAWA Journal, 10*(4), 395-403.

Sauter, J. J., & van Cleve, B. (1994). Storage, mobilization and interrelations of starch, sugars, protein and fat in the ray storage tissue of poplar trees. *Trees, 8*, 297-304.

Sauter, J. J., & Wellenkamp, S. (1998). Seasonal changes in content of starch, protein and sugars in the twig wood of Salix caprea L. *Holzforschung-International Journal of the Biology, Chemistry, Physics and Technology of Wood, 52*(3), 255-262.

Savidge, R. A. (1983). The role of plant hormones in higher plant cellular differentiation. II. Experiments with the vascular cambium, and sclereid and tracheid differentiation in the pine, Pinus contorta. *The Histochemical journal, 15*(5), 447-466.

Scheible, W.-R., Gonzalez-Fontes, A., Lauerer, M., Muller-Rober, B., Caboche, M., & Stitt, M. (1997). Nitrate acts as a signal to induce organic acid metabolism and repress starch metabolism in tobacco. *The Plant Cell, 9*(5), 783-798.

Scheidel, U., & Bruelheide, H. (2004). The impact of altitude and simulated herbivory on the growth and carbohydrate storage of Petasites albus. *Plant Biol (Stuttg), 6*(6), 740-745.

Scheres, B. (2007). Stem-cell niches: nursery rhymes across kingdoms. *Nat Rev Mol Cell Biol, 8*(5), 345-354.

Scheres, B., Wolkenfelt, H., Willemsen, V., Terlouw, M., Lawson, E., Dean, C., & Weisbeek, P. (1994). Embryonic origin of the Arabidopsis primary root and root meristem initials. *Development, 120*(9), 2475-2487.

Schmidt, M. A., & Herman, E. M. (2008). Suppression of soybean oleosin produces micro-oil bodies that aggregate into oil body/ER complexes. *Mol Plant, 1*(6), 910-924.

Schulz, H., & Kunau, W.-H. (1987). Beta-oxidation of unsaturated fatty acids: a revised pathway. *Trends in Biochemical Sciences, 12*, 403-406.

Schwall, G. P., Safford, R., Westcott, R. J., Jeffcoat, R., Tayal, A., Shi, Y.-C., Gidley, M. J., & Jobling, S. A. (2000). Production of very-high-amylose potato starch by inhibition of SBE A and B. *Nature biotechnology, 18*(5), 551-554.

Scofield, G. N., Ruuska, S. A., Aoki, N., Lewis, D. C., Tabe, L. M., & Jenkins, C. L. (2009). Starch storage in the stems of wheat plants: localization and temporal changes. *Ann Bot, 103*(6), 859-868.

Searle, I., He, Y., Turck, F., Vincent, C., Fornara, F., Kröber, S., Amasino, R. A., & Coupland, G. (2006). The transcription factor FLC confers a flowering response to vernalization by repressing meristem competence and systemic signaling in Arabidopsis. *Genes Dev, 20*(7), 898-912.

Secchi, F., & Zwieniecki, M. A. (2016). Accumulation of sugars in the xylem apoplast observed under water stress conditions is controlled by xylem pH. *Plant Cell Environ, 39*(11), 2350-2360.

Sehr, E. M., Agusti, J., Lehner, R., Farmer, E. E., Schwarz, M., & Greb, T. (2010). Analysis of secondary growth in the Arabidopsis shoot reveals a positive role of jasmonate signalling in cambium formation. *Plant J, 63*(5), 811-822.

Servaites, J. C., Fondy, B. R., Li, B., & Geiger, D. R. (1989). Sources of carbon for export from spinach leaves throughout the day. *Plant Physiology, 90*(3), 1168-1174.

Sherrard, M. E., & Maherali, H. (2006). The adaptive significance of drought escape in Avena barbata, an annual grass. *Evolution, 60*(12), 2478-2489.

Shimada, T. L., & Hara-Nishimura, I. (2015). Leaf oil bodies are subcellular factories producing antifungal oxylipins. *Curr Opin Plant Biol, 25*, 145-150.

Shimada, T. L., Shimada, T., Takahashi, H., Fukao, Y., & Hara-Nishimura, I. (2008). A novel role for oleosins in freezing tolerance of oilseeds in Arabidopsis thaliana. *Plant J, 55*(5), 798-809.

Shockey, J. M., Gidda, S. K., Chapital, D. C., Kuan, J. C., Dhanoa, P. K., Bland, J. M., Rothstein, S. J., Mullen, R. T., & Dyer, J. M. (2006). Tung tree DGAT1 and DGAT2 have nonredundant functions in triacylglycerol biosynthesis and are localized to different subdomains of the endoplasmic reticulum. *Plant Cell, 18*(9), 2294-2313.

Silva, F. G. d., Cangussu, L. M. B., Paula, S. L. A. d., Melo, G. A., & Silva, E. A. (2013). Seasonal changes in fructan accumulation in the underground organs of Gomphrena marginata Seub.(Amaranthaceae) under rock-field conditions. *Theoretical and Experimental Plant Physiology, 25*(1), 46-55.

Šimášková, M., O'Brien, J. A., Khan, M., Van Noorden, G., Ötvös, K., Vieten, A., De Clercq, I., Van Haperen, J. M. A., Cuesta, C., Hoyerová, K., Vanneste, S., Marhavý, P., Wabnik, K., Van

Breusegem, F., Nowack, M., Murphy, A., Friml, J., Weijers, D., Beeckman, T., & Benkova, E. (2015). Cytokinin response factors regulate PIN-FORMED auxin transporters. *Nat Commun, 6*, 8717.

Simon, E. (1974). Phospholipids and plant membrane permeability. *New Phytologist, 73*(3), 377-420.

Smith, A. M., & Zeeman, S. C. (2020). Starch: A Flexible, Adaptable Carbon Store Coupled to Plant Growth. *Annu Rev Plant Biol, 71*, 217-245.

Ståhl, U., Carlsson, A. S., Lenman, M., Dahlqvist, A., Huang, B., Banas, W., Banas, A., & Stymne, S. (2004). Cloning and functional characterization of a phospholipid:diacylglycerol acyltransferase from Arabidopsis. *Plant Physiol, 135*(3), 1324-1335.

Stitt, M., & Zeeman, S. C. (2012). Starch turnover: pathways, regulation and role in growth. *Curr Opin Plant Biol, 15*(3), 282-292.

Stobart, K., Mancha, M., Lenman, M., Dahlqvist, A., & Stymne, S. (1997). Triacylglycerols are synthesised and utilized by transacylation reactions in microsomal preparations of developing safflower (Carthamus tinctorius L.) seeds. *Planta, 203*(1), 58-66.

Suer, S., Agusti, J., Sanchez, P., Schwarz, M., & Greb, T. (2011). WOX4 imparts auxin responsiveness to cambium cells in Arabidopsis. *Plant Cell, 23*(9), 3247-3259.

Sundberg, B. (2000). Cambial growth and auxin gradients. *Cell and molecular biology of wood formation*, 169-188.

Thiam, A. R., Farese, R. V., Jr., & Walther, T. C. (2013). The biophysics and cell biology of lipid droplets. *Nat Rev Mol Cell Biol, 14*(12), 775-786.

Thomas, H. (2013). Senescence, ageing and death of the whole plant. *New Phytol, 197*(3), 696-711.

Tsai, C. H., Zienkiewicz, K., Amstutz, C. L., Brink, B. G., Warakanont, J., Roston, R., & Benning, C. (2015). Dynamics of protein and polar lipid recruitment during lipid droplet assembly in Chlamydomonas reinhardtii. *Plant J, 83*(4), 650-660.

Tuominen, H., Puech, L., Fink, S., & Sundberg, B. (1997). A radial concentration gradient of indole-3-acetic acid is related to secondary xylem development in hybrid aspen. *Plant Physiology, 115*(2), 577-585.

Usami, T., Horiguchi, G., Yano, S., & Tsukaya, H. (2009). The more and smaller cells mutants of Arabidopsis thaliana identify novel roles for SQUAMOSA PROMOTER BINDING PROTEIN-LIKE genes in the control of heteroblasty. *Development, 136*(6), 955-964.

Uggla, C., Mellerowicz, E. J., & Sundberg, B. (1998). Indole-3-acetic acid controls cambial growth in Scots pine by positional signaling. *Plant Physiology, 117*(1), 113-121.

Uggla, C., Moritz, T., Sandberg, G., & Sundberg, B. (1996). Auxin as a positional signal in pattern formation in plants. *Proceedings of the National Academy of Sciences of the United States of America*, *93*(17), 9282–9286.

van der Schoot, C., Paul, L. K., Paul, S. B., & Rinne, P. L. (2011). Plant lipid bodies and cell-cell signaling: a new role for an old organelle? *Plant Signal Behav, 6*(11), 1732-1738.

van Wijk, K. J., & Kessler, F. (2017). Plastoglobuli: Plastid Microcompartments with Integrated Functions in Metabolism, Plastid Developmental Transitions, and Environmental Adaptation. *Annu Rev Plant Biol, 68*, 253-289.

Vayssières, A., Mishra, P., Roggen, A., Neumann, U., Ljung, K., & Albani, M. C. (2020). Vernalization shapes shoot architecture and ensures the maintenance of dormant buds in the perennial Arabis alpina. *New Phytol, 227*(1), 99-115.

Vieira, C., & Figueiredo□Ribeiro, R. (1993). Fructose□containing carbohydrates in the tuberous root of Gomphrena macrocephala St.□Hil.(Amaranthaceae) at different phenological phases. *Plant, Cell & Environment, 16*(8), 919-928.

Visser, R. G., Vreugdenhil, D., Hendriks, T., & Jacobsen, E. (1994). Gene expression and carbohydrate content during stolon to tuber transition in potatoes (Solanum tuberosum). *Physiologia Plantarum, 90*(2), 285-292.

Waldie, T., McCulloch, H., & Leyser, O. (2014). Strigolactones and the control of plant development: lessons from shoot branching. *Plant J, 79*(4), 607-622.

Walther, T. C., Chung, J., & Farese, R. V., Jr. (2017). Lipid Droplet Biogenesis. *Annu Rev Cell Dev Biol, 33*, 491-510.

Wang, R., Albani, M. C., Vincent, C., Bergonzi, S., Luan, M., Bai, Y., Kiefer, C., Castillo, R., & Coupland, G. (2011). Aa TFL1 confers an age-dependent response to vernalization in perennial Arabis alpina. *Plant Cell, 23*(4), 1307-1321.

Wang, R., Farrona, S., Vincent, C., Joecker, A., Schoof, H., Turck, F., Alonso-Blanco, C., Coupland, G., & Albani, M. C. (2009). PEP1 regulates perennial flowering in Arabis alpina. *Nature, 459*(7245), 423-427.

Wang, G., Lin, Q., & Xu, Y. (2007). Tetraena mongolica Maxim can accumulate large amounts of triacylglycerol in phloem cells and xylem parenchyma of stems. *Phytochemistry, 68*(15), 2112-2117.

Wang, C., & Tillberg, J. E. (1996). Effects of nitrogen deficiency on accumulation of fructan and fructan metabolizing enzyme activities in sink and source leaves of barley (Hordeum vulgare). *Physiologia Plantarum, 97*(2), 339-345.

Wang, C., Van den Ende, W., & Tillberg, J.-E. (2000). Fructan accumulation induced by nitrogen deficiency in barley leaves correlates with the level of sucrose: fructan 6-fructosyltransferase mRNA. *Planta, 211*(5), 701-707.

Wani, S. H., Kumar, V., Shriram, V., & Sah, S. K. (2016). Phytohormones and their metabolic engineering for abiotic stress tolerance in crop plants. *The Crop Journal, 4*(3), 162-176.

Watanabe, M., Netzer, F., Tohge, T., Orf, I., Brotman, Y., Dubbert, D., Fernie, A. R., Rennenberg, H., Hoefgen, R., & Herschbach, C. (2018). Metabolome and Lipidome Profiles of Populus x canescens Twig Tissues During Annual Growth Show Phospholipid-Linked Storage and Mobilization of C, N, and S. *Front Plant Sci, 9*, 1292.

Wewer, V., Dombrink, I., vom Dorp, K., & Dormann, P. (2011). Quantification of sterol lipids in plants by quadrupole time-of-flight mass spectrometry. *J Lipid Res, 52*(5), 1039-1054.

Whitford, R., Fernandez, A., De Groodt, R., Ortega, E., & Hilson, P. (2008). Plant CLE peptides from two distinct functional classes synergistically induce division of vascular cells. *Proceedings of the National Academy of Sciences, 105*(47), 18625-18630.

Whyte, R. O. (1977). The botanical Neolithic revolution. *Human Ecology, 5*(3), 209-222.

Wildhagen, H., Durr, J., Ehlting, B., & Rennenberg, H. (2010). Seasonal nitrogen cycling in the bark of field-grown Grey poplar is correlated with meteorological factors and gene expression of bark storage proteins. *Tree Physiol, 30*(9), 1096-1110.

Willing, E. M., Rawat, V., Mandakova, T., Maumus, F., James, G. V., Nordström, K. J. V., Becker, C., Warthmann, N., Chica, C., Szarzynska, B., Zytnicki, M., Albani, M. C., Kiefer, C., Bergonzi, S., Castaings, L., Mateos, J. L. Berns, M. C., Bujdoso, N., Piofczyk, T., de Lorenzo, L., Barrero-Sicilia, C., Mateos, I., Piednoël, M., Hagmann, J., Chen-Min-Tao, R., Iglesias-Fernández, R., Schuster, S. C., Alonso-Blanco, C., Roudier, F., Carbonero, P., Paz-Ares, J., Davis, S. J., Pecinka, A., Quesneville, H., Colot, V., Lysak, M. A., Weigel, D., Coupland, G., & Schneeberger, K. (2015). Genome expansion of Arabis alpina linked with retrotransposition and reduced symmetric DNA methylation. *Nat Plants, 1*, 14023.

Willmann, M. R., & Poethig, R. S. (2011). The effect of the floral repressor FLC on the timing and progression of vegetative phase change in Arabidopsis. *Development, 138*(4), 677-685.

Wyka, T. (1999). Carbohydrate storage and use in an alpine population of the perennial herb, Oxytropis sericea. *Oecologia, 120*(2), 198-208.

Xu, C., Hartel, H., Wada, H., Hagio, M., Yu, B., Eakin, C., & Benning, C. (2002). The pgp1 mutant locus of Arabidopsis encodes a phosphatidylglycerolphosphate synthase with impaired activity. *Plant Physiol, 129*(2), 594-604.

Xu, M., Hu, T., Zhao, J., Park, M. Y., Earley, K. W., Wu, G., Yang, L., & Poethig, R. S. (2016). Developmental Functions of miR156-Regulated SQUAMOSA PROMOTER BINDING PROTEIN-LIKE (SPL) Genes in Arabidopsis thaliana. *PLoS Genet, 12*(8), e1006263.

Xue, H.-W., Hosaka, K., Plesch, G., & Mueller-Roeber, B. (2000). Cloning of Arabidopsis thaliana phosphatidylinositol synthase and functional expression in the yeast pis mutant. *Plant Molecular Biology, 42*(5), 757-764.

Yen, C. L., Stone, S. J., Koliwad, S., Harris, C., & Farese, R. V., Jr. (2008). Thematic review series: glycerolipids. DGAT enzymes and triacylglycerol biosynthesis. *J Lipid Res, 49*(11), 2283-2301.

Yu, T. S., Kofler, H., Häusler, R. E., Hille, D., Flügge, U. I., Zeeman, S. C., Smith, A. M., Kossmann, J., Lloyd, J., Ritte, G., Steup, M., Lue, W. L., Chen, J., & Weber, A. (2001). The Arabidopsis sex1 mutant is defective in the R1 protein, a general regulator of starch degradation in plants, and not in the chloroplast hexose transporter. *The Plant Cell, 13*(8), 1907-1918.

Zhang, M., Fan, J., Taylor, D. C., & Ohlrogge, J. B. (2009). DGAT1 and PDAT1 acyltransferases have overlapping functions in Arabidopsis triacylglycerol biosynthesis and are essential for normal pollen and seed development. *Plant Cell, 21*(12), 3885-3901.

Zhang, Z., Cheng, Z. J., Gan, L., Zhang, H., Wu, F. Q., Lin, Q. B., Wang, J. L., Wang, J., Guo, X. P., Zhang, X., Zhao, Z. C, Lei, C. L., Zhu, S. S., Wang, C. M., & Wan, J. M. (2016). OsHSD1, a hydroxysteroid dehydrogenase, is involved in cuticle formation and lipid homeostasis in rice. *Plant Science, 249*, 35-45.

Zheng, Z., Xia, Q., Dauk, M., Shen, W., Selvaraj, G., & Zou, J. (2003). Arabidopsis AtGPAT1, a member of the membrane-bound glycerol-3-phosphate acyltransferase gene family, is essential for tapetum differentiation and male fertility. *Plant Cell, 15*(8), 1872-1887.

Zhou, C. M., Zhang, T. Q., Wang, X., Yu, S., Lian, H., Tang, H., Feng, Z. Y., Zozomova-Lihová, J., & Wang, J. W. (2013). Molecular basis of age-dependent vernalization in Cardamine flexuosa. *Science, 340*(6136), 1097-1100.

Zou, J., Wei, Y., Jako, C., Kumar, A., Selvaraj, G., & Taylor, D. C. (1999). The Arabidopsis thaliana TAG1 mutant has a mutation in a diacylglycerol acyltransferase gene. *The Plant Journal, 19*(6), 645-653.

7 Manuscript 1

Cytokinin-promoted secondary growth and nutrient storage in the perennial stem zone of *Arabis alpina*

Cytokinin-promoted secondary growth and nutrient storage in the perennial stem zone of *Arabis alpina*

Anna Sergeeva[1,4], Hongjiu Liu[1], Hans-Jörg Mai[1], Tabea Mettler-Altmann[2,4], Christiane Kiefer[3], George Coupland[3,4], Petra Bauer[1,4]

[1] Heinrich Heine University, Institute of Botany, D-40225 Düsseldorf, Germany

[2] Heinrich Heine University, Institute of Plant Biochemistry, D-40225 Düsseldorf, Germany

[3] Max Planck Institute for Plant Breeding Research, Department of Plant Developmental Biology, D-50829 Cologne, Germany

[4]Cluster of Excellence on Plant Science (CEPLAS), Heinrich Heine University, Düsseldorf, Germany

Correspondence to: Petra Bauer, Institute of Botany, Heinrich Heine University, Universitätstrasse 1, D-40225 Düsseldorf, Germany

Email: petra.bauer@uni-duesseldorf.de

Tel: +49 211 81-13479, Fax: +49 211 81-12881

Anna Sergeeva, Anna.Sergeeva@uni-duesseldorf.de
Hongjiu Liu, liured9@nwafu.edu.cn
Hans-Jörg Mai, Hans-Joerg.Mai@hhu.de
Tabea Mettler-Altmann, tabeam@yahoo.de
Christiane Kiefer, christiane.kiefer@cos.uni-heidelberg.de
George Coupland, coupland@mpipz.mpg.de
Petra Bauer, Petra.Bauer@hhu.de

Running title

Secondary growth and nutrient storage in *Arabis alpina*

Highlight

Arabis alpina stems have a perennial zone with secondary growth, where cambium and derivatives store high molecular weight compounds independent of vernalization. Cytokinins are signals for the perennial secondary growth zone.

Keywords (10)

Cambium, cytokinin, lipid body, nutrient storage, perennial, phloem parenchyma, secondary growth, starch, triacylglycerol, vernalization

Abbreviations

ACC, 1-aminocyclopropane-1-carboxylic acid

ANOVA, analysis of variance

AZ, annual growth zone

BAP, benzylaminopurine

C, carbon

CDS, coding sequences

EA-IRMS, elemental analysis isotope ratio mass spectrometry

FAME, fatty acid methylester

FCA, fuchsine, chrysoidine, astra blue

FLC, FLOWERING LOCUS C

GA, gibberellin

GC-MS, gas chromatography-mass spectrometry

GO, gene ontology

HC, hierarchical clustering

I, inflorescence zone

N, nitrogen

NAA, naphthaleneacetic acid

NAD, nicotinamide adenine dinucleotide

Paj, Pajares

PCA, Principal Component Analysis

PEP1, PERPETUAL FLOWERING 1

PZ, perennial growth zone

RNA-seq, RNA-sequencing

SPL, SQUAMOSA PROMOTER BINDING PROTEIN-LIKE

TAG, triacylglycerol

TPM, transcripts per million

V, vegetative growth zone

Abstract

Perennial plants maintain their life span through several growth seasons. *Arabis alpina* serves as model Brassicaceae species to study perennial traits. *A. alpina* lateral stems have a proximal vegetative zone with a dormant bud zone, and a distal senescing seed-producing inflorescence zone. We addressed the questions of how this zonation is distinguished at the anatomical level, whether it is related to nutrient storage, and which signals affect the zonation. We found that the vegetative zone exhibits secondary growth, which we termed the perennial growth zone (PZ). High molecular weight carbon compounds accumulate there in cambium and cambium derivatives. Neither vernalization nor flowering were requirements for secondary growth and sequestration of storage compounds. The inflorescence zone with only primary growth, termed annual growth zone (AZ), or roots exhibited different storage characteristics. Following cytokinin application, cambium activity was enhanced and secondary phloem parenchyma was formed in the PZ and also in the AZ. In transcriptome analysis, cytokinin-related genes represented enriched gene ontology terms and were expressed at higher level in the PZ than the AZ. Thus, *A. alpina* uses primarily the vegetative PZ for nutrient storage, coupled to cytokinin-promoted secondary growth. This finding lays a foundation for future studies addressing signals for perennial growth.

Introduction

Perennial plants sustain their life span through several growth seasons and many of these plants are polycarpic and reproduce multiple times (Bergonzi and Albani, 2011). This allows plants to maintain space in their environment, to exploit and defend light and soil resources, and to survive harsh conditions. In contrast, annual plants are usually monocarpic and reproduce only once before they die (Thomas, 2013), a life style of advantage in lowland dry habitats with animal foraging and agriculture in favor of juvenile survival.

Vegetative above-ground shoots of perennial plants may grow in diameter over the years. This production of new tissues in the lateral dimension is termed secondary growth and is initiated by two secondary meristems. The fascicular and interfascicular cambium produces new vasculature in the form of secondary xylem and secondary phloem and corresponding parenchyma, leading to the formation of wood and bast. The cork cambium or phellogen produces outward cork and inward phelloderm to generate new protective outer layers, periderm, with increasing stem diameter. A diverse set of phytohormones and signals influences cambial activity in stems (Fischer *et al.*, 2019). Hormonal profiling across the *Populus trichocarpa* stem identified a specific but interconnected distribution of hormones (Immanen *et al.*, 2016). Cytokinins peaked in the developing phloem tissue, while auxin had its maximum in the dividing cambial cells, and developing xylem tissue was marked by bioactive gibberellin (Immanen *et al.*, 2016). Cytokinins are key regulators of cambium initiation, and cambial activity is affected in cytokinin biosynthetic mutants and by cytokinin supply (Matsumoto-Kitano *et al.*, 2008; Nieminen *et al.*, 2008). Cambial auxin concentration is relevant for activity and maintenance of cambium (Immanen *et al.*, 2016), for example through homeobox transcription factors regulating auxin-dependent cambium proliferation (Suer *et al.*, 2011; Kucukoglu *et al.*, 2017). Gibberellins act in the xylem region promoting xylem cell differentiation and lignification (Denis *et al.*, 2017). Secondary growth is coupled with nutrient allocation. In *Populus*, carbon storage, in the form of triacylglycerols (TAGs), galactose and raffinose, is present in the stem bark and wood tissues (Sauter and van Cleve, 1994; Sauter and Wellenkamp, 1998; Watanabe *et al.*, 2018). Nutrient deposition in storage organs is also affected by plant hormones, and cytokinins may play a dual role in some perennials to direct secondary growth and nutrient storage therein (Hartmann *et al.*, 2011; Eviatar-Ribak *et al.*, 2013).

The perennial life strategy is usually regarded to be ancestral (Hu *et al.*, 2003; Grillo *et al.*, 2009) which is also true for the tribe Arabideae within the Brassicaceae. Interestingly, in this tribe annuality has evolved multiple times independently from a perennial background in different lineages (Karl and Koch, 2013). This suggests that this complex life style decision may be determined by a limited set of regulatory events. Phylogenetic reconstruction has shown that perennial *Arabis alpina* and annual *Arabis montbretiana* are sister species. Hence, these two taxa have been established as a model system to study the perennial-annual transition (Kiefer *et al.*, 2017; Heidel *et al.*, 2016).

A. alpina Pajares (Paj), an accession from Spain, was used to characterize the perennial life cycle of the species. These plants have above-ground vegetative perennial parts and stems as well as reproductive ones that senesce and die during the growth season (Wang *et al.*, 2009). A characteristic of perennial vegetative stems is the transition from juvenile to adult phase, which results in flowering (Bergonzi and Albani, 2011; Hyun *et al.*, 2017). Competence to flower in perennial *A. alpina* like in annual *Arabidopsis thaliana* can be conferred by the ecologically relevant adaptive trait of vernalization during a cold winter period which suppresses flowering until the action of repressors is released (Kim *et al.*, 2009; Wang *et al.*, 2009). The positions of individual flowers, dormant buds, non-flowering and flowering lateral branches vary along the stems of *A. alpina*. From bottom to top, three types of vegetative (V1, V2, V3) and two inflorescence (I1, I2) subzones are distinguished, established during and after vernalization (Lazaro *et al.*, 2018). V1 has full lateral branches resembling the main shoot axis in terms of the zonation pattern. V2 has dormant axillary buds, and the short V3 subzone axillary vegetative branches. I1 has lateral branches forming inflorescences, while I2 is an inflorescence and forms individual flowers (Lazaro *et al.*, 2018). The signals and genetic networks triggering the differentiation of V and I zones are not fully understood. *A. alpina PERPETUAL FLOWERING 1* (*PEP1*) similar to its orthologue in *Arabidopsis*, *FLOWERING LOCUS C* (*FLC*), is a regulator of flowering in response to vernalization and acts as floral repressor (Wang *et al.*, 2009). The *pep1-1* mutant, a derivative of the wild-type accession Paj, shows constant reproduction. Despite lower longevity and the absence of the sub-zonation of the vegetative stem zone, *pep1-1* plants show perennial growth characteristics and have the ability to form continuously new lateral branches until the end of the growth season (Wang *et al.*, 2009; Hughes *et al.*, 2019). Thus, flowering control pathways are regulated by the age control systems to maintain the perennial life style (Hyun *et al.*, 2019). Besides vernalization auxin signals are also involved (Vayssières *et al.*, 2020).

The regulation of nutrient allocation is fundamental for the perennial life cycle to re-initiate growth. In this study, we provide evidence that the proximal vegetative stem zone is characterized by secondary growth where nutrient storage takes place (termed here perennial zone, PZ), irrespective of flowering control by *PEP1*. In contrast, the distal reproductive zone has primary growth (here annual zone, AZ). We furthermore show that cytokinin is effective in initiating secondary growth and we propose a heterochronic model for PZ-AZ transitioning.

Materials and Methods

Plant material, growth conditions and plant harvesting

Perennial *Arabis alpina* wild type Pajares (Paj) accession, perpetual flowering mutant *pep1-1* (Wang *et al.*, 2009) and annual *A. montbretiana* (Kiefer *et al.*, 2017) plants were grown on potting soil (Vermehrungssubstrat, Stender GmbH, Schermbeck, Germany) with a humidity of 70 % in a plant growth chamber (Percival Scientific, CLF Plant Climatics) under controlled long-day (16 h light and 8

h dark, at 20 °C) or short-day (8 h light and 16 h dark, at 4 °C for vernalization) conditions and harvested at stages I, II, III, and II', as described in the Result section and corresponding figures. Plants were fertilized every second week using universal Wuxal (Aglukon, Germany). All experiments were performed with 3-7 biological replicate plants, as indicated in the text. For anatomical analysis, 4-11 internode cross sections were prepared per lateral stem sample and stored in 70 % ethanol (Supplemental Figure S1).

Biochemical analysis was conducted with lateral stems from nodes 1 to 5 of the main axis in the case of Paj and *pep1-1* or all lateral stems of *A. montbretiana*. Internodes of one plant were dissected and pooled as one biological replicate, deep-frozen in liquid nitrogen, and stored at -80 °C. Entire root systems of single plants were harvested as one root sample and residual soil was removed. Plant samples were freeze-dried using a lyophilizer and ground to fine powder in a mixer mill (Mixer Mill MM 200, Retsch, Haan, Germany). All biochemical measurements were conducted with the same plant samples (Supplemental Figure S1).

For hormone treatments, *pep1-1* plants were grown as above under long-day conditions for 4 to 5 weeks. The two lateral branches with one elongated internode in a juvenile PZ stage were treated with 300 µl of either 2 mM 6-benzylaminopurine (BAP), 0.5 mM 1-naphthaleneacetic acid (NAA), 4 mM gibberellin GA_3 (GA) or 2 mM 1-aminocyclopropane-1-carboxylic acid (ACC) solution (or mock-treated, in 50 % ethanol, mixed with 10 mg lanolin and pasted with a brush along the first internode). The treatment was repeated after 4 days, and internodes were harvested after eight days. AZ treatment was initiated when the plants were 18 weeks old and two elongated internodes of the AZ were formed. Both internodes of five replicate plants were treated with 2 mM BAP solution, as described above. The treatment was performed for 46 days until siliques and uppermost part of the AZ of the control plants started to senesce. Every newly formed and already present internodes were treated every fourth day. Harvested AZs were divided into three regions ("top", "middle", and "bottom") comprising two to three internodes.

For RNA-sequencing (RNA-seq), 12 *pep1-1* plants were grown per biological replicate. Three biological replicates were used for each examined sampling stage, as described in the text and corresponding figures. Plant samples were immediately deep-frozen in liquid nitrogen, stored at -80 °C and ground to fine powder before use.

Microscopic analysis

50-100 µm hand-made cross internode sections were incubated for 5-8 minutes in 1 mg/ml fuchsine, 1 mg/ml chrysoidine, 1 mg/ml astra blue, 0.025 ml/ml acetic acid staining (= FCA staining) solution, washed in water and alcohol solutions and mounted. For starch staining, sections were incubated for 5 minutes in 50 % Lugol solution (Sigma-Aldrich GmbH), rinsed in water and mounted. For lipid staining, sections were incubated for 30 minutes in a filtered solution of 0.5 % Sudan IV in 50 % isopropanol, rinsed in water and mounted. Pictures were taken with an Axio Imager 2 microscope

(Carl Zeiss Microscopy, Jena, Germany), equipped with an Axiocam 105 color camera (Carl Zeiss Microscopy, Jena, Germany) using bright-field illumination. Images were processed and tissue width quantified via ZEN 2 (blue edition) software (Carl Zeiss Microscopy, Jena, Germany).

Starch quantification

Starch was quantified enzymatically according to Smith and Zeeman (2006). Briefly, starch was extracted by boiling 10 mg lyophilized plant material in 80 % ethanol. Extracted starch granules were gelatinized at 100 °C. After incubation with α-amyloglucosidase and α-amylase the samples were assayed for glucose in a microplate reader (Tecan Group, Männedorf, Switzerland) using hexokinase and glucose 6-phosphate dehydrogenase to monitor reduction of NAD^+ at 340 nm (extinction coefficient 6220 l/mol cm).

Triacylglycerol (TAG) quantification

TAGs were obtained by fractionation of glycerolipids and quantified based on their fatty acid contents, normalized to plant sample dry weight (Sergeeva *et al.*, Manuscript 2). Briefly, lipids were isolated from dried plant samples according to a modified acidic chloroform/methanol extraction method for glycerolipids (Hajra *et al.*, 1974; Wewer *et al.*, 2011). TAGs were separated from glycolipid and phospholipid fractions by successive elution with chloroform, acetone/isopropanol, methanol. Fatty acid methylesters (FAMEs) of the TAG fatty acids or of the total fatty acids from plant samples were analyzed by gas chromatography-mass spectrometry (GC-MS) and resulting peaks integrated for quantification (Sergeeva *et al.*, Manuscript 2).

Protein content determination

10 mg lyophilized plant material was taken up in 200 µl (for stems) or 300 µl (for roots) of Laemmli buffer (2 % SDS, 10 % glycerol, 60 mM Tris-HCl pH 6.8, 0.005 % bromphenol blue, 0.1 M DTT) and heated at 95 °C for 10 minutes. Total protein contents were assayed using the 2-D Quant Kit (GE Healthcare, Little Chalfont, UK), measuring OD_{480} in a microplate reader (Tecan Group, Männedorf, Switzerland) using a bovine serum albumin mass standard curve.

Determination of carbon (C) and nitrogen (N)

For C and N quantification, 2 mg of lyophilized plant material, packed into tin containers, was applied to elemental analysis isotope ratio mass spectrometry (EA-IRMS) (Elementar Analysensysteme, Germany). C/N ratios were calculated from C and N values.

RNA isolation

Total RNA from plant samples was isolated using the RNeasy Plant Mini Kit (Qiagen, Hilden, Germany), including DNase I digestion via the RNase-Free DNase Set to remove traces of genomic DNA (Qiagen, Hilden, Germany). Quality and quantity of the isolated RNA was examined with the

Fragment Analyzer (Advanced Analytical Technologies GmbH, Heidelberg, Germany). All samples had a suitable RNA quality number above 7.0 (RQN mean = 8.9).

RNA sequencing and analysis

RNA-seq analysis was conducted for three biological replicates per sample. For gene expression profiling, libraries were prepared using the Illumina TruSeq® Stranded mRNA Library Prep kit. Prepared libraries were sequenced on the HiSeq3000 system (Illumina Inc. San Diego, CA, USA) with a read setup of 1 x 150 bp and an expected number of 28 Mio reads.

Using the latest publicly available versions of the *A. alpina* genome assembly (Arabis_alpina.MPIPZ.V5.chr.all.fasta and Arabis_alpina.MPIPZ.V5.chr.all.liftOverV4.v3.gff3, both downloaded from arabis-alpina.org), 34.220 coding sequences (CDS) were assembled. Closest *A. thaliana* orthologues were determined by blasting *A. alpina* CDS assemblies against the most recent version of the *A. thaliana* proteome sequences (TAIR10_pep_20101214_updated; downloaded from TAIR) using the *blastx* algorithm of the Blast+ suite (Altschul *et al.*, 1990) with an E-value threshold of < 1E5. Among multiple resulting hits, the *Arabidopsis* proteins with the highest bit score followed by the lowest E value were accepted as the closest orthologues if the percentage of identity was > 25 % of the aligned amino acids (Doolittle, 1986) and the E-value was < 1E-15. Single end reads were trimmed with *trimmomatic* (Bolger *et al.*, 2014) and the quality of the trimmed reads was evaluated with *fastqc* (Andrews, 2010). Using *kallisto* (Bray *et al.*, 2016), the trimmed reads were mapped to the *A. alpina* CDS assemblies and quantified, which resulted in estimated counts and transcripts per million (TPM) values per gene. As a control, the trimmed reads were mapped to the genome assembly with *hisat2* (Kim *et al.*, 2015) and transcripts were quantified with *htseq-count* (Anders *et al.*, 2015) using a gene transfer format (*.gtf) file that was generated from the general feature format (*.gff3) file. The resulting counts were transformed to TPM and used for Principal Component Analysis (PCA, R: *prcomp*) and hierarchical clustering (HC, R: *dist*, *hclust*). Estimated counts were used for statistical analysis using *edgeR* (Robinson *et al.*, 2010; McCarthy *et al.*, 2012). Resulting p-values were adjusted with the Bonferroni method. Fold-change values of gene expression were calculated in pairwise comparisons between samples and pooled PZ and AZ samples. The above-described calculations were performed with the values obtained from *kallisto* and with those obtained from *hisat2* and *htseq-count*. Genes were accepted as differentially regulated if $P < 0.01$ with both mapping and quantification methods. Graphs were produced with TPMs obtained by *kallisto*.

Gene ontology (GO) analysis was carried out using *topGO* (Alexa and Rahnenfuhrer, 2010) with the closest *A. thaliana* ortholog Locus ID's (AGI code) using the latest publicly available *A. thaliana* GO annotations (go_ensembl_arabidopsis_thaliana.gaf; downloaded from Gramene) applying Fisher's exact test. GO terms were enriched with $P < 0.05$.

The full transcriptome data set is available under the GEO no. GSE152417.

Gene expression by reverse transcription-qPCR

Total RNA was reverse-transcribed into cDNA using oligo dT primer and diluted cDNA used for qPCR, as described (Ben Abdallah and Bauer, 2016). Absolute normalized gene expression values were calculated based on mass standard curve analysis and reference gene normalization (Stephan *et al.*, 2019). Primers for qPCR are listed in Supplemental Table S1.

Statistical analysis

R software was used to perform statistical analyses by one-way analysis of variance (ANOVA) in conjunction with Tukey's HSD (honest significant difference) test ($\alpha = 0.05$). Significant differences with $P < 0.05$ are indicated by different letters.

Results

Lateral stems of *A. alpina* plants have a perennial secondary growth and annual primary growth zone

To investigate nutrient storage in *A. alpina* stems, we first inspected the anatomy of stem internode cross sections. Since nutrient storage might be coupled with signals for vernalization, we included besides vernalization-dependent wild-type Pajares (Paj) also its mutant derivative *perpetual flowering 1-1* (*pep1-1*), that flowers independently of vernalization. We performed comparisons of perennial lines to annual sister species *A. montbretiana* which does not require vernalization, either. We focused on internodes of the lateral branches, formed in the V1 subzone of the main axis at the lower first to fifth nodes. Sub-zonation into three V zones (V1, V2, and V3) is present in Paj, but absent in *pep1-1*. Instead, *pep1-1* has a single V zone, V1, and all axillary buds develop into flowering branches (Wang *et al.*, 2009; Vayssières *et al.*, 2020). Thus, by investigating lateral branches from V1 we were able to study the role of *PEP1* in stem development and nutrient allocation.

The anatomy of these lateral branches changed from the vegetative (V) to inflorescence (I) zone. Paj V internodes displayed secondary growth with cambium and cork cambium activities. Since advanced secondary growth is a perennial trait, we termed this zone "perennial zone" ("PZ", Figure 1). I zone internodes had only primary growth characteristics in Paj, and accordingly, we termed this zone "annual zone" ("AZ", Figure 1). *pep1-1* showed a PZ and an AZ as Paj, while *A. montbretiana* lateral stems displayed the AZ pattern (Figure 1).

Next, we inspected lateral stem anatomy more closely at specific growth stages during development of the PZ and AZ, namely at stage I (after 8 weeks, before vernalization), at stages II and III (after 20 and 35 weeks including vernalization) and at stage II' (after 20 weeks without vernalization) (Figure 2, see Supplemental Figure S2 for detailed descriptions of plant growth). At stages I and II, lateral branches had vegetative character (Figure 2B) and all elongated internodes corresponded to PZ with beginning secondary growth, similar in Paj and *pep1-1* (PZ in Figure 3A, Figure 3B). At stage I

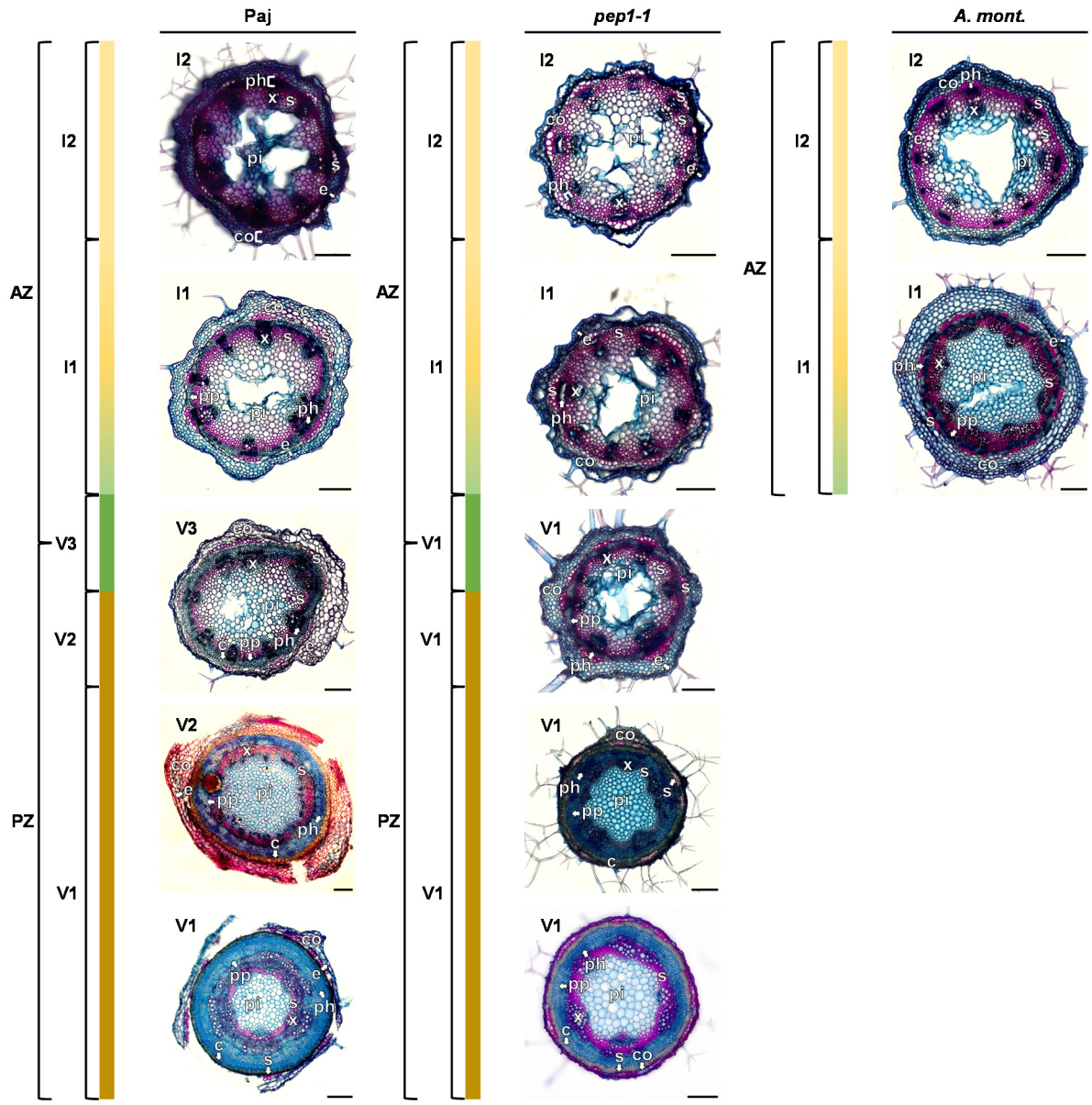

Figure 1. Overview of lateral stem internode anatomy of perennial and annual *Arabis* plants. 100 µm cross sections of lateral stems formed at the lower nodes of main stems from perennial *A. alpina* Pajares (Paj, wild type), its *perpetual flowering1-1* (*pep1-1*) mutant derivative, and annual *A. montbretiana* (*A. mont.*). Plants were harvested at different growth stages (see Figure 2, red triangles indicate positions of cross sections). A „perennial zone" (PZ) with secondary growth characteristics is found at the proximal side of lateral branches, corresponding to the vegetative zone (V1, V2, described for main stems in Lazaro *et al.*, 2018), while an „annual zone" (AZ) with primary growth overlaps with inflorescence zone (I1, I2, described in main stems in Lazaro *et al.*, 2018). PZ and AZ are separated by a transition zone (V3, described for main stems in Lazaro *et al.*, 2018). Anatomy, investigated following FCA staining, in blue, staining of non-lignified cell walls (parenchyma, phloem, meristematic cells), in red, staining of lignified cell walls, and greenish, staining of suberized cell walls (xylem, sclerenchyma, cork). Abbreviations used in microscopic images: c, cork; co, cortex; e, epidermis; ph, phloem including primary phloem, secondary phloem, phloem parenchyma; pi, pith; pp, secondary phloem parenchyma; s, sclerenchyma; x, xylem including primary xylem, secondary xylem, xylem parenchyma. Arrows point to respective tissues. Scale bars, 200 µm.

(Figure 3A), epidermis and cortex were separated from the central pith by a ring of vascular bundles. Cambium was narrow, surrounded by few layers of secondary phloem. We noted a ring of cork

cambium below the sclerenchyma cap in vascular bundles and below the outer cortex in the interfascicular region. Cork cells were formed already in some regions (note that this tissue became more evident at later stages). At stage II (Figure 3B), cork formation underneath the outer cortex had progressed to a multi-cell-layer-thick ring in the PZ. Cortical and epidermal cells were compressed and showed lignification (appeared reddish by FCA staining, Figure 3B). At stage III, lateral branches of Paj flowered and formed green siliques, and those of *pep1-1* were in a more advanced reproductive state and already senescent (Figure 2B). Secondary growth was further progressed in the PZ (PZ in Figure 3C). The lower lateral stem internodes of Paj and *pep1-1* had hardly any outer cortex left, and if present, the cortex cells were compressed. Frequently, sclerenchyma, outer cortex and epidermis peeled off as fibers during preparation. The cambium had formed a large ring of secondary phloem and secondary xylem with parenchyma. The upper lateral stem internodes of the AZ showed the annual growth pattern (AZ in Figure 3C). Interestingly, in the AZ, interfascicular cambium and a ring of phloem parenchyma adjacent to the fascicular phloem were found in both, Paj and *pep1-1* (for Paj visible in stage III, Figure 3C, but for *pep1-1* this was only visible between stages II and III as shown, Supplemental Figure S3A). This interfascicular cambium and phloem parenchyma were no longer visible at later stages of the AZ development, but instead sclerenchyma tissue had formed, suggesting that cambium and phloem parenchyma had transformed into sclerenchyma in the AZ (for *pep1-1* visible at stage III, Figure 3C, but for Paj visible only later than stage III as shown in Supplemental Figure S3B). The pith regions became hollow in the two lines, and upper stem regions began to senesce. The border of PZ and AZ coincided with a transition region with short internodes. Phloem parenchyma and cork gradually became narrower, until they were no longer apparent (Supplemental Figure S3C, S3D). At stage II', lateral branches of Paj retained vegetative character and consisted only of PZ internodes (Figure 2B). Contrary to that, lateral branches of *pep1-1* formed the AZ and flowered. Secondary growth was advanced in the PZ, comparable to stage III (PZ, Figure 3D). The upper AZ (only present in *pep1-1* but not in Paj) showed again primary growth (AZ, Figure 3D). *A. montbretiana* plants formed lateral branches and were marked by green siliques (Figure 2B). Lateral stems of *A. montbretiana*, only available at stage II', showed primary growth (AZ in Figure 3D). Only in a very thin zone close to the main stem secondary growth was apparent in the lateral stems of *A. montbretiana*, presumably necessary for stability (Supplemental Figure S3E).

Taken together, the characteristic zonation into an upper reproductive and senescent annual growth zone, the AZ, and a lower vegetative perennial growth zone, the PZ, with secondary growth is a property of perennial *Arabis alpina* Paj and *pep1-1*, not affected by perpetual flowering and vernalization. This zonation was absent in the annual *A. montbretiana*.

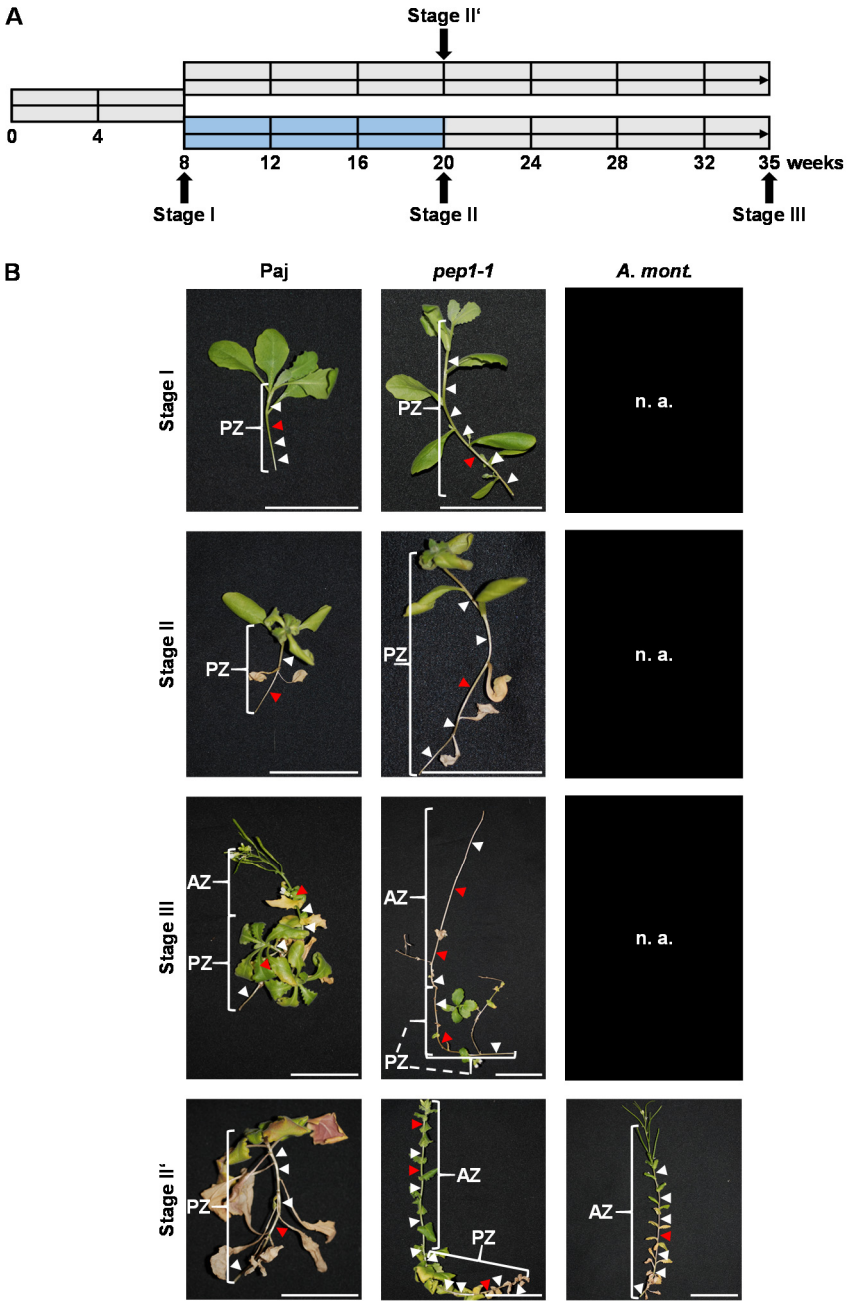

Figure 2. Plant growth and morphology (A) Plant growth scheme and harvesting stages. Time scale of plant growth under, grey color, long-day conditions at 20 °C, blue color, short-day conditions at 4 °C (vernalization); harvesting stages I, II, III or alternatively II'. (B) Lateral stem morphology at different growth stages. Representative photos of lateral stems from lower nodes of the main axis at stage I, II, III, and II'; perennial *A. alpina* Pajares (Paj, wild type), its *perpetual flowering1-1* (*pep1-1*) mutant derivative and annual *A. montbretiana* (*A. mont.*); for whole plant morphology (Supplemental Figure S2). Red triangles, positions of cross sections in Figure 3, similar as shown in Figure 1; white triangles, other regions examined by microscopy; n. a., lateral stems not present at this stage. Scale bars, 5 cm.

Starch and lipids are stored in secondary growth tissues of the PZ

Secondary growth in the PZ of lateral stems might be linked to nutrient storage. We investigated the deposition of C storage biopolymers starch and lipids (triacylglycerols, TAGs), by staining of tissue sections and biochemical quantification (Figure 3, Figure 4).

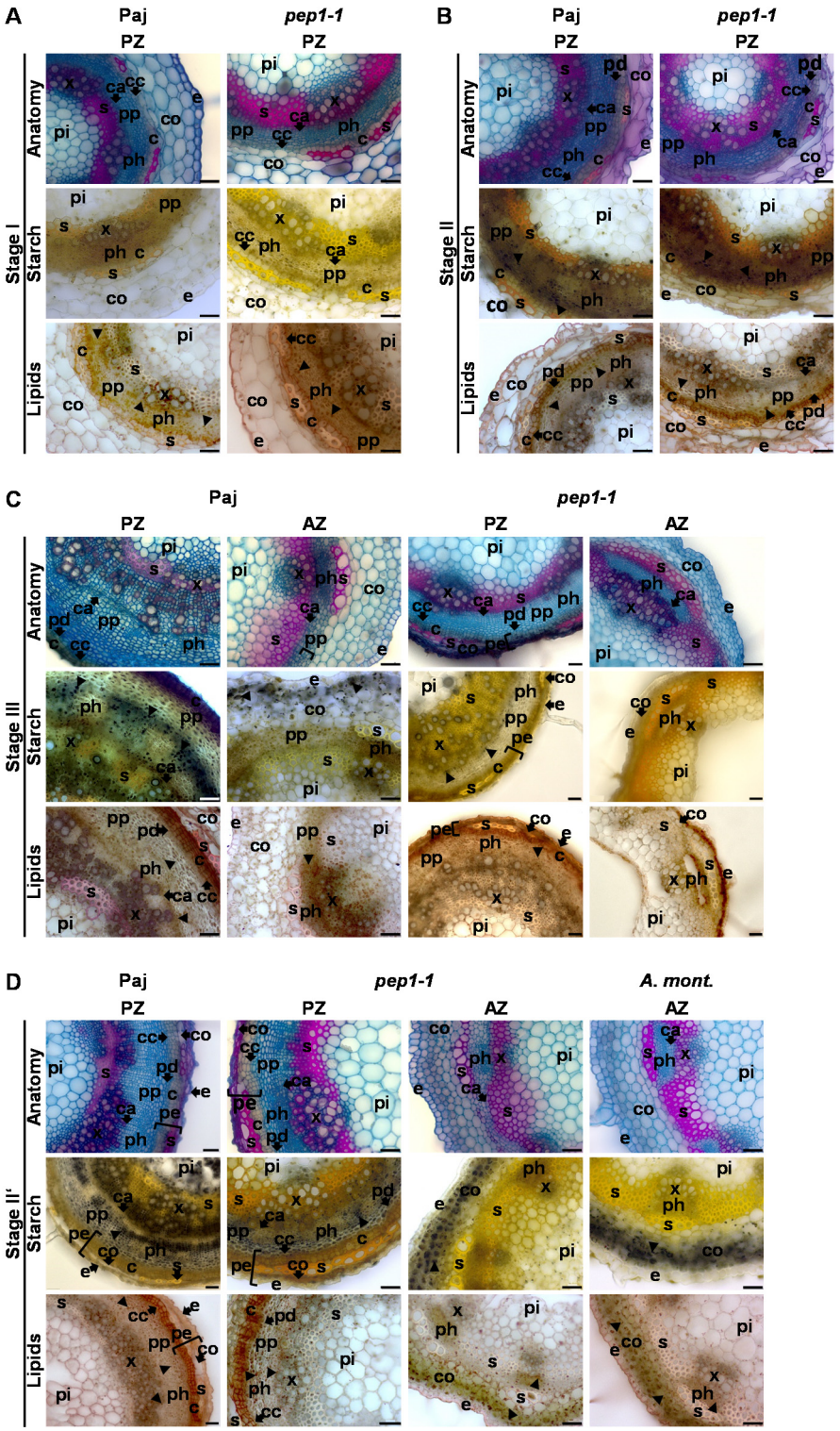

Figure 3. Anatomy, starch, and lipid body staining of lateral stem internodes. Representative lateral stem internode cross sections at (A), stage I; (B), stage II; (C), stage III; (D), stage II', prepared from perennial *A. alpina* Pajares (Paj, wild type), its *perpetual flowering1-1* (*pep1-1*) mutant derivative, and annual *A. montbretiana* (*A. mont.*) in the perennial zone (PZ) and annual zone (AZ). Anatomy, investigated following FCA staining, in blue, staining of non-lignified cell walls (parenchyma, phloem, meristematic cells), in red, staining of lignified cell walls, and greenish, staining of suberized cell walls (xylem, sclerenchyma, cork). Starch, visualized following Lugol's iodine staining, dark violet-black color. Lipids, detected by Sudan IV staining, orange pinkish color of lipid bodies and yellowish color of suberized and lignified cell wall structures. *(legend continued on next page)*

Black triangles, starch and lipid bodies. Abbreviations used in microscopic images: c, cork; ca, cambium; co, cortex; e, epidermis; pd, phelloderm; pe, periderm; ph, phloem including primary phloem, secondary phloem, phloem parenchyma; pi, pith; pp, secondary phloem parenchyma; s, sclerenchyma; x, xylem including primary xylem, secondary xylem, xylem parenchyma. Arrows point to respective tissues. Scale bars, 50 µm.

Starch was hardly detectable at stage I in PZ in Paj and *pep1-1* (Figure 3A), confirmed by starch contents below 5 mg/g dry matter (Figure 4A). At stage II, starch was formed in the ring of secondary phloem parenchyma in Paj and *pep1-1* (Figure 3B). Starch contents were between 20 and 30 mg/g dry matter (Figure 4A). At stage III, starch was also present in secondary phloem parenchyma of the PZ in Paj and *pep1-1* and contents ranged between 7-12 mg/g dry weight (Figure 3C, 4A). In the AZ, starch was detected in the outer cortex of Paj, but hardly in *pep1-1* (Figure 3C). Indeed, starch contents were higher in the AZ of Paj compared to *pep1-1* (28 mg/g in Paj compared to 0.6 mg/g dry weight in *pep1-1*, Figure 4A). Since the AZ development was advanced in *pep1-1* compared to Paj, we figured that starch was consumed and degraded with progression of senescence in the AZ. In stage II', starch was found deposited in the secondary phloem parenchyma ring of the PZ in Paj and *pep1-1*, while it was confined to the outer cortex of the AZ in *pep1-1* and *A. montbretiana* (Figure 3D). Starch contents were high in stage II' samples ranging from 18 to 32 mg/g dry matter in *pep1-1* and *A. montbretiana*, and up to even 54 mg/g dry matter in the PZ of Paj (Figure 4A). Significant differences with regard to starch contents between PZs of Paj and *pep1-1* at stage II' and between PZs of Paj at stage II' and III not only support the storage property of PZ, but also indicate the active turnover of stored starch resources during flowering.

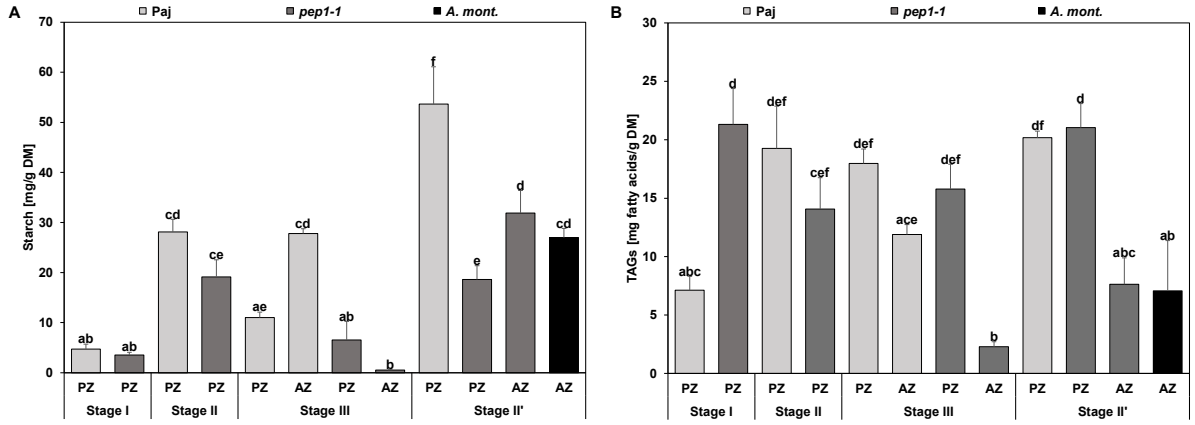

Figure 4. Contents of C-containing storage compounds in lateral stem internodes. Stem diagrams represent contents per dry matter (DM) of (A), starch, and (B), triacylglycerols (TAGs). Lateral stem internodes were harvested at stages I, II, III, and II', corresponding to perennial zone (PZ) and annual zone (AZ) of *A. alpina* Pajares (Paj, wild type), its *perpetual flowering1-1* (*pep1-1*) mutant derivative, and annual *A. montbretiana* (*A. mont.*). Data are represented as mean +/- SD (n = 3-7). Different letters indicate statistically significant differences, determined by one-way ANOVA-Tukey's HSD test ($P < 0.05$).

Lipid staining patterns were similar but not identical with starch staining. The main difference was that in the PZ, lipid bodies were found in all stages in the secondary phloem parenchyma, and in addition also in the secondary phloem, secondary xylem and in the cambium (Figure 3A-D). In the AZ,

lipid bodies were present in the outer cortex and in addition in the phloem and cambium of vascular bundles in Paj*, pep1-1*, and *A. montbretiana* (Figure 3C, 3D). TAG contents did not vary significantly between the PZs of different stages and lines, except at stage I in Paj, where it was lowest in accordance with the presence of lipid bodies in the developing secondary parenchyma (Figure 4B). In all AZ samples, TAG contents were lower than in the corresponding PZ samples, in agreement with anatomical observations (Figure 4B).

In summary, the tissues derived from secondary growth play a predominant role in C storage in the form of starch and TAGs in the PZ, irrespective of the flowering status and vernalization.

Carbon storage is reflected by carbon/nitrogen (C/N) ratio

An elevated C and C/N ratio is an indicator for carbon storage. Total C contents of all stem samples ranged between 360 and 440 mg/g dry matter (Figure 5A). In the PZ, significant increases of the C contents were noted from stage I to stages II and II' and then remained rather constant. At stage III, a lower C content was found in the AZ compared to the PZ, which was significant in *pep1-1* (Figure 5A). Total N contents developed in an opposite pattern to the C contents and decreased significantly from 20-25 mg/g dry matter at stage I to 5-10 mg/g dry matter at stages II and II' and then remained at a constant low level in stage III (Figure 5B). This finding speaks against usage of N storage compounds. Total protein contents were highest with 110-140 mg/g dry matter in stages I and II and in the PZ of Paj at stage III, while they were lower and varied between the AZ and the PZ and between lines without apparent pattern at stages III and II' (Figure 5C). Perhaps the lower N contents indicate a lower metabolic activity of the fully developed PZ. The C/N ratios were lowest at stage I and increased in stages II, III and II', however, a distinction of the PZ and the AZ was not possible and noticeable differences between the lines were not observed (Figure 5D). The C storage capacity of the PZ and possible turnover of C storage compounds during flowering is reflected by C/N ratio of the PZs of Paj at stage III and II'. The C/N ratio of the PZ retaining vegetative character at stage II' was significantly higher than that of the PZ corresponding to flowering at stage III. As a comparison to stems, roots may also serve as a C storage reservoir, however, in this case TAGs would be primary C storage products but not starch (Supplemental Figure S4).

Taken together, the total C content increased slightly with the progression of the development of the PZ. This slight increase may reflect storage of starch and TAGs but also may comprise the increases in cell walls.

Hormones affect secondary growth in lateral stems

We tested effects of hormone application to internodes in a juvenile PZ stage prior to visible secondary growth. First, we applied synthetic 6-benzylaminopurine (BAP) for eight or 46 days to PZ and AZ internodes respectively. In the PZ, cambium and phloem parenchyma regions were increased in width (Figure 6A, 6B, "Anatomy"). The increase in width corresponded to a doubling of cambium cells from two to about four cells and additional one or two cells of phloem parenchyma in the fascicular

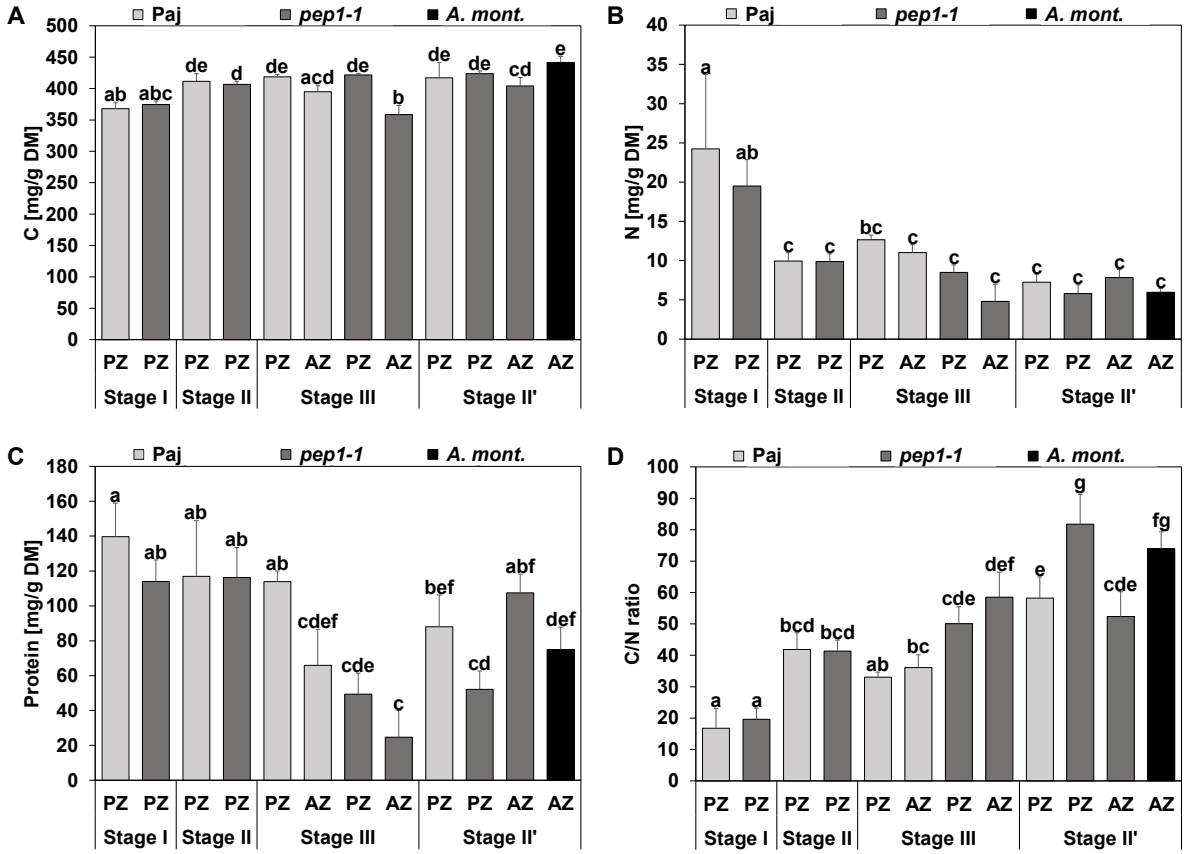

Figure 5. Carbon, nitrogen, and protein contents in lateral stem internodes. Stem diagrams represent contents per dry matter (DM) of (A), carbon (C), (B), nitrogen (N), (C), protein, (D), C/N ratios. Lateral stem internodes were harvested at stages I, II, III, and II', corresponding to perennial zone (PZ) and annual zone (AZ) of *A. alpina* Pajares (Paj, wild type), its *perpetual flowering1-1* (*pep1-1*) mutant derivative, and annual *A. montbretiana* (*A. mont.*). Data are represented as mean +/- SD (n = 3-7). Different letters indicate statistically significant differences, determined by one-way ANOVA-Tukey's HSD test ($P < 0.05$).

and interfascicular regions (Figure 6A-D). Interestingly, the increase in width was also found in the newly developed second internode that had not been treated with BAP directly, showing that a cytokinin-induced signal acted in the adjacent internode (Figure 6C, 6D). Similar to the control plants, starch did not accumulate in the secondary phloem parenchyma of the treated plants. Patterns of lipid bodies were similar in treated and control stems (Figure 6A, 6B, "Starch", "Lipids"). After 46 days of BAP treatment, the AZ internodes also increased in width (Supplemental Figure S5B). Additionally, flowering was delayed and a second zone with short internodes, as found in the PZ-AZ transition zone, was formed two to three internodes above the first (Supplemental Figure S5B). Cambium and phloem parenchyma regions were considerably increased in width in the AZ (Figure 7A, 7B, "Anatomy", 7C, 7D). Secondary phloem parenchyma was formed in the interfascicular regions of "Top" and "Middle" areas of the AZ. In the control, the corresponding areas would differentiate into sclerenchyma (Figure 7B, "Anatomy": "Top" and "Middle", 7D). Furthermore, cork cambium and cork were formed in the "Middle" area in the fascicular and interfascicular regions of the treated stems (Figure 7A, 7B). A difference with regard to starch accumulation was observed only for the "Bottom" area (Figure 7A, 7B,

"Starch": "Bottom"). Starch accumulated in secondary phloem parenchyma in the treated AZ stems, while starch was not observed in the corresponding tissue of the control. The observed starch accumulation in the AZ supports the strong involvement of cytokinins in the development of the perennial stem with a storing function. Patterns of lipid bodies in cambium and phloem parenchyma were similar between the treated and the untreated stems (Figure 7A, 7B, "Lipids").

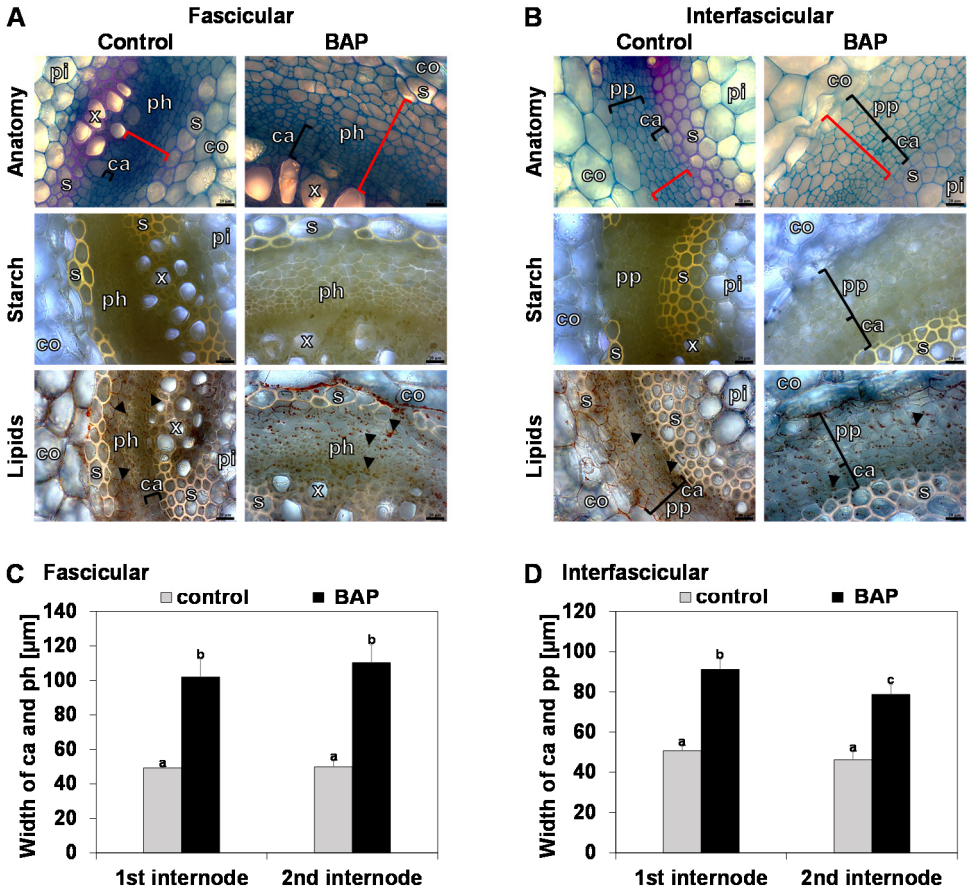

Figure 6. Effect of cytokinin treatment on cambium activity in the perennial zone (PZ). (A, B), Lateral stem first internode cross sections of (A), the fascicular region, (B), the interfascicular region of *A. alpina perpetual flowering 1-1* (*pep1-1*), following treatment with cytokinin (2 mM 6-benzylaminopurine, BAP) or mock control for eight days to the first internode. Representative images are shown. Anatomy, investigated following FCA staining, in blue, staining of non-lignified cell walls (parenchyma, phloem, meristematic cells), in red, staining of lignified cell walls, and in greenish, staining of suberized cell walls (xylem, sclerenchyma, cork). Starch, visualized following Lugol's iodine staining, dark violet-black color. Lipids, detected by Sudan IV staining, orange pinkish color of lipid bodies and yellowish color of suberized and lignified cell wall structures. Black triangles, lipid bodies; black brackets, responsive cambium and phloem/secondary phloem parenchyma; red brackets, quantified tissue width in (C) and (D). Abbreviations used in microscopic images: c, cork; ca, cambium; co, cortex; e, epidermis; pd, phelloderm; pe, periderm; ph, phloem including primary phloem, secondary phloem, phloem parenchyma; pi, pith; pp, secondary phloem parenchyma; s, sclerenchyma; x, xylem including primary xylem, secondary xylem, xylem parenchyma. Scale bars, 20 µm. (C, D) Quantified cambium and phloem/secondary phloem width in, (C), fascicular, and (D), interfascicular internode regions for first and second internodes. Data are represented as mean +/- SD (n = 3). Different letters indicate statistically significant differences, determined by one-way ANOVA-Tukey's HSD test ($P < 0.05$).

Auxin (1-naphthaleneacetic acid, NAA), gibberellic acid (GA_3) and ethylene precursor (1-aminocyclopropane-1-carboxylic acid, ACC) also influenced cambial activity in the first internode of the PZ upon application during eight days. Cambium and phloem parenchyma regions were increased in width, but in contrast to BAP to a maximum of 30 % and only in the treated first internode but not the second (Supplemental Figure S6, S7, S8). No changes with regard to starch and lipid body accumulation were observed (Supplemental Figure S6, S7, S8).

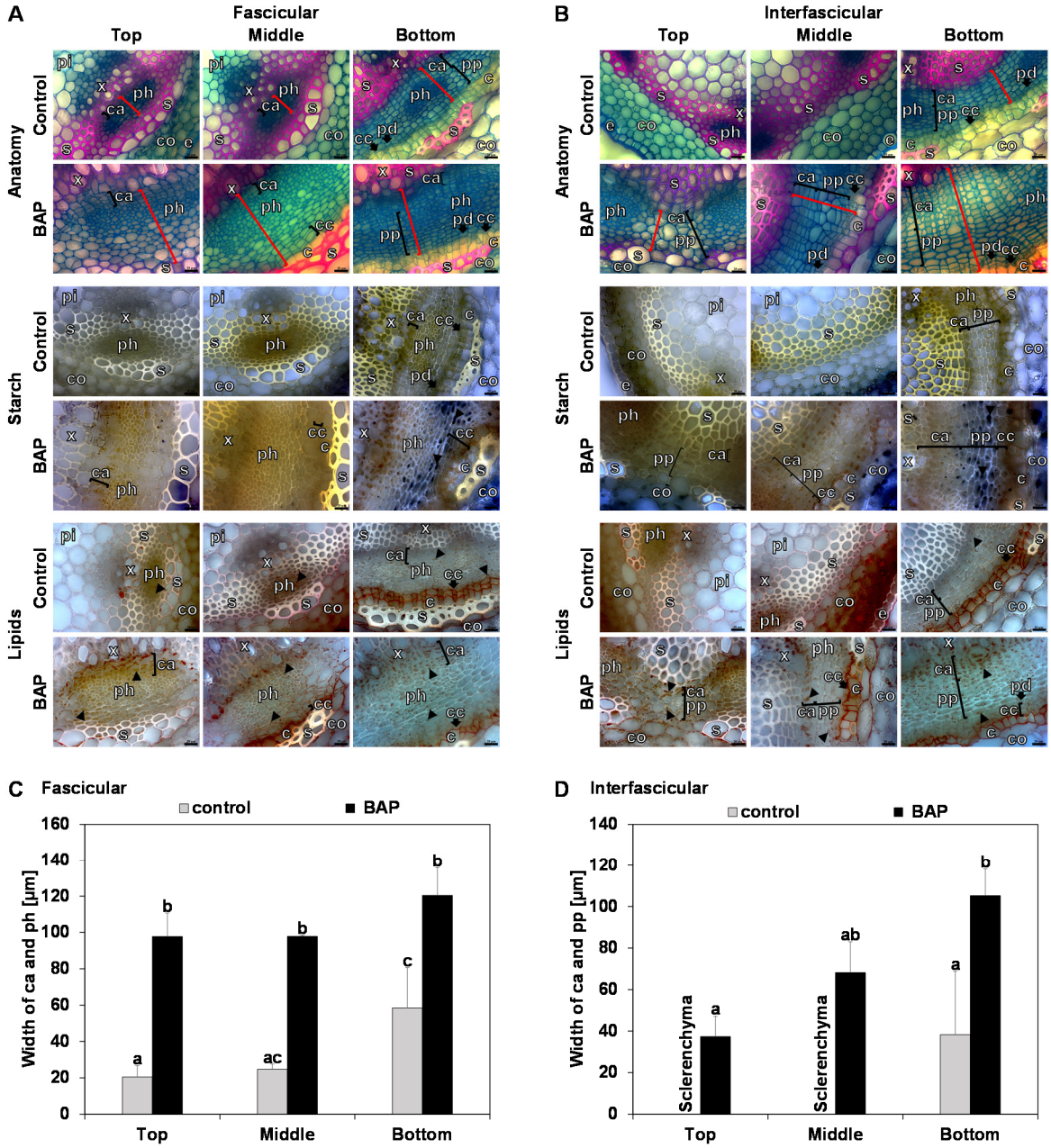

Figure 7. Effect of cytokinin treatment on cambium activity in the annual zone (AZ). (A, B), Lateral stem first internode cross sections of top, middle, and bottom parts of the AZ (see also Supplemental Figure S5) in (A), the fascicular region, (B), the interfascicular region of *A. alpina perpetual flowering1-1* (*pep1-1*) mutant, following treatment with cytokinin (2 mM 6-benzylaminopurine, BAP) or mock control for 46 days to all developing internodes of the AZ. Representative images are shown. Anatomy, investigated following FCA staining, in blue, staining of non-lignified cell walls (parenchyma, phloem, meristematic cells), *(legend continued on next page)*

in red, staining of lignified cell walls, and in greenish, staining of suberized cell walls (xylem, sclerenchyma, cork). Starch, visualized following Lugol's iodine staining, dark violet-black color. Lipids, detected by Sudan IV staining, orange pinkish color of lipid bodies and yellowish color of suberized and lignified cell wall structures. Black triangles, starch and lipid bodies; black brackets, responsive cambium and phloem/secondary phloem parenchyma; red brackets, quantified tissue width in (C) and (D). Abbreviations used in microscopic images: c, cork; ca, cambium; co, cortex; e, epidermis; pd, phelloderm; pe, periderm; ph, phloem including primary phloem, secondary phloem, phloem parenchyma; pi, pith; pp, secondary phloem parenchyma; s, sclerenchyma; x, xylem including primary xylem, secondary xylem, xylem parenchyma. Scale bars, 20 µm. (C, D) Quantified cambium and phloem/secondary phloem width in, (C), fascicular, and (D), interfascicular internode regions in top, middle, and bottom parts of the AZ. Data are represented as mean +/- SD (n = 3). Different letters indicate statistically significant differences, determined by one-way ANOVA-Tukey's HSD test ($P < 0.05$).

Taken together, among all tested hormones, cytokinin had the highest effect in the PZ on secondary growth. Cytokinin application to the AZ caused a shift in the zonation pattern and promoted secondary growth in the AZ, indicating that cytokinins act as signals to induce secondary growth. At an early growth stage, starch accumulation was not stimulated by cytokinins, whereas this was the case upon a prolonged treatment.

Transcriptome analysis reflects cytokinin effects in the PZ

To provide support for PZ and AZ activities and obtain hints on signaling, we conducted a gene expression profiling experiment with *pep1-1* lateral stem internodes using RNA-seq at 4- and 5-week-old juvenile developmental PZ stages (stage I_PZ and stage II_PZ), a 7-week-old PZ stage with secondary growth and lipid bodies (stage III_PZ) and a 30-week-old mature PZ stage (stage IV_PZ) with advanced secondary growth and accumulated starch and lipid bodies, and AZ internodes either in close proximity to the formed inflorescence (stage IV_AZ_if) or in the region with short internodes of the AZ (stage IV_AZ_si) (Figure 8A; Supplemental Table S2). Hierarchical clustering (HC) and Principal Component Analysis (PCA) confirmed the close relationships of three biological replicates of each sample and quality of RNA-seq data (Supplemental Figure S9). In HC, four distinct clusters were apparent, one cluster with stages IV_AZ_si and IV_AZ_if, a second one with stages I_PZ and II_PZ, grouping closely with AZ samples. The third and fourth cluster were stages III_PZ and IV_PZ, whereby the latter was most distant from all other groups (Supplemental Figure S9A). PCA analysis confirmed the expected variation between the samples. PC1 separated between the age of the internodes, similar as the first clusters in HC, while PC2 grouped according to PZ and AZ (Supplemental Figure S9B).

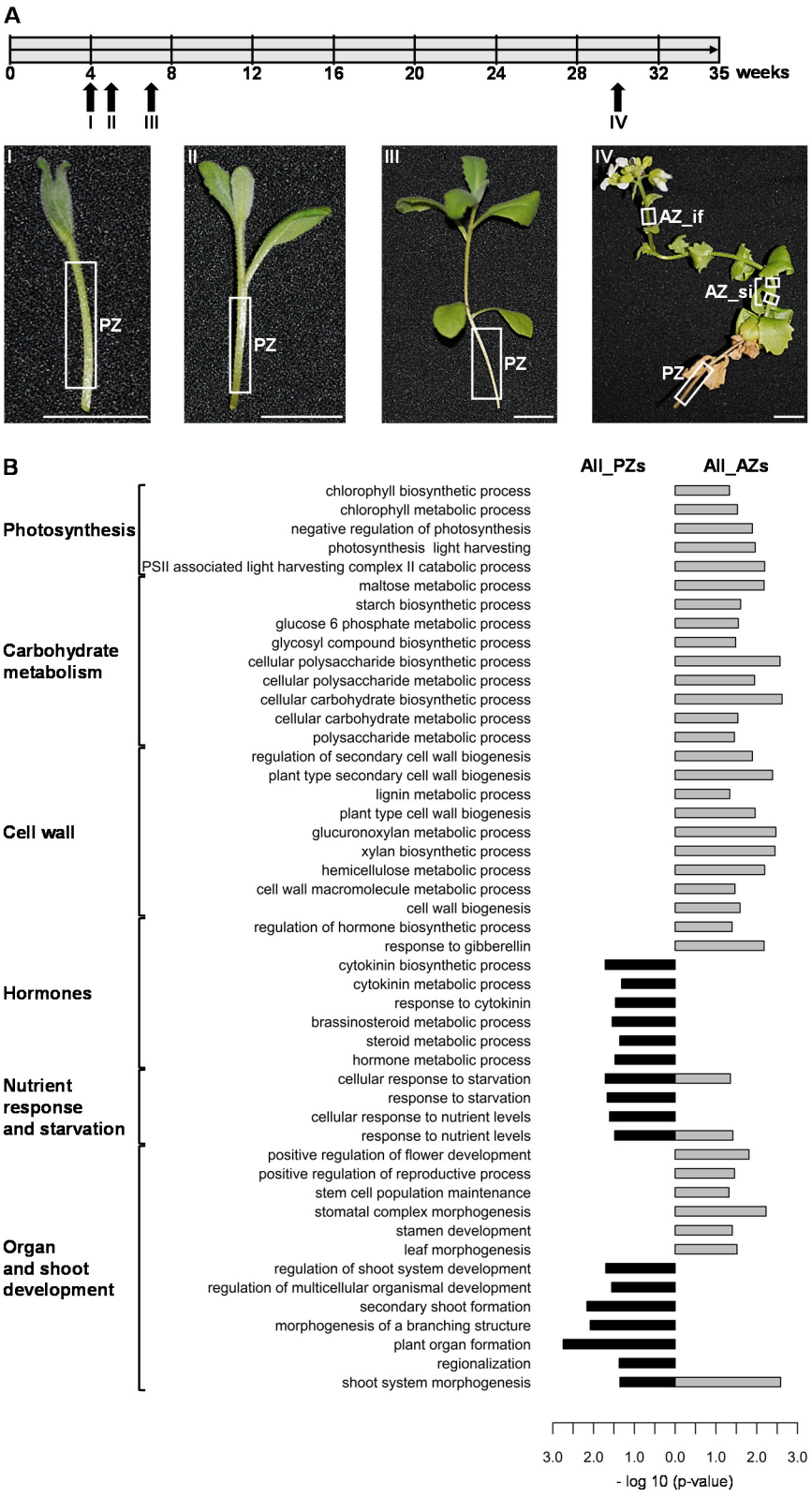

Figure 8. Transcriptome analysis of perennial (PZ) and annual (AZ) lateral stem zones. (A) Plant growth and morphology. Upper part, plant growth scheme and harvesting stages I-IV for RNA-sequencing (RNA-seq), long-day conditions at 20 °C, *A. alpina perpetual flowering1-1* (*pep1-1*) mutant. Bottom part, lateral stem morphology at each harvesting stage. Representative photos, white rectangles, harvested parts, stage I_PZ and stage II_PZ, PZs both prior to visible secondary growth in a juvenile phase, stage III_PZ and stage IV_PZ, PZs with visible secondary growth, stage IV_AZ_si, small internode region, stage IV_AZ_if, *(legend continued on next page)*

inflorescence region. Scale bars, 1 cm. (B) GO term enrichment analysis of PZ versus AZ. PZ comprised the sum of stages I to IV_PZ, while AZ comprised stage IV_AZ_si and _if combined. GO terms were assigned to the indicated categories photosynthesis, carbohydrate metabolism, cell wall, hormones, nutrient response and starvation, organ and shoot development. Enriched GO terms, $P < 0.05$, represented as –log 10 values. Further information about the GO term enrichment analysis in Supplemental Table S18.

As we were seeking gene expression differences between the PZ and the AZ, we conducted meaningful crosswise enrichment analysis of gene ontology (GO) terms (Supplemental Tables S3-S17). Cytokinin terms were enriched in comparisons of stages II_PZ and IV_AZ_if, III_PZ and IV_AZ_si or IV_AZ_if (Supplemental Tables S11, S13, S14). By grouping the data and comparing all PZ with all AZ stages, enrichment analysis resulted in a total of 48 PZ- and 89 AZ-enriched GO terms, among them cytokinin-related terms (Figure 8B, Supplemental Table S18; confirmed by gene expression validation in Fig. 9). Other PZ-enriched GO terms were related to organ and shoot development, nutrient response and starvation genes, and other hormone responses (Figure 8B, Supplemental Table S18). AZ-enriched terms were cell wall, carbohydrate metabolism, and photosynthesis categories (Figure 8B, Supplemental Table S18). GA biosynthesis and response terms were enriched in the AZ (Figure 8B, Supplemental Table S18).

In summary, the PZ shows a high responsiveness to cytokinins as compared to the AZ, confirming that cytokinins play an important role in the differentiation of the PZ.

Discussion

The complex perennial lifestyle of *A. alpina* comprises an allocation of nutrients and storage of high-energy C compounds in the proximal vegetative perennial zone (PZ), characterized by secondary growth. The distal inflorescence annual zone (AZ) remains in a primary growth stage.

A. alpina stems have proximal perennial (PZ) and distal annual zones (AZ) with C sequestration in the cambium and derivatives in the PZ

The vegetative growth zone (V) coincided with the PZ characterized by secondary growth, while the distal inflorescence zone (I) represented the AZ with primary growth. In the PZ-AZ transition zone secondary growth gradually shifted to primary growth. At the beginning of stem development, the anatomy of stem cross sections was similar in the PZ in *A. alpina* and AZ of *A. alpina* and *A. montbretiana*. With continuation of development, secondary growth was initiated by activities of cambium at first and then cork cambium. At the bottom of annual stems in *A. montbretiana* secondary growth was also found, where it may serve for general stability of upright stems, as described in *A. thaliana* (Agusti *et al.*, 2011). Moreover, perennial life strategy is regarded to be ancestral (Hu *et al.*, 2003; Grillo *et al.*, 2009). Secondary growth at the bottom of *A. montbretiana* stems may still occur to some extent due to regulatory events retained from perennial to annual transition. In the AZ, the interfascicular cambium and inner layer of the cortex differentiate into sclerenchyma during progression

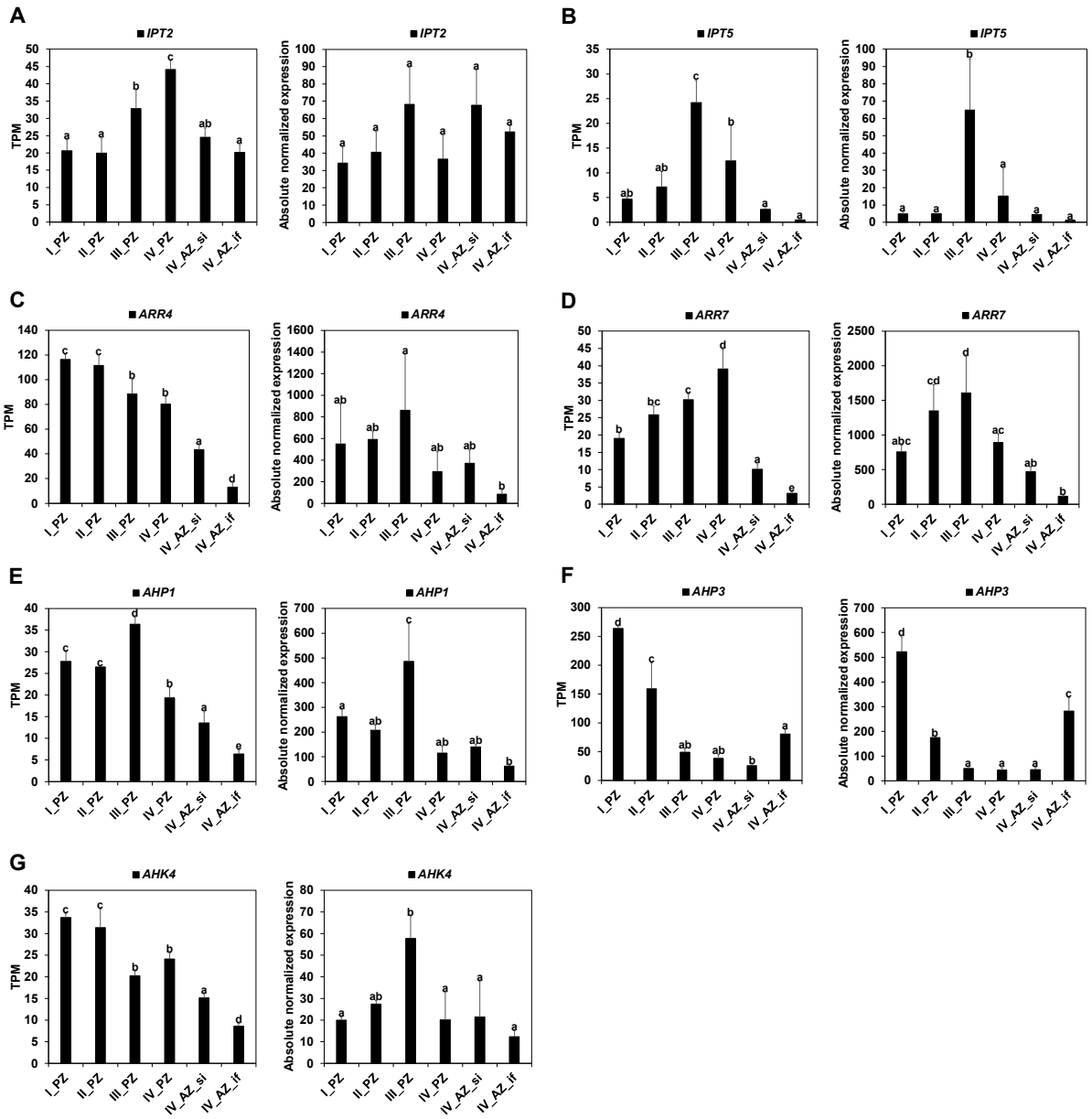

Figure 9. Gene expression of orthologues of *Arabidopsis* cytokinin signaling and response genes in lateral stem internodes. Gene expression was tested at different stages of the development of the perennial zone (PZ) and the annual zone (AZ) in *A. alpina perpetual flowering1-1* (*pep1-1*) mutant derivative (see Figure 8A). Represented are RNA-sequencing data (left; TPM, transcripts per million) and reverse transcription-qPCR data (right; Absolute normalized expression). (A), *IPT2*, *ISOPENTENYLTRANSFERASE 2*; (B) *IPT5*, *ISOPENTENYLTRANSFERASE 5*; (C) *ARR4*, *ARABIDOPSIS RESPONSE REGULATOR 4;* (D) *ARR7*, *ARABIDOPSIS RESPONSE REGULATOR 7*; (E) *AHP1, ARABIDOPSIS HISTIDINE-CONTAINING PHOSPHOTRANSMITTER 1*; (F) *AHP3, ARABIDOPSIS HISTIDINE-CONTAINING PHOSPHOTRANSMITTER 3*; (G) *AHK4, ARABIDOPSIS HISTIDINE KINASE 4*. Data are represented as mean +/- SD (n = 3). Different letters indicate statistically significant differences, determined by one-way ANOVA-Tukey's HSD test ($P < 0.05$).

of development, perhaps for stabilization during flowering and silique production. The occurrence of PZ and AZ regions in all stems in *A. alpina* wild type Paj and *pep1-1* suggests that the genetically encoded signals for the PZ-AZ transition do not require vernalization treatment. Instead, we propose that a heterochronic regulation might control it. In the PZ, cambium and its derivatives store high

molecular weight C compounds in the form of starch and TAGs, in agreement with the rise in C contents and C/N ratios. The GO terms related to cell wall were enriched in the AZ but not in the PZ, suggesting that the elevated C content in the PZ was not primarily due to cell wall biosynthesis. The enrichment of nutrient response and starvation GO terms in the PZ speaks in favor of a nutrient storage reservoir. Starch is present in the secondary phloem parenchyma of the PZ and the outer cortex of the AZ. This could be the reason why the GO term starch biosynthesis was not enriched in the PZ. Starch deposition begins with the end of vegetative growth, usually coinciding with a cold treatment, however it is also in place in the absence of the cold treatment and increases up to the flowering stage and also during the senescence of leaves present in the PZ. C-containing compounds are presumably re-mobilized from senescing leaves to be allocated to adjacent storage tissue in the PZ. Interestingly, sequestration of C to phloem tissue of stems has been detected in trees, where functions are attributed to C supply during stress and in early spring (reviewed by Furze *et al.*, 2018). In tree species storage also occurs in pith cells, wood ray and bark parenchyma (Netzer *et al.*, 2018). Thus, it is not unusual that *A. alpina* uses different types of tissues for storage of different compounds. Lipid bodies occur in the cambium and cambium derivatives of the PZ and in cortex and phloem of the AZ, and this parallels generally a trend toward higher TAG content in the PZ than in the AZ. This suggests that lipids are used as storage compounds in the PZ. The N pool in *A. alpina* stems coincided with the protein pool, noteworthy in the early PZ but decreasing with development. Thus, N utilization in storage is not likely. Roots acted differently from stems and are not perennial starch storage organs in *A. alpina* but might be involved in lipid storage. In summary, C storage is more important than N storage, and the PZ of the stem has higher storage capacity than roots in *A. alpina*.

Cytokinins are signals for demarcation of annual and perennial growth zones

The open question is which events are responsible to demarcate the sharp PZ-AZ transition. The PZ-AZ boundary separates besides secondary/primary growth and C storage also organ differentiation at the nodes and in axils, such as bud outgrowth into fully developed lateral stems, bud dormancy, bud differentiation into a singular flower or bud outgrowth into flowering secondary and tertiary branches. The small PZ-AZ transition zone has short internodes and is marked by a gradual shift from secondary to primary growth. Multiple signals could act in these differentiation processes in the PZ and AZ.

One possible explanation is that the PZ state is an initial ground state. In this scenario, the progression to the PZ becomes halted later in developmental time in the AZ. In this model, the PZ to AZ transition is a heterochrony or developmental phase transition. Since regulation of bud fate is under control of meristem identity genes, mutants in those genes affect developmental phase transitions. In annuals, some progression to the PZ may take place in a rudimentary manner at the bottom of stems or during senescence onset for stabilization reasons, however, a full progression to the PZ is prevented. We exclude that flowering or vernalization emit signals for the PZ-AZ transition in Paj and *pep1-1*. The

pep1-1 mutant has also the PZ-AZ transition. Even though the presence of flowers was not a requirement for PZ-AZ transition, upstream regulators of flowering and developmental phase transition, namely the regulatory network of microRNA miR156, SQUAMOSA PROMOTER BINDING PROTEIN-LIKE (SPL) proteins, and Mediator complex subunits may well control aspects of stem differentiation (Park *et al.*, 2017; Bergonzi *et al.*, 2013; Guo *et al.*, 2017; Hyun *et al.*, 2019; Zhang and Guo, 2020).

Developmental decisions are often taken under the influence of plant hormones and they affect stem differentiation, flowering, and developmental phase transition. Cytokinin application shifted the PZ-AZ transition and might be coupled to a heterochronic signal. A cytokinin effect was further confirmed by enrichment of cytokinin biosynthesis and response gene expression in the developing PZ. Even application directly to the AZ caused an extension of the PZ into the AZ. Thus, cytokinins might be signals that promote the progression during developmental phase transitions, and cytokinin depletion rather than decreased sensitivity might trigger the precocious halting in the AZ. Cytokinins play also a crucial role in the regulation of source and sink relationships including starch deposition (Thomas, 2013). Cytokinins are likely signals in the PZ to promote secondary growth and later in combination with flowering and senescence also sink activity and starch formation. Cytokinins also retard senescence which is partly explained by cytokinin-modified source-sink relationships (Thomas, 2013). Together, this suggests that cytokinins are less likely to act in the AZ but rather contribute to the maintenance of an adult vegetative state in the PZ.

GA, auxin, and ethylene also promoted secondary growth in the PZ. Yet, these hormones acted only locally on the same internode and not to the same extent as cytokinin. Auxin produced in V3 lateral branches may cause bud dormancy in V2, according to an auxin canalization model. This growth inhibition effect is also under the control of vernalization and further promoted by enhanced sinks for nutrients in the AZ and V3 lateral branches (Vayssières *et al.*, 2020). In our experiments, auxin did not stimulate secondary growth in the neighboring internodes, that had not been treated, in the way that cytokinin did. Auxin signaling may give rise to distinctive V subzones in the PZ, but not the PZ-AZ transition. Gibberellins (GAs) are influential in the xylem region promoting xylem cell differentiation and lignification (Denis *et al.*, 2017). Interestingly, this stronger lignification of vascular cells resembles the anatomy which has been detected in our study in the AZ of Paj and *pep1-1* as well as in *A. montbretiana* at later developmental stages. Perhaps GA signals explain the sensitivity of cambium in the AZ to develop lignified cell walls and differentiate into sclerenchyma. Indeed, GA-related GO terms were enriched in AZ versus PZ, supporting this idea.

To test whether hormone gradients and developmental phase transition regulation are responsible for the secondary to primary growth transition, transgenic approaches will be helpful in the future to manipulate these responses in the different growth zones.

Conclusions

The functional complexity of stem differentiation in *Arabis* offers the possibility to study regulation of perennial (advanced secondary growth and storage) and annual (primary growth and senescence) traits using the same model species. The close relationship among Brassicaceae and the similarities of secondary growth processes in trees and *Arabidopsis* can be exploited to unveil signaling pathways and regulators for stem differentiation in *A. alpina* in future projects. Further studies need to show whether heterochronic PZ-AZ transition genes and plant hormones determine the transport of effectors, the sensitivity to respond to effectors or to alter specific long-distance signaling processes, and how these processes link flowering control and secondary growth.

Supplemental Material

Supplemental Figures S1-S10 and Supplemental Table S1 are represented at the end of the manuscript. Supplemental Tables S2-S19 are available as "Supplementary Material" online (https://doi.org/10.1101/2020.06.01.124362).

Supplemental Figure S1: Experimental outline.
Supplemental Figure S2: Whole plant morphology.
Supplemental Figure S3: Additional internode cross section analysis.
Supplemental Figure S4: Analysis of nutrient storage in roots.
Supplemental Figure S5: Effect of prolonged cytokinin treatment and dissection of the annual zone (AZ).
Supplemental Figure S6: Effect of auxin treatment on cambium activity in the perennial zone (PZ).
Supplemental Figure S7: Effect of gibberellic acid (GA) treatment on cambium activity in the perennial zone (PZ).
Supplemental Figure S8: Effect of ethylene on cambium activity in the perennial zone (PZ).
Supplemental Figure S9: Hierarchical clustering (HC) and Principal Component Analysis (PCA) of RNA-sequencing data.
Supplemental Figure S10: Expression of genes, involved in cambial activity and maintenance, in lateral stem internodes.
Supplemental Table S1: RT-qPCR primers.
Supplemental Table S2: Spreadsheet with RNA-sequencing (RNA-seq) gene expression data set.
Supplemental Table S3: Enriched GO terms in the comparison stage I_PZ and stage II_PZ.
Supplemental Table S4: Enriched GO terms in the comparison stage I_PZ and stage III_PZ.
Supplemental Table S5: Enriched GO terms in the comparison stage I_PZ and stage IV_PZ.
Supplemental Table S6: Enriched GO terms in the comparison stage I_PZ and stage IV_AZ_si.
Supplemental Table S7: Enriched GO terms in the comparison stage I_PZ and stage IV_AZ_if.

Supplemental Table S8: Enriched GO terms in the comparison stage II_PZ and stage III_PZ.
Supplemental Table S9: Enriched GO terms in the comparison stage II_PZ and stage IV_PZ.
Supplemental Table S10: Enriched GO terms in the comparison stage II_PZ and stage IV_AZ_si.
Supplemental Table S11: Enriched GO terms in the comparison stage II_PZ and stage IV_AZ_if.
Supplemental Table S12: Enriched GO terms in the comparison stage III_PZ and stage IV_PZ.
Supplemental Table S13: Enriched GO terms in the comparison stage III_PZ and stage IV_AZ_si.
Supplemental Table S14: Enriched GO terms in the comparison stage III_PZ and stage IV_AZ_if.
Supplemental Table S15: Enriched GO terms in the comparison stage IV_PZ and stage IV_AZ_si.
Supplemental Table S16: Enriched GO terms in the comparison stage IV_PZ and stage IV_AZ_if.
Supplemental Table S17: Enriched GO terms in the comparison stage IV_AZ_si and stage IV_AZ_if.
Supplemental Table S18: Enriched GO terms in the comparison all PZ stages (stage I_, II_, III_, IV_PZ) and all AZ stages (stage IV_AZ_si, _if).
Supplemental Table S19: Gene expression data of cytokinin signaling, biosynthesis, and catabolism genes.

Author Contributions

AS, TMA, and PB planned and designed the research. AS and HL performed the experiments. AS and HJM analyzed data. AS and PB wrote the manuscript. HL, HJM, TMA, CK, and GC reviewed the article. PB acquired funding.

Acknowledgements

We acknowledge the excellent technical assistance of M. Graf, E. Klemp, and K. Weber for GC-MS and EA-IRMS measurements. We thank Vera Wewer (University of Cologne) for her advice regarding the establishment of the lipid extraction protocol. The authors thank E. Wieneke for help with gene expression studies. We are grateful to Maria C. Albani (University of Cologne) for critical reading of the manuscript. This project was funded by the Deutsche Forschungsgemeinschaft (DFG) under Germany´s Excellence Strategy – EXC 2048/1 – project 390686111. H.L. was the recipient of a doctoral fellowship from Northwest A&F University, College of Horticulture, Yangling, China.

References

Agusti J, Lichtenberger R, Schwarz M, Nehlin L, Greb T (2011) Characterization of transcriptome remodeling during cambium formation identifies MOL1 and RUL1 as opposing regulators of secondary growth. PLoS Genet **7:** e1001312

Alexa A, Rahnenfuhrer J (2010) topGO: enrichment analysis for gene ontology. R package version 2

Altschul SF, Gish W, Miller W, Myers EW, Lipman DJ (1990) Basic local alignment search tool. J Mol Biol **215:** 403-410

Anders S, Pyl PT, Huber W (2015) HTSeq—a Python framework to work with high-throughput sequencing data. Bioinformatics **31:** 166-169

Andrews S (2010) FastQC: a quality control tool for high throughput sequence data (https://www.bioinformatics.babraham.ac.uk/projects/fastqc/)

Ben Abdallah H, Bauer P (2016) Quantitative Reverse Transcription-qPCR-based gene expression analysis in plants. In: Botella J., Botella M. (eds) Plant Signal Transduction. Methods in Molecular Biology **1363**. Humana Press, New York, NY

Bergonzi S, Albani MC (2011) Reproductive competence from an annual and a perennial perspective. J Exp Bot **62:** 4415-4422

Bergonzi S, Albani MC, van Themaat EVL, Nordström KJ, Wang R, Schneeberger K, Moerland PD, Coupland G (2013) Mechanisms of age-dependent response to winter temperature in perennial flowering of Arabis alpina. Science **340:** 1094-1097

Bolger AM, Lohse M, Usadel B (2014) Trimmomatic: a flexible trimmer for Illumina sequence data. Bioinformatics **30:** 2114–2120

Bray NL, Pimentel H, Melsted P, Pachter L (2016) Near-optimal probabilistic RNA-seq quantification. Nat Biotechnol **34:** 525–527

Denis E, Kbiri N, Mary V, Claisse G, Conde ESN, Kreis M, Deveaux Y (2017) WOX14 promotes bioactive gibberellin synthesis and vascular cell differentiation in Arabidopsis. Plant J **90:** 560-572

Doolittle R.F (1986) Of URFs and ORFs: A primer on how to analyze derived amino acid sequences. University Science Books

Eviatar-Ribak T, Shalit-Kaneh A, Chappell-Maor L, Amsellem Z, Eshed Y, Lifschitz E (2013) A cytokinin-activating enzyme promotes tuber formation in tomato. Curr Biol **23:** 1057-1064

Fischer U, Kucukoglu M, Helariutta Y, Bhalerao RP (2019) The Dynamics of Cambial Stem Cell Activity. Annual review of plant biology **70:** 293-319

Furze ME, Trumbore S, Hartmann H (2018) Detours on the phloem sugar highway: stem carbon storage and remobilization. Curr Opin Plant Biol **43:** 89-95

Grillo MA, Li C, Fowlkes AM, Briggeman TM, Zhou A, Schemske DW, Sang T (2009) Genetic architecture for the adaptive origin of annual wild rice, Oryza nivara. Evolution **63:** 870-883

Guo C, Xu Y, Shi M, Lai Y, Wu X, Wang H, Zhu Z, Poethig RS, Wu G (2017) Repression of miR156 by miR159 regulates the timing of the juvenile-to-adult transition in Arabidopsis. Plant Cell **29:** 1293-1304

Hajra AK (1974) On extraction of acyl and alkyl dihydroxyacetone phosphate from incubation mixtures. Lipids **9:** 502-505

Hartmann A, Senning M, Hedden P, Sonnewald U, Sonnewald S (2011) Reactivation of meristem activity and sprout growth in potato tubers require both cytokinin and gibberellin. Plant Physiol **155:** 776-796

Heidel AJ, Kiefer C, Coupland G, Rose LE (2016) Pinpointing genes underlying annual/perennial transitions with comparative genomics. BMC Genomics **17:** 921

Hu FY, Tao DY, Sacks E, Fu BY, Xu P, Li J, Yang Y, McNally K, Khush GS, Paterson AH, Li ZK (2003) Convergent evolution of perenniality in rice and sorghum. Proc Natl Acad Sci U S A **100:** 4050-4054

Hughes PW, Soppe WJJ, Albani MC (2019) Seed traits are pleiotropically regulated by the flowering time gene PERPETUAL FLOWERING 1 (PEP1) in the perennial Arabis alpina. Mol Ecol **28:** 1183-1201

Hyun Y, Richter R, Coupland G (2017) Competence to flower: Age-controlled sensitivity to environmental cues. Plant Physiol **173:** 36-46

Hyun Y, Vincent C, Tilmes V, Bergonzi S, Kiefer C, Richter R, Martinez-Gallegos R, Severing E, Coupland G (2019) A regulatory circuit conferring varied flowering response to cold in annual and perennial plants. Science **363:** 409-412

Immanen J, Nieminen K, Smolander OP, Kojima M, Alonso Serra J, Koskinen P, Zhang J, Elo A, Mahonen AP, Street N, Bhalerao RP, Paulin L, Auvinen P, Sakakibara H, Helariutta Y (2016) Cytokinin and auxin display distinct but interconnected distribution and signaling profiles to stimulate cambial activity. Curr Biol **26:** 1990-1997

Karl R, Koch MA (2013) A world-wide perspective on crucifer speciation and evolution: phylogenetics, biogeography and trait evolution in tribe Arabideae. Ann Bot **112:** 983-1001

Kiefer C, Severing E, Karl R, Bergonzi S, Koch M, Tresch A, Coupland G (2017) Divergence of annual and perennial species in the Brassicaceae and the contribution of cis-acting variation at FLC orthologues. Mol Ecol **26:** 3437-3457

Kim DH, Doyle MR, Sung S, Amasino RM (2009) Vernalization: Winter and the timing of flowering in plants. Annual Review of Cell and Developmental Biology **25:** 277-299

Kim D, Langmead B, Salzberg SL (2015) HISAT: a fast spliced aligner with low memory requirements. Nat Methods **12:** 357□360

Kucukoglu M, Nilsson J, Zheng B, Chaaboukimni S, Nilsson O (2017) WUSCHEL-RELATED HOMEOBOX4 (WOX4)-like genes regulate cambial cell division activity and secondary growth in Populus trees. New Phytol **215:** 642-657

Lazaro A, Obeng-Hinneh E, Albani MC (2018) Extended vernalization regulates inflorescence fate in Arabis alpina by stably silencing PERPETUAL FLOWERING1. Plant Physiol **176:** 2819-2833

Matsumoto-Kitano M, Kusumoto T, Tarkowski P, Kinoshita-Tsujimura K, Vaclavikova K, Miyawaki K, Kakimoto T (2008) Cytokinins are central regulators of cambial activity. Proc Natl Acad Sci U S A **105:** 20027-20031

McCarthy DJ, Chen Y, Smyth GK (2012) Differential expression analysis of multifactor RNA-Seq experiments with respect to biological variation. Nucleic acids research **40:** 4288-4297

Netzer F, Herschbach C, Oikawa A, Okazaki Y, Dubbert D, Saito K, Rennenberg H (2018) Seasonal alterations in organic phosphorus metabolism drive the phosphorus economy of annual growth in F. sylvatica trees on P-impoverished soil. Front Plant Sci **9:** 723

Nieminen K, Immanen J, Laxell M, Kauppinen L, Tarkowski P, Dolezal K, Tähtiharju S, Elo A, Decourteix M, Ljung K, Bhalerao R, Keinonen K, AlbertVA, Helariutta Y (2008) Cytokinin signaling regulates cambial development in poplar. Proc Natl Acad Sci U S A **105**: 20032-20037

Park JY, Kim H, Lee I (2017) Comparative analysis of molecular and physiological traits between perennial Arabis alpina Pajares and annual Arabidopsis thaliana Sy-0. Scientific reports **7:** 13348

Robinson MD, McCarthy DJ, Smyth GK (2010) edgeR: a Bioconductor package for differential expression analysis of digital gene expression data. Bioinformatics **26:** 139-140

Sauter JJ, van Cleve B (1994) Storage, mobilization and interrelations of starch, sugars, protein and fat in the ray storage tissue of poplar trees. Trees **8:** 297-304

Sauter JJ, Wellenkamp S (1998) Seasonal changes in content of starch, protein and sugars in the twig wood of Salix caprea L. Holzforschung-International Journal of the Biology, Chemistry, Physics and Technology of Wood **52:** 255-262

Smith AM, Zeeman SC (2006) Quantification of starch in plant tissues. Nat Protoc **1:** 1342-1345

Stephan L, Tilmes V, Hülskamp M (2019) Selection and validation of reference genes for quantitative Real-Time PCR in Arabis alpina. PLoS One **14:** e0211172.

Suer S, Agusti J, Sanchez P, Schwarz M, Greb T (2011) WOX4 imparts auxin responsiveness to cambium cells in Arabidopsis. Plant Cell **23:** 3247-3259

Thomas H (2013) Senescence, ageing and death of the whole plant. New Phytol **197:** 696-711

Vayssières A, Mishra P, Roggen A, Neumann U, Ljung K, Albani MC (2020) Vernalization shapes shoot architecture and ensures the maintenance of dormant buds in the perennial Arabis alpina. New Phytol

Wang R, Farrona S, Vincent C, Joecker A, Schoof H, Turck F, Alonso-Blanco C, Coupland G, Albani MC (2009) PEP1 regulates perennial flowering in Arabis alpina. Nature **459:** 423-427

Watanabe M, Netzer F, Tohge T, Orf I, Brotman Y, Dubbert D, Fernie AR, Rennenberg H, Hoefgen R, Herschbach C (2018) Metabolome and lipidome profiles of Populus x canescens twig tissues during annual growth show phospholipid-linked storage and mobilization of C, N, and S. Front Plant Sci **9:** 1292

Wewer V, Dombrink I, vom Dorp K, Dörmann P (2011) Quantification of sterol lipids in plants by quadrupole time-of-flight mass spectrometry. J Lipid Res **52:** 1039-1054.

Zhang L, Guo C (2020) The important function of Mediator complex in controlling the developmental transitions in plants. Int J Mol Sci. **21:** E2733

Supplemental Figures

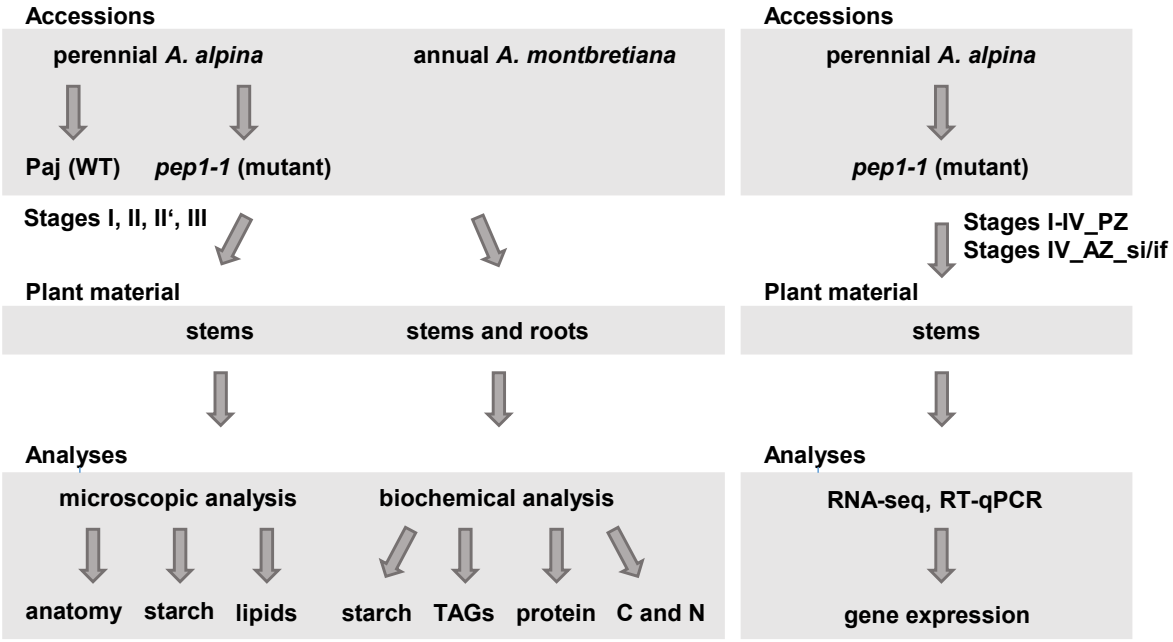

Supplemental Figure S1. Experimental outline. Abbreviations: perennial *A. alpina* Pajares (Paj WT, wild type); its *perpetual flowering1-1* (*pep1-1*) mutant derivative; perennial zone (PZ); annual zone (AZ); short internode zone (si); inflorescence zone (if); triacylglycerol (TAG); carbon (C); nitrogen (N); RNA-sequencing (RNA-seq); reverse transcription-qPCR (RT-qPCR).

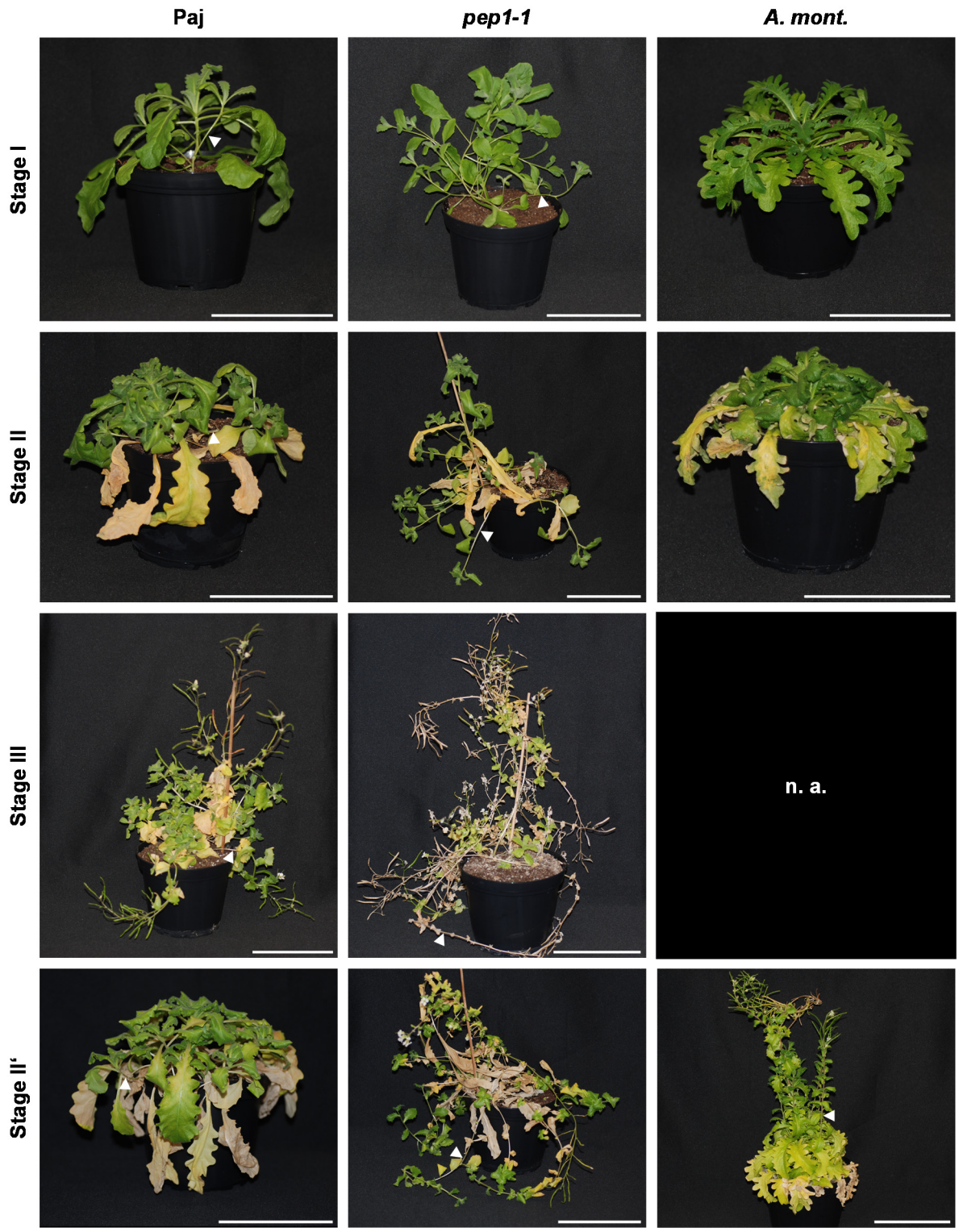

Supplemental Figure S2. Whole plant morphology. Representative photos of plants at stage I, stage II, stage III, stage II' for microscopic and biochemical analysis; perennial *A. alpina* Pajares (Paj, wild type), its *perpetual flowering1-1* (*pep1-1*) mutant derivative and annual *A. montbretiana* (*A. mont.*). White triangles indicate representative lateral stems used in analyses (see Figure 2); n. a., plants not available at this stage. Scale bar, 10 cm.

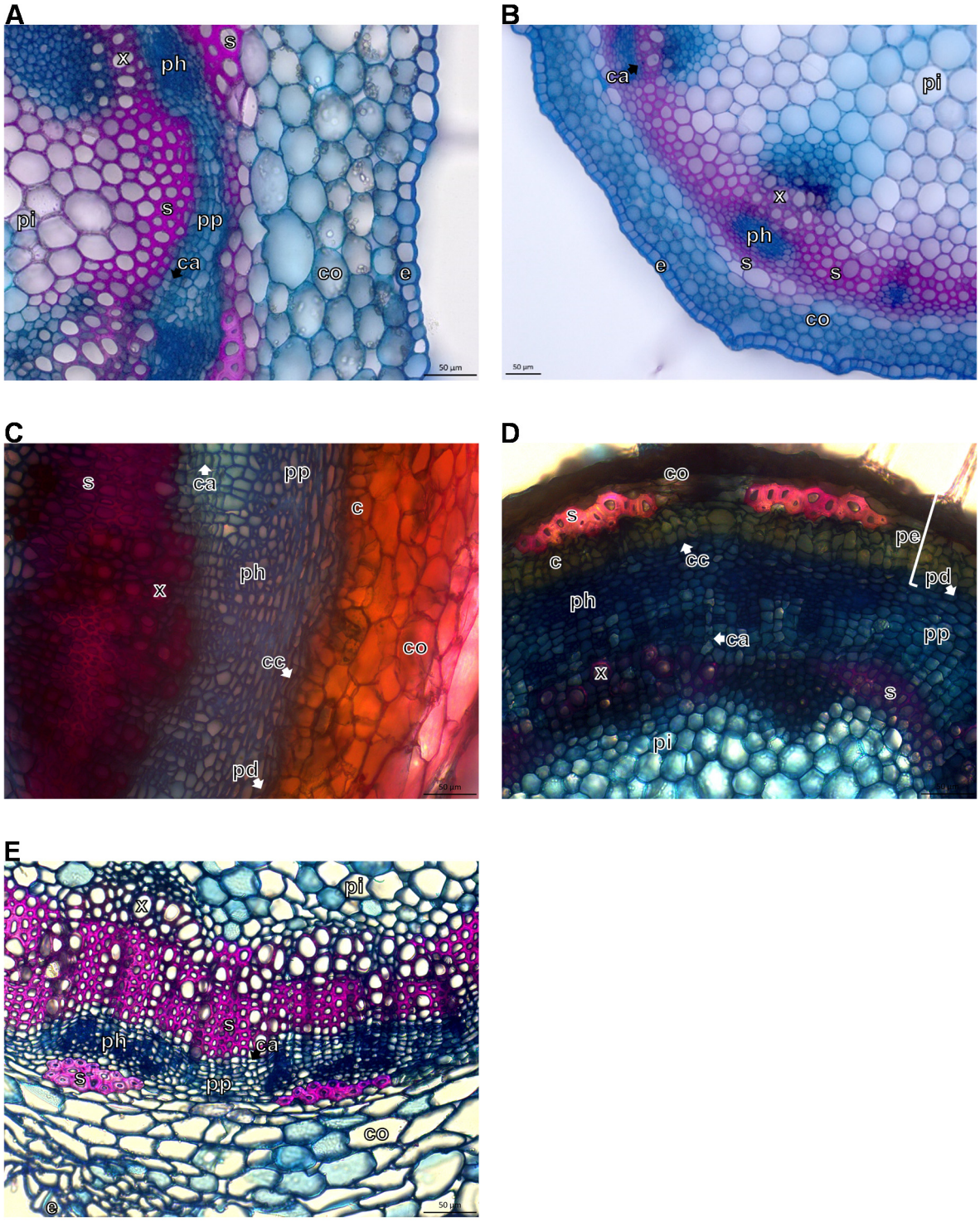

Supplemental Figure S3. Additional internode cross section analysis. (A) Early stage of development between stages II and III of the upper annual stem zone of *perpetual flowering1-1* (*pep1-1*) mutant; the center of the image shows the interfascicular region. (B) Late stage of development beyond stage III of the annual stem zone of wild type Pajares (Paj). (C, D), Transition regions at stage III in (C), Paj, and (D), *pep1-1*. (E) Internode region of *A. montbretiana* at stage II' close to the main axis. Abbreviations used in microscopic images: c, cork; ca, cambium; co, cortex; e, epidermis; pd, phelloderm; pe, periderm; ph, phloem including primary phloem, secondary phloem, phloem parenchyma; pi, pith; pp, secondary phloem parenchyma; s, sclerenchyma; x, xylem including primary xylem, secondary xylem, xylem parenchyma. Arrows point to respective tissues. Scale bars, 50 µm.

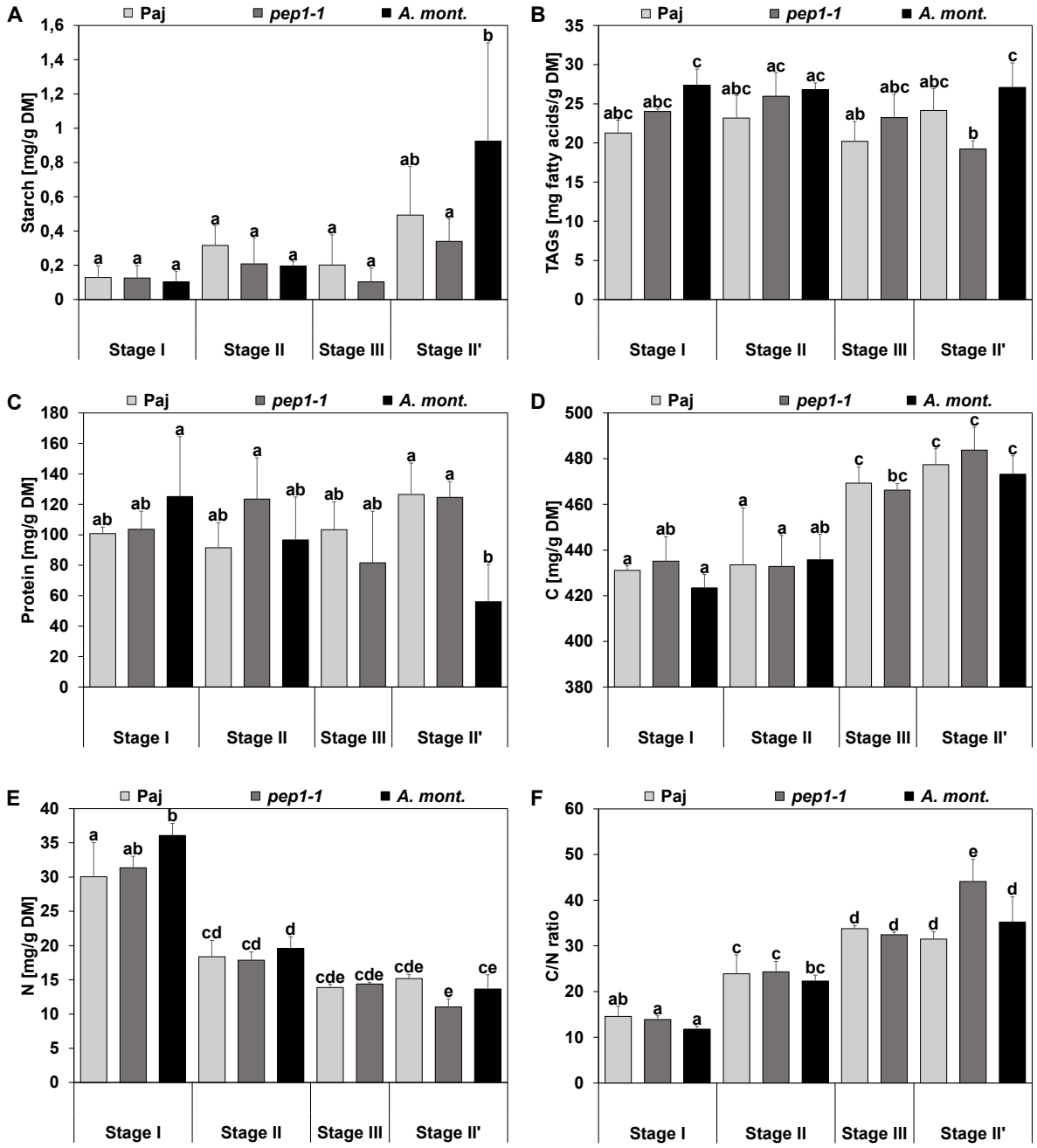

Supplemental Figure S4. Analysis of nutrient storage in roots. Stem diagrams represent contents per dry matter (DM) of (A), starch, (B), triacylglycerols (TAGs), (C), protein, (D), carbon (C), (E), nitrogen (N), (F), C/N ratios. Entire root systems were harvested at stages I, II, III, and II' of *A. alpina* Pajares (Paj, wild type), its *perpetual flowering 1-1* (*pep1-1*) mutant derivative, and annual *A. montbretiana* (*A. mont.*). Data are represented as mean +/- SD (n = 3-7). Different letters indicate statistically significant differences, determined by one-way ANOVA-Tukey's HSD test ($P < 0.05$).

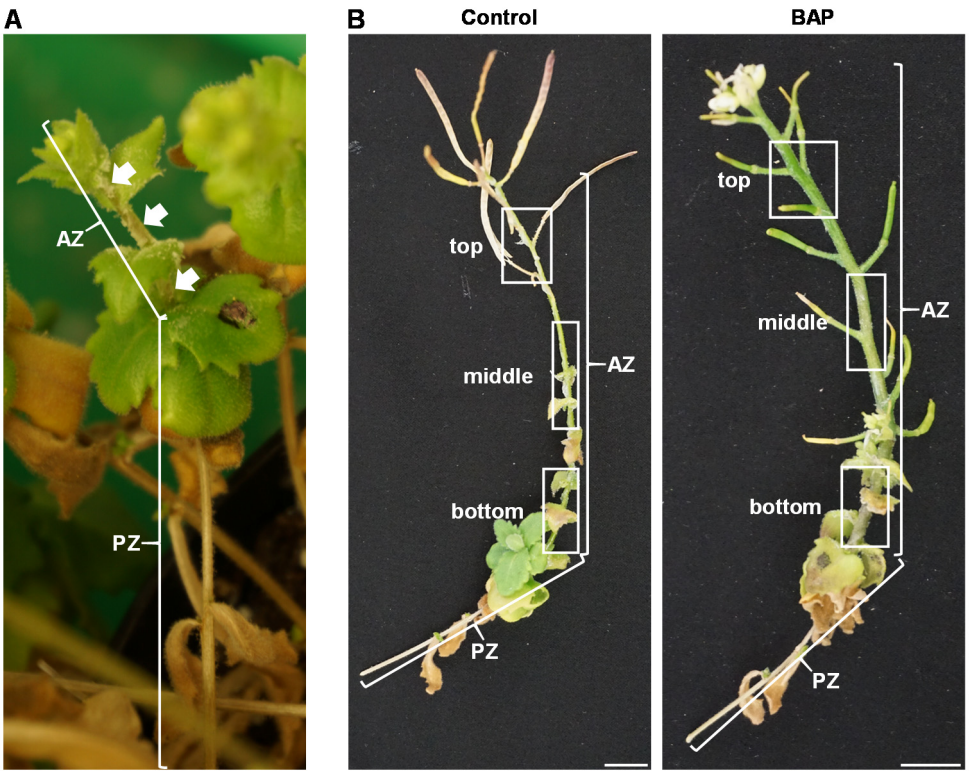

Supplemental Figure S5. Effect of prolonged cytokinin treatment and dissection of the annual zone (AZ). (A) Representative lateral branch of *perpetual flowering 1-1* (*pep1-1*) mutant before treatment. Three internodes belonging to the AZ were treated on day 1 (arrows) with 2 mM 6-benzylaminopurine (BAP) or mock treatment. These and following newly formed internodes were treated every fourth day until the experiment was stopped after 46 days. (B) Representative lateral branches after 46-day BAP and mock treatment (control). For the microscopic analysis, the AZ was divided into three regions (boxes: top, middle, and bottom), which were comparable between control and cytokinin treatment with regard to the overall size of the formed AZ. Each investigated region comprised two to three internodes.

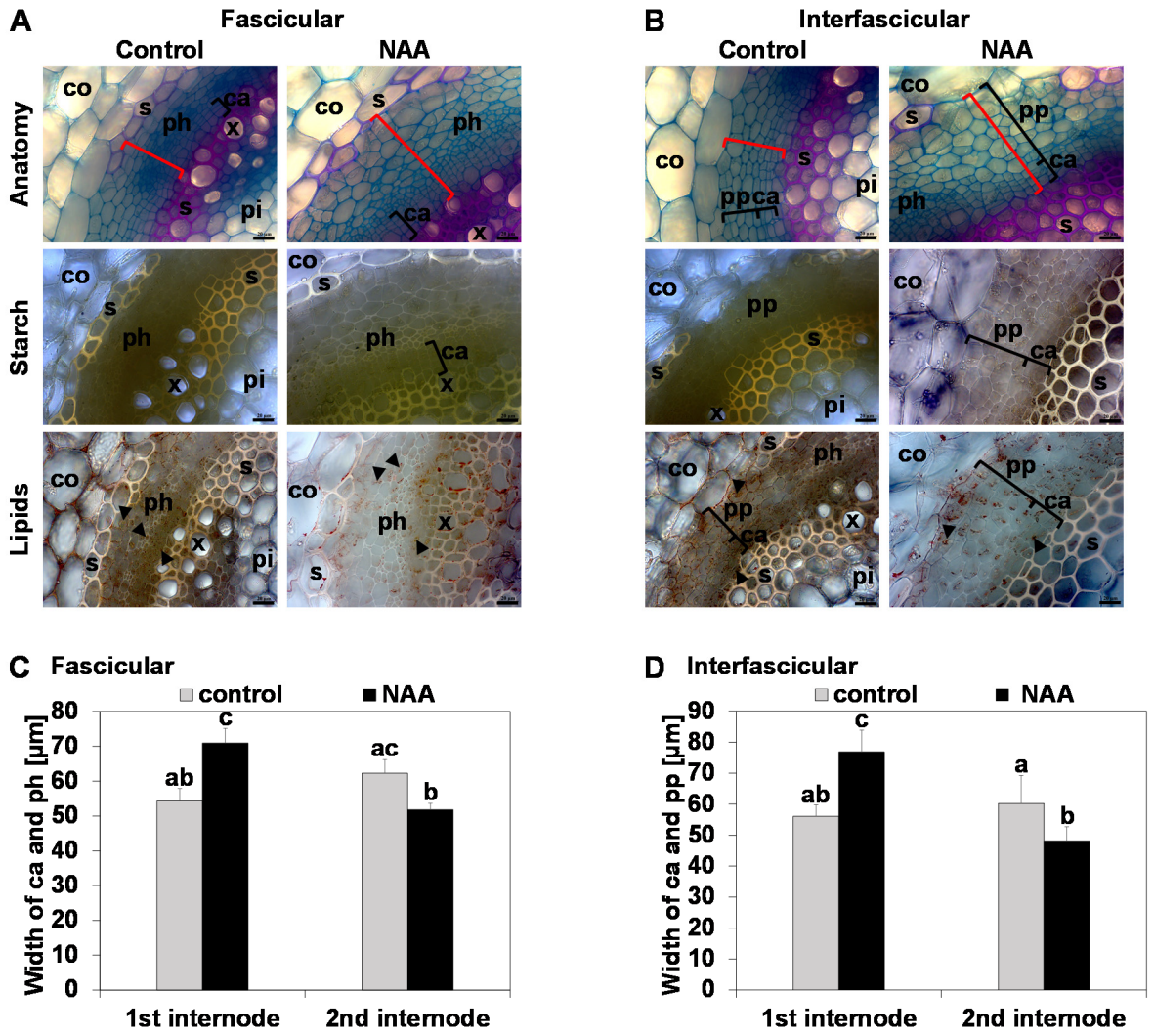

Supplemental Figure S6. Effect of auxin treatment on cambium activity in the perennial zone (PZ). (A, B), Lateral stem first internode cross sections of (A), the fascicular region, (B), the interfascicular region of *A. alpina perpetual flowering 1-1* (*pep1-1*) mutant, following treatment with auxin (0.5 mM 1-naphthaleneacetic acid, NAA) or mock control for eight days to the first internode. Representative images are shown. Anatomy, investigated following FCA staining, in blue, staining of non-lignified cell walls (parenchyma, phloem, meristematic cells), in red, staining of lignified cell walls, and in greenish, staining of suberized cell walls (xylem, sclerenchyma, cork). Starch, visualized following Lugol's iodine staining, dark violet-black color. Lipids, detected by Sudan IV staining, orange pinkish color of lipid bodies and yellowish color of suberized and lignified cell wall structures. Black triangles, lipid bodies; black brackets, responsive cambium and phloem/secondary phloem parenchyma; red brackets, quantified tissue width in (C) and (D). Abbreviations used in microscopic images: c, cork; ca, cambium; co, cortex; e, epidermis; pd, phelloderm; pe, periderm; ph, phloem including primary phloem, secondary phloem, phloem parenchyma; pi, pith; pp, secondary phloem parenchyma; s, sclerenchyma; x, xylem including primary xylem, secondary xylem, xylem parenchyma. Scale bars, 20 µm. (C, D) Quantified cambium and phloem/secondary phloem width in, (C), fascicular, and (D), interfascicular internode regions for first and second internodes. Data are represented as mean +/- SD (n = 5). Different letters indicate statistically significant differences, determined by one-way ANOVA-Tukey's HSD test ($P < 0.05$).

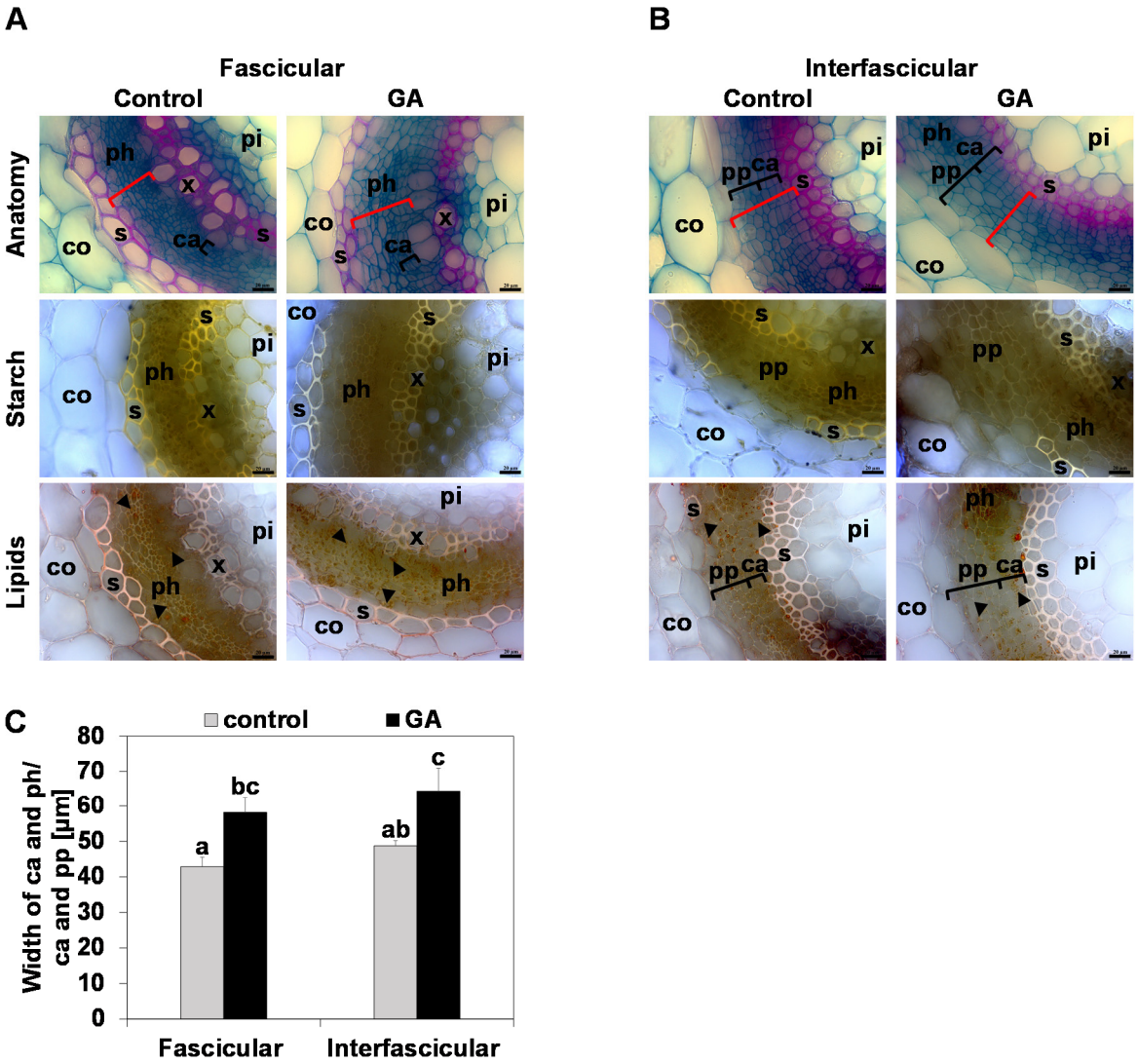

Supplemental Figure S7. Effect of gibberellic acid (GA) treatment on cambium activity in the perennial zone (PZ). (A, B), Lateral stem first internode cross sections of (A), the fascicular region, (B), the interfascicular region of *A. alpina perpetual flowering1-1* (*pep1-1*) mutant, following treatment with GA (4 mM gibberellin A_3) or mock control for eight days to the first internode. Representative images are shown. Anatomy, investigated following FCA staining, in blue, staining of non-lignified cell walls (parenchyma, phloem, meristematic cells), in red, staining of lignified cell walls, and in greenish, staining of suberized cell walls (xylem, sclerenchyma, cork). Starch, visualized following Lugol's iodine staining, dark violet-black color. Lipids, detected by Sudan IV staining, orange pinkish color of lipid bodies and yellowish color of suberized and lignified cell wall structures. Black triangles, lipid bodies; black brackets, responsive cambium and phloem/secondary phloem parenchyma; red brackets, quantified tissue width in (C). Abbreviations used in microscopic images: c, cork; ca, cambium; co, cortex; e, epidermis; pd, phelloderm; pe, periderm; ph, phloem including primary phloem, secondary phloem, phloem parenchyma; pi, pith; pp, secondary phloem parenchyma; s, sclerenchyma; x, xylem including primary xylem, secondary xylem, xylem parenchyma. Scale bars, 20 µm. (C) Quantified cambium and phloem/secondary phloem width in fascicular and interfascicular internode regions for first internode. Data are represented as mean +/- SD (n = 3). Different letters indicate statistically significant differences, determined by one-way ANOVA-Tukey's HSD test ($P < 0.05$).

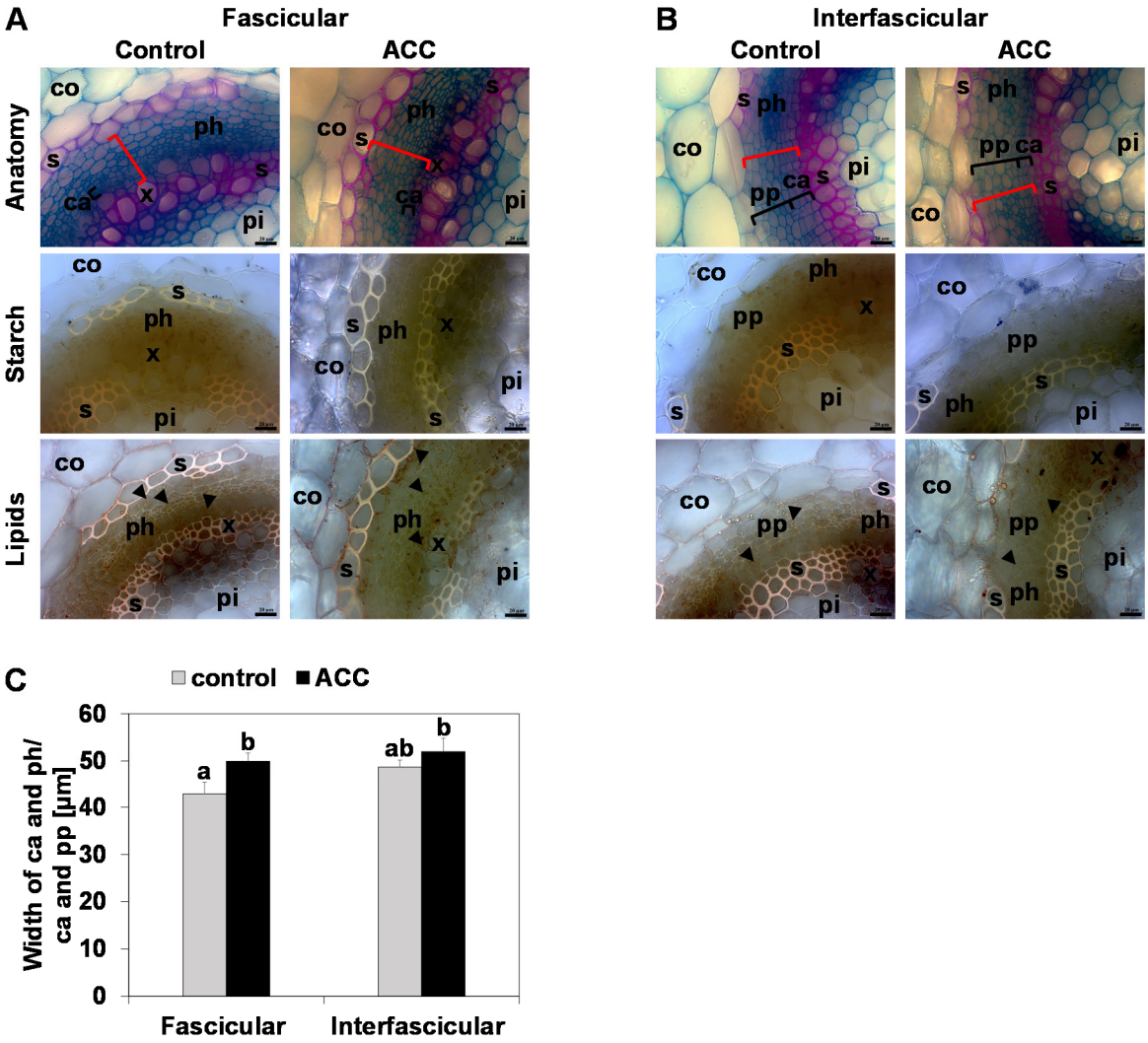

Supplemental Figure S8. Effect of ethylene on cambium activity in the perennial zone (PZ). (A, B), Lateral stem first internode cross sections of (A), the fascicular region, (B), the interfascicular region of *A. alpina perpetual flowering1-1* (*pep1-1*) mutant, following treatment with 2 mM 1-aminocyclopropane-1-carboxylic acid (ACC) or mock control for eight days to the first internode. Representative images are shown. Anatomy, investigated following FCA staining, in blue, staining of non-lignified cell walls (parenchyma, phloem, meristematic cells), in red, staining of lignified cell walls, and in greenish, staining of suberized cell walls (xylem, sclerenchyma, cork). Starch, visualized following Lugol's iodine staining, dark violet-black color. Lipids, detected by Sudan IV staining, orange pinkish color of lipid bodies and yellowish color of suberized and lignified cell wall structures. Black triangles, lipid bodies; black brackets, responsive cambium and phloem/secondary phloem parenchyma; red brackets, quantified tissue width in (C). Abbreviations used in microscopic images: c, cork; ca, cambium; co, cortex; e, epidermis; pd, phelloderm; pe, periderm; ph, phloem including primary phloem, secondary phloem, phloem parenchyma; pi, pith; pp, secondary phloem parenchyma; s, sclerenchyma; x, xylem including primary xylem, secondary xylem, xylem parenchyma. Scale bars, 20 µm. (C) Quantified cambium and phloem/secondary phloem width in fascicular and interfascicular internode regions for first internode. Data are represented as mean +/- SD (n = 3). Different letters indicate statistically significant differences, determined by one-way ANOVA-Tukey's HSD test ($P < 0.05$).

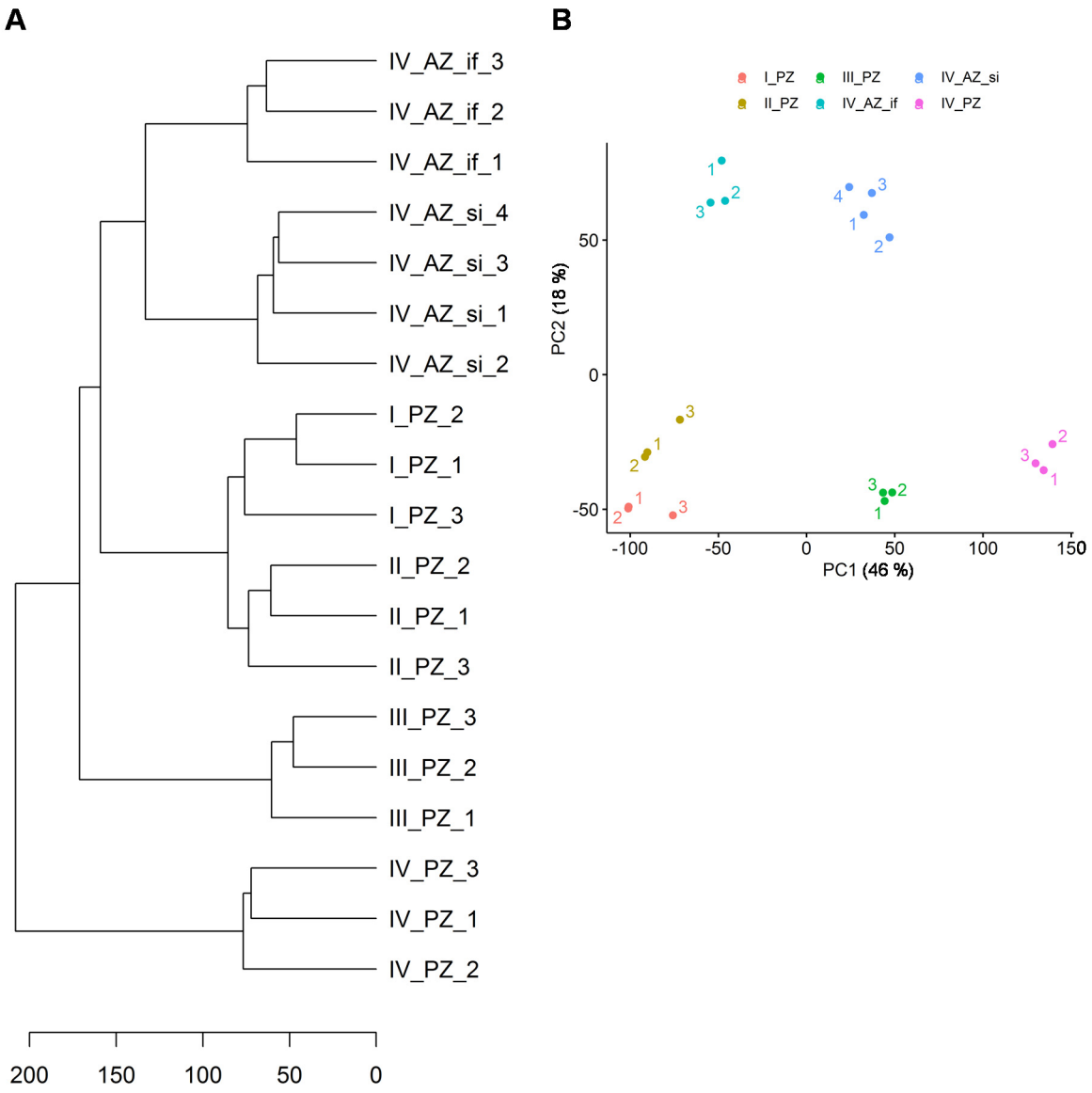

Supplemental Figure S9. Hierarchical clustering (HC) and Principal Component Analysis (PCA) of RNA-sequencing data. (A) HC and (B) PCA corresponding to internode samples harvested at different stages from perennial (PZ) and annual (AZ) lateral stem zones, stage I_PZ, stage II_PZ, stage III_PZ, stage IV_PZ, stage IV_AZ_si, stage IV_AZ_if; biological replicates 1-3 or 1-4 (compare with Figure 8A).

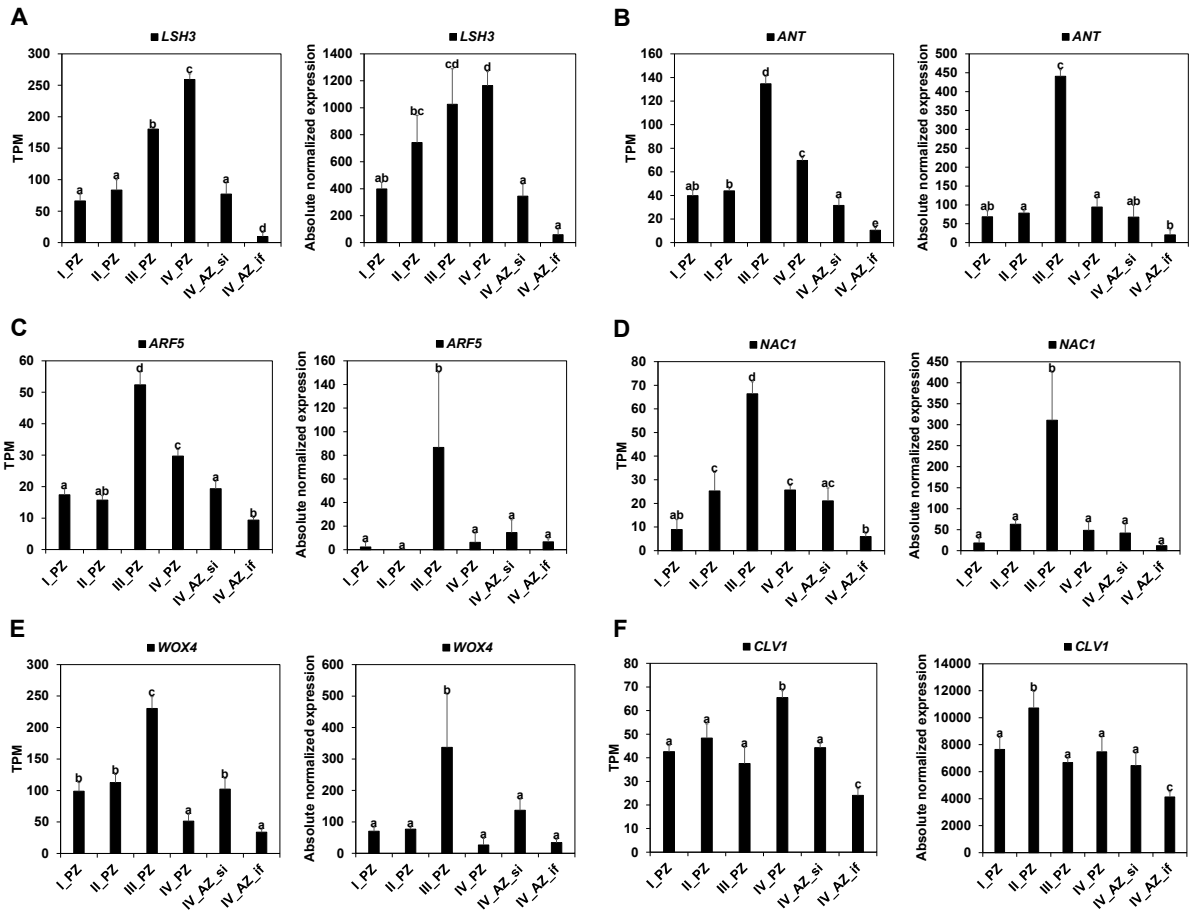

Supplemental Figure S10. Expression of genes, involved in cambial activity and maintenance, in lateral stem internodes. Gene expression was tested at different stages of the development of the perennial zone (PZ) and annual zone (AZ) in *A. alpina perpetual flowering1-1* (*pep1-1*) mutant derivative (see Figure 8A). Represented are RNA-sequencing data (left; TPM, transcripts per million) and reverse transcription-qPCR data (right; Absolute normalized expression). (A), *LSH3*, *LIGHT SENSITIVE HYPOCOTYLS 3*; (B) *ANT*, *AINTEGUMENTA*; (C) *ARF5*, *AUXIN RESPONSE FACTOR 5;* (D) *NAC1*, *NAC DOMAIN CONTAINING PROTEIN 1*; (E) *WOX4, WUSCHEL RELATED HOMEOBOX 4*; (F) *CLV1, CLAVATA 1*. In accordance with the observation of the established vascular cambium, these genes are higher expressed at the developmentally more progressed PZ stages (II_PZ, III_PZ or IV_PZ) in comparison to the AZ. Data are represented as mean +/- SD ($n = 3$). Different letters indicate statistically significant differences, determined by one-way ANOVA-Tukey's HSD test ($P < 0.05$).

Supplemental Table S1. RT-qPCR primers.

	arabis_transcript_id	Ath_AGI	Name	Forward (F) Primer (5' to 3')	Reverse (R) Primer (5' to 3')	Amplicon length [bp]
Reference	Aa_G26240	AT5G46630	*CLATHRIN ADAPTOR COMPLEX MEDIUM SUBUNIT* (*CAC*)	TGGACAAGACCACCAATCCA (Stephan *et al.*, 2019)	CACTCGACCGTGTTGTAACC (Stephan *et al.*, 2019)	113
	Aa_G472320	AT3G13920	*EUKARYOTIC TRANSLATION INITIATION FACTOR 4A1* (*EIF4a*)	CCAGCTTCTCCCACCCAAGA (Stephan *et al.*, 2019)	GCTCGTCACGCTTCACCAAG (Stephan *et al.*, 2019)	122
Genomic DNA control	Aa_G26240	AT5G46630	*CLATHRIN ADAPTOR COMPLEX MEDIUM SUBUNIT* (*CAC*)	CATTGGAAGCGTGGATGAAA	CTCCGAATCCACTTCAATCTCC	230
	Aa_G472320	AT3G13920	*EUKARYOTIC TRANSLATION INITIATION FACTOR 4A1* (*EIF4a*)	AAGAGCGGAAACAAGGGAAG	AAATGCAAAGCTCGGAACAC	129
Cytokinin	Aa_G918240	AT2G27760	*ISOPENTENYLTRANSFERASE 2* (*IPT2*)	CCTGTGGCAGCAAACAGAAT	ACCAGGGTTTCAGCGTCTAA	185
	Aa_G83560	AT5G19040	*ISOPENTENYLTRANSFERASE 5* (*IPT5*)	GGAGACGGCGATTGAGAAGA	GAACCTATCGACTGCGAGTGC	205
	Aa_G226650	AT1G10470	*ARABIDOPSIS RESPONSE REGULATOR 4* (*ARR4*)	TTCTGATTCCGTCCAAACTCC	TCTAAACCGGGACTCCTCATC	213
	Aa_G762130	AT1G19050	*ARABIDOPSIS RESPONSE REGULATOR 7* (*ARR7*)	GCCAATCTAACAAGAGGAAGCT	TGAAGATGAAATGTCCTTGACA	101
	Aa_G388620	AT3G21510	*ARABIDOPSIS HISTIDINE-CONTAINING PHOSPHOTRANSMITTER 1* (*AHP1*)	TGTGTCGTCTTCCGTAGCTTC	TCATCCCACCAGAGGCTACA	151
	Aa_G245600	AT5G39340	*ARABIDOPSIS HISTIDINE-CONTAINING PHOSPHOTRANSMITTER 3* (*AHP3*)	TAGCTTTAGATCAGACAGGAAATGT	TGAAGCTTTGCCTTCAATGA	211
	Aa_G312320	AT2G01830	*ARABIDOPSIS HISTIDINE KINASE 4* (*AHK4*)	TCATCTCCCGCAACACTCAA	TCTCCATCATCCTTATCTGACGA	250
Cambial activity and maintenance	Aa_G359500	AT2G31160	*LIGHT SENSITIVE HYPOCOTYLS 3* (*LSH3*)	CCACAAACCTAAGCATCATCG	CGTAACGGCTTGAGTTTCCT	111
	Aa_G95190	AT4G37750	*AINTEGUMENTA* (*ANT*)	TGGAAGGAGGAAGAGGAGAAG	CATTAAGCAAAGAGAACCATCAG	209
	Aa_G329270	AT1G19850	*AUXIN RESPONSE FACTOR 5* (*ARF5*)	CGAGTCCGAACCTACACTAAGG	TGTGGGCGACAGTATCCTTAT	258
	Aa_G108910	AT1G56010	*NAC DOMAIN CONTAINING PROTEIN 1* (*NAC1*)	CCCTGCTTCTCCAATTTGTC	GCTGCCTTCACCGTTACTCT	240
	Aa_G171170	AT1G46480	*WUSCHEL RELATED HOMEOBOX 4* (*WOX4*)	ATATCACATCTCAGCTCGGTAAG	CCTGATGTCTAGCGACGATG	206
	Aa_G702580	AT1G75820	*CLAVATA 1* (*CLV1*)	TTCGGAGTGGTTCTATTGGAG	CGTGTTCCTCACCCACCTA	93

Author contributions to Manuscript 1

Anna Sergeeva

Designed, performed, and analyzed all of the described experiments, except for the following sections: RNA-seq data analysis (from assembling of the coding sequences until the gene ontology analysis (generation of excel tables containing GO terms): s. Materials and Methods: RNA sequencing and analysis), conducting of RT-qPCRs (Figure 9, Supplemental Figure S10), microscopy and measurements of cambium, phloem, and phloem parenchyma regions of lateral stem internodes treated with auxin, GA, and ACC (Supplemental Figures S6, S7, S8). Supervised RT-qPCR and hormone experiments. Prepared figures and tables, wrote the manuscript, reviewed/edited the manuscript.

Hongjiu Liu

Performed the following experiments: RT-qPCRs (Figure 9, Supplemental Figure S10), microscopy and measurements of cambium, phloem, and phloem parenchyma regions of lateral stem internodes treated with auxin, GA, and ACC (Supplemental Figures S6, S7, S8). Helped with microscopy and measurements of the AZ internodes treated with cytokinin (Figure 7). Reviewed/edited the manuscript.

Hans-Jörg Mai

Performed the RNA-seq data analysis (from assembling of the coding sequences until the gene ontology analysis (generation of excel tables containing GO terms): s. Materials and Methods: RNA sequencing and analysis). Provided R scripts for generation of HC, PCA, and horizontal bar plots (Figure 8B, Supplemental Figure S9). Reviewed/edited the manuscript.

Tabea Mettler-Altmann

Helped in designing and analyzing of the following experiments: TAG quantification (Figure 4B and Supplemental Figure S4B), C and N determination (Figure 5A, B, D and Supplemental Figure S4D, E, F). Reviewed/edited the manuscript.

Christiane Kiefer

Provided initial information about *A. alpina* and *A. montbretiana*, and seeds of all mentioned genotypes. Reviewed/edited the manuscript.

George Coupland

Provided initial information about *A. alpina* and *A. montbretiana*. Reviewed/edited the manuscript.

Petra Bauer

Designed and supervised the study. Acquired funding. Wrote the manuscript, reviewed/edited the manuscript.

8 Manuscript 2

Lipid metabolism distinguishes perennial and annual stem zones in the perennial model plant *Arabis alpina*

Lipid metabolism distinguishes perennial and annual stem zones in the perennial model plant *Arabis alpina*

Anna Sergeeva[1,2], Tabea Mettler-Altmann[2,3], Hongjiu Liu[1], Hans-Jörg Mai[1], Petra Bauer[1,2]

[1]Heinrich Heine University, Institute of Botany, D-40225 Düsseldorf, Germany

[2]Cluster of Excellence on Plant Science (CEPLAS), Heinrich Heine University, Düsseldorf, Germany

[3]Heinrich Heine University, Institute of Plant Biochemistry, D-40225 Düsseldorf, Germany

Correspondence to: Petra Bauer, Institute of Botany, Heinrich Heine University, Universitätstraße 1, D-40225 Düsseldorf, Germany

Email: petra.bauer@uni-duesseldorf.de

Tel: +49 211 81-13479, Fax: +49 211 81-12881

Anna Sergeeva, Anna.Sergeeva@hhu.de
Tabea Mettler-Altmann, tabeam@yahoo.de
Hongjiu Liu, liured9@nwafu.edu.cn
Hans-Jörg Mai, Hans-Joerg.Mai@hhu.de
Petra Bauer, petra.bauer@hhu.de

Running title: Lipid storage in *Arabis*

Highlight

Glycerolipid amounts increase in the developing vegetative perennial stem zone. Expression of corresponding lipid metabolism genes correlates with lipid species, and such genes are targets for studying the perennial-annual phase transition.

Key words (6-10)

Arabis alpina, cambium, fatty acid, glycerolipid, lipid, *pep1*, perennial, secondary growth, triacylglycerol

Abbreviations

ACT1, ACYLTRANSFERASE 1
ACX, ACYL-COA OXIDASE
AIM1, ABNORMAL INFLORESCENCE MERISTEM 1
ANOVA, analysis of variance
AZ, annual zone
CAC, CLATHRIN ADAPTOR COMPLEX MEDIUM SUBUNIT
DGD1, DIGALACTOSYL DIACYLGLYCEROL DEFICIENT 1
DSEL, DAD1-LIKE SEEDLING ESTABLISHMENT-RELATED LIPASE
ECH2, ENOYL-COA HYDRATASE 2
ECI1, Δ3, Δ2-ENOYL COA ISOMERASE 1
EIF4a, EUKARYOTIC TRANSLATION INITIATION FACTOR 4A1
ER, endoplasmic reticulum
FA, fatty acid
FAME, fatty acid methylester
FLC, FLOWERING LOCUS C
GC-MS, gas chromatography-mass spectrometry
GL, glycolipid
GO, gene ontology
HSD, honest significant difference
KAT2, 3-KETOACYL-COA THIOLASE 2
KCS4, 3-KETOACYL-COA SYNTHASE 4
LB, lipid body
LCFA, long-chain fatty acid
LPCAT1, LYSOPHOSPHATIDYLCHOLINE ACYLTRANSFERASE 1
MFP2, MULTIFUNCTIONAL PROTEIN 2
NL, neutral lipid
Paj, Pajares
PEP1, PERPETUAL FLOWERING 1
PES1, PHYTYL ESTER SYNTHASE 1
PL, phospholipid
PLDζ2, PHOSPHOLIPASE D ζ 2
PLIP3, PLASTID LIPASE 3
PNC1, PEROXISOMAL ADENINE NUCLEOTIDE CARRIER 1
pPLAIIIβ, PATATIN-RELATED PHOSPHOLIPASE A IIIβ
PZ, perennial zone
QTOF, quadrupole time-of-flight
SDP1, SUGAR-DEPENDENT 1
TAG, triacylglycerol
VLCFA, very long-chain fatty acid
WRI1, WRINKLED 1

Abstract

The perennial life style is a successful ecological strategy, and *Arabis alpina* is a recently developed model Brassicaceae species for studying it. One aspect, poorly investigated until today, concerns the differing patterns of allocation, storage and metabolism of nutrients between perennials and annuals and the yet unknown signals that regulate this process. *A. alpina* has a complex lateral stem architecture with a proximal vegetative perennial (PZ) and a distal annual flowering zone (AZ), allowing to study nutrient allocation to either PZ or AZ inside the same stems. Lipid bodies (LBs) with triacylglycerol (TAG) accumulate in the PZ. To decipher processes of lipid metabolism linked with the perennial lifestyle, we analyzed lipid species in the PZ versus AZ. Glycerolipid fractions, including neutral lipids with mainly TAGs, phospholipids, and glycolipids were present at higher levels in the PZ as compared to the AZ or roots. Concomitantly, contents of specific long-chain and very long-chain fatty acids increased during formation of the PZ. Corresponding gene expression data, gene ontology term enrichment and correlation analysis with lipid species pinpoint glycerolipid-related genes active during the development of the PZ. Lipid metabolism genes are targets of regulatory mechanisms specifying PZ differentiation in *A. alpina*.

Introduction

Perennial plants survive and reproduce throughout many years, and in most natural settings the perennial life style is of advantage to secure a dominant position in the environment. *Arabis alpina* is a herbaceous hemicryptophyte with perennial vegetative branches above the soil (according to the Raunkiaer's system of plant life forms). This species has attracted attention as a model for studying its specific perennial characters. *A. alpina* is polycarpic and produces new flowers during every new growth season at the distal ends of the main shoot and lateral branches. In proximal vegetative parts of the stems, buds develop either into non-flowering branches, remain as perennating buds or develop into flowering lateral branches that maintain vegetative growth (Lazaro *et al.*, 2018; Vayssières *et al.*, 2020). This complex architecture of *A. alpina* is established during and after vernalization, a required cold season that induces flowering. The *Arabis* clade belongs to the Brassicaceae family (Karl and Koch, 2013; Kiefer *et al.* 2017) and genome sequence information, techniques, and tools developed for *Arabidopsis thaliana* and other Brassicaceae, are employed to study *Arabis* perennial behavior. Flowering repressor PERPETUAL FLOWERING 1 (PEP1), the orthologue of the *Arabidopsis* FLOWERING LOCUS C (FLC), controls the flowering response and plant architecture (Michaels and Amasino, 1999; Wang *et al.*, 2009; Wang *et al.*, 2011; Albani *et al.*, 2012; Lazaro *et al.*, 2018; Hughes *et al.*, 2019). *pep1-1* mutant plants continuously form new lateral branches irrespective of a cold season, each of them with proximal vegetative and distal reproductive character (Wang *et al.*, 2009).

The vegetative part of the stem has secondary growth, coupled with high molecular weight carbon storage in a so-called perennial zone (PZ). Here, carbon accumulates in the form of starch and triacylglycerol (TAG) in cambium and cambium-derived secondary phloem tissues (Sergeeva *et al.*, Manuscript 1). These stored nutrients likely serve bud outgrowth in the following season. In contrast to that, reproductive parts of the main shoot and lateral shoots show primary growth and after flowering and seed formation turn senescent, so-called annual zone (AZ). Starch and lipid bodies (LBs) accumulate there in cortical parenchyma tissue (Sergeeva *et al.*, Manuscript 1). Additionally, LBs but not starch accumulate in the AZ in fascicular cambium and phloem of the vascular bundles (Sergeeva *et al.*, Manuscript 1). In the AZ, these high-energy carbon-rich nutrients are used during reproduction.

Lipids play key roles in metabolism and nutrient storage in plants. Lipid composition is a key for membrane identity. For example, the plasma membrane contains primarily phosphoglycerolipids (Simon, 1974; Wewer *et al.*, 2011), while predominant constituents of the chloroplast thylakoid membranes are galactoglycerolipids (Hurlock *et al.*, 2014; LaBrant *et al.*, 2018; Karki *et al.*, 2019). Besides that, lipids are carbon storage products in plants and animals (Lu *et al.*, 2011; Tan *et al.*, 2011; Shi *et al.*, 2012; Haslam *et al.*, 2013; Vanhercke *et al.*, 2013; van Erp *et al.*, 2014; Li *et al.*, 2015). Plants store lipids mainly as TAG in LBs. TAG-containing LBs are present in oilseeds of various plant species (Cao and Huang, 1986; Loer and Herman, 1993; Lee *et al.*, 1995; Lacey *et al.*, 1999; Shockey *et al.*, 2006; Cai *et al.*, 2017), but also in vegetative tissues, such as leaves (Pyc *et al.*, 2017; Brocard *et al.*,

2017), stems (Sauter and Cleve, 1994; Madey *et al.*, 2002; Wang *et al.*, 2007), and roots (Næsted *et al.*, 2000; Chinnasamy *et al.*, 2003). The biosynthesis pathways of different glycerolipid classes are interconnected in plants. Lipids are synthesized in the prokaryotic pathway in the chloroplast and in the eukaryotic pathway in the endoplasmic reticulum (ER) (Li-Beisson *et al.*, 2013; Jayawardhane *et al.*, 2018). Biosynthesis of neutral lipid (NL) TAG takes place in the ER in the *Kennedy* or *glycerol phosphate pathway* (Li-Beisson *et al.*, 2013). Diacylglycerol functions as the intermediate for TAG biosynthesis and as the backbone for the biosynthesis of glycolipids (GLs) and the phospholipids (PLs), phosphatidylcholine and phosphatidylethanolamine. Diacylglycerol is therefore an important intermediate for the synthesis of storage and membrane lipids. GLs, representative for plastidic membranes, are produced in the prokaryotic pathway. In addition, phosphatidylglycerol can be synthesized in the plastid in a series of sequential reactions. Phosphatidic acid is the intermediate for the biosynthesis of above-mentioned GLs and also PLs produced in the eukaryotic pathway in the ER. PLs mainly represent structural elements of extraplastidic membranes. The nature of fatty acids (FAs) of glycerolipids is indicative for their function. The *de novo* FA synthesis takes place in the plastid, and after their transport to the ER, FAs may be elongated to yield very long-chain fatty acids (VLCFAs) (Joubès *et al.*, 2008).

Here, we study a new aspect of stem architecture related to lipid metabolism. The simultaneous presence of the PZ and the AZ poses the conflict of nutrient allocation and usage for either seed production or development of perennating storage tissues. This raises the question which genes and signals regulate this process. We compared glycerolipid profiles between PZ and AZ and found that they differed between PZ and AZ. Using transcriptome data, we identified differentially regulated lipid metabolism genes, that are targets of PZ and AZ differentiation. Lipid metabolism gene ontology terms were enriched, that correlated with lipid species. These findings serve to investigate the regulation of TAG storage and lipid metabolism as a perennial trait in a Brassicaceae species and to study the differentiation signals in the PZ.

Materials and methods

Lipid analysis of plant material

Freeze-dried plant samples from different developmental stages of the PZ and AZ of *A. alpina* wild type Pajares (Paj) and its mutant derivative *perpetual flowering 1-1* (*pep1-1*) were used for lipid analysis (Fig. 1; Sergeeva *et al.*, Manuscript 1). At first, total amounts of glycerolipids were extracted using an acidic modified chloroform-methanol method (Hajra *et al*., 1974, https://www.imbio.uni-bonn.de/molekulare-biotechnologie/lipidomics-platform/acidic-chloroform-methanol, Wewer *et al*., 2011), (Supplementary Fig. S1). Ten mg of lyophilized and ground (fine-powdered in a Mixer Mill MM 200, Retsch, Haan, Germany) plant material was vortexed with 0.4 ml chloroform/methanol/formic acid (1:1:0.1) and 0.2 ml solution containing 0.2 M phosphoric acid and 1 M potassium chloride. After 5-minute centrifugation at 5000 rpm the resulting lower phase with glycerolipids was transferred to a new

glass tube. Chloroform extractions were repeated twice and bottom phases combined as the glycerolipid fraction, which included nonpolar and polar lipids.

Separation into nonpolar lipids (NL, triacylglycerol (TAG) and diacylglycerol) and polar lipids containing glycolipids (GL, monogalactosyldiacylglycerol, digalactosyldiacylglycerol, sulfoquinovosyldiacylglycerol) and phospholipids (PL, phosphatidic acid, phosphatidylserine, phosphoinositide, phosphatidylethanolamine, phosphatidylglycerol and phosphatidylcholine) was performed using silica-based solid phase extraction columns (55 µm, 70 Å) (Phenomenex, Torrance, USA) (Supplementary Fig. S1) (Wewer *et al.*, 2011), equilibrated with 1 ml chloroform. Glycerolipid fractions were applied to the column after equilibration and the flow through collected in a new glass tube. The NL fraction was eluted into the same glass tube with 1 ml chloroform. One milliliter of acetone/isopropanol (1:1) was added to the same column to elute the GL fraction, which was collected in a second glass tube. The flow through containing the PL fraction, eluted by addition of 1 ml methanol, was retrieved in a third tube. Finally, organic solvents were evaporated from the tubes in a desiccator coupled to a vacuum pump.

Resulting NL, GL, and PL fractions were immediately applied to prepare fatty acid methylesters (FAMEs) according to Hielscher *et al.* (2017) (Supplementary Fig. S1), using heptadecanoic acid (C17) (1 mg/ml) as internal standard. One milliliter of 3 N methanolic hydrochloric acid and 20 µl of the C17 internal standard were added to each sample. The samples were incubated for 60 min at 90 °C, cooled down at room temperature for 5 min. One milliliter n-hexane as well as 1 ml 1% (w/v) sodium chloride were added. Tubes were vortexed for 10 s and centrifuged for 5 min at 2000 rpm for phase separation. The upper hexane phase was transferred to a gas chromatography (GC) vial and stored at -20 °C until further analysis.

The analysis of FAME extracts was performed by GC-mass spectrometry (GC-MS) using a 7200-GC-quadrupole time-of-flight mass spectrometer (GC-QTOF) (Agilent Technologies, Santa Clara, USA) (Supplementary Fig. S1). Mass Hunter Software (Agilent Technologies, Santa Clara, USA) was used for integration of the resulting peaks. Absolute amounts of FAs in each sample were determined by relating the integrated peak area of detected FAs to the integrated peak area and known concentration of the C17 standard.

Gene expression analysis of lipid metabolism genes

The RNA-seq dataset consisting of three biological replicates per sample that had been described (Sergeeva *et al.*, Manuscript 1) was used to extract RNA-seq gene expression data corresponding to lipid metabolism (Supplementary Table S1; derived from the full transcriptome data set available under the GEO no. GSE152417). Gene ontology (GO) term enrichment analysis was performed according to Sergeeva *et al.* (Manuscript 1) to identify enriched lipid metabolism GO terms with a $P < 0.05$ (Supplementary Tables S2-S7). GO terms “NL metabolic process”, “galactolipid metabolic process”, “phosphatidylglycerol metabolic process”, “PL biosynthetic process”, “FA

biosynthetic process", and "FA catabolic process" (Supplementary Tables S2, S3) were screened for genes involved in NL, GL, PL, and FA biosynthesis and catabolism.

Validation of lipid metabolism gene expression was performed by reverse transcription-qPCR using the cDNA samples and procedures as described (Sergeeva *et al.*, Manuscript 1) and qPCR primers listed (Supplementary Table S8). Absolute quantification of normalized gene expression was obtained using mass standard curve analysis (Ben Abdallah and Bauer, 2016) and normalization with reference genes *CLATHRIN ADAPTOR COMPLEX MEDIUM SUBUNIT* (*CAC*) and *EUKARYOTIC TRANSLATION INITIATION FACTOR 4A1* (*EIF4a*) (Stephan *et al.*, 2019).

Statistical and correlation analysis

One-way analysis of variance (ANOVA) combined with Tukey's honest significant difference (HSD) test ($\alpha = 0.05$) was performed using the R software. Different letters in the diagrams represent significant differences with $P < 0.05$.

Pearson correlation analysis was conducted via the R software, between individual gene expression and biochemical lipid analysis data, using stages III_PZ, IV_PZ, stage I, and stage II' for PZ and stage IV_AZ_if, and stage II' for AZ, respectively. Only correlation coefficients with significant levels of correlation ($P < 0.05$) are displayed in the diagrams.

Results

Levels of glycerolipids increase during development of the PZ

The PZ differentiates during development to form secondary growth tissues, in which TAG-containing LBs accumulate, e.g. for lipid storage (Sergeeva *et al.*, Manuscript 1). The identity of lipids and TAGs had not been further elucidated previously. Moreover, not only TAG among the neutral lipids (NLs), but also two more glycerolipid types are linked with lipid storage and metabolism in plants, glycolipids (GLs) and phospholipids (PLs). These latter form cell and organellar membranes and membranous compartments for nutrient storage. Here, we subfractionated glycerolipid fractions into NLs, GLs, and PLs and determined their proportion as compared to total lipid amounts. Plant samples were lateral stem internodes divided into PZ and AZ and for comparison roots of *A. alpina* wild type Pajares (Paj) and mutant *perpetual flowering1-1* (*pep1-1*). These samples had been harvested along a developmental gradient at different growth stages during differentiation of the PZ and AZ, namely stages I, II, III, and II' (for descriptions see Fig. 1). *pep1-1* does not require vernalization for triggering flowering, and Paj and *pep1-1* differ in the timing but not the outcome of the PZ and AZ formation (Fig. 1; Sergeeva *et al.*, Manuscript 1).

NL, GL, and PL fractions were present at all stages in stems and roots of Paj and *pep1-1* (Fig. 2). They were highest in the PZ at stages III and II' in Paj and *pep1-1*, and lower in the PZ at stage I in Paj and stage II in *pep1-1* (Fig. 2A, Fig. 2B). Together, the three glycerolipid fractions reached about 60 % of total lipids in the PZ of Paj and even 80 % or more in *pep1-1*. On the other hand, the AZ of Paj

and *pep1-1* contained lowest amounts of all three glycerolipid fractions. These findings point to a significant increase of storage-related lipid forms in the PZ. In roots, on the other hand, NL, GL, and PL fractions remained constant and significant differences in their contents were not noted during the development at the same stages of Paj and *pep1-1* (Fig. 2C, Fig. 2D). Glycerolipid fractions together did not exceed 30-35 % of all lipids in roots, which was lower than in most PZ stem samples.

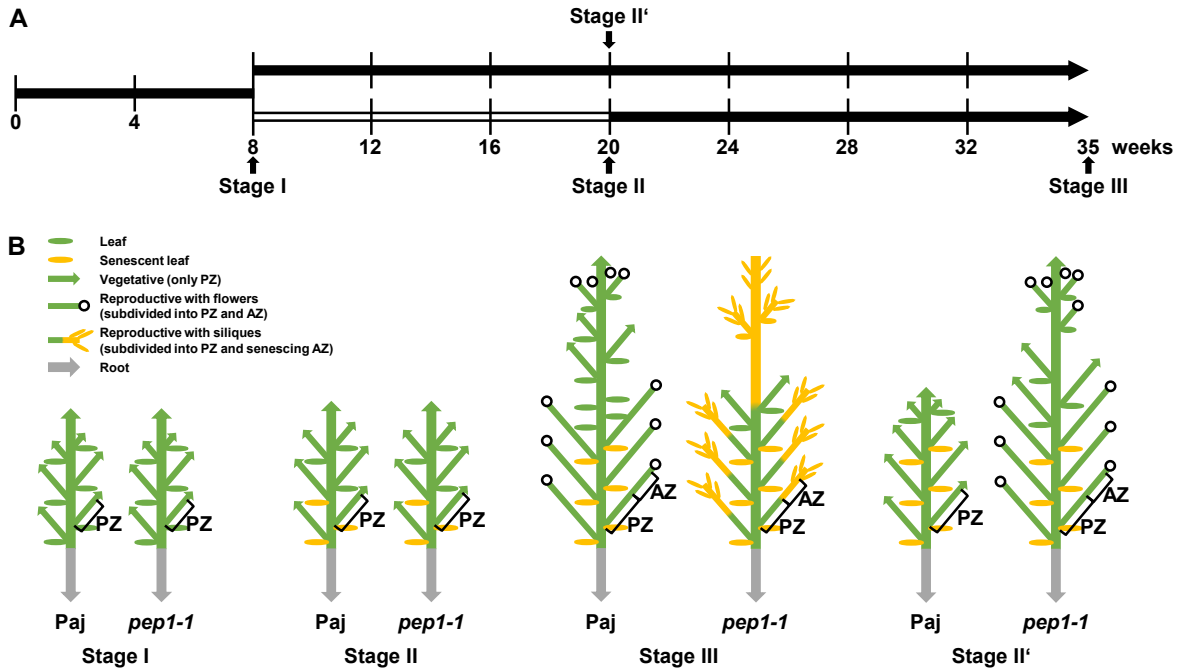

Fig. 1. Schematic representation of plant growth stages for *A. alpina* Pajares (Paj, wild type) and its *perpetual flowering 1-1* (*pep1-1*) mutant derivative used in lipid analysis. (A) Plant growth and harvesting scheme. Solid black lines, long-day conditions at 20 °C; open line, short-day conditions at 4 °C (vernalization); four developmental stages for harvesting, I, II, III, and II‘. (B) Schematic representation of Paj and *pep1-1* architecture of lateral stems at stages I, II, III, and II‘. Lateral stems were harvested, subdivided into perennial (PZ) and annual (AZ) zones, as indicated (see also Sergeeva *et al*., Manuscript 1). In addition to lateral stems, entire root systems of single plants were harvested as one root sample. The schematic plant representation was partially adopted from Wang *et al.* (2009), Lazaro *et al.* (2018), and Vayssières *et al.* (2020).

Taken together, these data show the highest amounts of glycerolipids in the developed PZ of lateral stems rather than roots or the AZ, indicating the importance of lipid metabolism and lipid storage in the PZ. Moreover, Paj and *pep1-1* were similar in this respect showing that vernalization was not a requirement for glycerolipid accumulation.

NLs with long-chain and very long-chain fatty acids increase during development of the PZ

The nature of FAs contained in glycerolipids is important to estimate their function. Generally, storage lipids contain long-chain FAs (LCFAs), comprising predominantly C16 and C18 FAs (palmitic (16:0), linoleic (18:2) and linolenic (18:3) acids), and very long-chain FAs (VLCFAs), including C20, C22 and C24 FAs (arachidic (20:0), behenic (22:0) and lignoceric (24:0) acids).

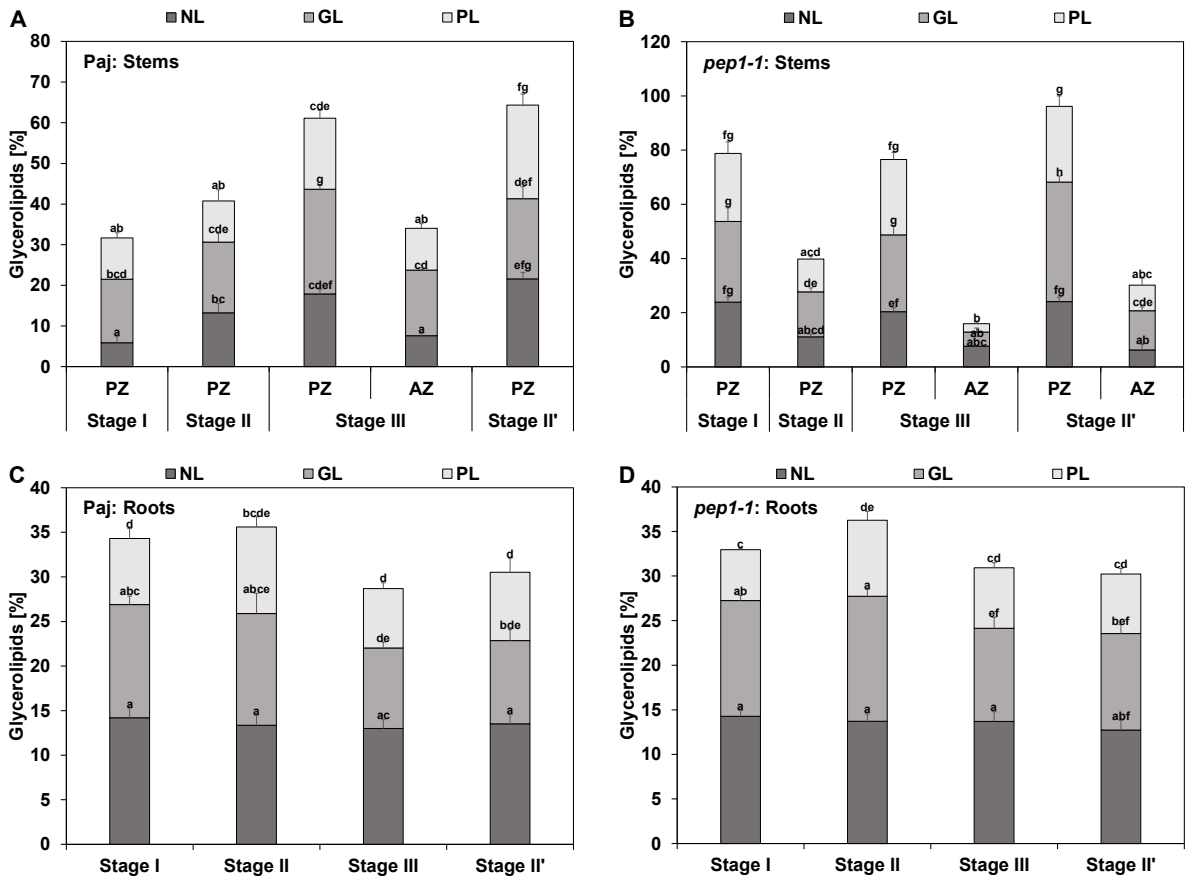

Fig. 2. Glycerolipid accumulation in stems and roots. The three glycerolipid fractions are neutral lipids (NL), glycolipids (GL), and phospholipids (PL), represented as percentage of their fatty acids (FAs) in relation to total FA contents (as 100 %) of dry matter of (A, B) perennial and annual internode stem zones (PZ, AZ) and (C, D) entire root systems of (A, C) *A. alpina* Pajares (Paj, wild type) and (B, D) *perpetual flowering 1-1* (*pep1-1*) mutant derivative. Plant material was harvested at four different developmental stages, stage I, II, III, and II‘, as indicated in Fig. 1A. Data are represented as mean +/- SD (n = 3-7). Different letters indicate statistically significant differences, determined by one-way ANOVA-Tukey‘s HSD test ($P < 0.05$).

At first, FAs present in the NL fraction of each investigated stage and line were therefore subdivided into total LCFAs (total of 14:0, 16:0, 16:1, 18:2, 18:3 and 18:1 FAs), and total VLCFAs (total of 20:0, 22:1, 22:0, 24:1, 24:0 FAs) (Fig. 3). Contents of total LCFAs were higher than those of total VLCFAs in all stem samples of Paj and *pep1-1*. Generally, amounts of total LCFAs and total VLCFAs were higher in PZ than in AZ samples. Interestingly, contents of total VLCFAs increased in the PZ with the progression of the development and reached highest levels at stage II’ (Fig. 3A, Fig. 3B). Levels of total LCFAs and total VLCFAs in the NL fraction were not significantly differing from each other at every single investigated developmental stage in roots of Paj and *pep1-1* (Fig. 3C, Fig. 3D). Contrary to stems, contents of total LCFAs and total VLCFAs in roots did not change during root development in both lines.

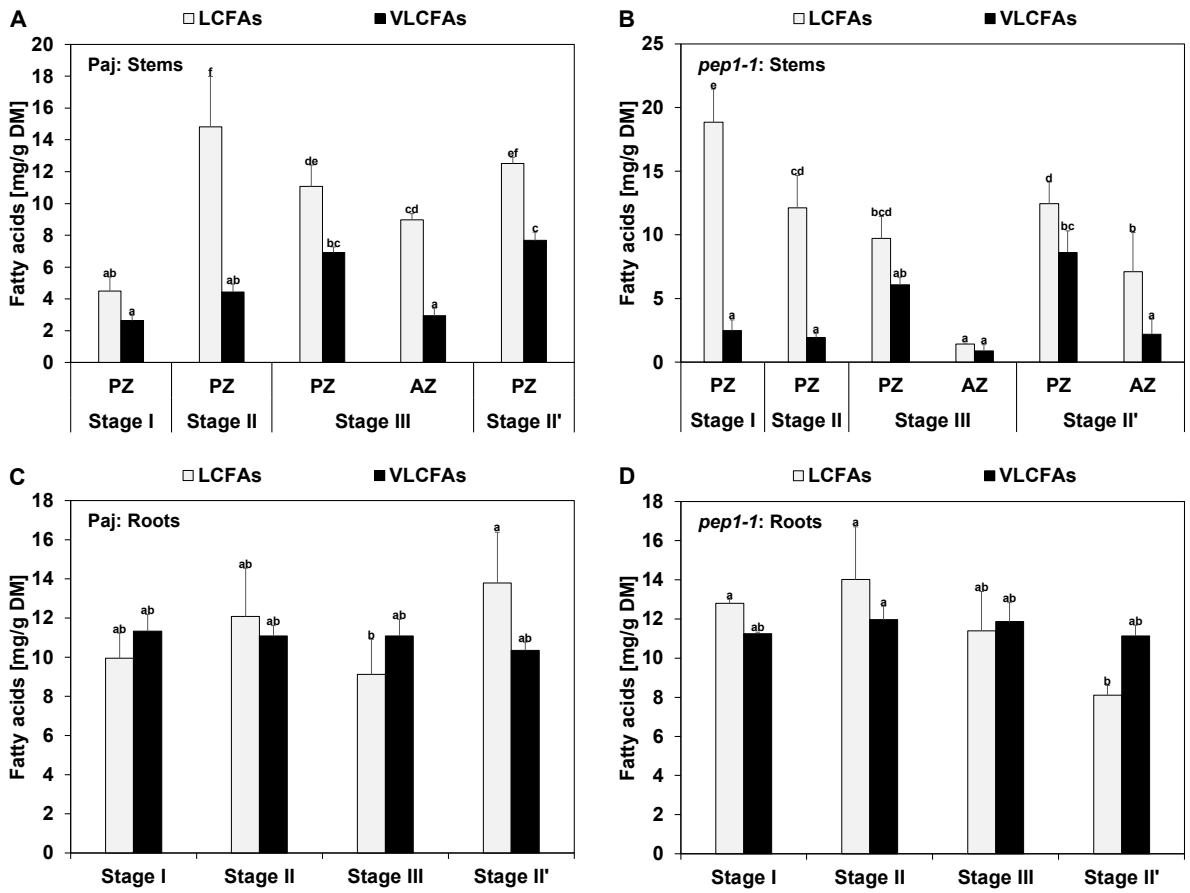

Fig. 3. Long-chain and very long-chain fatty acid contents (LCFAs, VLCFAs) in neutral lipid (NL) fractions in stems and roots. Represented are the contents of NL fraction-derived total LCFAs (total of 14:0, 16:0, 16:1, 18:2, 18:3, 18:1) and total VLCFAs (total of 20:0, 22:1, 22:0, 24:1, 24:0) per dry matter (DM) of (A, B) perennial (PZ) and annual (AZ) internode stem zones and (C, D) entire root systems of (A, C) *A. alpina* Pajares (Paj, wild type) and (B, D) *perpetual flowering 1-1* (*pep1-1*) mutant derivative. Plant material was harvested at four different developmental stages, stage I, II, III, and II‘, as indicated in Fig. 1A. Data are represented as mean +/- SD (n = 3-7). Different letters indicate statistically significant differences, determined by one-way ANOVA-Tukey’s HSD test ($P < 0.05$).

Next, we investigated individual LCFAs and VLCFAs. In NLs of both genotypes, 16:0 palmitic acid was the most abundant FA at examined stages, while in the same samples 14:0, 16:1, 18:1, 22:1, and 24:1 FAs were not abundant nor varied significantly (Fig. 4A, Fig. 4B). However, contents of 18:2 and 18:3 FAs along with VLCFAs 20:0, 22:0, and 24:0 increased markedly with progression of PZ development in both genotypes and only slightly during development of the AZ. Therefore, the increase of LCFAs 18:2 and 18:3 and of VLCFAs 20:0, 22:0, and 24:0 in the PZ supports the storage character of the PZ and the relevance of NLs (Fig. 4A, Fig. 4B). Interestingly, in *pep1-1* LCFAs 18:2 and 18:3 peaked at stage I and II in the PZ, but then declined (Fig. 4B). Perhaps this decline is caused by catabolic activities during seed formation. GL and PL fractions of Paj and *pep1-1* stems, PZ and AZ, were mainly composed of LCFAs 16:0, 18:2, and 18:3 at every investigated developmental stage (Supplementary Fig. S2). Contrary to the NL fraction, amounts of VLCFAs, such as 20:0, 22:0, and 24:0, were low in the GL and PL fractions (Supplementary Fig. S2). Interestingly, the amounts of 18:2 and 18:3 FAs in

the PL fraction of Paj increased slightly from stage I to stage III and II' (Supplementary Fig. S2B), perhaps partially related to incorporation of these FAs in the PL monolayer of LBs that accumulate in the PZ. In roots, NLs of Paj and *pep1-1* were predominantly composed of LCFAs, 16:0, 18:2, and 18:3 and VLCFAs, 20:0, 22:0, and 24:0, that did not significantly vary between stages (Fig. 4C, Fig. 4D). Differing from stems, 16:0 and 20:0 FAs represented the most abundant FAs at every investigated developmental stage in roots of Paj and *pep1-1* (Fig. 4C, Fig. 4D). The absence of a regulatory pattern of NL FAs across the root stages suggests again that roots do not develop as primary lipid storage organs. The GL fractions of the roots of Paj and *pep1-1* plants were marked by high contents of LCFAs 16:0, 18:2, and 18:3 and relatively large amounts of VLCFAs, 20:0, 22:0, and 24:0 (Supplementary Fig. S3A and Supplementary Fig. S3C). The PL fractions of Paj and *pep1-1* roots had also high levels of LCFAs 16:0, 18:2, and 18:3, but low contents of all other investigated FAs (Supplementary Fig. S3B and Supplementary Fig. S3D). Only slight variations of FA contents were noted for the PL and GL fractions in root samples across stages. Again, the high amount of LCFAs 16:0, 18:2, and 18:3 in the PL fraction may reflect their accumulation in the PL monolayer of LBs.

In summary, the FA profiles of glycerolipids show that the PZ is the primary place for lipid metabolic processes, while the AZ and roots play minor roles in this. Similar patterns in Paj and *pep1-1* indicate that vernalization itself is not a requirement for these processes.

Gene ontology (GO) term enrichment and lipid metabolism gene expression confirm enhanced lipid metabolism during progression of the PZ

Enriched lipid metabolism GO terms in RNA-seq data reflect importance of the respective pathways. To identify such, we examined GO term enrichment in three consecutive juvenile to adult *pep1-1* stages I_PZ (very early stage, prior to secondary growth), III_PZ, and IV_PZ in comparison with inflorescence stage IV_AZ_if, for which RNA-seq-based transcriptome data are available (Fig. 5A, see also Sergeeva *et al.*, Manuscript 1). We selected GO terms related to lipid metabolism (Fig. 5B, Supplementary Tables S1 and S2-S7).

When comparing the stages I_PZ with III_PZ, lipid biosynthesis GO term enrichment was pronounced at stage I_PZ, while this was the case for lipid catabolism at stage III_PZ (Fig. 5B, Supplementary Table S2). Interestingly, stage I_PZ showed an enrichment of PL and FA biosynthetic GO terms, while stage III_PZ was enriched in NL and GL biosynthetic GO terms. When comparing stages I_PZ and IV_PZ, general lipid metabolism, PL and FA-related GO terms were similarly enriched

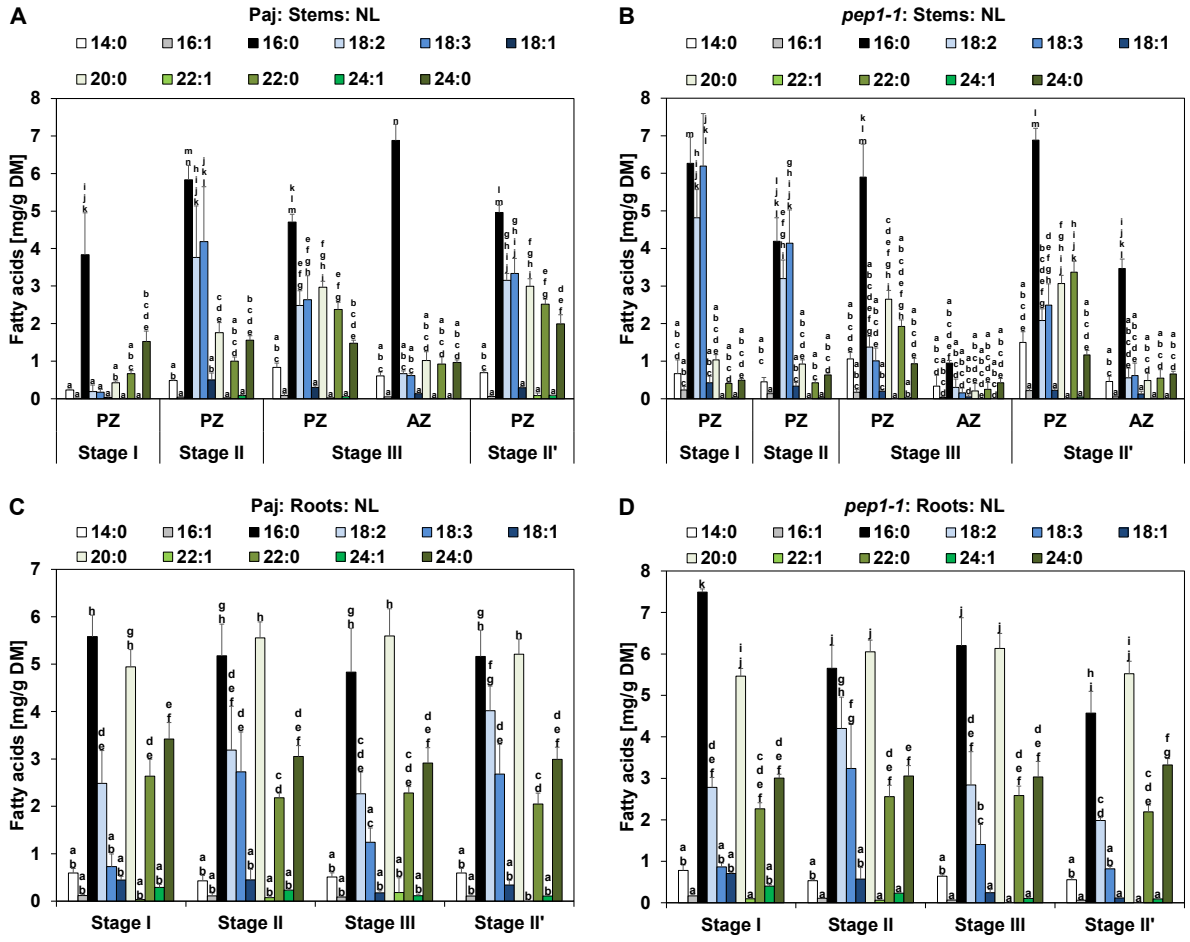

Fig. 4. Long-chain (LC) and very long-chain fatty acid (VLCFA) contents in neutral lipid (NL) fractions in stems and roots. Represented are the contents of NL fraction-derived individual LCFAs (14:0, 16:1, 16:0, 18:2, 18:3, 18:1) and individual VLCFAs (20:0, 22:1, 22:0, 24:1, 24:0) per dry matter (DM) of (A, B) perennial (PZ) and annual (AZ) internode stem zones and (C, D) entire root systems of (A, C) *A. alpina* Pajares (Paj, wild type) and (B, D) *perpetual flowering 1-1* (*pep1-1*) mutant derivative. Plant material was harvested at four different developmental stages, stage I, II, III, and II‘, as indicated in Fig. 1A. In addition, the PZ of *pep1-1* contained low contents of other FAs (compare with B), namely 16:3 FA at stages I and II (0.03 mg/g DM) and 20:1 FA at stages I and III (0.07 mg/g DM and 0.54 mg/g DM). For comparable representation, these FAs are not shown in the diagram, but were included in all calculations. Data are represented as mean +/- SD (n = 3-7). Different letters indicate statistically significant differences, determined by one-way ANOVA-Tukey’s HSD test ($P < 0.05$).

but this was no longer the case for GL and NL categories (Fig. 5C, Supplementary Table S3). In general, all three single comparisons between IV_AZ_if and each PZ stage were marked by an enrichment of PL and FA biosynthetic GO terms in the AZ (Supplementary Tables S5-S7). The enrichment of PL and FA biosynthetic GO terms in the AZ internodes indicates that lipid-related metabolic processes are rather similar to those occurring in the early stage I_PZ.

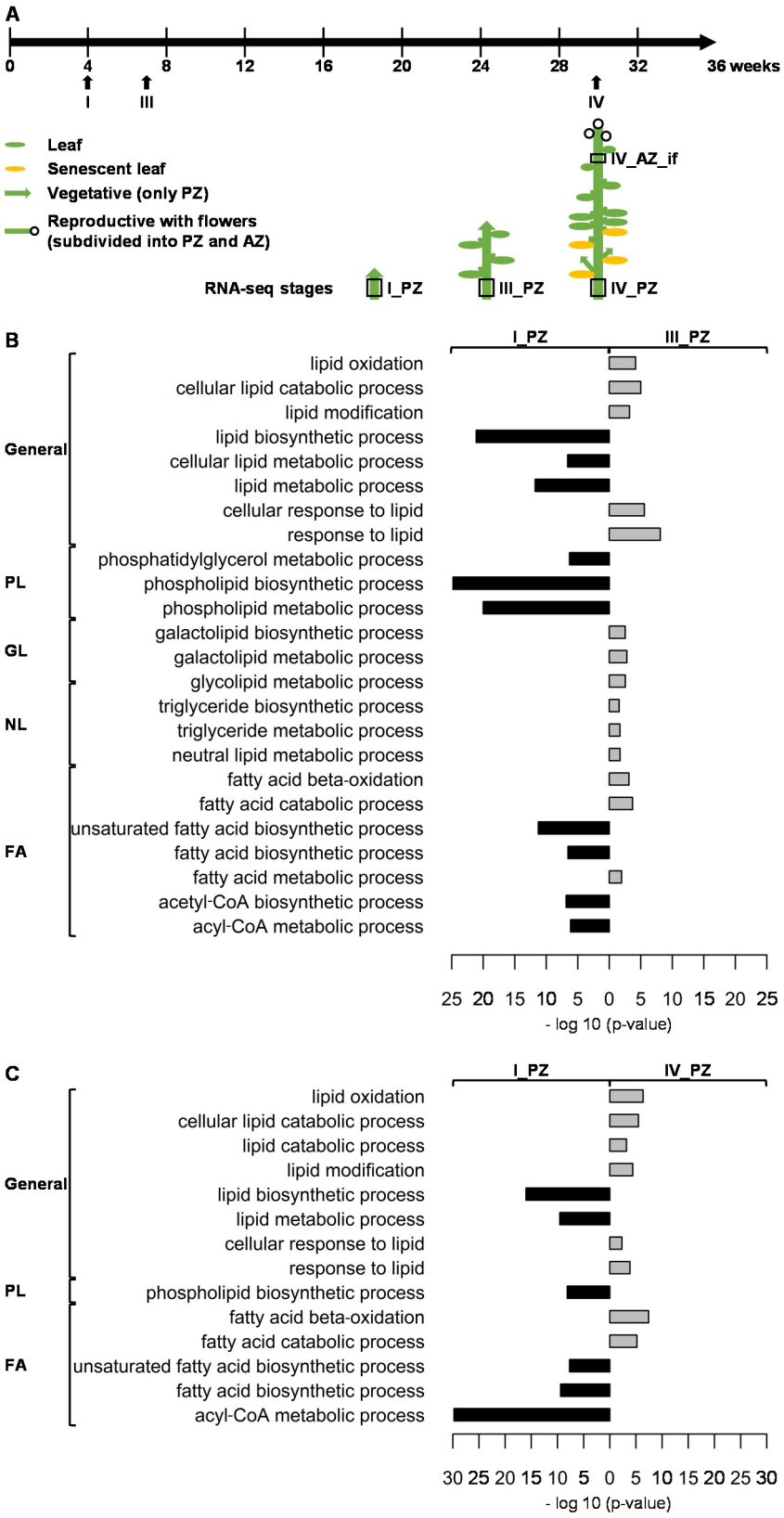

Fig. 5. Lipid metabolism-related GO term enrichment analysis of RNA-seq data. (A) Plant growth and harvesting scheme for *A. alpina perpetual flowering 1-1* (*pep1-1*) mutant with schematic representation of *pep1-1* architecture of the first and second lateral stems formed at lower internodes of the main stem at different stages. Solid black line, long-day conditions at 20 °C; three developmental RNA-seq stages were considered, stages I_PZ, III_PZ, and IV_PZ as well as IV_AZ_if (see also Sergeeva *et al.*, Manuscript 1). *(legend continued on next page)*

Lateral stem internodes had been subdivided into perennial (PZ) and annual (AZ) zones, as indicated. The schematic plant representation was partially adopted from Wang *et al.*, (2009), Lazaro *et al.*, (2018), and Vayssières *et al.*, (2020). (B, C) Lipid metabolism-related GO terms enriched in (B) stage I_PZ (represented in black) versus stage III_PZ (represented in grey) and in (C) stage I_PZ (represented in black) versus stage IV_PZ (represented in grey). GO terms were assigned to the different categories, general, phospholipids (PL), glycolipids (GL), neutral lipids (NL), and fatty acids (FA). GO terms with a p-value $P < 0.05$ are enriched; p-values, represented as –log 10 values. Further information about the represented GO term enrichment analysis is provided in Supplementary Tables S2 and S3.

We selected and compared 50 individual genes for lipid metabolism out of the NL, GL, PL, and FA-related GO categories (Fig. 6 and Supplementary Table S1). Nineteen of them were first, up-regulated during PZ progression from stage I_PZ to stages III_PZ and/or IV_PZ and second, up-regulated at either stage III_PZ or stage_IV_PZ or both versus stage IV_AZ_if (Fig. 6, genes marked in red; Supplementary Table S1; Supplementary Fig. 4). In the GO category "NL metabolic process" (Supplementary Table S2), *LYSOPHOSPHATIDYLCHOLINE ACYLTRANSFERASE 1* (*LPCAT1*), *WRINKLED 1* (*WRI1*), *PHYTYL ESTER SYNTHASE 1* (*PES1*), *DAD1-LIKE SEEDLING ESTABLISHMENT-RELATED LIPASE* (*DSEL*), and *SUGAR-DEPENDENT 1* (*SDP1*) fulfilled these criteria (Fig. 6A and Supplementary Fig. S4A-E). All five genes were significantly up-regulated from stage I_PZ to stage III_PZ. Expression of *LPCAT1*, *PES1*, *DSEL*, and *SDP1* increased from stage I_PZ to stage IV_PZ (Fig. 6A and Supplementary Fig. S4A, C, D, E). The five genes were less expressed at stage IV_AZ_if versus stages III_ and/or IV_PZ (Fig. 6A and Supplementary Fig. S4A-E). Among the examined GL genes, all assigned to GO term "GL metabolic process" (Supplementary Table S2), *PHOSPHOLIPASE D ζ 2* (*PLDζ2*), *PATATIN-RELATED PHOSPHOLIPASE A IIIβ* (*pPLAIIIβ*), *DIGALACTOSYL DIACYLGLYCEROL DEFICIENT 1* (*DGD1*), and *PLASTID LIPASE 3* (*PLIP3*) fulfilled the above criteria (Fig. 6A and Supplementary Fig. S4F-I). *PLDζ2*, *pPLAIIIβ*, and *PLIP3* were significantly up-regulated from stage I_PZ to stage III_PZ (Fig. 6A and Supplementary Fig. S4F, G, I). Expression of *DGD1* increased from stage I_PZ to stage IV_PZ, where it was highest (Fig. 6A and Supplementary Fig. S4H). For the four genes expression was lower at stage IV_AZ_if versus stages III_ and/or IV_PZ (Fig. 6A and Supplementary Fig. S4F-I). Among the PL-related genes, we examined closely genes of the GO terms "phosphatidylglycerol metabolic process" and "PL biosynthetic process" (Supplementary Tables S2, S3). Only a single gene, *ACYLTRANSFERASE 1* (*ACT1*), fulfilled the criteria, as it was significantly up-regulated from stage I_PZ to stage IV_PZ, but down-regulated in stage IV_AZ_if (Fig. 6A and Supplementary Fig. S4J). Among FA-related genes of GO terms "FA biosynthetic process" (Supplementary Tables S2, S3) and "FA catabolic process" (Supplementary Tables S2, S3), nine genes fulfilled the criteria, *3-KETOACYL-COA SYNTHASE 4* (*KCS4*), *ACYL-COA OXIDASE 3* (*ACX3*), *Δ3, Δ2-ENOYL COA ISOMERASE 1* (*ECI1*), *3-KETOACYL-COA THIOLASE 2* (*KAT2*), *PEROXISOMAL ADENINE NUCLEOTIDE CARRIER 1* (*PNC1*), *MULTIFUNCTIONAL PROTEIN 2* (*MFP2*), *ACYL-COA OXIDASE 4* (*ACX4*), *ENOYL-COA HYDRATASE 2* (*ECH2*), and *ABNORMAL INFLORESCENCE MERISTEM 1* (*AIM1*) (Fig. 6B and Supplementary Fig. S4K-S).

Expression of *KCS4* decreased from stage I_PZ to stages III_PZ and IV_PZ and was lowest at stage IV_AZ_if (Fig. 6B and Supplementary Fig. S4K). *ACX3*, *ECI1*, *KAT2*, *PNC1*, *MFP2*, *ACX4*, *ECH2*, and *AIM1* were significantly up-regulated from stage I_PZ to stage III_ and/or IV_PZ and down-regulated at stage IV_AZ_if (Fig. 6B and Supplementary Fig. S4L-S)

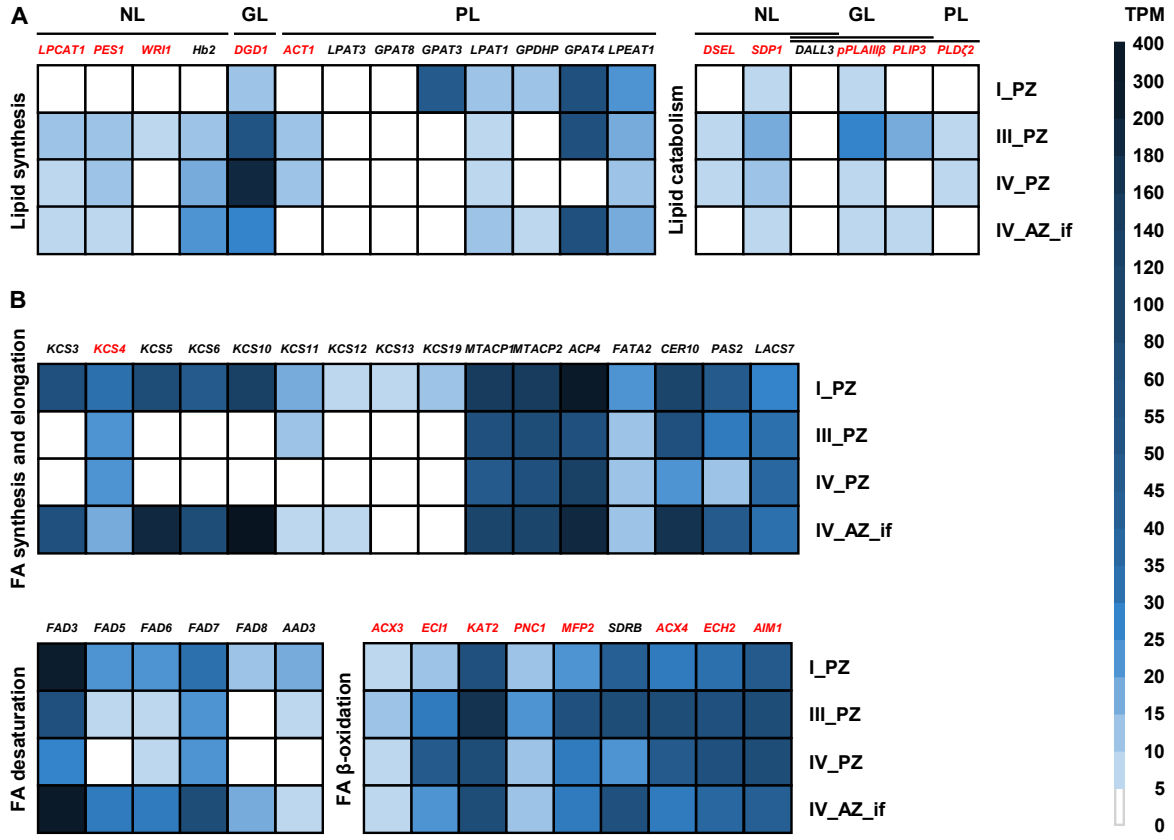

Fig. 6. Gene expression profiles of 50 individual genes out of the NL, GL, PL, and FA-related GO categories. Represented are RNA-seq data (TPM, transcripts per million) of *A. alpina perpetual flowering 1-1* (*pep1-1*) mutant lateral stem internodes of perennial (PZ) and annual (AZ) zones at stages I_PZ, III_PZ, IV_PZ, and IV_AZ_if (see Fig. 5A). (A) NL, GL, and PL genes involved in lipid synthesis and catabolism: *LPCAT1*, *LYSOPHOSPHATIDYLCHOLINE ACYLTRANSFERASE 1*, *PES1*, *PHYTYL ESTER SYNTHASE 1, WRI1*, *WRINKLED 1*, *Hb2, HAEMOGLOBIN 2*, *DGD1*, *DIGALACTOSYL DIACYLGLYCEROL DEFICIENT 1*, *ACT1*, *ACYLTRANSFERASE 1*, *LPAT3*, *LYSOPHOSPHATIDYL ACYLTRANSFERASE 3*, *GPAT8*, *GLYCEROL-3-PHOSPHATE SN-2-ACYLTRANSFERASE 8*, *GPAT3*, *GLYCEROL-3-PHOSPHATE SN-2-ACYLTRANSFERASE 3*, *LPAT1*, *LYSOPHOSPHATIDIC ACID ACYLTRANSFERASE 1*, *GPDHP*, *GLYCEROL-3-PHOSPHATE DEHYDROGENASE PLASTIDIC*, *GPAT4*, *GLYCEROL-3-PHOSPHATE SN-2-ACYLTRANSFERASE 4*, *LPEAT1*, *LYSOPHOSPHATIDYLETHANOLAMINE ACYLTRANSFERASE 1*, *DSEL*, *DAD1-LIKE SEEDLING ESTABLISHMENT-RELATED LIPASE*, *SDP1, SUGAR-DEPENDENT1*, *DALL3*, *DAD1-LIKE LIPASE 3*, *pPLAIIIβ*, *PATATIN-RELATED PHOSPHOLIPASE A IIIβ*, *PLIP3*, *PLASTID LIPASE 3, PLDζ2*, *PHOSPHOLIPASE D ζ 2*; (B) Genes involved in FA synthesis, elongation, desaturation, and β-oxidation: *KCS3*, *KCS4*, *KCS5*, *KCS6*, *KCS10*, *KCS11*, *KCS12*, *KCS13*, *KCS19*, *KETOACYL-COA SYNTHASEs*, *MTACP1*, *MITOCHONDRIAL ACYL CARRIER PROTEIN 1*, *MTACP2*, *MITOCHONDRIAL ACYL CARRIER PROTEIN 2*, *ACP4*, *ACYL CARRIER PROTEIN 4*, *FATA2*, *OLEOYL-ACYL CARRIER PROTEIN THIOESTERASE 2*, *CER10*, *ECERIFERUM 10*, *PAS2*, *PASTICCINO 2*, *LACS7*, *LONG-CHAIN ACYL-COA SYNTHETASE 7*, *FAD3*, *FAD5*, *FAD6*, *FAD7*, *FAD8*, *FATTY ACID DESATURASEs*, *AAD3*, *ACYL-ACYL CARRIER PROTEIN DESATURASE 3*, *ACX3*, *ACYL-COA OXIDASE 3*, *ECI1*, *Δ3, Δ2-ENOYL COA ISOMERASE 1*, *KAT2*, *3-KETOACYL-COA THIOLASE 2*, *PNC1*, *PEROXISOMAL ADENINE NUCLEOTIDE CARRIER 1*, *(legend continued on next page)*

MFP2, *MULTIFUNCTIONAL PROTEIN 2*, *SDRB*, *SHORT-CHAIN DEHYDROGENASE-REDUCTASE B*, *ACX4*, *ACYL-COA OXIDASE 4*, *ECH2*, *ENOYL-COA HYDRATASE 2*, *AIM1*, *ABNORMAL INFLORESCENCE MERISTEM 1*. Candidate genes differentially regulated between the PZ and the AZ are represented in red. Data are represented as mean (n = 3).

Taken together, during progression of stage I_PZ to stage III_PZ, an enrichment of GL and NL-related GO terms and analysis of individual genes support the biochemical data with increased presence of glycerolipids during progression of the PZ. The occurrence of catabolic processes related to lipid metabolism in the PZ at stages III_PZ and IV_PZ may indicate active turnover of lipids.

Biochemical lipid analysis and gene expression are correlated

We confirmed differentially regulated lipid metabolism by correlation analysis of the amounts of single FAs of NL, GL, and PL fractions and the expression levels of 50 genes in PZ and AZ samples (see Materials and Methods). We found clearly more correlations related to the PZ than AZ, supporting the coordinated presence of lipid species and involvement of corresponding genes in the PZ (Fig. 7, 8 and Supplemenary Fig. S5, S6, S7).

We investigated meaningful individual correlations in more detail. For example, NL gene expression levels of *LPCAT1* positively correlated with amounts of 16:0, 18:2, and 18:3 FAs of the NL fraction of the PZ (Fig. 7A, PZ). Gene expression levels of *PES1* highly correlated with the amounts of 16:0 and 18:3 FAs. Positive correlation was also detected between *WRI1* and the amounts of 18:3 FAs. Furthermore, 16:0 FAs positively correlated with gene expression levels of *DSEL*. Negative correlation was seen between *SDP1* and VLCFAs, 24:0, 20:0, and 22:0 in the PZ, as well as between 16:1 FAs, *PES1* and *SDP1* in the AZ (Fig. 7A). In addition, among the identified genes of the GO term "galactolipid metabolic process", *DGD1*, *pPLAIIIβ*, *PLIP3*, and *PLDζ2*, up-regulated at stage III_PZ and/or IV_PZ versus stage IV_AZ_if (Fig. 6A), *DGD1* positively correlated with 16:0, 18:2, 18:3, 22:0, and 24:0 FAs of the GL fraction of the PZ (Fig. 7B). In the AZ, significant positive correlation for *DGD1* was only detected with 16:0 FA. Negative correlation was detected for *pPLAIIIβ* and *PLIP3* with 22:0 and 24:0 FAs in the PZ, while in the AZ *pPLAIIIβ* and *PLIP3* negatively correlated with 16:1 and 14:0 FAs respectively. Expression levels of *PLDζ2* positively correlated with the amounts of 16:0, 18:2, and 18:3 FAs of the GL fraction of the PZ, but only with 16:0 FA in the AZ (Fig. 7B).

Finally, among the PL-related genes, *ACT1* fulfilled the criteria of being expressed at a higher level at stages III_PZ and IV_PZ than at stage IV_AZ_if (Fig. 6A). *ACT1* encodes a plastidic enzyme involved in the first step of phosphatidic acid biosynthesis (Li-Beisson *et al.*, 2013). No positive correlation was observed between *ACT1* gene expression and amounts of single FAs of the PL fraction of the PZ (Fig. 7C). Surprisingly, *ACT1* positively correlated with 24:0 FAs in the AZ, indicating in fact a minor role in PL metabolism in the PZ. In addition to their involvement in GL metabolism, PLDζ2, pPLAIIIβ, and PLIP3 were reported to hydrolyze PLs (Li *et al.*, 2011; Su *et al.*, 2018; Wang *et al.*, 2018). Therefore, we analyzed correlation of these genes with FAs present in the PL fraction, assuming a negative

correlation (Supplementary Fig. S7B). Indeed, the three genes negatively correlated with 16:1 and 22:0 FAs in the PZ. In addition, the analysis resulted in negative correlation between *PLDζ2* and 20:0 FAs.

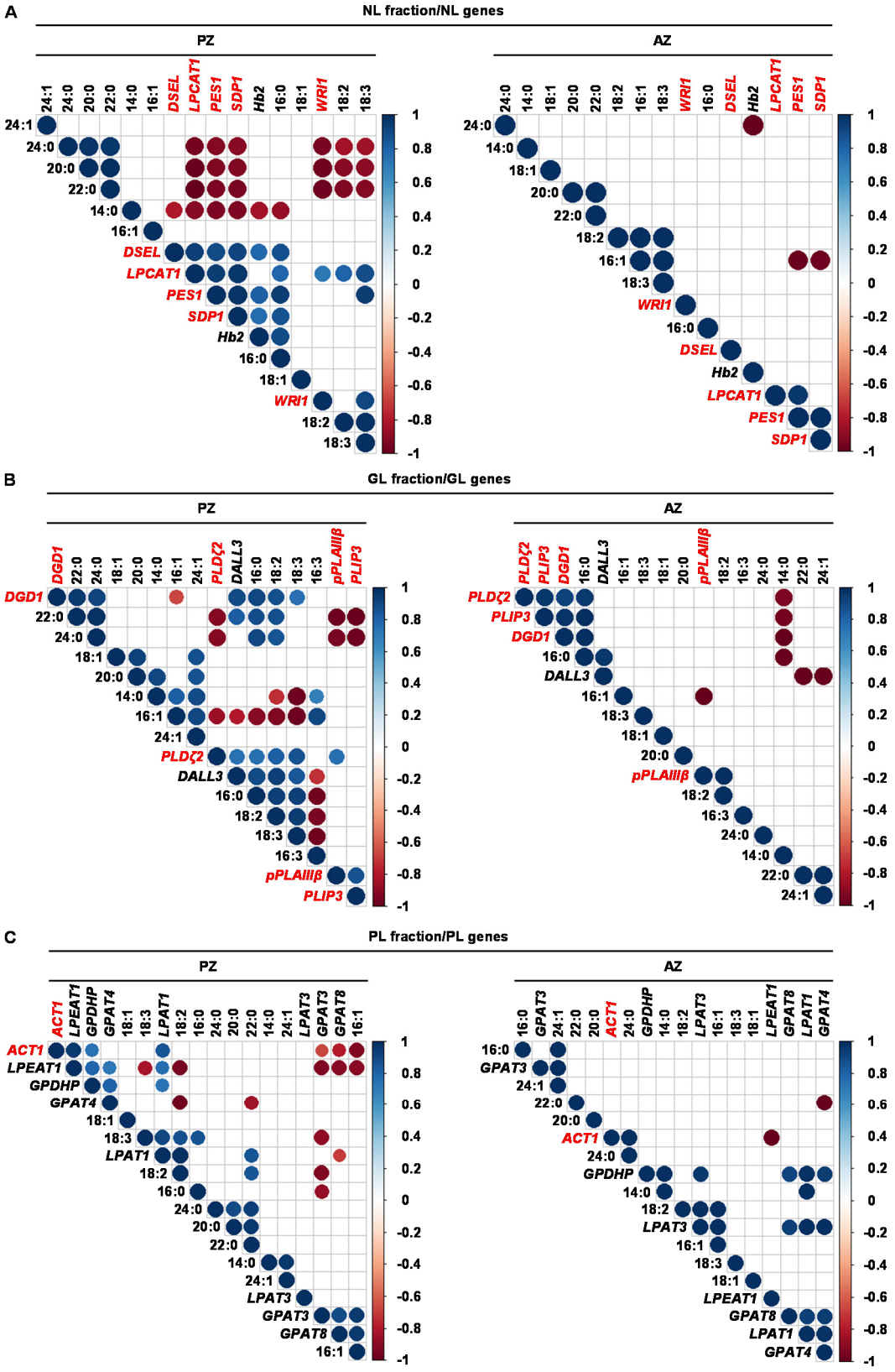

Fig. 7. Pearson correlation analysis between gene expression levels of lipid metabolism genes and the amounts of individual FAs of the NL, GL, and PL fraction *(legend continued on next page)*

of *A. alpina perpetual flowering 1-1* (*pep1-1*) mutant lateral stem internodes of perennial (PZ) and annual (AZ) zones. The analysis was performed between stages III_PZ, IV_PZ and I', II' for PZ, and IV_AZ_if and II' for AZ (see Fig. 1 and Fig. 5A). (A) Correlation analysis between NL-derived FAs and NL metabolism-related genes. *DSEL*, *DAD1-LIKE SEEDLING ESTABLISHMENT-RELATED LIPASE*, *Hb2, HAEMOGLOBIN 2*, *LPCAT1*, *LYSOPHOSPHATIDYLCHOLINE ACYLTRANSFERASE 1*, *PES1*, *PHYTYL ESTER SYNTHASE 1, SDP1, SUGAR-DEPENDENT1, WRI1*, *WRINKLED 1*. (B) Correlation analysis between GL-derived FAs and GL metabolism-related genes. *DALL3*, *DAD1-LIKE LIPASE 3*, *DGD1*, *DIGALACTOSYL DIACYLGLYCEROL DEFICIENT 1*, *PLDζ2*, *PHOSPHOLIPASE D ζ 2*, *PLIP3*, *PLASTID LIPASE 3*, *pPLAIIIβ*, *PATATIN-RELATED PHOSPHOLIPASE A IIIβ*. (C) Correlation analysis between PL-derived FAs and PL metabolism-related genes. *ACT1*, *ACYLTRANSFERASE 1*, *GPAT3*, *GLYCEROL-3-PHOSPHATE SN-2-ACYLTRANSFERASE 3*, *GPAT4*, *GLYCEROL-3-PHOSPHATE SN-2-ACYLTRANSFERASE 4*, *GPAT8*, *GLYCEROL-3-PHOSPHATE SN-2-ACYLTRANSFERASE 8*, *GPDHP*, *GLYCEROL-3-PHOSPHATE DEHYDROGENASE PLASTIDIC*, *LPAT1*, *LYSOPHOSPHATIDIC ACID ACYLTRANSFERASE 1*, *LPAT3*, *LYSOPHOSPHATIDYL ACYLTRANSFERASE 3*, *LPEAT1*, *LYSOPHOSPHATIDYLETHANOLAMINE ACYLTRANSFERASE 1*. Only correlation coefficients with significant levels of correlation ($P < 0.05$) are displayed in the diagrams. Candidate genes differentially regulated between the PZ and the AZ are represented in red.

Among the identified FA genes, *KCS4*, *ACX3*, *ECI1*, *KAT2*, *PNC1*, *MFP2*, *ACX4*, *ECH2*, and *AIM1* were regulated according to the above-described criteria (Fig. 6B). While *KCS4* is involved in the elongation of VLCFAs, the other FA genes are needed for the peroxisomal FA β-oxidation (Li-Beisson *et al.*, 2013). Therefore, we assumed that the importance of these genes for NL, GL, and PL metabolism in the PZ would be reflected by positive correlation between *KCS4* and single FAs and by negative correlation between the genes of peroxisomal FA β-oxidation and individual FAs. Gene expression levels of *KCS4* did not positively correlate with any of the identified FAs of the three lipid fractions present in the PZ and AZ (Fig. 8). Supporting the assumption, significant negative correlation between the gene expression levels and the amounts of individual FAs of each fraction of the PZ was detected for all of the mentioned FA β-oxidation genes except for *ECH2* (Fig. 8A, B, C). In the NL fraction of the PZ, *ECI1* and *AIM1* negatively correlated with 18:2 and 18:3 FAs (Fig. 8A). Gene expression levels of *PNC1*, *ACX3*, *ACX4*, *KAT2*, and *MFP2* negatively correlated with the amounts of VLCFAs, 20:0, 22:0, and 24:0. Except for *MFP2* and *PNC1*, no correlation was detected between the candidate genes and the amounts of NL-derived FAs in the AZ (Fig. 8A). Analysis between the FA genes and FAs of the GL fraction of the PZ resulted in high negative correlation between *ACX4*, *KAT2*, *MFP2*, *ACX3*, *PNC1* and 16:0, 22:0, 24:0 FAs (Fig. 8B). In addition, *KAT2*, *MFP2*, and *PNC1* negatively correlated with 18:2 FAs. Except for *ACX3* negatively correlating with 20:0 FAs, no correlation was detected between the FA β-oxidation-related genes and the amounts of GL-derived FAs in the AZ (Fig. 8B). Gene expression levels of *ACX3*, *ACX4*, *KAT2*, *MFP2*, and *PNC1* negatively correlated with 18:2 and 22:0 FAs present in the PL fraction of the PZ (Fig. 8C). In addition, the analysis resulted here in negative correlation between *ACX3* and 18:3 FAs. Expression levels of the FA β-oxidation-related genes did not correlate with the amounts of PL-derived FAs in the AZ (Fig. 8C).

Taken together, we detected many concordant correlations between NL, GL, PL, and FA biosynthesis gene expression and the measured contents of the respective FA species in the various

glycerolipid fractions in the PZ, but less so in the AZ. Correlation analysis therefore confirmed involvement of candidate genes in lipid metabolism in the PZ.

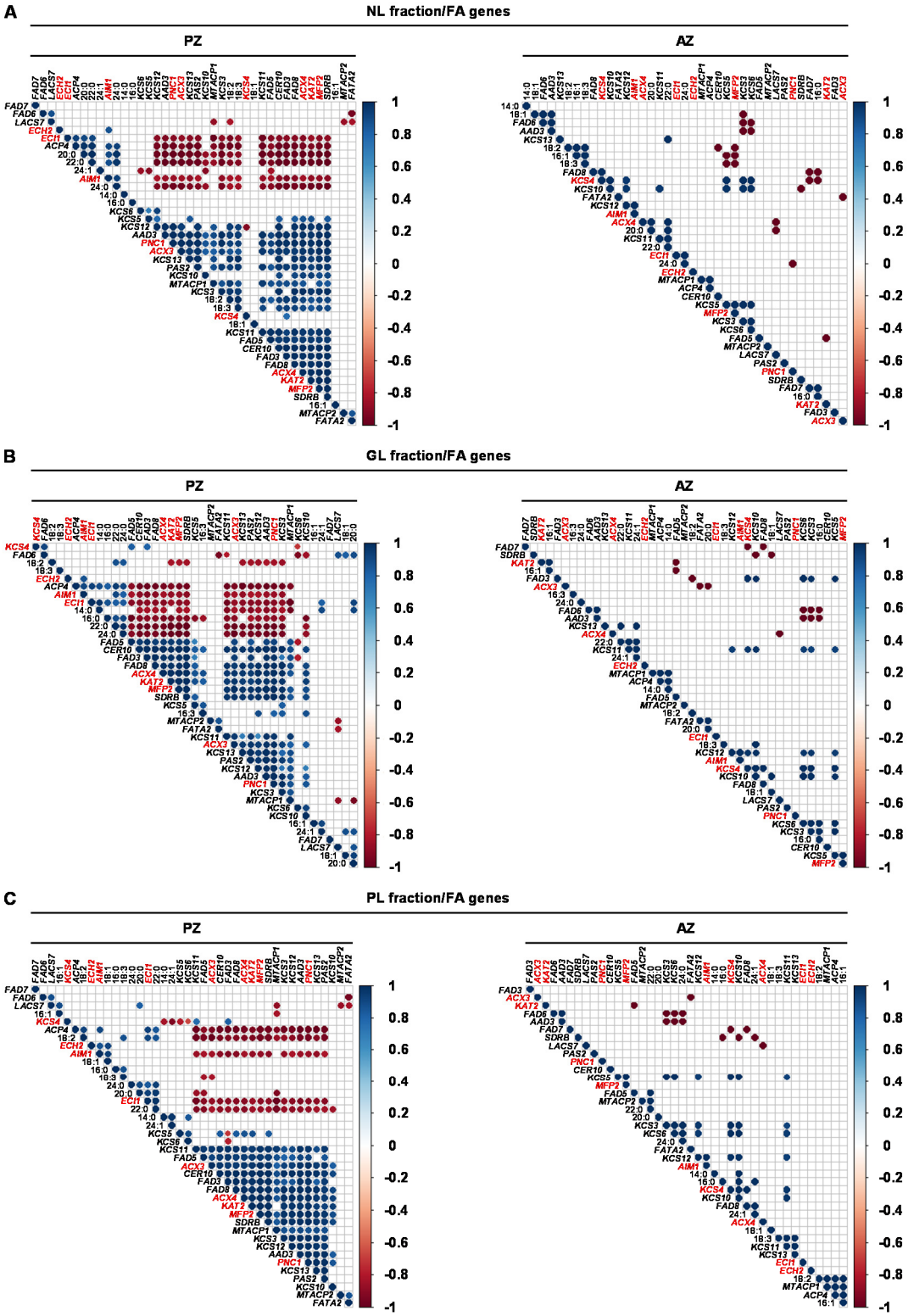

Fig. 8. Pearson correlation analysis between gene expression levels of lipid metabolism genes and the amounts of individual FAs of the NL, GL, and PL fraction of *A. alpina perpetual flowering 1-1* (*pep1-1*) mutant lateral stem internodes of perennial (PZ) and annual (AZ) zones. *(legend continued on next page)*

The analysis was performed between stages III_PZ, IV_PZ and I‘, II‘ for PZ, and IV_AZ_if and II‘ for AZ (see Fig. 1 and Fig. 5A). Correlation analysis between (A) NL-derived, (B) GL-derived, (C) PL-derived FAs and FA synthesis, elongation, desaturation, and β-oxidation-related genes. *AAD3*, *ACYL-ACYL CARRIER PROTEIN DESATURASE 3*, *ACP4*, *ACYL CARRIER PROTEIN 4*, *ACX3*, *ACYL-COA OXIDASE 3*, *ACX4*, *ACYL-COA OXIDASE 4*, *AIM1*, *ABNORMAL INFLORESCENCE MERISTEM 1*, *CER10*, *ECERIFERUM 10*, *ECH2*, *ENOYL-COA HYDRATASE 2*, *ECI1*, *Δ3, Δ2-ENOYL COA ISOMERASE 1*, *FAD3*, *FAD5*, *FAD6*, *FAD7*, *FAD8*, *FATTY ACID DESATURASEs*, *FATA2*, *OLEOYL-ACYL CARRIER PROTEIN THIOESTERASE 2*, *KAT2*, *3-KETOACYL-COA THIOLASE 2*, *KCS3*, *KCS4*, *KCS5*, *KCS6*, *KCS10*, *KCS11*, *KCS12*, *KCS13*, *KCS19*, *KETOACYL-COA SYNTHASEs*, *LACS7*, *LONG-CHAIN ACYL-COA SYNTHETASE 7*, *MFP2*, *MULTIFUNCTIONAL PROTEIN 2*, *MTACP1*, *MITOCHONDRIAL ACYL CARRIER PROTEIN 1*, *MTACP2*, *MITOCHONDRIAL ACYL CARRIER PROTEIN 2*, *PAS2*, *PASTICCINO 2*, *PNC1*, *PEROXISOMAL ADENINE NUCLEOTIDE CARRIER 1*, *SDRB*, *SHORT-CHAIN DEHYDROGENASE-REDUCTASE B*. Only correlation coefficients with significant levels of correlation ($P < 0.05$) are displayed in the diagrams. Candidate genes differentially regulated between the PZ and the AZ are represented in red.

Discussion

Glycerolipids in *A. alpina* contain predominantly LCFAs and additionally VLCFAs in the NL fraction, more abundant in the PZ than AZ, pointing towards an active lipid metabolic function in the PZ. We have identified 19 lipid metabolism genes that have an expression pattern in favor of their function in storage and different steps of NL, GL, PL, and FA metabolism in the PZ, and all of them show correlation with certain FA species amounts. Positive and negative correlations of these 19 enzymatic functions support their involvement in biosynthesis or catabolism of NL, GL, and PL-related lipid species in the PZ. These genes could be targets of signals that regulate PZ development and delimit PZ and AZ.

Biosynthesis and catabolism of NLs are differentially regulated during progression of the PZ and between the PZ and the AZ

The high proportion of glycerolipids among total lipids is indicative of carbon storage. The TAG-containing NL fraction increased during development of the PZ in Paj and *pep1-1*. Significant amounts of VLCFAs are known to be present in TAGs. Millar and Kunst (1999) demonstrated that seed oil from 100 ecotypes of *A. thaliana* contained large proportions of VLCFAs, including C20 and C22 FAs. These long-chain FAs are more energy-rich than short-chain FAs. Interestingly, VLCFA contents indeed increased in the NL fractions of the PZ, but were unchanged in corresponding PL and GL fractions, during PZ progression. These findings support that PZs of lateral branches of *A. alpina* are high-energy lipid storage sites.

Elongation of VLCFAs occurs in a sequence of reactions in the ER (Fig. 9). The first enzyme involved in the process of FA elongation is KCS. KCS catalyzes condensation of a long-chain acyl-CoA with malonyl-CoA. *A. thaliana* has 21 *KCS* genes (Joubès *et al.*, 2008). Characterization of the members of the KCS family showed their diverse chain-length specificities (Yang *et al.*, 2018). We identified *KCS4* to be differentially regulated during PZ progression. The exact chain-length specificity for KCS4 has still to be elucidated. However, Blacklock and Jaworski (2006) hypothesized the possible

activity of several KCS proteins including KCS4 toward acyl-CoAs longer than C20. Beside 20:0 FAs, levels of 22:0 and 24:0 FAs increased in the NL fraction during PZ progression. Moreover, lowest levels of expression of *KCS4* were detected in the AZ in comparison to the PZ tissues indicating the possible involvement of *KCS4* in the synthesis of TAG-derived VLCFAs in the PZ. However, gene expression levels of *KCS4* neither correlated with any of the TAG-derived FAs nor with FAs from the GL and PL fraction. KCS4 may therefore also be involved in the elongation of FAs deriving from other lipid classes, e. g. cuticular waxes. Thus, the exact role of KCS4 in lipid metabolism of *A. alpina* has to be elucidated in future studies.

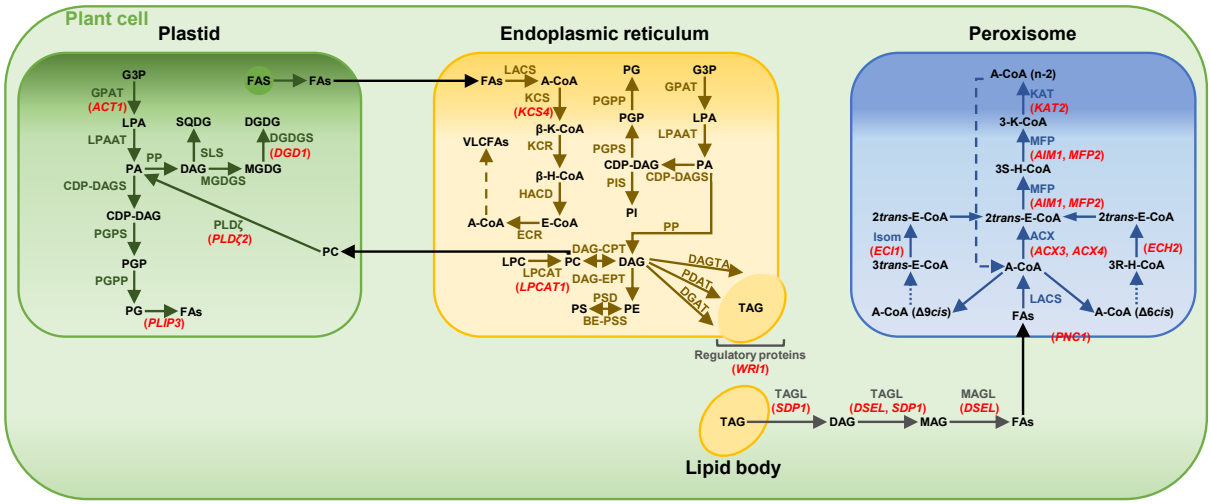

Fig. 9. Candidate genes for lipid metabolism and their involvement in glycerolipid biosynthesis and fatty acid β-oxidation. Overview of prokaryotic and eukaryotic glycerolipid biosynthesis pathways and fatty acid β-oxidation in the plastid, in or at the endoplasmic reticulum (ER), and in the peroxisome, showing the interconversion of pathways. Candidate genes differentially regulated between the PZ and the AZ are represented in red, except *PES1* and *pPLAIIIβ*. Abbreviations: A-CoA: acyl-CoA; ACX: acyl-CoA thioesterase; β/3R/3S-H-CoA: β/3R/3S-hydroxyacyl-CoA; β/3-K-CoA: β/3-ketoacyl-CoA; BE-PSS: base-exchange-type phosphatidylserine synthase; CDP-DAGS: CDP-DAG synthase; CoA: coenzyme A; DAG: diacylglycerol; DAGTA: diacylglycerol transacylase; DAG-CPT: CDP-choline:diacylglycerol cholinephosphotransferase; DAG-EPT: CDP-ethanolamine:diacylglycerol cholinephosphotransferase; DGAT: diacylglycerol acyltransferase; DGDG: digalactosyldiacylglycerol; DGDGS: digalactosyldiacylglycerol transferase; E-CoA: enoyl-CoA; ECR: enoyl-CoA reductase; FAS: fatty acid synthase; FAs: fatty acids; G3P: glycerol 3-phosphate; GPAT: glycerol-3-phosphate acyltransferase; HACD: hydroxyacyl-CoA dehydratase; Isom: isomerase; KAT: 3-ketothiolase; KCR: ketoacyl-CoA reductase; KCS: 3-ketoacyl-CoA synthase; LACS: long-chain acyl-CoA synthetase; LPA: lysophosphatidic acid; LPAAT: lysophosphatidic acid acyltransferase; LPC: lysophosphatidylcholine; LPCAT: lysophosphatidylcholine acyltransferase; MAG: monoacylglycerol; MAGL: monoacylglycerol lipase; MFP: multifunctional protein; MGDG: monogalactosyldiacylglycerol; MGDGS: monogalactosyldiacylglycerol transferase; PA: phosphatidic acid; PC: phosphatidylcholine; PDAT: phospholipid:diacylglycerol acyltransferase; PE: phosphatidylethanolamine; PG: phosphatidylglycerol; PGP: phosphatidylglycerol phosphate; PGPP: phosphatidylglycerol phosphate phosphatase; PGPS: phosphatidylglycerol phosphate synthase; PI: phosphatidylinositol; PIS: PI synthase; PP: phosphatidate phosphatase; PS: phosphatidylserine; PSD: phosphatidylserine decarboxylae; SLS: sulfolipid synthase; SQDG: sulfoquinovosyldiacylglycerol; TAG: triacylglycerol; TAGL: triacylglycerol lipase; VLCFAs: very long-chain fatty acids. Adopted from Li-Beisson *et al.* (2013). Candidate genes: *ACT1*, *ACYLTRANSFERASE 1*, *ACX3*, *ACYL-COA OXIDASE 3*, *ACX4*, *ACYL-COA OXIDASE 4*, *AIM1*, *ABNORMAL INFLORESCENCE MERISTEM 1*, *DGD1*, *DIGALACTOSYL DIACYLGLYCEROL DEFICIENT 1*, *DSEL*, *DAD1-LIKE SEEDLING ESTABLISHMENT-RELATED LIPASE*, *ECH2*, *ENOYL-COA HYDRATASE 2*, *(legend continued on next page)*

ECI1, *Δ3, Δ2-ENOYL COA ISOMERASE 1*, *KAT2*, *3-KETOACYL-COA THIOLASE 2*, *KCS4*, *3-KETOACYL-COA SYNTHASE 4*, *LPCAT1*, *LYSOPHOSPHATIDYLCHOLINE ACYLTRANSFERASE 1*, *MFP2*, *MULTIFUNCTIONAL PROTEIN 2*, *PES1*, *PHYTYL ESTER SYNTHASE 1, PLDζ2*, *PHOSPHOLIPASE D ζ 2*, *PLIP3*, *PLASTID LIPASE 3, PNC1*, *PEROXISOMAL ADENINE NUCLEOTIDE CARRIER 1*, *pPLAIIIβ*, *PATATIN-RELATED PHOSPHOLIPASE A IIIβ*, *SDP1, SUGAR-DEPENDENT1*, *WRI1*, *WRINKLED 1*. Acyl-CoA chains with a *cis* double bond on an even-numbered carbon are exemplified by Δ6*cis*, while fatty acids with *cis* double bonds at odd-numbered positions are exemplified by Δ9*cis*.

LPCAT1, *WRI1*, *PES1*, *DSEL*, and *SDP1* encode enzymes and regulators for TAG metabolism. These genes are expressed at higher level during development of the PZ and correlate with LCFAs and VLCFAs in comparison to the AZ, which supports their function in the accumulation of TAGs in the PZ, but not in the AZ. LPCAT1 is involved in acylation of lysophosphatidylcholine during acyl editing, the entry point of FAs into phosphatidylcholine (Bates *et al.*, 2012) (Fig. 9). In the ER, PC can be further converted to diacylglycerol, a precursor of TAG biosynthesis. Moreover, Bates *et al.* (2012) demonstrated decreased polyunsaturated FA contents in TAGs in *lpcat1 lpcat2* mutant *Arabidopsis* plants. Polyunsaturated 18:2 and 18:3 FAs constitute a great proportion of total NL-derived FAs in Paj and *pep1-1*. Thus, the increased expression of *LPCAT1* and the positive correlation with 18:2 and 18:3 FAs not only supports TAG biosynthesis and storage in the PZ, but also indicates that the pool of these polyunsaturated FAs in TAGs may derive from PC produced via the activity of LPCAT1.

In accordance with the observed accumulation of TAGs in the PZ, we detected increased expression of *PES1* and high positive correlation with 16:0 and 18:3 FAs in the same tissues. Involvement of PES1 in TAG biosynthesis was demonstrated by lower accumulation of TAGs, a phenotype of *Arabidopsis pes1 pes2* mutants (Lippold *et al.*, 2012). Regulation of TAG biosynthesis involves a complex of numerous transcription factors. One transcription factor, WRI1, known to regulate genes responsible for carbon allocation from starch to FAs of TAG (Cernac and Benning, 2004; Baud *et al.*, 2007; Maeo *et al.*, 2009), was most expressed at stage III_PZ. This indicates the enhanced rate of TAG biosynthesis in this stage with preferentially 18:3 FAs according to the correlation analysis. According to Sergeeva *et al.* (Manuscript 1), starch accumulates in well-developed PZ stages with visible secondary growth. WRI1 may therefore be involved in TAG and starch deposition in a well-developed PZ stage. Secondary growth and thus establishment of secondary phloem parenchyma tissue for TAG storage do not occur in the AZ, which is indirectly reflected by low expression and no FA-related correlation of *WRI1* in the AZ.

An intriguing finding was that NL genes did not correlate positively with VLCFAs. We explain this with the higher amounts of LCFAs in the PZ in comparison with VLCFAs at every investigated stage. Some of the genes there could have VLCFA catabolic activity. SDP1 is a key enzyme of TAG hydrolysis (Kelly *et al.*, 2013; Fan *et al.*, 2017) and can also hydrolyze diacylglycerol (Eastmond, 2006) (Fig. 9). The observed negative correlation between *SDP1* and NL-derived VLCFAs, 20:0, 22:0, and 24:0 may be indicative of catabolic processes related to VLCFA-containing TAGs accumulated in the PZ at later stages of development.

The acylhydrolase DSEL catalyzes the hydrolysis of di- and monoacylglycerol (Kim *et al.*, 2011) (Fig. 9). Moreover, DSEL was suggested to negatively regulate storage oil mobilization by a still unknown mechanism. Likewise, DSEL may not only participate in the TAG hydrolysis pathway, but may also influence levels of available energy by preventing TAG hydrolysis. Higher expression levels of *DSEL* in developmentally more progressed PZs fit with accumulation of TAG-containing LBs in these tissues (Sergeeva *et al.*, Manuscript 1). Contrary to that, *DSEL* expression in the AZ and early PZ was low, indirectly stressing the importance of oil storage in the developmentally advanced PZ.

In summary, TAG storage in advanced stages of the PZ correlates with NL biosynthesis and catabolism gene expression, suggesting that these genes are involved in lipid storage in the PZ. *WRI1* and *DSEL* showed the most striking difference of gene expression between the PZ and the AZ. Thus, these two candidates may represent important regulators of lipid metabolism, discriminating PZ-AZ transition.

Catabolism of PLs is characteristic in late PZ stages and differentiates between the PZ and the AZ

GLs and PLs function primarily as structural elements of organellar membranes and membranous compartments. As the pathways of NL, GL, and PL biosynthesis are interconnected, GLs and PLs also contribute to storage in TAG-containing LBs and energy storage in general. GLs and PLs were present at higher amounts at PZ stages than corresponding AZ stages and generally there was an increase from stages I and II to stage III and/or stage II'. Levels of *DGD1* raised up to stage IV_PZ, positively correlated with GL-derived 16:0, 18:2, 18:3, 22:0 and 24:0 FAs in the PZ, but were low in stage IV_AZ_if. DGD1 catalyzes synthesis of galactolipid digalactosyldiacylglycerol, constituent of plastid membranes (Dörmann *et al.*, 1995; Benning and Ohta, 2005) (Fig. 9). The gradual increase of *DGD1* expression and enhanced digalactosyldiacylglycerol biosynthesis for incorporation into plastid membranes may be indicative of cell division, cell differentiation and plastid differentiation during secondary growth. On the other side, *DGD1* activity alone may also indicate a requirement for phosphate mobilization at the late PZ stage. Under phosphate deficiency, extraplastidial PLs are replaced by galactolipids (Essigmann *et al.*, 1998; Härtel *et al.*, 1998; Härtel *et al.*, 2000; Kelly and Dörmann, 2002; Kelly *et al.*, 2003; Jouhet *et al.*, 2004; Pant *et al.*, 2015). A corresponding PL decrease indicative of remobilization of phosphate was not found and speaks against phosphate mobilization taking place in the PZ. Interestingly, the turnover of PLs and GLs was supported by negative correlation of three catabolic lipase genes *PLDζ2*, *PLIP3*, and *pPLAIIIβ* with PL- and GL-derived FAs of the PZ. The expression of *PLDζ2* raised during progression of the development of the PZ with highest levels of expression at stage III_PZ. *PLDζ2* is related to P_i deficiency (Li *et al.*, 2006; Su *et al.*, 2018). *PLDζ2* hydrolyzes phosphatidylcholine (Fig. 9) which finally leads to the synthesis of digalactosyldiacylglycerol and release of free phosphate (Cruz-Ramírez *et al.*, 2006; Su *et al.*, 2018). Perhaps, there is an active turnover of PLs and supposedly also GLs during progression of the

development of the PZ. We noted higher expression levels of *PLIP3* and *pPLAIIIβ* at stage III_PZ. In addition to phosphatidylglycerol (Fig. 9), both enzymes were reported to hydrolyze monogalactosyldiacylglycerol and digalactosyldiacylglycerol (Li *et al.*, 2011; Wang *et al.*, 2018). Moreover, higher expression of *PLDζ2*, *PLIP3*, and *pPLAIIIβ* in the developmentally more progressed PZ may indicate catabolic processes related to TAG-containing LBs. The TAG core of LBs is surrounded by a PL monolayer. Once hydrolysis of TAG occurs, PLs of the monolayer membrane are supposedly also subjected to catabolic processes. Expression levels of *PLDζ2*, *PLIP3*, and *pPLAIIIβ* correlate with the gene expression levels of TAG-hydrolyzing lipase *SDP1*, thus supporting this idea.

In general, our data indicate that regarding PL metabolism differences during development of the PZ and between the PZ and the AZ occur for PL catabolic processes. In addition to TAGs, PLs thus may represent a source of acetyl-CoA units as well as phosphate for developmental processes.

Enhanced FA β-oxidation during progression of the PZ indicates turnover of stored lipid resources

In peroxisomal β-oxidation FAs are broken down to yield finally C_2 acetyl units (Fig. 9). Especially FAs released from TAGs and PLs may be targets for the peroxisomal FA β-oxidation during progression of the PZ in comparison to the AZ. Eight genes, *ACX3*, *ECI1*, *KAT2*, *PNC1*, *MFP2*, *ACX4*, *ECH2*, and *AIM1*, involved in peroxisomal FA β-oxidation, were up-regulated during PZ progression and down-regulated in the AZ (Fig. 9). All of these genes, except for *ECH2*, negatively correlated with LCFAs and VLCFAs present in the three investigated lipid fractions, supporting catabolic processes related to NL, GL, and PL metabolism. The first step of peroxisomal FA β-oxidation, the conversion of acyl-CoA to 2*trans*-enoyl-CoA, is catalyzed by ACXs (Li-Beisson *et al.*, 2013). AIM1 is an isoform of multifunctional protein (MFP) involved in the second and the third step of the core β-oxidation pathway (Richmond and Bleeker, 1999; Li-Beisson *et al.*, 2013), leading to conversion of 2*trans*-enoyl-CoA to 3S-hydroxyacyl-CoA and production of 3-ketoacyl-CoA. KAT2 catalyzes cleavage of 3-ketoacyl-CoA into acyl-CoA. Acyl-CoA chains with a *cis* double bond on an even-numbered carbon are converted in the final step to 2*trans*-enoyl-CoA by ECH2, while 3*trans*-enoyl-CoA is converted to 2*trans*-enoyl-CoA by the isomerase ECI1 in the case of acyl-CoA chains with *cis* double bonds at odd-numbered positions (Li-Beisson *et al.*, 2013) (Fig. 9). Interestingly, the LCFAs 18:2 and 18:3, derived from NLs, decreased with progression of the development of the PZ, indicating that these FAs might be catabolized to generate acetyl-CoA for developmental processes and seed setting. This decrease fits to increasing levels of *ECI1* and *ECH2* expression and is supported by the negative correlation between *ECI1* and NL-derived 18:2 and 18:3 FAs. Moreover, ECH2 was demonstrated to play an important role with regard to mobilization of storage lipids (Strader *et al.*, 2011; Katano *et al.*, 2016; Li *et al.*, 2019). Finally, the peroxisomal adenine nucleotide carrier protein PNC1 catalyzes the import of ATP into peroxisomes, thus playing an important role with regard to energy supply for subsequent peroxisomal reactions (Linka *et al.*, 2008) (Fig. 9).

In summary, gene expression levels of enzymes involved in peroxisomal FA β-oxidation correlate with degradation of certain VLCFAs and LCFAs, indicating turnover of stored lipid resources.

Conclusions

This study sheds light on lipid metabolism and corresponding genes catalyzing and regulating metabolic steps that differentiate PZ and AZ in the perennial *A. alpina*. On one side, glycerolipids increase during PZ progression with a tendency for higher amounts of VLCFAs. On the other side, catabolic activities interconvert lipids or degrade them for energy consumption during specific developmental steps. In future studies, the exact role of these candidate genes in lipid metabolism and thereby the importance of metabolic steps themselves can be investigated. The lipid metabolism genes help to dissect the regulatory pathways for storage lipid deposition, potentially controlled by PZ-AZ transition signals.

Supplementary Material

Supplementary Fig. S1: Overview of biochemical lipid analysis.

Supplementary Fig. S2: Long-chain (LC) and very long-chain fatty acid (VLCFA) contents in glycolipid (GL) and phospholipid (PL) fractions in stems.

Supplementary Fig. S3: Long-chain (LC) and very long-chain fatty acid (VLCFA) contents in glycolipid (GL) and phospholipid (PL) fractions in roots.

Supplementary Fig. S4: Gene expression of lipid metabolism genes in lateral stem internodes.

Supplementary Fig. S5: Pearson correlation analysis between gene expression levels of lipid metabolism genes and amounts of individual FAs of the NL fraction of *A. alpina perpetual flowering 1-1* (*pep1-1*) lateral stem internodes of perennial (PZ) and annual (AZ) zones.

Supplementary Fig. S6: Pearson correlation analysis between gene expression levels of lipid metabolism genes and amounts of individual FAs of the GL fraction of *A. alpina perpetual flowering 1-1* (*pep1-1*) lateral stem internodes of perennial (PZ) and annual (AZ) zones.

Supplementary Fig. S7: Pearson correlation analysis between gene expression levels of lipid metabolism genes and amounts of individual FAs of the PL fraction of *A. alpina perpetual flowering 1-1* (*pep1-1*) lateral stem internodes of perennial (PZ) and annual (AZ) zones.

Supplementary Table S1: Lipid metabolism RNA-seq gene expression data.

Supplementary Table S2: Selected GO terms from the GO enrichment analysis related to lipid metabolism: Comparison I_PZ and III_PZ.

Supplementary Table S3: Selected GO terms from the GO enrichment analysis related to lipid metabolism: Comparison I_PZ and IV_PZ.

Supplementary Table S4: Selected GO terms from the GO enrichment analysis related to lipid metabolism: Comparison III_PZ and IV_PZ.

Supplementary Table S5: Selected GO terms from the GO enrichment analysis related to lipid metabolism: Comparison I_PZ and IV_AZ_if.

Supplementary Table S6: Selected GO terms from the GO enrichment analysis related to lipid metabolism: Comparison III_PZ and IV_AZ_if.

Supplementary Table S7: Selected GO terms from the GO enrichment analysis related to lipid metabolism: Comparison IV_PZ and IV_AZ_if.

Supplementary Table S8: Reverse transcription qPCR primers for lipid metabolism genes.

Author Contributions

AS, TMA, and PB planned and designed the research. AS and HL performed the experiments. AS and HJM analyzed data. AS and PB wrote the manuscript. HL, HJM, and TMA reviewed the article. PB acquired funding.

Acknowledgements

This work received funding from Germany's Excellence Strategy, EXC 2048/1, Project ID: 390686111. We acknowledge the excellent technical assistance of M. Graf, E. Klemp, and K. Weber for GC-MS measurements. We also want to thank Dr. Vera Wewer (University of Cologne) for her advice regarding the establishment of lipid extraction. The authors thank E. Wieneke for help with gene expression studies. H.L. was the recipient of a doctoral fellowship from Northwest A&F University, College of Horticulture, Yangling, China. The authors have no conflict of interest to declare.

References

Albani MC, Castaings L, Wotzel S, Mateos JL, Wunder J, Wang R, Reymond M, Coupland G. 2012. PEP1 of Arabis alpina is encoded by two overlapping genes that contribute to natural genetic variation in perennial flowering. PLoS Genet **8**, e1003130.

Bates PD, Fatihi A, Snapp AR, Carlsson AS, Browse J, Lu C. 2012. Acyl editing and headgroup exchange are the major mechanisms that direct polyunsaturated fatty acid flux into triacylglycerols. Plant Physiol **160**, 1530-1539.

Baud S, Santos Mendoza M, To A, Harscoët E, Lepiniec L, Dubreucq B. 2007. WRINKLED1 specifies the regulatory action of LEAFY COTYLEDON2 towards fatty acid metabolism during seed maturation in Arabidopsis. The Plant J **50**, 825-838.

Ben Abdallah H, Bauer P. 2016. Quantitative Reverse Transcription-qPCR-Based Gene Expression Analysis in Plants. In: Botella J., Botella M. (eds) Plant Signal Transduction. Methods in Molecular Biology **1363**. Humana Press, New York, NY

Benning C, Ohta H. 2005. Three enzyme systems for galactoglycerolipid biosynthesis are coordinately regulated in plants. J Biol Chem **280**, 2397-2400.

Brocard L, Immel F, Coulon D, Esnay N, Tuphile K, Pascal S, Claverol S, Fouillen L, Bessoule JJ, Brehelin C. 2017. Proteomic Analysis of Lipid Droplets from Arabidopsis Aging Leaves Brings New Insight into Their Biogenesis and Functions. Front Plant Sci **8**, 894.

Cai Y, McClinchie E, Price A, Nguyen TN, Gidda SK, Watt SC, Yurchenko O, Park S, Sturtevant D, Mullen RT, Dyer JM, Chapman KD. 2017. Mouse fat storage-inducing transmembrane protein 2 (FIT2) promotes lipid droplet accumulation in plants. Plant Biotechnol J **15**, 824-836.

Cao Y, Huang AHC. 1986. Diacylglycerol acyltransferase in maturing oil seeds of maize and other species. Plant Physiol **82**, 813-820.

Cernac A, Benning C. 2004. WRINKLED1 encodes an AP2/EREB domain protein involved in the control of storage compound biosynthesis in Arabidopsis. The Plant J **40**, 575-585.
Chinnasamy G, Davis PJ, Bal AK. 2003. Seasonal changes in oleosomic lipids and fatty acids of perennial root nodules of beach pea. J Plant Physiol **160**, 355-365.
Cruz-Ramírez A, Oropeza-Aburto A, Razo-Hernández F, Ramírez-Chávez E, Herrera-Estrella L. 2006. Phospholipase DZ2 plays an important role in extraplastidic galactolipid biosynthesis and phosphate recycling in Arabidopsis roots. Proc Natl Acad Sci U S A **103**, 6765-6770.
Dörmann P, Hoffmann-Benning S, Balbo I, Benning C. 1995. Isolation and characterization of an Arabidopsis mutant deficient in the thylakoid lipid digalactosyl diacylglycerol. The Plant Cell **7**, 1801-1810.
Eastmond PJ. 2006. SUGAR-DEPENDENT1 encodes a Patatin Domain Triacylglycerol Lipase that initiates storage oil breakdown in germinating Arabidopsis seeds. Plant Cell **18**, 665-675.
Essigmann B, Güler S, Narang RA, Linke D, Benning C. 1998. Phosphate availability affects the thylakoid lipid composition and the expression of SQD1, a gene required for sulfolipid biosynthesis in Arabidopsis thaliana. Proc Natl Acad Sci U S A **95**, 1950-1955.
Fan J, Yu L, Xu C. 2017. A central role for triacylglycerol in membrane lipid breakdown, fatty acid beta-oxidation, and plant survival under extended darkness. Plant Physiol **174**, 1517-1530.
Hajra AK. 1974. On extraction of acyl and alkyl dihydroxyacetone phosphate from incubation mixtures. Lipids **9**, 502-505.
Härtel H, Essigmann B, Lokstein H, Hoffmann-Benning S, Peters-Kottig M, Benning C. 1998. The phospholipid-deficient pho1 mutant of Arabidopsis thaliana is affected in the organization, but not in the light acclimation, of the thylakoid membrane. Biochimica et Biophysica Acta **1415**, 205-218.
Härtel H, Dörmann P, Benning C. 2000. DGD1-independent biosynthesis of extraplastidic galactolipids after phosphate deprivation in Arabidopsis. Proc Natl Acad Sci U S A **97**, 10649-10654.
Haslam RP, Ruiz-Lopez N, Eastmond P, Moloney M, Sayanova O, Napier JA. 2013. The modification of plant oil composition via metabolic engineering--better nutrition by design. Plant Biotechnol J **11**, 157-168.
Hielscher B, Charton L, Mettler-Altmann T, Linka N. 2017. Analysis of peroxisomal β-oxidation during storage oil mobilization in Arabidopsis thaliana seedlings. In: Schrader M. (eds) Peroxisomes. Methods in Molecular Biology, **1595**.
Huang AHC. 2018. Plant lipid droplets and their associated proteins: Potential for rapid advances. Plant Physiol **176**, 1894-1918.
Huang S, Jiang L, Zhuang X. 2019. Possible roles of membrane trafficking components for lipid droplet dynamics in higher plants and green algae. Front Plant Sci **10**, 207.
Hughes PW, Soppe WJJ, Albani MC. 2019. Seed traits are pleiotropically regulated by the flowering time gene PERPETUAL FLOWERING 1 (PEP1) in the perennial Arabis alpina. Mol Ecol **28**, 1183-1201.
Hurlock AK, Roston RL, Wang K, Benning C. 2014. Lipid trafficking in plant cells. Traffic **15**, 915-932.
Jayawardhane KN, Singer SD, Weselake RJ, Chen G. 2018. Plant sn-glycerol-3-phosphate acyltransferases: Biocatalysts involved in the biosynthesis of intracellular and extracellular lipids. Lipids **53**, 469-480.
Joubès J, Raffaele S, Bourdenx B, Garcia C, Laroche-Traineau J, Moreau P, Domergue F, Lessire R. 2008. The VLCFA elongase gene family in Arabidopsis thaliana: phylogenetic analysis, 3D modelling and expression profiling. Plant Mol Biol **67**, 547-566.
Jouhet J, Marechal E, Baldan B, Bligny R, Joyard J, Block MA. 2004. Phosphate deprivation induces transfer of DGDG galactolipid from chloroplast to mitochondria. J Cell Biol **167**, 863-874.
Karki N, Johnson BS, Bates PD. 2019. Metabolically distinct pools of phosphatidylcholine are involved in trafficking of fatty acids out of and into the chloroplast for membrane production. Plant Cell **31**, 2768-2788.
Karl R, Koch MA. 2013. A world-wide perspective on crucifer speciation and evolution: phylogenetics, biogeography and trait evolution in tribe Arabideae. Ann Bot **112**, 983-1001.
Katano M, Takahashi K, Hirano T, Kazama Y, Abe T, Tsukaya H, Ferjani A. 2016. Suppressor screen and phenotype analyses revealed an emerging role of the monofunctional peroxisomal Enoyl-CoA Hydratase 2 in compensated cell enlargement. Front Plant Sci **7**, 132.

Kelly AA, Dörmann P. 2002. DGD2, an arabidopsis gene encoding a UDP-galactose-dependent digalactosyldiacylglycerol synthase is expressed during growth under phosphate-limiting conditions. J Biol Chem **277**, 1166-1173.
Kelly AA, Froehlich JE, Dörmann P. 2003. Disruption of the two digalactosyldiacylglycerol synthase genes DGD1 and DGD2 in Arabidopsis reveals the existence of an additional enzyme of galactolipid synthesis. Plant Cell **15**, 2694-2706.
Kelly AA, van Erp H, Quettier AL, Shaw E, Menard G, Kurup S, Eastmond PJ. 2013. The sugar-dependent1 lipase limits triacylglycerol accumulation in vegetative tissues of Arabidopsis. Plant Physiol **162**, 1282-1289.
Kiefer C, Severing E, Karl R, Bergonzi S, Koch M, Tresch A, Coupland G. 2017. Divergence of annual and perennial species in the Brassicaceae and the contribution of cis-acting variation at FLC orthologues. Mol Ecol **26**, 3437-3457.
Kim EY, Seo YS, Kim WT. 2011. AtDSEL, an Arabidopsis cytosolic DAD1-like acylhydrolase, is involved in negative regulation of storage oil mobilization during seedling establishment. J Plant Physiol **168**, 1705-1709.
LaBrant E, Barnes AC, Roston RL. 2018. Lipid transport required to make lipids of photosynthetic membranes. Photosynth Res **138**, 345-360.
Lacey DJ, Beaudoin F, Dempsey CE, Shewry PR, Napier JA. 1999. The accumulation of triacylglycerols within the endoplasmic reticulum of developing seeds of Helianthus annuus. The Plant J **17**, 397-405.
Lazaro A, Obeng-Hinneh E, Albani MC. 2018. Extended vernalization regulates inflorescence fate in Arabis alpina by stably silencing PERPETUAL FLOWERING1. Plant Physiol **176**, 2819-2833.
Lee K, Ratnayake C, Huang AHC. 1995. Genetic dissection of the co-expression of genes encoding the two isoforms of oleosins in the oil bodies of maize kernel. The Plant J **7**, 603-611.
Li-Beisson Y, Shorrosh B, Beisson F, Andersson MX, Arondel V, Bates PD, Baud S, Bird D, Debono A, Durrett TP, Franke RB, Graham IA, Katayama K, Kelly AA, Larson T, Markham JE, Miquel M, Molina I, Nishida I, Rowland O, Samuels L, Schmid KM, Wada H, Welti R, Xu C, Zallot R, Ohlrogge J. 2013. Acyl-lipid metabolism. Arabidopsis Book **11**, e0161.
Li M, Qin C, Welti R, Wang X. 2006. Double knockouts of phospholipases Dzeta1 and Dzeta2 in Arabidopsis affect root elongation during phosphate-limited growth but do not affect root hair patterning. Plant Physiol **140**, 761□770.
Li M, Bahn SC, Guo L, Musgrave W, Berg H, Welti R, Wang X. 2011. Patatin-related phospholipase pPLAIIIβ-induced changes in lipid metabolism alter cellulose content and cell elongation in Arabidopsis. Plant Cell **23**, 1107-1123.
Li M, Wei F, Tawfall A, Tang M, Saettele A, Wang X. 2015. Overexpression of patatin-related phospholipase AIIIdelta altered plant growth and increased seed oil content in camelina. Plant Biotechnol J **13**, 766-778.
Li Y, Liu Y, Zolman BK. 2019. Metabolic Alterations in the Enoyl-CoA Hydratase 2 Mutant Disrupt Peroxisomal Pathways in Seedlings. Plant Physiol **180**, 1860-1876.
Linka N, Theodoulou FL, Haslam RP, Linka M, Napier JA, Neuhaus HE, Weber APM. 2008. Peroxisomal ATP import is essential for seedling development in Arabidopsis thaliana. Plant Cell **20**, 3241-3257.
Lippold F, vom Dorp K, Abraham M, Holzl G, Wewer V, Yilmaz JL, Lager I, Montandon C, Besagni C, Kessler F, Stymne S, Dörmann P. 2012. Fatty acid phytyl ester synthesis in chloroplasts of Arabidopsis. Plant Cell **24**, 2001-2014.
Loer DS, Herman EM. 1993. Cotranslational integration of soybean (Glycien max) oil body membrane protein oleosin into microsomal membranes. Plant Physiol **101**, 993-998.
Lu C, Napier JA, Clemente TE, Cahoon EB. 2011. New frontiers in oilseed biotechnology: meeting the global demand for vegetable oils for food, feed, biofuel, and industrial applications. Curr Opin Biotechnol **22**, 252-259.
Madey E, Nowack LM, Thompson JE. 2002. Isolation and characterization of lipid in phloem sap of canola. Planta **214**, 625-634.
Maeo K, Tokuda T, Ayame A, Mitsui N, Kawai T, Tsukagoshi H, Ishiguro S, Nakamura K. 2009. An AP2-type transcription factor, WRINKLED1, of Arabidopsis thaliana binds to the AW-box

sequence conserved among proximal upstream regions of genes involved in fatty acid synthesis. The Plant J **60**, 476-487.
Michaels SD, Amasino RM. 1999. FLOWERING LOCUS C encodes a novel MADS domain protein that acts as a repressor of flowering. The Plant Cell **11**, 949-956.
Millar AA, Kunst L. 1999. The natural genetic variation of the fatty-acyl composition of seed oild in different ecotypes of Arabidopsis thaliana. Phytochemistry **52**, 1029-1033.
Næsted H, Frandsen GI, Jauh GY, Hernandez-Pinzon I, Nielsen HB, Murphy DJ, Rogers JC, Mundy J. 2000. Caleosins: Ca^{2+}-binding proteins associated with lipid bodies. Plant Mol Biol **44**, 463-476.
Pant BD, Burgos A, Pant P, Cuadros-Inostroza A, Willmitzer L, Scheible WR. 2015. The transcription factor PHR1 regulates lipid remodeling and triacylglycerol accumulation in Arabidopsis thaliana during phosphorus starvation. J Exp Bot **66**, 1907-1918.
Pyc M, Cai Y, Greer MS, Yurchenko O, Chapman KD, Dyer JM, Mullen RT. 2017. Turning Over a New Leaf in Lipid Droplet Biology. Trends Plant Sci **22**, 596-609.
Richmond TA, Bleecker AB. 1999. A defect in beta-oxidation causes abnormal inflorescence development in Arabidopsis. Plant Cell **11**, 1911□1924.
Sauter JJ, van Cleve B. 1994. Storage, mobilization and interrelations of starch, sugars, protein and fat in the ray storage tissue of poplar trees. Trees **8**, 297-304.
Sergeeva A, Liu H, Mai HJ, Mettler-Altmann T, Kiefer C, Coupland G, Bauer P. 2020. Cytokinin-promoted secondary growth and nutrient storage in the perennial stem zone of Arabis alpina. Biorxiv doi.org/10.1101/2020.06.01.124362.
Shi L, Katavic V, Yu Y, Kunst L, Haughn G. 2012. Arabidopsis glabra2 mutant seeds deficient in mucilage biosynthesis produce more oil. Plant J **69**, 37-46.
Shockey JM, Gidda SK, Chapital DC, Kuan JC, Dhanoa PK, Bland JM, Rothstein SJ, Mullen RT, Dyer JM. 2006. Tung tree DGAT1 and DGAT2 have nonredundant functions in triacylglycerol biosynthesis and are localized to different subdomains of the endoplasmic reticulum. Plant Cell **18**, 2294-2313.
Simon EW. 1974. Phospholipids and plant membrane permeability. New Phytol **73**, 377-420.
Stephan L, Tilmes V, Hulskamp M. 2019. Selection and validation of reference genes for quantitative Real-Time PCR in Arabis alpina. PLoS One **14**, e0211172.
Strader LC, Wheeler DL, Christensen SE, Berens JC, Cohen JD, Rampey RA, Bartel B. 2011. Multiple facets of Arabidopsis seedling development require indole-3-butyric acid-derived auxin. Plant Cell **23**, 984-999.
Su Y, Li M, Guo L, Wang X. 2018. Different effects of phospholipase Dζ2 and non-specific phospholipase C4 on lipid remodeling and root hair growth in Arabidopsis response to phosphate deficiency. The Plant J **94**, 315-326.
Tan H, Yang X, Zhang F, Zheng X, Qu C, Mu J, Fu F, Li J, Guan R, Zhang H, Wang G, Zuo J. 2011. Enhanced seed oil production in canola by conditional expression of Brassica napus LEAFY COTYLEDON1 and LEC1-LIKE in developing seeds. Plant Physiol **156**, 1577-1588.
van der Schoot C, Paul LK, Paul SB, Rinne PL. 2011. Plant lipid bodies and cell-cell signaling: a new role for an old organelle? Plant Signal Behav **6**, 1732-1738.
van Erp H, Kelly AA, Menard G, Eastmond PJ. 2014. Multigene engineering of triacylglycerol metabolism boosts seed oil content in Arabidopsis. Plant Physiol **165**, 30-36.
Vanhercke T, Wood CC, Stymne S, Singh SP, Green AG. 2013. Metabolic engineering of plant oils and waxes for use as industrial feedstocks. Plant Biotechnol J **11**, 197-210.
Vayssières A, Mishra P, Roggen A, Neumann U, Ljung K, Albani MC. 2020. Vernalization shapes shoot architecture and ensures the maintenance of dormant buds in the perennial Arabis alpina. New Phytol.
Wang G, Lin Q, Xu Y. 2007. Tetraena mongolica Maxim can accumulate large amounts of triacylglycerol in phloem cells and xylem parenchyma of stems. Phytochemistry **68**, 2112-2117.
Wang R, Farrona S, Vincent C, Joecker A, Schoof H, Turck F, Alonso-Blanco C, Coupland G, Albani MC. 2009. PEP1 regulates perennial flowering in Arabis alpina. Nature **459**, 423-427.
Wang R, Albani MC, Vincent C, Bergonzi S, Luan M, Bai Y, Kiefer C, Castillo R, Coupland G. 2011. Aa TFL1 confers an age-dependent response to vernalization in perennial Arabis alpina. Plant Cell **23**, 1307-1321.

Wang K, Guo Q, Froehlich JE, Hersh HL, Zienkiewicz A, Howe GA, Benning C. 2018. Two abscisic acid-responsive plastid lipase genes involved in jasmonic acid biosynthesis in Arabidopsis thaliana. Plant Cell **30**, 1006-1022.
Wewer V, Dombrink I, vom Dorp K, Dormann P. 2011. Quantification of sterol lipids in plants by quadrupole time-of-flight mass spectrometry. J Lipid Res **52**, 1039-1054.
Yang X, Wang Z, Feng T, Li J, Huang L, Yang B, Zhao H, Jenks MA, Yang P, Lü S. 2018. Evolutionarily conserved function of the sacred lotus (Nelumbo nucifera Gaertn.) CER2-LIKE family in very-long-chain fatty acid elongation. Planta **248**, 715□727.

Supplementary Figures and Tables

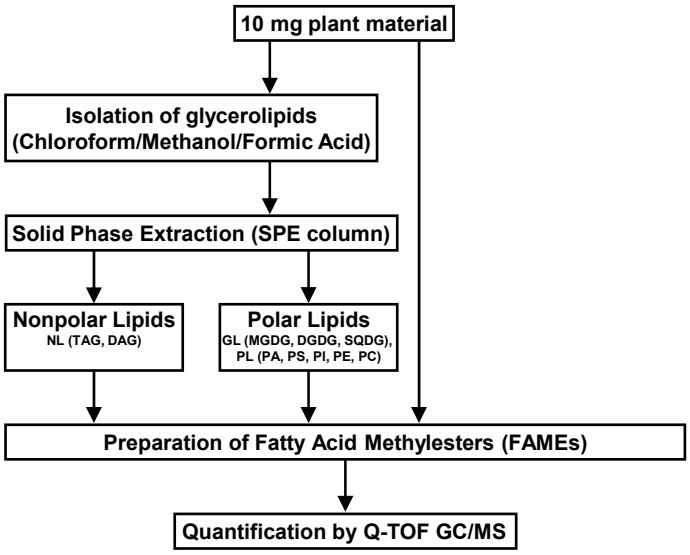

Supplementary Fig. S1. Overview of biochemical lipid analysis. Ten mg of dry starting plant material was either used for preparation of glycerolipids or directly applied for preparation of fatty acid methylesters (FAMEs). Extracted glycerolipids were fractionated into neutral lipids (NL), glycolipids (GL), and phospholipids (PL) on solid phase extraction (SPE) columns. The NL fraction contained triacylglycerol (TAG) and diacylglycerol (DAG). The GL fraction comprised monogalactosyldiacylglycerol (MGDG), digalactosyldiacylglycerol (DGDG), and sulfoquinovosyldiacylglycerol (SQDG). The PL fraction included phosphatidic acid (PA), phosphatidylserine (PS), phosphoinositide (PI), phosphatidylethanolamine (PE), and phosphatidylcholine (PC). Fractionated lipids were applied to the preparation of FAMEs. FAMEs were finally quantified by Q-TOF GC/MS analysis.

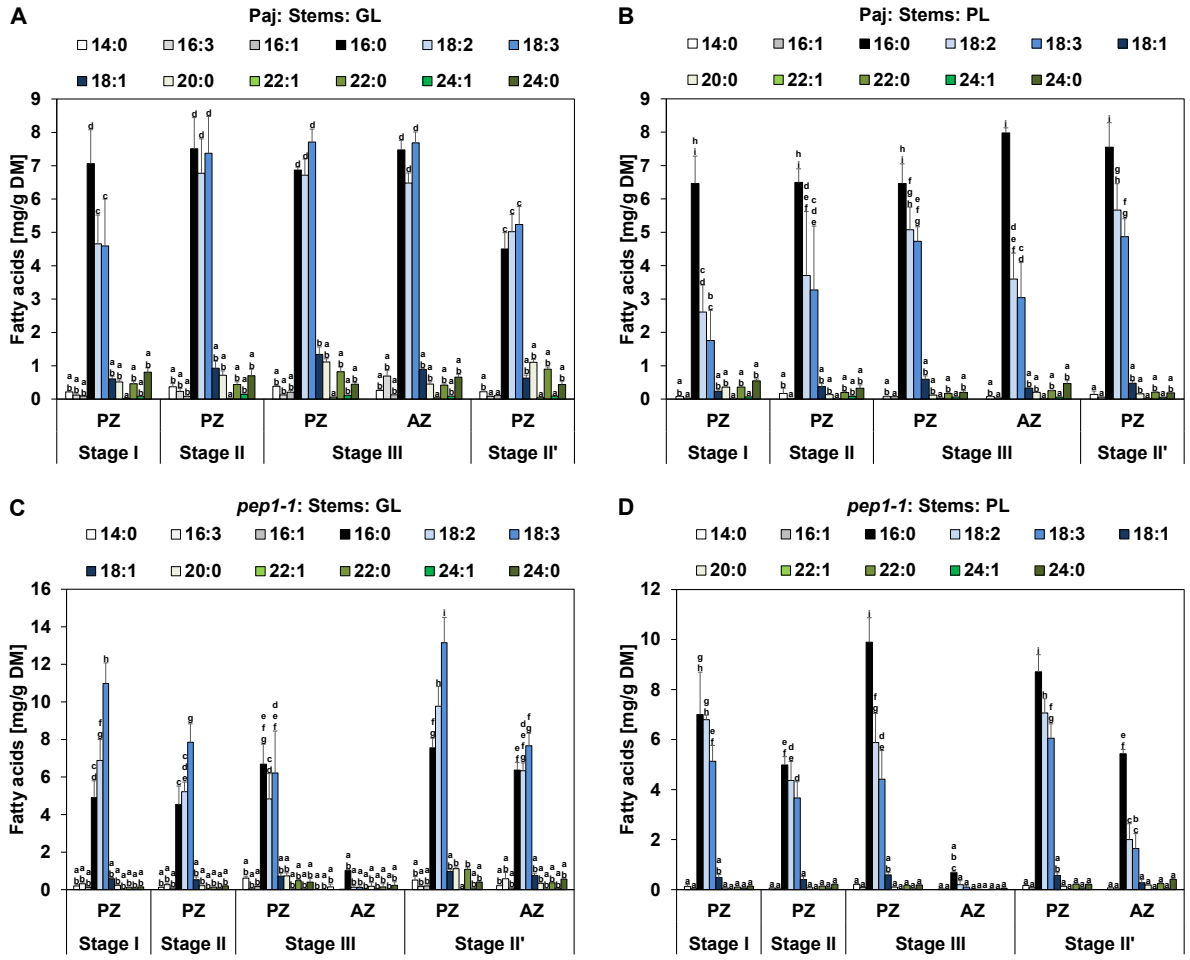

Supplementary Fig. S2. Long-chain (LC) and very long-chain fatty acid (VLCFA) contents in glycolipid (GL) and phospholipid (PL) fractions in stems. Represented are the contents of (A, C) GL and (B, D) PL fraction-derived individual LCFAs (14:0, 16:3, 16:1, 16:0, 18:2, 18:3, 18:1) and individual VLCFAs (20:0, 22:1, 22:0, 24:1, 24:0) per dry matter (DM) of perennial (PZ) and annual (AZ) internode stem zones of (A, C) *A. alpina* Pajares (Paj, wild type) and (B, D) *perpetual flowering 1-1* (*pep1-1*) mutant derivative. Plant material was harvested at four different developmental stages, stage I, II, III, and II‘, as indicated in Fig. 1A. In addition, the PZ of *pep1-1* contained low contents of other FAs in the GL fraction (compare in C), namely 16:2 FAs at stages I, II, and II’ (0.02 mg/g DM, 0,02 mg/g DM, and 0.05 mg/g DM) and 20:1 FAs at stages I and II (0.04 mg/g DM and 0.32 mg/g DM). For comparable representation, these FAs are not shown in the diagram, but were included in all calculations. Data are represented as mean +/- SD (n = 3-7). Different letters indicate statistically significant differences, determined by one-way ANOVA-Tukey’s HSD test ($P < 0.05$).

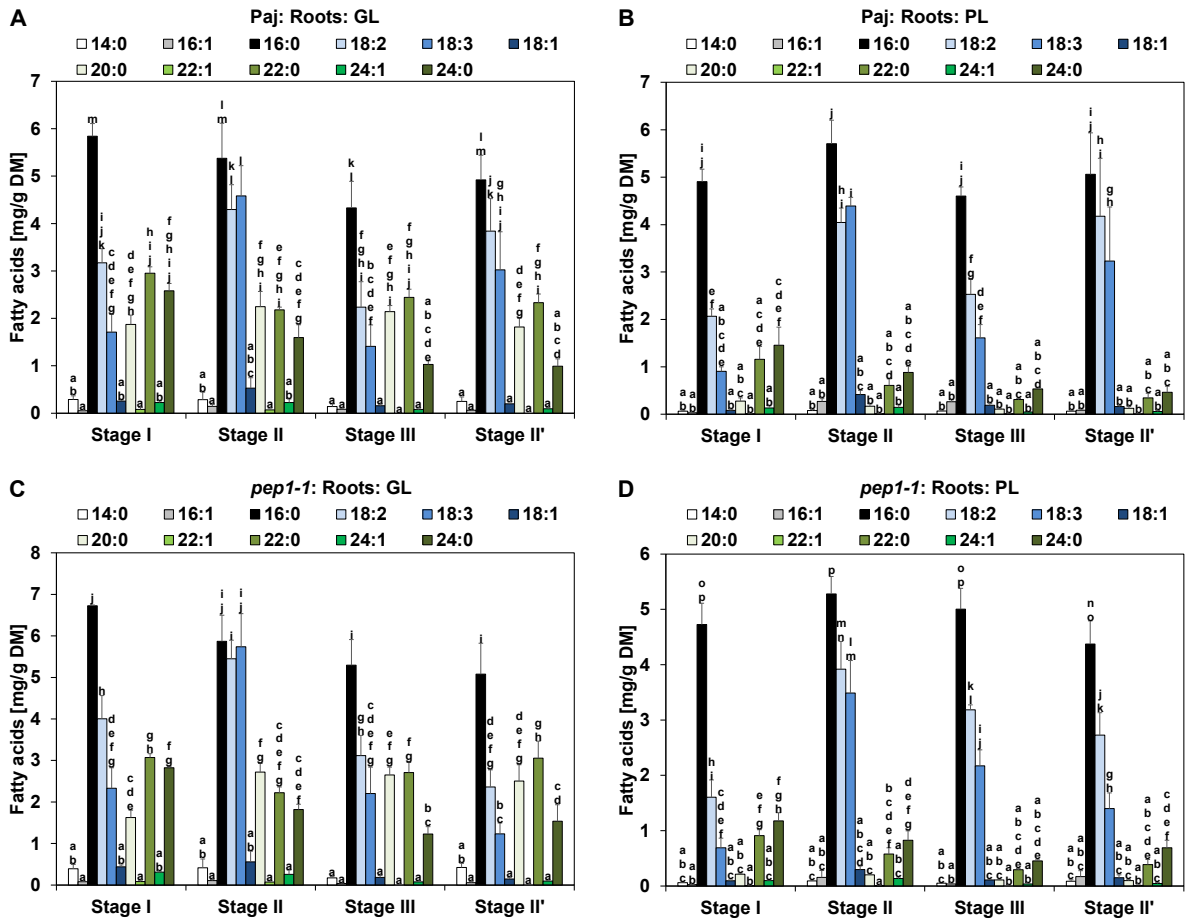

Supplementary Fig. S3. Long-chain (LC) and very long-chain fatty acid (VLCFA) contents in glycolipid (GL) and phospholipid (PL) fractions in roots. Represented are the contents of (A, C) GL and (B, D) PL fraction-derived individual LCFAs (14:0, 16:1, 16:0, 18:2, 18:3, 18:1) and individual VLCFAs (20:0, 22:1, 22:0, 24:1, 24:0) per dry matter (DM) in roots of (A, C) *A. alpina* Pajares (Paj, wild type) and (B, D) *perpetual flowering 1-1* (*pep1-1*) mutant derivative. Plant material was harvested at four different developmental stages, stage I, II, III, and II‘, as indicated in Fig. 1A. Data are represented as mean +/- SD (n = 3-7). Different letters indicate statistically significant differences, determined by one-way ANOVA-Tukey’s HSD test ($P < 0.05$).

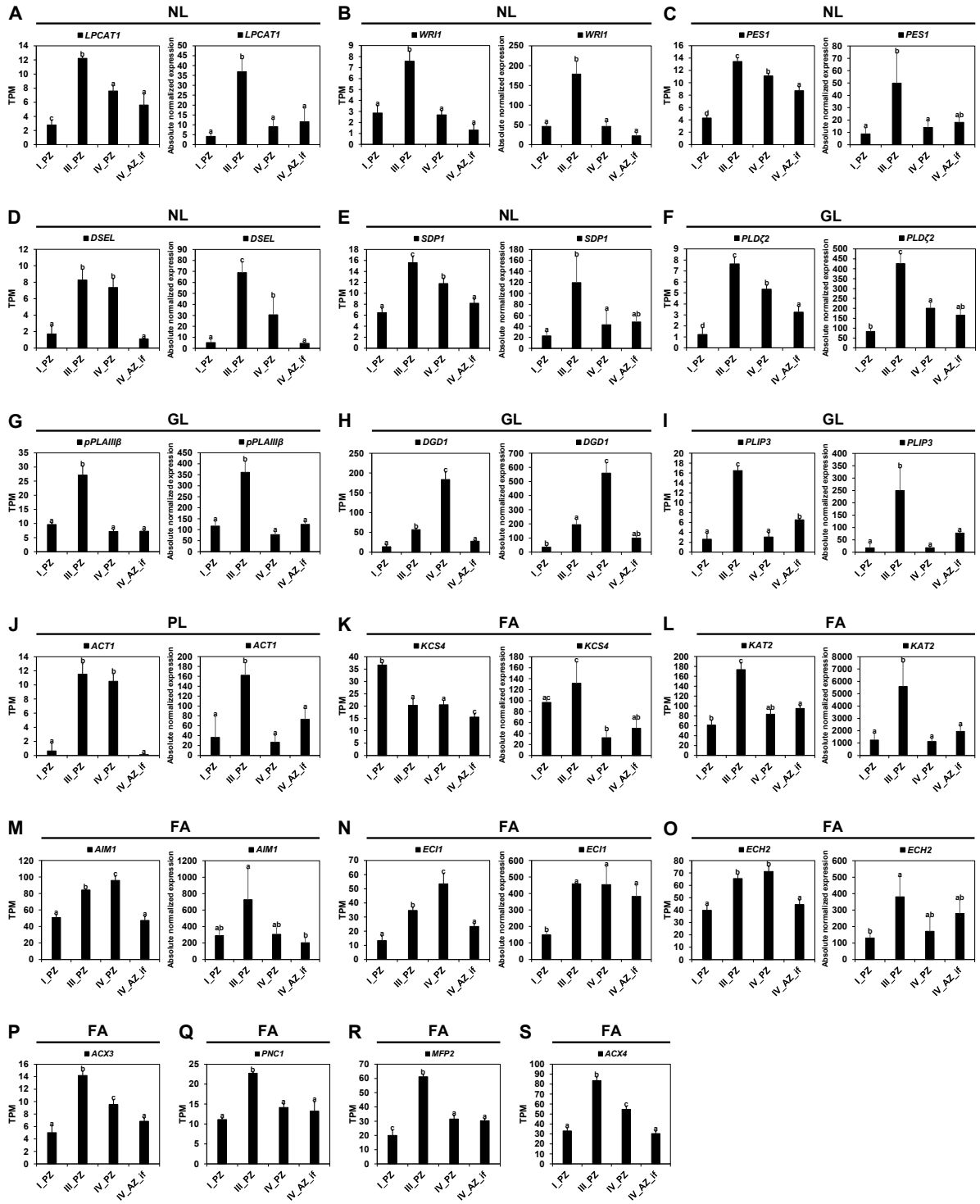

Supplementary Fig. S4. Gene expression of lipid metabolism genes in lateral stem internodes. Represented are RNA-seq data (left; TPM, transcripts per million) and reverse transcription-qPCR data (right; absolute normalized expression) of *A. alpina perpetual flowering 1-1* (*pep1-1*) lateral stem internodes of perennial (PZ) and annual (AZ) zones of RNA-seq at stages I_PZ, III_PZ, IV_PZ, and IV_AZ_if (see Fig. 5A). (A-E) NL genes (A) *LPCAT1*, *LYSOPHOSPHATIDYLCHOLINE ACYLTRANSFERASE 1*, (B) *WRI1*, *WRINKLED 1*, (C) *PES1*, *PHYTYL ESTER SYNTHASE 1,* (D) *DSEL*, *DAD1-LIKE SEEDLING ESTABLISHMENT-RELATED LIPASE*, (E) *SDP1, SUGAR-DEPENDENT1;* (F-I) GL genes (F) *PLDζ2*, *PHOSPHOLIPASE D ζ 2*, (G) *pPLAIIIβ*, *PATATIN-RELATED PHOSPHOLIPASE A IIIβ*, (H) *DGD1*, *DIGALACTOSYL DIACYLGLYCEROL DEFICIENT 1*, (I) *PLIP3*, *PLASTID LIPASE 3;* (J) PL gene *ACT1*, *ACYLTRANSFERASE 1*; *(legend continued on next page)*

(K-S) FA genes (K) *KCS4*, *3-KETOACYL-COA SYNTHASE 4*, (L) *KAT2*, *3-KETOACYL-COA THIOLASE 2*, (M) *AIM1*, *ABNORMAL INFLORESCENCE MERISTEM 1*, (N) *ECI1*, *Δ3, Δ2-ENOYL COA ISOMERASE 1*, (O) *ECH2*, *ENOYL-COA HYDRATASE 2*, (P) *ACX3*, *ACYL-COA OXIDASE 3*, (Q) *PNC1*, *PEROXISOMAL ADENINE NUCLEOTIDE CARRIER 1*, (R) *MFP2*, *MULTIFUNCTIONAL PROTEIN 2*, (S) *ACX4*, *ACYL-COA OXIDASE 4*. Data are represented as mean +/- SD (n = 3). Different letters indicate statistically significant differences, determined by one-way ANOVA-Tukey's HSD test ($P < 0.05$). Reverse transcription-qPCR data for *ACX3*, *PNC1*, *MFP2*, and *ACX4* are not shown.

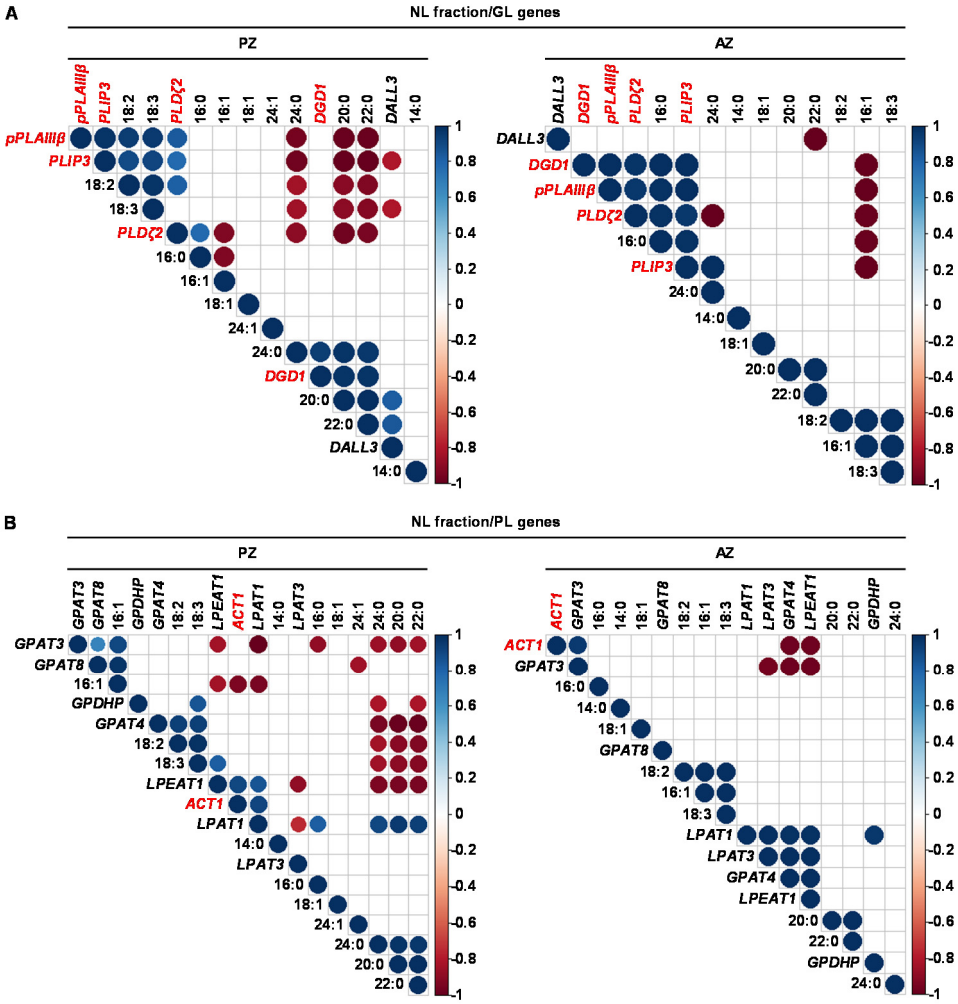

Supplementary Fig. S5. Pearson correlation analysis between gene expression levels of lipid metabolism genes and amounts of individual FAs of the NL fraction of *A. alpina perpetual flowering 1-1* (*pep1-1*) lateral stem internodes of perennial (PZ) and annual (AZ) zones. The analysis was performed between stages III_PZ, IV_PZ and I', II' for PZ, and IV_AZ_if and II' for AZ (see Fig. 1 and Fig. 5A). Correlation analysis between NL-derived FAs and (A) GL metabolism-related genes, *DALL3*, *DAD1-LIKE LIPASE 3*, *DGD1*, *DIGALACTOSYL DIACYLGLYCEROL DEFICIENT 1*, *PLDζ2*, *PHOSPHOLIPASE D ζ 2*, *PLIP3*, *PLASTID LIPASE 3*, *pPLAIIIβ*, *PATATIN-RELATED PHOSPHOLIPASE A IIIβ*; and (B) PL metabolism-related genes, *ACT1*, *ACYLTRANSFERASE 1*, *GPAT3*, *GLYCEROL-3-PHOSPHATE SN-2-ACYLTRANSFERASE 3*, *GPAT4*, *GLYCEROL-3-PHOSPHATE SN-2-ACYLTRANSFERASE 4*, *GPAT8*, *GLYCEROL-3-PHOSPHATE SN-2-ACYLTRANSFERASE 8*, *GPDHP*, *GLYCEROL-3-PHOSPHATE DEHYDROGENASE PLASTIDIC*, *LPAT1*, *LYSOPHOSPHATIDIC ACID ACYLTRANSFERASE 1*, *LPAT3*, *LYSOPHOSPHATIDYL ACYLTRANSFERASE 3*, *LPEAT1*, *LYSOPHOSPHATIDYLETHANOLAMINE ACYLTRANSFERASE 1*. Only correlation coefficients with significant levels of correlation ($P < 0.05$) are displayed in the diagrams. Putative candidate genes that may regulate the PZ development and the delimitation of the PZ and the AZ are represented in red.

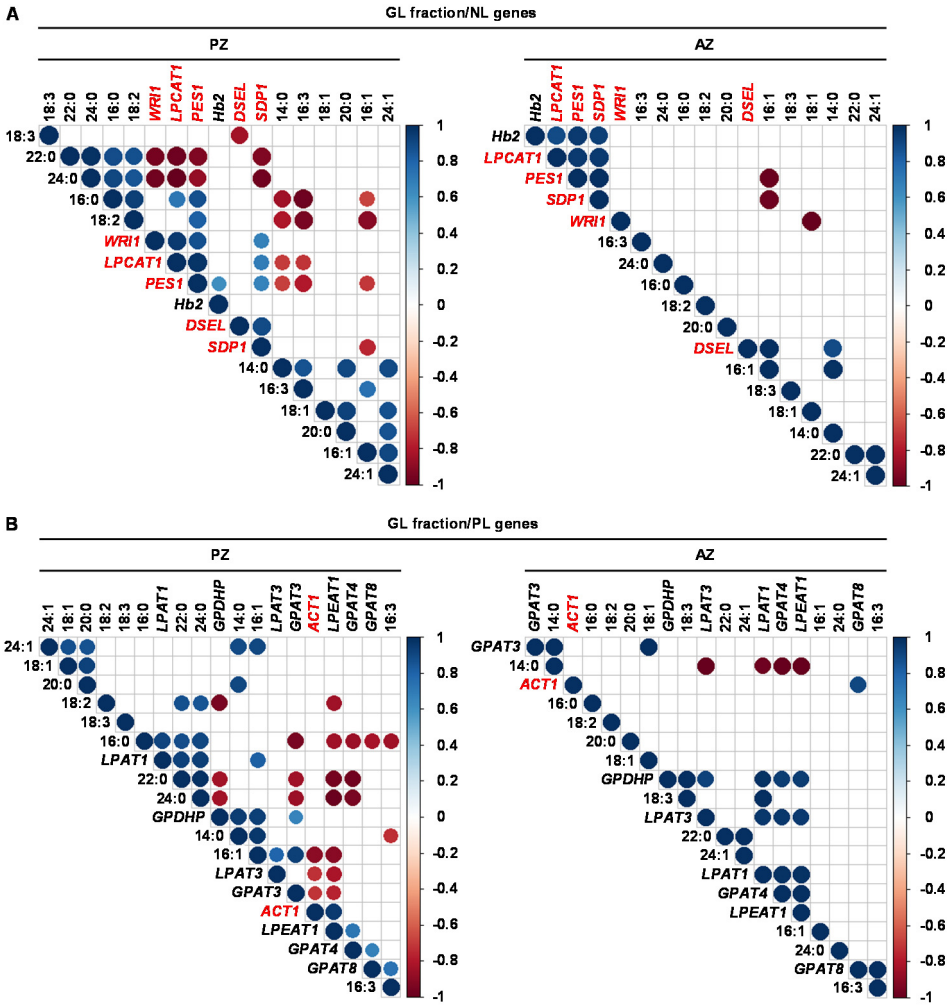

Supplementary Fig. S6. Pearson correlation analysis between gene expression levels of lipid metabolism genes and amounts of individual FAs of the GL fraction of *A. alpina perpetual flowering 1-1* (*pep1-1*) lateral stem internodes of perennial (PZ) and annual (AZ) zones. The analysis was performed between stages III_PZ, IV_PZ and I', II' for PZ, and IV_AZ_if and II' for AZ (see Fig. 1 and Fig. 5A). Correlation analysis between GL-derived FAs and (A) NL metabolism-related genes, *DSEL*, *DAD1-LIKE SEEDLING ESTABLISHMENT-RELATED LIPASE*, *Hb2, HAEMOGLOBIN 2*, *LPCAT1*, *LYSOPHOSPHATIDYLCHOLINE ACYLTRANSFERASE 1*, *PES1*, *PHYTYL ESTER SYNTHASE 1, SDP1, SUGAR-DEPENDENT1, WRI1*, *WRINKLED 1*; and (B) PL metabolism-related genes, *ACT1*, *ACYLTRANSFERASE 1*, *GPAT3*, *GLYCEROL-3-PHOSPHATE SN-2-ACYLTRANSFERASE 3*, *GPAT4*, *GLYCEROL-3-PHOSPHATE SN-2-ACYLTRANSFERASE 4*, *GPAT8*, *GLYCEROL-3-PHOSPHATE SN-2-ACYLTRANSFERASE 8*, *GPDHP*, *GLYCEROL-3-PHOSPHATE DEHYDROGENASE PLASTIDIC*, *LPAT1*, *LYSOPHOSPHATIDIC ACID ACYLTRANSFERASE 1*, *LPAT3*, *LYSOPHOSPHATIDYL ACYLTRANSFERASE 3*, *LPEAT1*, *LYSOPHOSPHATIDYLETHANOLAMINE ACYLTRANSFERASE 1*. Only correlation coefficients with significant levels of correlation ($P < 0.05$) are displayed in the diagrams. Putative candidate genes that may regulate the PZ development and the delimitation of the PZ and the AZ are represented in red.

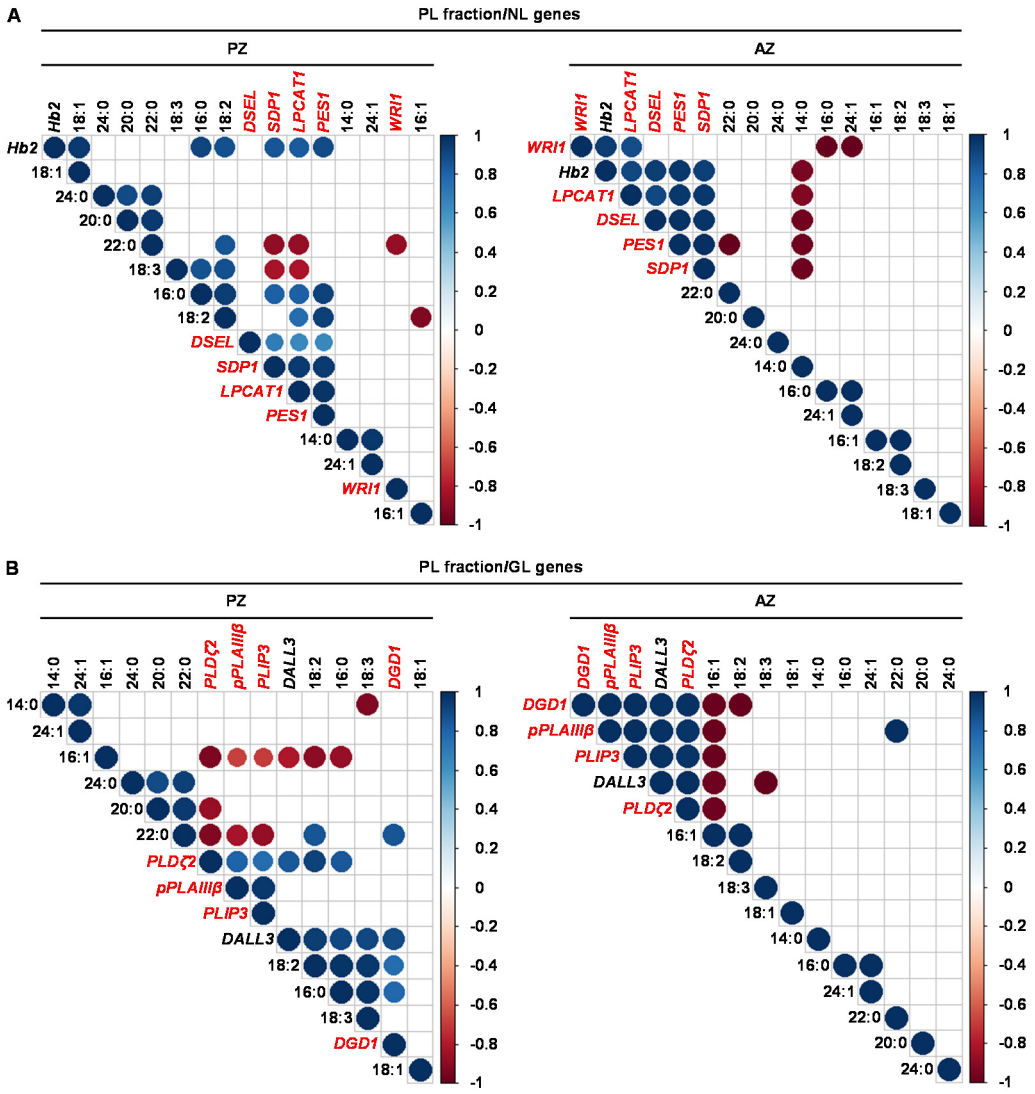

Supplementary Fig. S7. Pearson correlation analysis between gene expression levels of lipid metabolism genes and amounts of individual FAs of the PL fraction of *A. alpina perpetual flowering 1-1* (*pep1-1*) lateral stem internodes of perennial (PZ) and annual (AZ) zones. The analysis was performed between stages III_PZ, IV_PZ and I‘, II‘ for PZ, and IV_AZ_if and II‘ for AZ (see Fig. 1 and Fig. 5A). Correlation analysis between PL-derived FAs and (A) NL metabolism-related genes, *DSEL*, *DAD1-LIKE SEEDLING ESTABLISHMENT-RELATED LIPASE*, *Hb2, HAEMOGLOBIN 2*, *LPCAT1*, *LYSOPHOSPHATIDYLCHOLINE ACYLTRANSFERASE 1*, *PES1*, *PHYTYL ESTER SYNTHASE 1, SDP1, SUGAR-DEPENDENT1, WRI1*, *WRINKLED 1*; and (B) GL metabolism-related genes, *DALL3*, *DAD1-LIKE LIPASE 3*, *DGD1*, *DIGALACTOSYL DIACYLGLYCEROL DEFICIENT 1*, *PLDζ2*, *PHOSPHOLIPASE D ζ 2*, *PLIP3*, *PLASTID LIPASE 3*, *pPLAIIIβ*, *PATATIN-RELATED PHOSPHOLIPASE A IIIβ*. Only correlation coefficients with significant levels of correlation ($P < 0.05$) are displayed in the diagrams. Putative candidate genes that may regulate the PZ development and the delimitation of the PZ and the AZ are represented in red.

Supplementary Table S1. Lipid metabolism RNA-seq gene expression data. *AAD3*, *ACYL-ACYL CARRIER PROTEIN DESATURASE 3*, *ACP4*, *ACYL CARRIER PROTEIN 4*, *ACT1*, *ACYLTRANSFERASE 1*, *ACX3*, *ACYL-COA OXIDASE 3*, *ACX4*, *ACYL-COA OXIDASE 4*, *AIM1*, *ABNORMAL INFLORESCENCE MERISTEM 1*, *CER10*, *ECERIFERUM 10*, *DALL3*, *DAD1-LIKE LIPASE 3*, *DGD1*, *DIGALACTOSYL DIACYLGLYCEROL DEFICIENT 1*, *DSEL*, *DAD1-LIKE SEEDLING ESTABLISHMENT-RELATED LIPASE*, *ECH2*, *ENOYL-COA HYDRATASE 2*, *ECI1*, *Δ3, Δ2-ENOYL COA ISOMERASE 1*, *FAD3*, *FAD5*, *FAD6*, *FAD7*, *FAD8*, *FATTY ACID DESATURASEs*, *FATA2*, *OLEOYL-ACYL CARRIER PROTEIN THIOESTERASE 2*, *GPAT3*, *GLYCEROL-3-PHOSPHATE SN-2-ACYLTRANSFERASE 3*, *GPAT4*, *GLYCEROL-3-PHOSPHATE SN-2-ACYLTRANSFERASE 4*, *GPAT8*, *GLYCEROL-3-PHOSPHATE SN-2-ACYLTRANSFERASE 8*, *GPDHP*, *GLYCEROL-3-PHOSPHATE DEHYDROGENASE PLASTIDIC*, *Hb2, HAEMOGLOBIN 2*, *KAT2*, *3-KETOACYL-COA THIOLASE 2*, *KCS3*, *KCS4*, *KCS5*, *KCS6*, *KCS10*, *KCS11*, *KCS12*, *KCS13*, *KCS19*, *KETOACYL-COA SYNTHASEs*, *LACS7*, *LONG-CHAIN ACYL-COA SYNTHETASE 7*, *LPAT1*, *LYSOPHOSPHATIDIC ACID ACYLTRANSFERASE 1*, *LPAT3*, *LYSOPHOSPHATIDYL ACYLTRANSFERASE 3*, *LPCAT1*, *LYSOPHOSPHATIDYLCHOLINE ACYLTRANSFERASE 1*, *LPEAT1*, *LYSOPHOSPHATIDYLETHANOLAMINE ACYLTRANSFERASE 1*, *MFP2*, *MULTIFUNCTIONAL PROTEIN 2*, *MTACP1*, *MITOCHONDRIAL ACYL CARRIER PROTEIN 1*, *MTACP2*, *MITOCHONDRIAL ACYL CARRIER PROTEIN 2*, *PAS2*, *PASTICCINO 2*, *PES1*, *PHYTYL ESTER SYNTHASE 1, PLDζ2*, *PHOSPHOLIPASE D ζ*, *2PLIP3*, *PLASTID LIPASE 3, pPLAIIIβ*, *PATATIN-RELATED PHOSPHOLIPASE A IIIβ*, *PNC1*, *PEROXISOMAL ADENINE NUCLEOTIDE CARRIER 1*, *SDP1, SUGAR-DEPENDENT1*, *SDRB*, *SHORT-CHAIN DEHYDROGENASE-REDUCTASE B*, *WRI1*, *WRINKLED 1*.

	arabis_transcript_id	Ath_AGI	Ath_Symbols	TPM_Kallisto_I_PZ_1	TPM_Kallisto_I_PZ_2	TPM_Kallisto_I_PZ_3	TPM_Kallisto_III_PZ_1	TPM_Kallisto_III_PZ_2	TPM_Kallisto_III_PZ_3	TPM_Kallisto_IV_PZ_1	TPM_Kallisto_IV_PZ_2	TPM_Kallisto_IV_PZ_3	TPM_Kallisto_IV_AZ_if_1	TPM_Kallisto_IV_AZ_if_2	TPM_Kallisto_IV_AZ_if_3
Neutral Lipids (NL)	Aa_G319790.h1	AT1G12640	*LPCAT1*	2,43844	2,47036	3,493	12,3732	12,3483	11,9762	7,61295	8,29088	6,90127	6,39823	3,86507	6,60306
	Aa_G510110.h1	AT1G54570	*PES1*	4,29696	3,94718	4,65103	13,5411	12,8609	13,9638	11,0228	10,8191	11,4723	9,17445	8,02171	8,93584
	Aa_G300490.h1	AT3G54320	*WRI1*	3,05629	2,15287	3,38178	8,27032	6,60246	7,86098	2,74384	3,00782	2,33804	1,82445	1,02805	1,08704
	Aa_G339910.h1	AT4G18550	*DSEL*	1,70487	0,861477	2,61409	9,54489	8,32044	6,92501	6,18839	8,25489	7,59073	1,08399	1,19952	1,07155
	Aa_G259000.h1	AT5G04040	*SDP1*	5,87678	6,22315	7,29024	16,7643	15,0951	14,9281	11,9329	12,5274	10,8354	8,15638	7,53087	8,89106
	Aa_G302800.h1	AT3G10520	*HB2*	2,12105	0,795116	2,63186	11,8802	11,8797	12,9763	17,1131	19,0495	10,8017	26,4765	20,3482	16,5968
Glycolipids (GL)	Aa_G470340.h1	AT2G30550	*DALL3*	0,105446	0,0948679	0,297773	1,51463	1,06593	1,00536	1,70966	1,61315	1,76612	0,667394	0,653641	0,534436
	Aa_G51080.h1	AT3G05630	*PLDζ2*	0,963808	0,799849	1,9112	7,76428	8,12673	7,02665	5,72729	5,14511	5,16033	3,75128	3,24477	2,78379
	Aa_G695020.h1	AT3G11670	*DGD1*	11,9215	11,25	17,9114	55,9397	59,7334	55,2381	182,939	202,74	165,553	28,0866	27,7269	27,2599
	Aa_G301500.h1	AT3G54950	*pPLAIIIβ*	9,38649	9,32275	10,2401	23,8632	29,7291	28,0205	6,40037	7,36106	7,84445	7,102	7,5	7,20457
	Aa_G167830.h1	AT3G62590	*PLIP3*	1,87262	2,00825	3,96904	16,4679	17,4034	15,5689	2,99804	3,88589	2,35999	6,46348	6,56687	6,63379
Phospholipids (PL)	Aa_G275510.h1	AT1G32200	*ACT1*	0	0	1,91655	12,3239	9,80992	12,4221	9,68781	10,2838	11,5873	0,0982951	0,220677	0,0663563
	Aa_G415010.h1	AT1G51260	*LPAT3*	2,77688	2,2366	2,36272	0	0	0	0	0	0,215492	2,14814	2,17803	2,2293
	Aa_G299890.h1	AT4G00400	*GPAT8*	1,06917	1,33565	1,43618	0,996917	0,235101	0,653556	0,0351551	0	0	1,36695	1,15288	1,73073
	Aa_G46570.h1	AT4G01950	*GPAT3*	53,5492	57,5355	53,0925	0,524914	0,568358	0,153886	0	0	0	0,0189176	0,238214	0,210489
	Aa_G432060.h1	AT4G30580	*LPAT1*	16,1116	14,1085	14,4842	7,36568	6,98664	7,62605	8,26052	8,22176	8,46139	11,5523	13,176	13,3678
	Aa_G266760.h1	AT5G40610	*GPDHP*	13,1344	14,8513	11,1506	1,01069	1,28856	1,59477	0,431885	1,00177	0,595811	5,40905	8,18312	8,4264
	Aa_G291150.h1	AT1G01610	*GPAT4*	78,4967	77,6089	80,723	63,5943	86,7666	77,5891	0,762809	0,427259	0,203293	73,2707	66,3146	71,8979
	Aa_G293630.h1	AT1G80950	*LPEAT1*	20,1723	19,9636	19,918	16,2611	17,3253	16,2987	11,2377	13,7236	10,9345	19,8607	18,2529	20,1997
Fatty acids (FA)	Aa_G375840.h1	AT1G07720	*KCS3*	63,5359	61,4864	62,3571	1,83761	1,46019	1,99643	0	0	0	73,9227	84,5022	68,9646
	Aa_G323710.h1	AT1G19440	*KCS4*	37,3095	35,7675	36,8696	17,5123	22,3418	21,1798	21,3254	21,8061	18,5914	14,1909	16,4551	15,9318
	Aa_G442270.h1	AT1G25450	*KCS5*	95,5496	98,9632	89,8917	2,02497	0,624903	0,817778	0	0	0	196,775	207,796	173,339
	Aa_G110400.h1	AT1G68530	*KCS6*	52,268	50,4215	48,3228	1,23403	0,0414672	0,307507	0	0	0	92,7077	99,4601	90,8533
	Aa_G734340.h1	AT2G26250	*KCS10*	135,987	129,229	123,459	6,81992	3,28889	3,24219	0,267799	0	0	166,21	197,965	199,002
	Aa_G304000.h1	AT2G26640	*KCS11*	18,2433	17,1225	17,623	9,85876	10,9604	9,61466	4,45066	2,62912	3,27014	8,02658	8,44298	11,797
	Aa_G627890.h1	AT2G28630	*KCS12*	8,65492	8,50439	8,10949	1,27552	1,0461	1,34997	0,20324	0,218568	0	4,2494	6,92265	6,06446
	Aa_G462220.h1	AT2G46720	*KCS13*	5,38812	4,87082	5,9566	1,08998	1,23966	1,52396	0	0	0	0,951836	1,25564	4,45636
	Aa_G73230.h1	AT5G04530	*KCS19*	13,4364	15,2437	12,2274	0	0	0	0	0	0	0	0	0
	Aa_G330010.h1	AT2G29980	*FAD3*	275,203	267,696	256,817	68,0006	63,739	66,4912	29,4105	27,4538	33,0701	318,632	302,382	313,832
	Aa_G233690.h1	AT3G15850	*FAD5*	23,2024	20,6338	20,002	5,95429	5,65109	4,52147	3,12773	2,49601	2,71678	32,5589	34,142	32,7336
	Aa_G437000.h1	AT4G30950	*FAD6*	25,5567	22,6066	25,7147	7,2174	8,12072	6,06096	6,64581	11,0629	8,43857	34,6619	31,0378	36,0234
	Aa_G195580.h1	AT3G11170	*FAD7*	40,7355	38,0922	40,4116	27,6219	23,8403	22,5738	20,2917	29,2924	23,0485	102,106	90,8682	93,3351
	Aa_G464270.h1	AT5G05580	*FAD8*	12,4413	12,8351	10,4805	2,02628	1,82117	1,95728	0,417285	0,287952	0,46893	18,3464	20,2014	19,8761
	Aa_G265090.h1	AT2G44620	*MTACP1*	151,091	153,009	151,981	70,8128	75,5659	74,6227	63,2454	46,6261	52,8785	112,515	118,425	128,566
	Aa_G474670.h1	AT1G65290	*MTACP2*	155,082	168,273	151,086	80,2115	81,0156	92,0744	78,4202	67,0595	86,1457	96,4777	105,389	98,3459
	Aa_G353680.h1	AT4G25050	*ACP4*	306,878	315,194	308,943	71,2348	60,2858	56,3521	118,754	127,758	115,625	148,168	188,32	250,902
	Aa_G356230.h1	AT4G13050	*FAT A2*	23,4944	20,9342	21,4262	12,7809	12,6062	16,0389	14,0926	9,70922	12,568	12,6454	15,1973	13,877
	Aa_G718090.h1	AT3G55360	*CER10*	108,484	110,581	101,881	63,6108	59,2236	60,4769	20,5921	19,3213	20,5162	172,31	173,64	166,365
	Aa_G98230.h1	AT5G10480	*PAS2*	52,6625	50,3617	50,4591	27,376	32,9444	33,7578	13,2093	14,8477	10,7646	58,6604	50,1294	47,3787
	Aa_G96860.h1	AT5G16230	*AAD3*	17,7455	14,9496	16,1308	8,59436	9,30764	9,68818	1,34167	1,21053	0,399985	6,03266	4,86868	6,44256
	Aa_G22950.h1	AT1G06290	*ACX3*	4,8438	4,00685	6,16231	13,9445	14,9395	13,7393	9,21237	10,3842	9,05093	7,28121	6,36264	6,8769
	Aa_G350320.h1	AT1G65520	*ECI1*	12,0416	11,0958	16,8529	36,2672	32,4747	35,1372	45,3908	58,0061	57,0157	21,6147	23,6058	24,6612
	Aa_G183660.h1	AT2G33150	*KAT2*	53,3696	58,9094	72,0068	188,003	169,74	163,189	75,8854	93,9996	80,2206	98,2433	89,4219	97,6495
	Aa_G5110.h1	AT3G05290	*PNC1*	10,8051	11,3125	11,2938	22,486	22,703	23,0262	14,1225	14,9206	13,4054	15,5706	12,9858	11,1176
	Aa_G47030.h1	AT3G06860	*MFP2*	16,8965	19,3231	23,8654	62,0979	61,6641	59,87	30,5154	34,0507	29,8754	30,6317	31,2556	29,1298
	Aa_G40050.h1	AT3G12800	*SDRB*	42,1682	43,9551	52,7724	95,8157	89,5513	88,7995	19,1104	27,7442	22,2117	73,6671	66,2058	66,4776
	Aa_G722850.h1	AT3G51840	*ACX4*	31,5421	31,3919	36,43	87,1937	80,9632	82,5511	55,9347	56,6056	51,6791	28,5809	29,5042	32,9836
	Aa_G87820.h1	AT1G76150	*ECH2*	36,2986	39,3401	43,936	68,645	62,1113	65,692	73,1776	73,8575	66,4874	41,198	44,5555	47,8047
	Aa_G186670.h1	AT4G29010	*AIM1*	49,2002	49,5094	54,0816	84,3924	84,0498	84,7897	99,4312	97,8479	90,2202	42,729	51,4566	48,2397
	Aa_G25930.h1	AT5G27600	*LACS7*	26,8932	25,3755	27,5765	40,2474	39,1255	38,7029	40,966	47,0023	41,1483	38,41	37,6606	35,5821

Supplementary Table S2. Selected GO terms from the GO enrichment analysis related to lipid metabolism: Comparison I_PZ and III_PZ.

Comparison I_PZ vs. III_PZ	GO.ID	Term	Annotated genes	Significant genes	Expected genes	classicFisher
Enriched in I_PZ	GO:0008654	phospholipid biosynthetic process	372	156	69,64	1,6E-25
	GO:0008610	lipid biosynthetic process	979	305	183,27	7,6E-22
	GO:0006644	phospholipid metabolic process	433	163	81,06	9,8E-21
	GO:0006629	lipid metabolic process	1469	380	275	1,7E-12
	GO:0006636	unsaturated fatty acid biosynthetic process	70	39	13,1	5,3E-12
	GO:0006084	acetyl-CoA metabolic process	82	36	15,35	0,00000014
	GO:0044255	cellular lipid metabolic process	1170	287	219,03	0,00000024
	GO:0006633	fatty acid biosynthetic process	198	67	37,07	0,00000028
	GO:0046471	phosphatidylglycerol metabolic process	59	28	11,04	0,00000048
	GO:0006637	acyl-CoA metabolic process	90	37	16,85	0,0000007
Enriched in III_PZ	GO:0033993	response to lipid	754	176	117,23	8,1E-09
	GO:0071396	cellular response to lipid	388	95	60,32	0,0000027
	GO:0044242	cellular lipid catabolic process	224	60	34,83	0,00001
	GO:0034440	lipid oxidation	164	45	25,5	0,000067
	GO:0009062	fatty acid catabolic process	196	50	30,47	0,0002
	GO:0016042	lipid catabolic process	334	75	51,93	0,00052
	GO:0030258	lipid modification	215	52	33,43	0,00061
	GO:0006635	fatty acid beta-oxidation	151	39	23,48	0,00074
	GO:0019374	galactolipid metabolic process	93	26	14,46	0,0016
	GO:0006664	glycolipid metabolic process	121	31	18,81	0,0028
	GO:0019375	galactolipid biosynthetic process	92	25	14,3	0,00297
	GO:0006631	fatty acid metabolic process	437	86	67,94	0,01124
	GO:0006638	neutral lipid metabolic process	19	7	2,95	0,01964
	GO:0006641	triglyceride metabolic process	15	6	2,33	0,01985
	GO:0019432	triglyceride biosynthetic process	12	5	1,87	0,02758

Supplementary Table S3. Selected GO terms from the GO enrichment analysis related to lipid metabolism: Comparison I_PZ and IV_PZ.

Comparison I_PZ vs. IV_PZ	GO.ID	Term	Annotated genes	Significant genes	Expected genes	classicFisher
Enriched in I_PZ	GO:0006637	acyl-CoA metabolic process	90	75	23,02	1,7E-30
	GO:0008610	lipid biosynthetic process	979	365	250,41	9,7E-17
	GO:0006629	lipid metabolic process	1469	479	375,74	2,7E-10
	GO:0006633	fatty acid biosynthetic process	198	91	50,64	4E-10
	GO:0008654	phospholipid biosynthetic process	372	145	95,15	7,4E-09
	GO:0006636	unsaturated fatty acid biosynthetic process	70	40	17,9	0,00000002
Enriched in IV_PZ	GO:0006635	fatty acid beta-oxidation	151	58	29,18	0,000000037
	GO:0034440	lipid oxidation	164	59	31,69	0,00000041
	GO:0044242	cellular lipid catabolic process	224	72	43,28	0,0000032
	GO:0009062	fatty acid catabolic process	196	64	37,87	0,0000062
	GO:0030258	lipid modification	215	66	41,54	0,000041
	GO:0033993	response to lipid	754	186	145,69	0,00014
	GO:0016042	lipid catabolic process	334	89	64,53	0,00063
	GO:0071396	cellular response to lipid	388	96	74,97	0,00474

Supplementary Table S4. Selected GO terms from the GO enrichment analysis related to lipid metabolism: Comparison III_PZ and IV_PZ.

Comparison III_PZ vs. IV_PZ	GO.ID	Term	Annotated genes	Significant genes	Expected genes	classicFisher
Enriched in III_PZ	GO:0006084	acetyl-CoA metabolic process	82	55	14,55	7,8E-23
	GO:0006637	acyl-CoA metabolic process	90	57	15,97	9,4E-22
	GO:0035383	thioester metabolic process	90	57	15,97	9,4E-22
	GO:0006633	fatty acid biosynthetic process	198	65	35,14	0,0000002
	GO:0006085	acetyl-CoA biosynthetic process	12	9	2,13	0,000023
	GO:0035384	thioester biosynthetic process	17	11	3,02	0,000023
	GO:0071616	acyl-CoA biosynthetic process	17	11	3,02	0,000023
	GO:0010583	response to cyclopentenone	113	36	20,06	0,00019
Enriched in IV_PZ	No GO terms identified					

Supplementary Table S5. Selected GO terms from the GO enrichment analysis related to lipid metabolism: Comparison I_PZ and IV_AZ_if.

Comparison I_PZ vs. IV_AZ_if	GO.ID	Term	Annotated genes	Significant genes	Expected genes	classicFisher
Enriched in I_PZ	No GO terms identified					
Enriched in IV_AZ_if	GO:0031407	oxylipin metabolic process	37	13	3,93	0,000065
	GO:0006636	unsaturated fatty acid biosynthetic process	70	19	7,44	0,00009
	GO:0033559	unsaturated fatty acid metabolic process	70	19	7,44	0,00009
	GO:0031408	oxylipin biosynthetic process	36	12	3,83	0,00022
	GO:0006633	fatty acid biosynthetic process	198	34	21,04	0,00334
	GO:0006631	fatty acid metabolic process	437	64	46,44	0,00509
	GO:0019216	regulation of lipid metabolic process	39	10	4,14	0,00637

Supplementary Table S6. Selected GO terms from the GO enrichment analysis related to lipid metabolism: Comparison III_PZ and IV_AZ_if.

Comparison III_PZ vs. IV_AZ_if	GO.ID	Term	Annotated genes	Significant genes	Expected genes	classicFisher
Enriched in III_PZ	GO:0033993	response to lipid	754	160	115,11	0,0000058
	GO:0010583	response to cyclopentenone	113	36	17,25	0,0000073
	GO:0071396	cellular response to lipid	388	85	59,23	0,00029
Enriched in IV_AZ_if	GO:0006644	phospholipid metabolic process	433	170	72,09	7,5E-30
	GO:0006629	lipid metabolic process	1469	399	244,56	5,3E-26
	GO:0006636	unsaturated fatty acid biosynthetic process	70	45	11,65	5,9E-19
	GO:0033559	unsaturated fatty acid metabolic process	70	45	11,65	5,9E-19
	GO:0044255	cellular lipid metabolic process	1170	298	194,78	2,2E-15
	GO:0006633	fatty acid biosynthetic process	198	68	32,96	9,5E-10
	GO:0006655	phosphatidylglycerol biosynthetic process	58	29	9,66	4,7E-09
	GO:0046471	phosphatidylglycerol metabolic process	59	29	9,82	7,7E-09

Supplementary Table S7. Selected GO terms from the GO enrichment analysis related to lipid metabolism: Comparison IV_PZ and IV_AZ_if.

Comparison IV_PZ vs. IV_AZ_if	GO.ID	Term	Annotated genes	Significant genes	Expected genes	classicFisher
Enriched in IV_PZ	GO:0006635	fatty acid beta-oxidation	151	40	26,96	0,00521
Enriched in IV_AZ_if	GO:0008610	lipid biosynthetic process	979	365	219,17	2,7E-27
	GO:0006629	lipid metabolic process	1469	486	328,87	1,3E-22
	GO:0006084	acetyl-CoA metabolic process	82	55	18,36	6,4E-18
	GO:0006637	acyl-CoA metabolic process	90	57	20,15	8,8E-17
	GO:0035383	thioester metabolic process	90	57	20,15	8,8E-17
	GO:0008654	phospholipid biosynthetic process	372	148	83,28	2,3E-14
	GO:0006644	phospholipid metabolic process	433	163	96,94	3,2E-13
	GO:0006636	unsaturated fatty acid biosynthetic process	70	43	15,67	2,4E-12
	GO:0033559	unsaturated fatty acid metabolic process	70	43	15,67	2,4E-12
	GO:0006633	fatty acid biosynthetic process	198	88	44,33	4E-12
	GO:0044255	cellular lipid metabolic process	1170	357	261,93	2,3E-11

Supplementary Table S8. Reverse transcription qPCR primers for lipid metabolism genes.

	arabis_transcript_id	Ath_AGI	Name	Forward (F) Primer (5' to 3')	Reverse (R) Primer (5' to 3')	Amplicon length [bp]
Reference	Aa_G26240	AT5G46630	*CLATHRIN ADAPTOR COMPLEX MEDIUM SUBUNIT (CAC)*	TGGACAAGACCACCAATCCA (Stephan *et al.*, 2019)	CACTCGACCGTGTTGTAACC (Stephan *et al.*, 2019)	113
	Aa_G472320	AT3G13920	*EUKARYOTIC TRANSLATION INITIATION FACTOR 4A1 (EIF4a)*	CCAGCTTCTCCCACCCAAGA (Stephan *et al.*, 2019)	GCTCGTCACGCTTCACCAAG (Stephan *et al.*, 2019)	122
Genomic DNA control	Aa_G26240	AT5G46630	*CLATHRIN ADAPTOR COMPLEX MEDIUM SUBUNIT (CAC)*	CATTGGAAGCGTGGATGAAA	CTCCGAATCCACTTCAATCTCC	230
	Aa_G472320	AT3G13920	*EUKARYOTIC TRANSLATION INITIATION FACTOR 4A1 (EIF4a)*	AAGAGCGGAAACAAGGGAAG	AAATGCAAAGCTCGGAACAC	129
Neutral lipids (NL)	Aa_G319790	AT1G12640	*LYSOPHOSPHATIDYLCHOLINE ACYLTRANSFERASE 1 (LPCAT1)*	CGATGGCAACAAGCTATCAG	GTAACTGAGCAGAAGCAATACAAC	201
	Aa_G510110	AT1G54570	*PHYTYL ESTER SYNTHASE 1 (PES1)*	ACGACCTGATGAAGATTCCAAT	ATCGGTTTCCCGAACAGGT	175
	Aa_G300490	AT3G54320	*WRINKLED 1 (WRI1)*	CGAGTCAGGATTTGAGGATAAC	AAGGCAAGACAACGGAGAAG	174
	Aa_G339910	AT4G18550	*DAD1-LIKE SEEDLING ESTABLISHMENT-RELATED LIPASE (DSEL)*	CTAATGCTCGTGACCAGGTGT	ACGGGACAAGACTTATCAGGAC	184
	Aa_G259000	AT5G04040	*SUGAR-DEPENDENT1 (SDP1)*	TCTGGTCCGTTTAGCCCACT	TTTGATTCCCGTTCGACGA	232
Glycolipids (GL)	Aa_G51080	AT3G05630	*PHOSPHOLIPASE D ζ 2 (PLDζ2)*	AGTGGTGGTGGCAGATTGG	TATCTTCGGGCTGGCTTGT	96
	Aa_G695020	AT3G11670	*DIGALACTOSYL DIACYLGLYCEROL DEFICIENT 1 (DGD1)*	GGCTGGATTGGCTTCTTCTT	TAGCTCGATCACGCATCAACT	149
	Aa_G301500	AT3G54950	*PATATIN-RELATED PHOSPHOLIPASE A IIIβ (pPLAIIIβ)*	GAGACACGGTGGCTATGGAG	GAAACTTGCTTTCGAGGATAGA	114
	Aa_G167830	AT3G62590	*PLASTID LIPASE 3 (PLIP3)*	AAGCCGAGCGGGATAAAT	GTGGGAGAAAGAAGATGATCAC	136
Phospholipids (PL)	Aa_G542320	AT1G32200	*ACYLTRANSFERASE 1 (ACT1)*	TATCCCATGTCTCTGCTTTGC	AATCTTGTATTGCTCGTGAACC	219
Fatty acids (FA)	Aa_G323710	AT1G19440	*3-KETOACYL-COA SYNTHASE 4 (KCS4)*	TGCAGCTTTCACCGGTTC	CAATCTTCCCAAGGACTGTTCT	232
	Aa_G350320	AT1G65520	*Δ3, Δ2-ENOYL COA ISOMERASE 1 (ECI1)*	CGTAAGGTTGGGAGAGGAGTTA	GAAAGGCTCTCATCTGAATCGA	117
	Aa_G183660	AT2G33150	*3-KETOACYL-COA THIOLASE 2 (KAT2)*	CACGTTGTGTCGCTACTTTGT	GTGTTTCAACTTTCCTCGCA	162
	Aa_G186670	AT4G29010	*ABNORMAL INFLORESCENCE MERISTEM (AIM1)*	AGGACCTTCTTTCCCTATTCAC	TGAACATGCGGTCACCATAC	193
	Aa_G87820	AT1G76150	*ENOYL-COA HYDRATASE 2 (ECH2)*	TTGCAATCAGGACAATCATCA	CACAGCTTTGTTCCTCTCCTTC	176

Author contributions to Manuscript 2

Anna Sergeeva

Designed, performed, and analyzed all of the described experiments, except for the following sections: RNA-seq data analysis (from assembling of the coding sequences until the gene ontology analysis (generation of excel tables containing GO terms): s. Manuscript 1: Materials and Methods: RNA sequencing and analysis), conducting of RT-qPCRs (Supplementary Fig. S4). Supervised RT-qPCR experiments. Prepared figures and tables, wrote the manuscript, reviewed/edited the manuscript.

Tabea Mettler-Altmann

Helped in designing and analyzing of the lipid analysis experiment (Fig. 2, 3, 4 and Supplementary Fig. S1, S2, S3). Reviewed/edited the manuscript.

Hongjiu Liu

Performed the RT-qPCRs (Supplementary Fig. S4). Reviewed/edited the manuscript.

Hans-Jörg Mai

Performed the RNA-seq data analysis (from assembling of the coding sequences until the gene ontology analysis (generation of excel tables containing GO terms): s. Manuscript 1: Materials and Methods: RNA sequencing and analysis). Provided R scripts for generation of horizontal bar plots (Figure 5B, C). Reviewed/edited the manuscript.

Petra Bauer

Designed and supervised the study. Acquired funding. Wrote the manuscript, reviewed/edited the manuscript.

9 Concluding Remarks

Resolution of regulatory mechanisms that confer perennial trait characteristics to plants might be extremely beneficial for development of perennial grain cropping systems. Previous studies extensively used the newly established perennial model species *Arabis alpina* to elucidate the differential behavior of meristems within the same plant (Wang *et al.*, 2009; Wang *et al.*, 2011; Bergonzi *et al.*, 2013; Park *et al.*, 2017; Lazaro *et al.*, 2018; Hyun *et al.*, 2019; Vayssières *et al.*, 2020). However, the efficient distribution of resources between seed producing organs and perennating tissues, in order to maintain perennial lifestyle, was so far an enigma in *A. alpina*. The study of this thesis provides new insights regarding the potential signals for perennial growth that are related to nutrient storage and thus, differential behavior of vegetative perennial (PZ) and annual (AZ) inflorescence stem zones.

A. alpina offers a possibility to investigate regulation of perennial and annual characteristics using the same model species due to a clear zonation pattern of lateral stems. The proximal PZ is maintained after flowering and gives rise to new axillary branches in the subsequent growth period. By contrast, the distal AZ completely senesces after seed setting. This differential behavior is also reflected on the anatomical and biochemical level. We identified the PZ to be marked by secondary growth tissues and long-term storage of starch and triacylglycerol (TAG)-containing lipid bodies (LBs) in cambium and cambium derivatives. The AZ was characterized by primary growth and sclerenchyma formation in the interfascicular regions. Production of secondary growth tissues, particularly of secondary phloem parenchyma, is clearly coupled with nutrient storage in stems of *A. alpina*. It is not unusual that *A. alpina* uses stem tissues for storage of high-energy carbon (C) compounds. Perennial herbaceous species *Tetraena mongolica* represents a similar example with starch and TAG-containing LB storage in phloem and xylem parenchyma of stems (Wang *et al.*, 2007). Accumulation of a diverse set of C, nitrogen (N), sulfur (S), and phosphorus (P) storage compounds in bark and wood tissues is well known for tree species (Sauter and Wellenkamp, 1998; Wildhagen *et al.*, 2010; Malcheska *et al.*, 2013; Netzer *et al*., 2018). Our data indicated that N storage is not likely to occur in the PZ of *A. alpina*. Yet, we cannot exclude long-term accumulation of S and P-containing metabolites. Future studies, addressing these compounds, might further stress the storage function of the PZ.

The described processes occurred in both, *A. alpina* Pajares (Paj) and its vernalization-independent mutant derivative *perpetual flowering 1-1* (*pep1-1*). By contrast, lateral stems of the annual sister species *A. montbretiana* displayed only the AZ pattern. Neither vernalization nor flowering were factors influencing secondary growth and accumulation of storage compounds in Paj and *pep1-1*.

Previous studies with *Arabidopsis* and *Populus* suggested cytokinin to be the major regulator of vascular cambium activity during secondary growth (Matsumoto-Kitano *et al.*, 2008; Nieminen *et al.*, 2008; Ohashi-Ito *et al.*, 2014; Immanen *et al.*, 2016). With our analyses using *A. alpina* we provide additional support and stress the role of cytokinin as a signal for demarcation of the AZ and the PZ.

Among all tested hormones, cytokinin application indeed greatly enhanced cambium activity and the formation of secondary phloem parenchyma in the PZ and even during the development of the AZ. In transcriptome analysis, cytokinin-related GO terms were enriched in the PZ and not in the AZ. Correspondingly, we identified a set of cytokinin biosynthesis and signaling-related genes that were higher expressed in the PZ in comparison to the AZ. The identified genes might represent targets for future studies, including generation of transgenic *A. alpina* plants with altered cytokinin levels or perception. Cytokinin biosynthesis is catalyzed by ISOPENTENYLTRANSFERASEs (IPTs), while CYTOKININ OXIDASEs (CKXs) are involved in cytokinin catabolic processes (Sakakibara, 2006). Cambium formation and secondary growth were completely absent in roots of the quadruple *atipt1;3;5;7 Arabidopsis* mutant (Matsumoto-Kitano *et al.*, 2008). Transgenic hybrid poplar trees overexpressing *CKX2* had decreased number of cambial cells and thinner stems in comparison to the wild type plants (Nieminen *et al.*, 2008). This raises an interesting question. Would transgenic *A. alpina* plants with impaired activity of IPTs or enhanced expression of CKXs still retain perennial characteristics of secondary growth and nutrient storage?

We identified the TAG-containing LBs to be present in abundance in cambium and cambium derivatives of the PZ throughout the life cycle of *A. alpina*. In addition to their storage function, LBs were proposed to be involved in various metabolic processes in plants (van der Schoot *et al.*, 2011; Tsai *et al.*, 2015; Brocard *et al.*, 2017; van Wijk and Kessler, 2017). In general, lipids play key roles in plant metabolism. According to our findings, we suggest that lipid metabolism might be another crucial factor differentiating the development of the PZ and the AZ. Glycerolipids, including neutral lipids, phospholipids, and glycolipids, were present at higher levels in the PZ of Paj and *pep1-1*, indicating their importance for the perennial lifestyle of *A. alpina*. The transcriptome analysis enabled us to identify 19 lipid metabolism-related genes that were differentially regulated between the PZ and the AZ. These genes rather correlated with individual fatty acids of investigated glycerolipid fractions of the PZ than AZ. Moreover, positive and negative correlations of these 19 identified lipid metabolism genes supported their involvement in biosynthetic and catabolic processes regarding glycerolipid species in the PZ. The functions of the enzymes encoded by the identified genes underpinned the observed accumulation of TAG-containing LBs in the PZ. In addition, our data demonstrated an enhanced fatty acid β-oxidation during progression of the PZ. This indicates the turnover of stored lipid resources, deriving for the most part presumably from neutral lipids and phospholipids. These genes represent potential targets for future studies in which regulatory mechanisms specifying the PZ differentiation in *A. alpina* will be addressed.

Taken together, our pioneer work regarding the perennial trait of nutrient allocation to perennating storage tissues present in lateral stems of *A. alpina* offers several starting points for further detailed analyses, aiming to elucidate the regulation of the sharp PZ-AZ transition. Secondary growth is linked with long-term storage in the PZ. On the one side, we provide evidence for cytokinin to be a putative important regulator of secondary growth promotion in stems of *A. alpina*. The already available

information about secondary growth processes in *Arabidopsis* and trees can be employed to reveal signaling pathways and regulators for differentiation of *A. alpina* stems in future studies. On the other side, our study indicates the importance of lipid metabolism for differentiation between the PZ and the AZ. The exact role of the suggested candidate genes and corresponding metabolic steps can be investigated in more detail in future experiments.

References

Bergonzi, S., Albani, M. C., van Themaat, E. V. L., Nordström K. J., Wang, R., Schneeberger, K., Moerland, P. D., & Coupland, G. (2013) Mechanisms of age-dependent response to winter temperature in perennial flowering of Arabis alpina. *Science*, 340, 1094-1097.

Brocard, L., Immel, F., Coulon, D., Esnay, N., Tuphile, K., Pascal, S., Claverol, S., Fouillen, L., Bessoule, J-J., & Brehelin, C. (2017). Proteomic Analysis of Lipid Droplets from Arabidopsis Aging Leaves Brings New Insight into Their Biogenesis and Functions. *Front Plant Sci, 8*, 894.

Hyun, Y., Vincent, C., Tilmes, V., Bergonzi, S., Kiefer, C., Richter, R., Martinez-Gallegos, R., Severing, E., & Coupland, G. (2019). A regulatory circuit conferring varied flowering response to cold in annual and perennial plants. *Science, 363*, 409-412.

Immanen, J., Nieminen, K., Smolander, O. P., Kojima, M., Alonso Serra, J., Koskinen, P., Zhang, J., Elo, A., Mähönen, P., Street, N., Bhalerao, R. P., Paulin, L., Auvinen, P., Sakakibara, H., & Helariutta, Y. (2016). Cytokinin and Auxin Display Distinct but Interconnected Distribution and Signaling Profiles to Stimulate Cambial Activity. *Curr Biol, 26*(15), 1990-1997.

Lazaro, A., Obeng-Hinneh, E., & Albani, M. C. (2018). Extended Vernalization Regulates Inflorescence Fate in Arabis alpina by Stably Silencing PERPETUAL FLOWERING1. *Plant Physiol, 176*(4), 2819-2833.

Malcheska, F., Honsel, A., Wildhagen, H., Durr, J., Larisch, C., Rennenberg, H., & Herschbach, C. (2013). Differential expression of specific sulphate transporters underlies seasonal and spatial patterns of sulphate allocation in trees. *Plant Cell Environ, 36*(7), 1285-1295.

Matsumoto-Kitano, M., Kusumoto, T., Tarkowski, P., Kinoshita-Tsujimura, K., Vaclavikova, K., Miyawaki, K., & Kakimoto, T. (2008). Cytokinins are central regulators of cambial activity. *Proc Natl Acad Sci U S A 105,* 20027-20031.

Netzer, F., Herschbach, C., Oikawa, A., Okazaki, Y., Dubbert, D., Saito, K., & Rennenberg, H. (2018). Seasonal Alterations in Organic Phosphorus Metabolism Drive the Phosphorus Economy of Annual Growth in F. sylvatica Trees on P-Impoverished Soil. *Front Plant Sci, 9*, 723.

Nieminen, K., Immanen, J., Laxell, M., Kauppinen, L., Tarkowski, P., Dolezal, K., Tähtiharju, S., Elo, A., Decourteix, M., Ljung, K., Bhalerao, R., Keinonen, K., Albert, V. A., & Helariutta, Y. (2008). Cytokinin signaling regulates cambial development in poplar. *Proceedings of the National Academy of Sciences, 105*(50), 20032-20037.

Ohashi-Ito, K., Saegusa, M., Iwamoto, K., Oda, Y., Katayama, H., Kojima, M., Sakakibara, H., & Fukuda, H. (2014). A bHLH complex activates vascular cell division via cytokinin action in root apical meristem. *Curr Biol, 24*(17), 2053-2058.

Park, J. Y., Kim, H., & Lee, I. (2017). Comparative analysis of molecular and physiological traits between perennial Arabis alpina Pajares and annual Arabidopsis thaliana Sy-0. *Sci Rep, 7*(1), 13348.

Sakakibara, H. (2006). Cytokinins: activity, biosynthesis, and translocation. *Annu Rev Plant Biol, 57*, 431-449.

Sauter, J. J., & Wellenkamp, S. (1998). Seasonal changes in content of starch, protein and sugars in the twig wood of Salix caprea L. *Holzforschung-International Journal of the Biology, Chemistry, Physics and Technology of Wood, 52*(3), 255-262.

Tsai, C. H., Zienkiewicz, K., Amstutz, C. L., Brink, B. G., Warakanont, J., Roston, R., & Benning, C. (2015). Dynamics of protein and polar lipid recruitment during lipid droplet assembly in Chlamydomonas reinhardtii. *Plant J, 83*(4), 650-660.

van der Schoot, C., Paul, L. K., Paul, S. B., & Rinne, P. L. (2011). Plant lipid bodies and cell-cell signaling: a new role for an old organelle? *Plant Signal Behav, 6*(11), 1732-1738.

van Wijk, K. J., & Kessler, F. (2017). Plastoglobuli: Plastid Microcompartments with Integrated Functions in Metabolism, Plastid Developmental Transitions, and Environmental Adaptation. *Annu Rev Plant Biol, 68*, 253-289.

Vayssières, A., Mishra, P., Roggen, A., Neumann, U., Ljung, K., & Albani, M. C. (2020). Vernalization shapes shoot architecture and ensures the maintenance of dormant buds in the perennial Arabis alpina. *New Phytol, 227*(1), 99-115.

Wang, R., Albani, M. C., Vincent, C., Bergonzi, S., Luan, M., Bai, Y., Kiefer, C., Castillo, R., & Coupland, G. (2011). Aa TFL1 confers an age-dependent response to vernalization in perennial Arabis alpina. *Plant Cell, 23*(4), 1307-1321.

Wang, R., Farrona, S., Vincent, C., Joecker, A., Schoof, H., Turck, F., Alonso-Blanco, C., Coupland, G., & Albani, M. C. (2009). PEP1 regulates perennial flowering in Arabis alpina. *Nature, 459*(7245), 423-427.

Wang, G., Lin, Q., & Xu, Y. (2007). Tetraena mongolica Maxim can accumulate large amounts of triacylglycerol in phloem cells and xylem parenchyma of stems. *Phytochemistry, 68*(15), 2112-2117.

Wildhagen, H., Durr, J., Ehlting, B., & Rennenberg, H. (2010). Seasonal nitrogen cycling in the bark of field-grown Grey poplar is correlated with meteorological factors and gene expression of bark storage proteins. *Tree Physiol, 30*(9), 1096-1110.